Thermal Neutron Capture Studies of ^{108}Ag and ^{110}Ag

A thesis submitted for the award of the degree of

Doctor of Philosophy of the University of London

Tomotaka MITSUNARI

University of London Reactor Centre

Imperial College of Science and Technology

October 1981

ABSTRACT

As a contribution to the systematic study of trends in the structure of odd-odd nuclei in the Z = 50 region, thermal neutron capture reactions in ^{107}Ag and ^{109}Ag have been investigated using a variety of techniques.

The internal conversion electrons in the ^{109}Ag(n,γe$^-$)^{110}Ag reaction have been measured with the electron spectrometer 'BILL', installed at the HFR in Grenoble. A target of enriched ^{109}Ag (99.7%, 3mg, 100μg/cm^2) evaporated onto aluminium foil was irradiated with a thermal neutron flux of 3×10^{14} ncm^{-2}sec^{-1}. More than 500 electron lines were observed in the range of 17 keV < E_e < 650 keV and 400 of them have been identified as the internal conversion electrons from more than 240 transitions in ^{110}Ag.

The gamma-transitions in the same reaction have been measured by the curved-crystal spectrometers 'GAMS' and by the pair-spectrometer 'PN4' both installed also at the HFR in Grenoble. A target of enriched ^{109}Ag (99.7%, 50mg, 100mg/cm^2) covered with aluminium foil was irradiated with a thermal neutron flux of 5×10^{14} ncm^{-2}sec^{-1}. 1100 gamma-transitions were observed in the range 35 keV < E_γ < 1500 keV by GAMS and the data have been combined with earlier data obtained at Risø. Multipolarities of about 200 transitions were determined by comparing gamma-ray and electron intensities. 740 gamma-transitions were observed in the range 1300 keV < E_γ < 6900 keV by PN4.

These transition data of ^{110}Ag and similar existing data of ^{108}Ag were fed into a series of computer programmes, which were designed especially for neutron capture studies, and detailed level schemes have been constructed, taking into account other experimental data on

the nuclei, such as γ-γ coincidence studies, (d,p), (p,nγ) and resonance neutron capture. The present level schemes consist of 50 levels below 1000 keV containing some 300 transitions and 75 levels below 1200 keV containing some 500 transitions in ^{108}Ag and ^{110}Ag, respectively.

Some proton-neutron multiplet configurations have been suggested and compared with the parabolic energy dependence on I(I + 1) suggested by Paar.

TABLE OF CONTENTS

LIST OF TABLES

LIST OF FIGURES

ACKNOWLEDGEMENTS

The author would like to express his gratitude for the encouragement and invaluable advice given by his supervisor, Dr. T. D. MacMahon.

The author is grateful to Dr. H. Faust, Dr. Barreau, Dr. S. Kerr and other members at the Institut Laue-Langevin for their help during the experiments and also the authorities of the Science Research Council for their financial support.

The author also appreciated Mr. M. Kerridge, the Director of the University of London Reactor Centre, for his kindness and the financial support.

The author would like to thank Dr. L. E. Culver and other staff of the Mechanical Engineering Department, Imperial College, for their contribution to the tuition fees.

The author sincerely thanks the members of the University of London Reactor Centre for their kind cooperation. Many thanks are due to Mr. S. M. Jefferies for his reading the manuscript, and to Mr. D. G. Russell for his printing the microfilm.

The author wishes special thanks to his parents and family for their financial support and patience.

CHAPTER 1.

INTRODUCTION

One of the principal slow neutron reactions is the radiative capture process in which the incident neutron is absorbed in the target nucleus followed by the emission of electromagnetic radiation. Since the slow neutron reactions were discovered in 1935 [1], extensive studies have been carried out both experimentally and theoretically. The compound nucleus concept of Bohr led to the systematic understanding of features of the neutron resonance phenomenon by employing an optical potential and complex phase shift in the scattering theory. This is known as the Breit-Wigner one-level formula.

However, more complicated properties in the neutron capture mechanism became evident after examining the distribution of partial radiation widths compared with the Porter-Thomas distribution [2]. These non-statistical effects are due to the direct and semi-direct capture processes as some correlations have been observed between the reduced widths and (d,p) spectroscopic factors. These processes have been formulated mathematically by Lane and Lynn [3].

Thermal neutron capture can be regarded as a combination of compound nucleus formation and direct capture components. Since the compound state is not uniquely defined because of thermalized neutron energies, this method is used mainly for nuclear structure studies rather than reaction studies by examining the accompaning electromagnetic radiations.

The improvements of gamma-ray detection techniques have enabled a precise determination of level energies with a few eV uncertainty up to 1 MeV excitation. However, the observable levels are rather limited depending

on the ground state spins of target nucleus and the next heavier isotope formed by neutron capture.

Thermal neutron capture gamma-ray spectroscopy is a powerful tool for investigating odd-odd nuclei, provided the target nucleus has a reasonable capture cross-section. Since a high level density is expected at low energy excitation due to the unpaired proton and neutron, gamma-ray measurements are favoured. In the present studies, ^{108}Ag and ^{110}Ag have been chosen to investigate recently reported interesting features of the nuclei around Z = 50 region, such as particle-rotational and particle-vibrational bands[4].

1.1. Neutron Capture Reaction

Basic understanding of the neutron capture mechanism is necessary to proceed with a physically consistent level scheme construction. Theoretical interpretation of the mechanism will be reviewed briefly both in compound nucleus formation and direct capture. Further formal theory of nuclear reactions has been developed by Feshbach [5] using channel projection operators.

1.1.1. Compound Nucleus Formation

A compound nucleus is formed by ~~an~~ the absorption of a neutron in the field of interaction between the neutron and the target nucleus. Since the kinetic energy of the incident neutron in the potential is distributed to the other nucleons in the nucleus by some collisions, a ~~slightly~~ relatively long-lived state will be achieved, in which particle emission channel widths are considerably suppressed for slow incident neutrons, and the decay mode of such a state does not depend on how it has been formed. Therefore, in this model, the neutron capture process is completely separated into the compound nucleus formation and its decay by the electromagnetic radiation emission, and the characteristics

of the compound nucleus will determine quantum mechanical probabilities of decay modes.

The process of compound nucleus formation can be described as a part of S-matrix formalism in the scattering theory [6]. The importance of incident s-wave slow neutrons in the process can be understood geometrically from the fact that the unitarity of the S-matrix sets up maxima of the partial cross-sections. However, the expressions for the cross-sections include implicit forms using the phase shift convention. For explicit expressions, the internal states of the system Hamiltonian have to be considered and the boundary condition must be satisfied at the channel radius.

The resonance phenomenon is an energy dependent event and its cross-section is very sensitive to the small value of the logarithmic derivative of the radial wave function at the channel radius. The resonance energies which give local maxima of total cross-section can be obtained very near to the internal level energies. Such energy shifts appear in the R-matrix formalism explicitly but not in the simple form of the Breit-Wigner formula [7]. In this well-known one-level formula, the radiation width appears as an imaginary energy term, from which the decay constant of the compound nucleus state can be deduced. This agrees with the uncertainty principle.

Since thermal neutrons have an approximately Maxwellian velocity distribution, the capture process has to be considered as a combination of several resonances including the negative levels which are lower than the neutron binding energy. However, the energy range covered by thermal neutrons is not wide enough to apply the statistical model of resonances to the thermal neutron capture process, because the level density and partial widths may not be correctly estimated around the

the neutron binding energy.

On the other hand, the selection rule of angular momentum plays an important role in the compound nucleus formation. Assuming a spin and parity $I_t^{\pi_t}$ of the target nucleus, the following compound nucleus states $J_c^{\pi_c}$ can be allowed in the angular momentum coupling scheme.

$$J_c = I_t \pm \frac{1}{2}\ ,\ \pi_c = \pi_t \qquad \text{for s-wave neutron capture}$$

$$J_c = \min\{|I_t - \tfrac{1}{2}|, |I_t - \tfrac{3}{2}|\},\ \cdots\ , I_t + \tfrac{3}{2}\ ,$$

$$\pi_c = -\pi_t \qquad \text{for p-wave neutron capture.}$$

This selection rule is obtained by the coupling of the three angular momenta, neutron intrinsic spin $\vec{i}$, orbital angular momentum $\vec{\ell}$ and the target spin $\vec{I}_t$, resulting in the compound nucleus spin $\vec{J}_c$.

$$\vec{J}_c = \vec{i} + \vec{I}_t + \vec{\ell}$$

In the coupling of three angular momenta, the representation of simultaneous eigenstates $|J_c M_c>$ of operators $\vec{J}_c^2$ and J_{cz} is not uniquely defined, but spans a definite subspace of $(2i+1)(2I_t+1)(2\ell+1)$ manifold [8].

By taking the channel spin coupling first as

$$\vec{I}_c = \vec{i} + \vec{I}_t\ ,$$

the dependence of the compound nucleus formation cross-section σ_c on angular momenta is expressed simply by the square of the Clebsch-Gordan coefficient [6],

$$\sigma_c \propto |<I_c M_c \ell m_\ell | J_c M>|^2 \qquad \text{or}$$

$$|<I_c M_c \ell 0 \ | J_c M>|^2 \qquad \text{if narrow beam.}$$

The above selection rule can be deduced by the triangular relationship of the coefficients.

1.1.2. Direct and Semi-direct Capture Processes

Non-statistical effects in thermal neutron capture and correlations of thermal (n,γ) intensities with $\ell = 1$ (d,p) intensities were discovered in 1953 [9], which stimulated the development of a mathematical formulation

of neutron capture mechanisms. Various models for the neutron capture mechanism have been established by Lane and Lynn [3]. The historical development of direct capture theories has been compiled by Lane[10].

These models are classified into three categories, which are known as

1) Direct Capture (Hard Sphere Capture)

2) Channel Capture (Valence Neutron Capture)

3) Semi-direct Capture (Doorway State Formation)

These processes can be considered as scattering of an incident neutron from the system potential and electromagnetic perturbation field to a low-lying state without forming a compound nucleus. The relationship of the hard sphere and valence neutron captures to the giant resonances in the gross-structure of total cross-section has been investigated [11] and these non-statistical effects seem to be present in mass regions where s-wave and p-wave neutron strength functions have peaks [12].

Since these single particle features exhibit much more complicated fine structures than the gross structure for heavier nuclei, the idea of the doorway state formation has been introduced to the 4s giant resonance mass region.

1.2. Electromagnetic Transitions

Electromagnetic transitions associated with neutron capture reactions are of great importance in nuclear structure studies as well as capture mechanisms in accordance with the development of high resolution gamma-ray detectors. However, the dynamical theories are very difficult to formalize due to the inclusion of the massless photon field.

The neutron binding energy or the excitation energy of the compound

nucleus is released in the form of electromagnetic radiation in several steps from the capture state to the ground state. The first transition from the capture state to an intermediate state is known as the primary transition and provides evidence for the existence of the intermediate state and also determines its excitation energy directly. Most of the excitation energy is carried off by the E1 or M1 primary transition. The rest of the excitation energy is carried off by other successive transitions, which are known as secondary transitions. They reveal the low-lying level structure by precise measurements of these low energy transitions.

1.2.1. Primary Transitions

The strengths of primary transitions are strongly related to the capture processes, and their decay amplitudes are expressed as a linear combination of various contributions [12].

$$\Gamma_{if}^{\frac{1}{2}} = C_1\Gamma_{(CN)if}^{\frac{1}{2}} + C_2\Gamma_{(HS)if}^{\frac{1}{2}} + C_3\Gamma_{(CV)if}^{\frac{1}{2}} + C_4\Gamma_{(DS)if}^{\frac{1}{2}}$$

where the terms on the right hand side correspond to compound nucleus formation, hard sphere capture, channel capture and doorway state formation, respectively. The statistics of the reduced intensities of the primary transitions depend on which contribution dominates in the expression.

It has been empirically investigated that the correlation between (d,p) spectroscopic factors $(2J+1)S_{dp}$ and the reduced primary gamma-ray intensities I_γ/E_γ^n shows different optimum values of the reduction factor n for various capture mechanisms, although the reduction factor $n = 2\ell+1$ is recommended theoretically, where ℓ is the multipolarity of the transition. According to the summary of the experimental data in the mass region from ^{27}Al to ^{66}Zn by Mughabghab [12], the region falls into three groups characterized by n = 1.1, 2.4 and 4.8, corresponding to

direct capture, valence capture and statistical regions, respectively.

The Porter-Thomas distribution [2] can be applicable to the primary transition reduced intensities if the compound nucleus formation dominates in the capture process. In the average resonance capture technique [14], it is a fundamental assumption that the dependence of the reduced intensities on the radial overlap integrals can be ignored due to the statistical distribution and the averaged contributions from many different resonances.

1.2.2. Secondary Transitions

Secondary transitions are not of interest in the neutron capture process, but supply very useful information in nuclear structure studies with the aid of the Ritz combination principle and the Kirchhoff's law. In thermal neutron capture, however, the excitation process is limited ~~within~~ to s-wave or p-wave neutron capture. Therefore, if the difference between the ground state spins of the target nucleus and the next heavier isotope is small, levels with very different spins cannot be populated in the decay of the compound nucleus.

Thermal neutron capture may not be a good method of nuclear excitation for the above reason to study complicated band structures, compared with other nuclear reactions. However, because of the fact that the energy precision of gamma-ray detectors is far superior ~~than the~~ to that of charged particle detectors, much more precise level energies can be deduced, provided correct assignments of the transitions in the level scheme are made.

Thousands of gamma-rays are emitted following neutron capture. A few hundreds of them can be detected using present experimental apparatus within a reasonable time. Since there are so many gamma-rays to be placed at an appropriate position in a level scheme, difficulty

arises in processing these data. Even with the high precision of curved-crystal spectrometer measurements, the Ritz combination principle may allow many possible combinations and can place a gamma-transition at several places in a level scheme.

One of the purposes of the present work is to develop the procedure and will be described in Chapter 3.

1.2.3. Gamma-ray Spectrum in Neutron Capture

The overall neutron capture gamma-ray spectrum can be calculated theoretically assuming E1 character for the transitions[3]. Since the transition probability from an excited state is given by the radiation width multiplied by the level density of final states, both characteristics have to be estimated between the ground state and neutron binding energy. The E1 radiation width can be obtained in the form of the photon strength function. This function is theoretically known to be proportional to the cube of the transition energy and is experimentally determined by photo-excitation reactions assuming that the strength is a function only of the photon energy. Several level density formulae can be used to obtain the best fit to the experimental results. In addition to these, it is necessary to normalize the contribution from each initial state such that the depopulation is equal to the population to the state.

Good agreement has been obtained in the comparison with experimental data for the nuclei with neutron number away from the magic numbers, e.g. neutron capture in Gd, Ta and Ag. In order to explain the Cs and Au spectra, however, it is necessary to assume a second peak in the gamma-ray strength function at an energy of about 5.5 MeV, which may be the M1 giant resonance predicted by Mottelson [15].

1.3. Nuclei around Z = 50 Region

It has been shown experimentally and theoretically that the nuclei around the Z = 50 region show interesting characteristics of quasi-particle-vibrational, quasi-particle-rotational and deformed states [4]. These features can be seen mostly in even-even and odd-even nuclei, and may be understood as the coupling of a proton group, the number of which is very close to the magic number 50, and a neutron group, the number of which is, on the contrary, just between two magic numbers 50 and 82.

Experimental studies in odd-odd nuclei are being carried out extensively as well as theoretical studies of the splitting of proton-neutron multiplets with some admixtures of collective motions [16]. A theoretical review will be given in Chapter 5.

^{108}Ag and ^{110}Ag are odd-odd nuclei with 47 protons and 61 or 63 neutrons, respectively. These nuclei have been studied at the University of London Reactor Centre and at the Institut Laue-Langevin using thermal neutron capture reactions in stable ^{107}Ag and ^{109}Ag in collaboration with some other institutions [17]. Since very high level density is expected at low excitation energy, very little was known about these nuclei. The present thermal neutron capture study has revealed the existence of some 50 to 60 low spin states up to 1 MeV in each nucleus. High spin states cannot be ~~deduced~~ observed very easily in the thermal neutron capture reactions for the reasons described before.

It is the main purpose of the present work to construct the level schemes using the results of thermal neutron capture reactions and to investigate the characteristics of ~~established~~ excited states including the spin and parity assignments, referring also to the results of other reactions.

CHAPTER 2.

EXPERIMENTS

Various types of experiments have been carried out in order to investigate the detailed level schemes of ^{108}Ag and ^{110}Ag, including (d,p) and (p,nγ) experiments. Those experiments referred to in the present work are listed in Table 1. Among these experiments, the internal conversion electron measurement ~~by~~ with 'BILL', the low energy gamma-ray measurement ~~by~~ with 'GAMS' and the high energy gamma-ray measurement ~~by~~ with 'PN4' in the reaction ^{109}Ag(n,γe$^-$)^{110}Ag were carried out by the present author and will be explained thoroughly. The other experiments are described in detail in the relevant references.

2.1. Measurement of Internal Conversion Electrons

In order to determine some multipolarities of the transitions in ^{110}Ag the reaction ^{109}Ag(n,e$^-$)^{110}Ag was ~~carried out~~ studied in July 1979 using the high resolution iron-core electron spectrometer BILL installed at the High Flux Reactor in Grenoble [30].

2.1.1. Instrument

The instrument consists of two independent flat electromagnets at the end of the vertical beam tube, 14m long and 10cm in diameter, which defines the solid angle of 3.4×10^{-6}str. Both magnets act as double focusing spectrometers by the use of the combination of homogeneous and 1/r fields. Electrons are detected by a five-wire proportional counter of the Charpak chamber type with aluminised mylar window (500μg/cm^2), several changable detector slits and 0.5mm thick aluminium walls between the tungsten wires to prevent cross talk. The resolution is defined mainly by the target width and thickness and by the detector slit, due to the high intrinsic resolution

Table 1. List of Experiments

$^{107}Ag(n,\gamma)^{108}Ag$

E_n	Measurement	Method	Place	Experimentalist	Year	Ref.
Thermal	γ,40∿1200keV	Crystal	Risø	Breitig	1969	18
Thermal	γ,20∿80keV	Si(Li)	Munich	Massoumi	1978	17
Thermal	γ,primary	Pair	Julich	Thein	1976	17
Thermal	e,17∿990keV	BILL	Grenoble	Massoumi	1978	17
Thermal	γ,primary	Pair	Julich	Bogdanovic	1979	19
Thermal	γ-γ coinc.	Ge(Li)	Leningrad	Sushkov	1980	20
16eV	γ,primary	Ge(Li)	Brookhaven	Kane	1978	21
2keV,24keV	γ,primary	Ge(Li)	Brookhaven	Kane	1978	22
Thermal	γ-γ coinc.	Na-Ge	Vinca	Bogdanovic	1977	23
Thermal	γ,primary	Ge(Li)	Argonne	Bolotin	1967	24

$^{109}Ag(n,\gamma)^{110}Ag$

E_n	Measurement	Method	Place	Experimentalist	Year	Ref.
Thermal	γ,40∿1200keV	Crystal	Risø	Breitig	1969	18
Thermal	γ,30∿1500keV	GAMS	Grenoble	Mitsunari	1980	
Thermal	γ,primary	PN4	Grenoble	Mitsunari	1980	
Thermal	e,18∿650keV	BILL	Grenoble	Mitsunari	1979	
Thermal	γ-γ coinc.	Na-Ge	Vinca	Bogdanovic	1978	25
Thermal	e,5∿300keV	electron	Munich	Elze	1967	26
Thermal	γ,primary	Pair	Julich	Bogdanovic	1979	19
Thermal	γ,50∿1200keV	A.Comp.	Ascot	Mitsunari	1980	
Thermal	γ-γ coinc.	Ge(Li)	Rossendorf	Winkler	1967	27
Thermal	γ,primary	Ge(Li)	Argonne	Bolotin	1967	24

Other Reactions

Reaction	Measurement	Method	Place	Experimentalist	Year	Ref.
(d,p)	protons	Si(Li)	Texas	Brient	1972	28
(p,nγ)	γ,50∿680keV	Ge(Li)	Tokyo	Hattori	1975	29

($\Delta p/p \simeq 1 \times 10^{-4}$, for $E_e > 100$ keV). For example, a 3cm wide target corresponds to $\Delta p/p \simeq 3 \times 10^{-4}$ and 2mm slit gives the same resolution.

2.1.2. Target

A target of 100μg/cm^2 (3.31mg total) was prepared by evaporation of enriched ^{109}Ag (99.7%) onto an aluminium foil of 0.25mg/cm^2 thick. A very thin target is required in order to reduce the ~~self-attenuation~~ loss of electron energy in the target, especially at the low energy range below 150 keV. Good uniformity is also required to achieve a good resolution. The target is stretched within a graphite ring approximately 12.5cm in diameter (shown in Fig. 1.) and is fixed by two clamps on the ring. The whole target arrangement is then inserted through the target changing tube into the irradiation position in the reactor, where a thermal neutron flux of 3×10^{14} ncm^{-2}sec^{-1} is available. The measurement may be started after a good vacuum of order 2×10^{-4} Torr in the beam tube is obtained.

2.1.3. Data Acquisition

The control of the magnetic fields and the data acquisition are carried out by a PDP 11 computer. The strengths of the magnetic fields progressing in logarithmic steps ($\Delta B\rho/B\rho = \Delta p/p$ = const.) are calculated such that an integer number of steps lies between two neighbouring wires of the detector, which are 4mm apart. It has been found that 1mm corresponds to the increment of $\Delta p/p = 1.5 \times 10^{-4}$. The energy range of 17 keV to 640 keV was scanned over twice and electron counts and counting time were recorded on a computer disk at each step automatically. The counting is controlled by counts measured by a neutron monitor on the top of the electron beam tube, and the counting time is kept roughly constant for each step.

In addition, demagnetization of the magnets is an inevitable

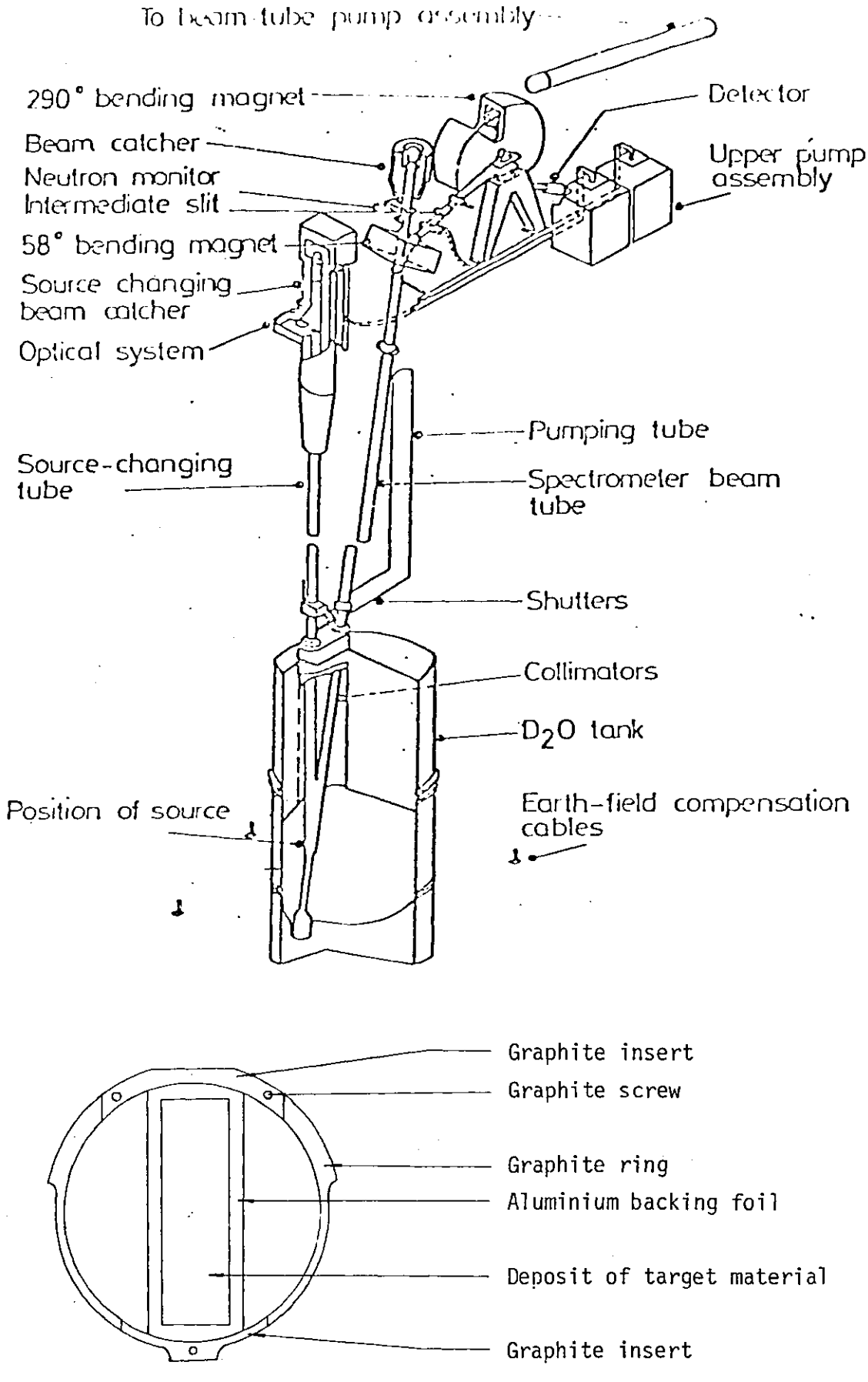

Fig. 1. Target Arrangement for BILL Spectrometer

problem because uncontrolled remanences can deteriorate the resolution and change the energy calibration of the spectrometer. This demagnetization can be done by a number of hysteresis loops with decreasing amplitudes, and is also controlled by the PDP 11 computer.

2.1.4. Data Evaluation

Data evaluation has been done following the flow-chart shown in Fig. 2.

2.1.4.1. ADD

Original five-wire data x_{ij} (i; wire number, j; step number) and counting time t_j are averaged at the points where they have the same energies. In the present experiment, the number of logarithmic steps which lies between two neighbouring wires was chosen to be four, therefore the data are added as follows:

$$X_j^{(n)} = \sum_{i=1}^{5} x_{i,j+4(i-1)} \qquad \text{(neutron normalization)}$$

$$X_j^{(t)} = \sum_{i=1}^{5} \frac{t_o}{t_{j+4(i-1)}} x_{i,j+4(i-1)} \qquad \text{(time normalization)}$$

where t_o is a normalization constant.

In the present analysis of the data, the neutron normalized spectra were used, since the reactor condition was not very stable during the experiment.

2.1.4.2. PLOT

In order to determine the background level before the peak fitting as will be described later, the normalized data are plotted as shown in Fig. 3.

2.1.4.3. BIFIT, SPECT

The line shape is fitted by a Gaussian form with an exponential tail at the low energy side, which is due to the loss of

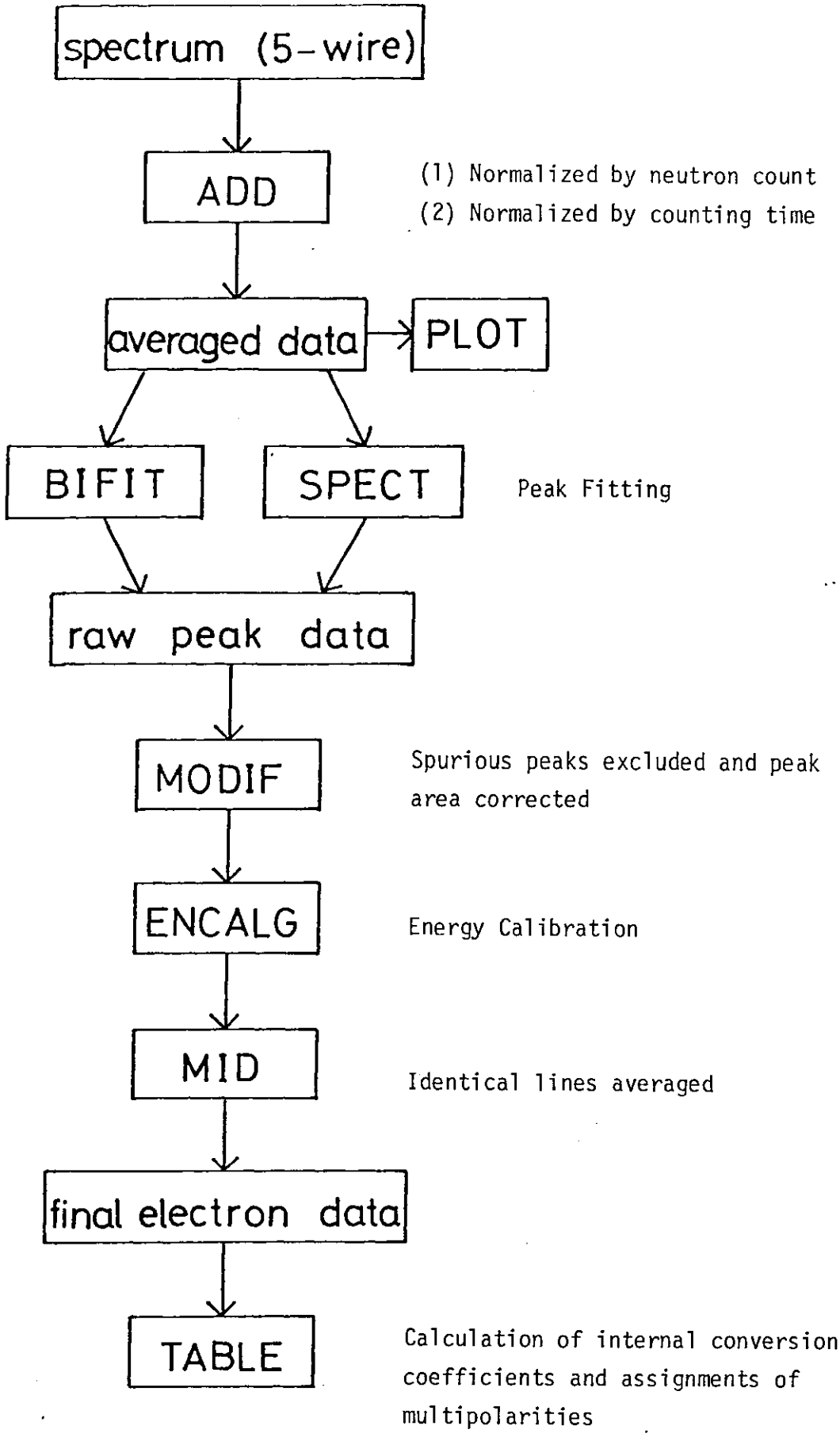

Fig. 2. Data Evaluation Flow for BILL Spectrometer

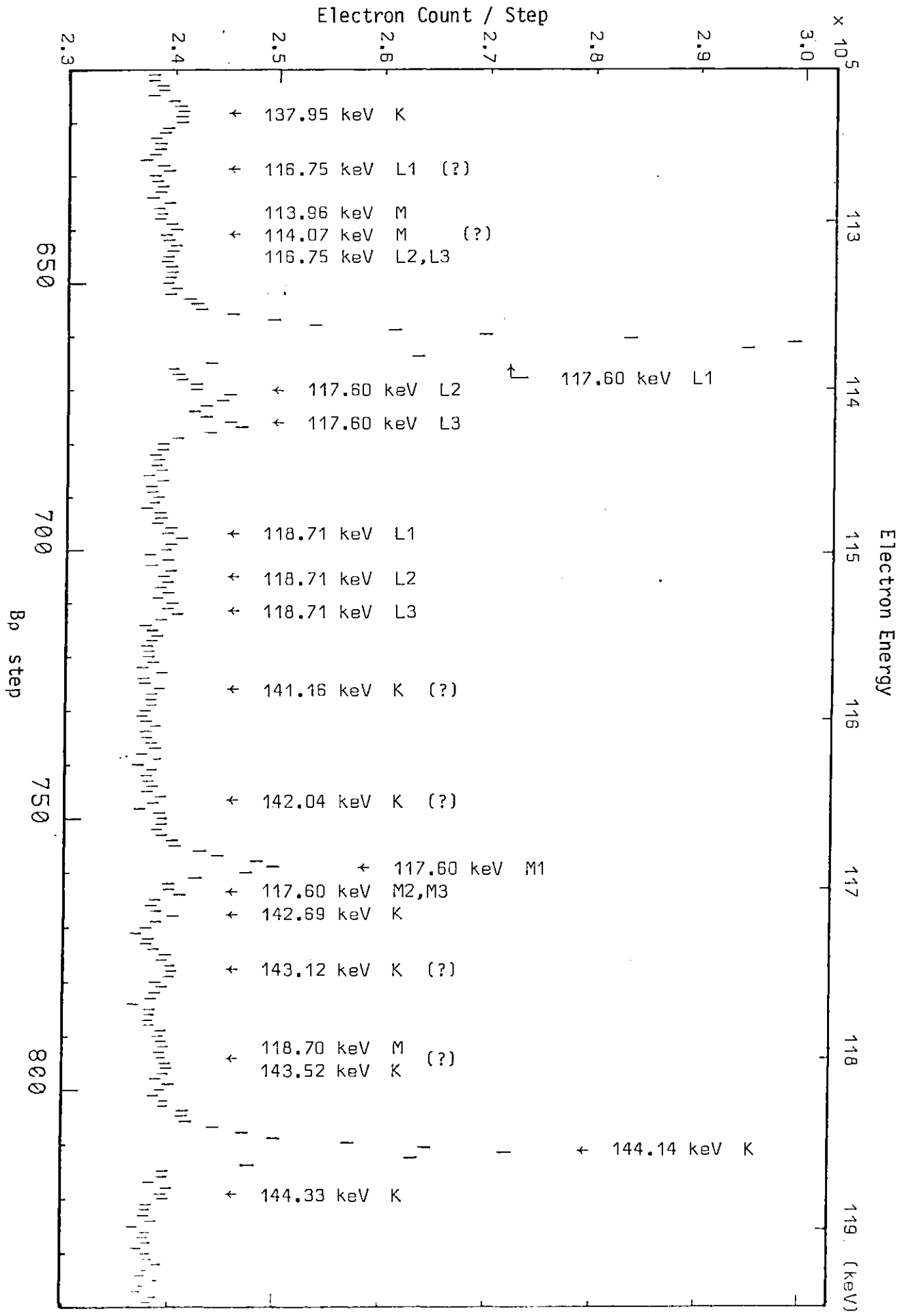

Fig. 3. Example of BILL Spectrum

electron energy in the target. This fitting function has been suggested by T. von Egidy and has the form

$$y = H \exp\{ -(x - x_o)^2 \, 4 \ln 2 / G^2\} + B.G. \qquad (x > x_o)$$

$$y = H \exp\{ -(x - x_o)^2 \, 4 \ln 2 / G^2\} + HS \exp\{(x - x_o + GG) \ln 2 / A\} \left[1 - \exp\{ -(x - x_o)^2 \, 4 \ln 2 / GG^2\}\right] + B.G. \qquad (x < x_o)$$

where x; step number

x_o; central position of the Gaussian

H; peak height

S, A, GG, G; shape parameters

B.G.; linear back ground

General trends of the four energy dependent shape parameters G, GG, S and A were obtained by the programme 'BIFIT' using some strong peaks in the spectrum. Then the automatic fitting routine 'SPECT' can be run by fixing the parameters in the fitting procedure.

2.1.4.4. MODIF

The automatic peak search routine in 'SPECT' may find some spurious peaks on the low energy tail of a strong peak. If these are found, this region has to be refitted without using the automatic peak search routine, or these spurious peaks may be excluded by this alternative programme 'MODIF'. Their intensities are distributed to the surrounding true peaks depending on the peak shapes. Since those intensities of the spurious peaks are small compared with the surrounding true peaks, it is expected that there is no influence on the peak positions. The identification of true peaks was done by inspection of plotted spectrum and the fitting result.

2.1.4.5. ENCALG

Observed Bρ-values, which are calculated from the fitted result,

are calibrated by this programme using some strong lines, the energies of which are obtained from gamma-ray data by subtracting the electron binding energy of the corresponding electron shell. The position which gives half maximum at the high energy side was used as the peak position rather than the central position of the Gaussian function in order to compensate for the attenuation of electron energy in the target, through the long beam path and by the detector window. This method does not differ very much from the method using the peak centre, unless the parameter G varies very much over the calibration region.

In this programme, observed Bρ-values $x_i \pm \Delta x_i$ are linearly fitted to the calibration Bρ-values $y_i \pm \Delta y_i$ calculated from energy. A systematic error of 1×10^{-5} times Bρ is quadratically added to the experimental error.

$$\Delta x_i' = \sqrt{(\Delta x_i)^2 + (1 \times 10^{-5} B\rho)^2}$$

The weighting factor W_i of each calibration line is calculated as follows:

$$W = 1 / (\Delta z)^2$$

$$(\Delta z)^2 = \{(\Delta x)^2 + (\Delta y)^2\}\cos\{\frac{\pi}{4} - \mathrm{Arctan}(\frac{\Delta x}{\Delta y})\}$$

where indices and primes are omitted. Δz is a projection of the total error to the 45^o line in the x-y plane.

This method includes both x and y errors without losing the linearity of minimization function derivatives with respect to the fitting parameters. There may be a problem in the choice of the weighting factor from the statistical point of view, but this is not very serious, since the coefficient of ~~the~~ linearity is expected to be approximately unity.

2.1.4.6. MID

At the final stage of analysis, several results ~~of~~ for a particular electron line are combined by taking averages of their energies and

intensities. Each correspondence is found line by line, by comparing energy and intensity, where the intensity comparison is not included in the computer programme.

Intensities have to be calibrated by the efficiency curve of the instrument, which has been given by the following equations.

$$\varepsilon = -0.00075\ E_e^{\,2} + 0.0675\ E_e - 0.848 \qquad (17\text{keV} < E_e < 40\text{keV})$$

$$\varepsilon = \min\{\ 1.,\ 0.278\ (E_e - 16.5)^{0.27}\ \} \qquad (E_e < 40\text{keV})$$

The usual correction of intensity by momentum width, which is defined by the detector slit, is not necessary because the logarithmic steps of Bρ-value have been introduced.

2.1.4.7. TABLE

Finally, in order to determine the transition multipolarities, calculation of experimental and theoretical internal conversion coefficients is carried out using the gamma-ray data from the same reaction. This will be described in detail in Chapters 3 and 4.

2.2. Measurement of Low Energy Gamma-Transitions

This experiment is to revise the earlier experiment carried out by Koch et al at Risø, in which the gamma-ray energies have large associated errors of 0.1keV or more above 500keV making the Ritz combination principle difficult to apply. Since a much higher level density was expected at the low energy excitation region in ^{110}Ag than in ^{108}Ag due to two extra neutrons, hence a much higher transition density as well, a precise low energy gamma-ray measurement in the reaction ^{109}Ag(n,γ)^{110}Ag was carried out in May 1980, using the curved crystal spectrometers 'GAMS 1' and 'GAMS 2/3' installed at the High Flux Reactor in Grenoble[31].

2.2.1. Instrument

Curved crystal spectrometers possess considerably better energy resolution and dynamic range for gamma-rays below 1MeV than Ge(Li) semi-conductor detectors, despite the fact that a high activity source is necessary because of the usual long gamma-ray path, the E_γ^{-2} dependence of crystal reflectivity and gamma-ray attenuation in the crystal[32]. They are, therefore, very useful tools in ~~the~~ neutron capture gamma-ray spectroscopy where many gamma-rays are emitted in the reactions.

The instrument 'GAMS' consists of two separate spectrometer systems of DuMond type with three main curved quartz crystals, one of focal length 5.76m (110 plane, 4mm thick, window 4cm in diameter, formerly installed at the Risø spectrometer) is used in the 'GAMS 1' and the others of focal length 24m (110 plane, 14mm thick, 6cm x 6cm window) in the 'GAMS 2/3'. Additional diffracting crystal (control crystal) of focal length 5.7m (110 plane, 2mm thick, window 4cm in diameter) is used in ~~the~~ GAMS 1 in order to measure the movement of the source by detecting an intense gamma-ray all the time. However, this assembly is not necessary in the GAMS 2/3 system, since the two spectrometers on top of each other operate symmetrically with respect to the beam axis and measure the same region of spectrum simultaneously. If a gamma-ray is found at the angle θ_2 on GAMS 2 and at θ_3 on GAMS 3, the Bragg angle will be given by $(\theta_2 + \theta_3)/2$, and will be independent of the source movement.

In both systems the reflection angle is measured by means of a He-Ne laser interferometer, whose relationship to the Bragg angle has been well established, This is ~~and~~ known as an interferometric functions ~~as follows;~~ and has the following forms;

$$\theta = -BB + \mathrm{Arcsin}\{\sin BB + K(F^{(1)} - F_o^{(1)})\} \qquad \text{(for GAMS 1)}$$

$$\sin\theta = A_1(F^{(23)} - F_o^{(23)}) + A_2(F^{(23)} - F_o^{(23)}) + A_3(F^{(23)} - F_o^{(23)}) \qquad \text{(for GAMS 2/3)}$$

where θ is the Bragg angle, $F^{(1)}$ and $F^{(23)} = F^{(2)} + F^{(3)}$ are interference fringe numbers of GAMS 1 and GAMS 2/3, respectively, and BB, K, $F_o^{(1)}$, A_1, A_2, A_3 and $F_o^{(23)}$ are parameters. One interference fringe corresponds to a rotation of approximately 0.45" of arc on GAMS 1 and 0.165" of arc on GAMS 2/3, which enables high precision measurement of gamma-ray energies.

The reflected gamma-rays are detected by a 2" × 2" NaI(Tl) scintillation detector (GAMS 1) and two 4" × 4" NaI(Tl) detectors (GAMS 2/3). By the use of NaI(Tl) detectors, all the orders of Bragg reflections, photo-peak energies of which are multiples of the first order energy, can be distinguished from each other by pulse height measurement. The counts of lower five orders and the integral counts are recorded by applying appropriate energy discriminations.

2.2.2. Target

A target of enriched ^{109}Ag (99.7%, 50mg 5mm × 10mm × 0.1mm) covered with aluminium foil was sandwiched between two parts of graphite source holder shown in Fig. 4. A thin target is required for a DuMond type spectrometer in order to achieve good focusing and hence good resolution. A 0.1mm thickness corresponds to 1.2" to 2.5" of arc depending on the flatness of the source.

The whole source arrangement is suspended in the source holder tube and is inserted by the source changing assembly into the irradiation position in the reactor, where a thermal neutron flux of $5.5 \times 10^{14} ncm^{-2}sec^{-1}$ is available.

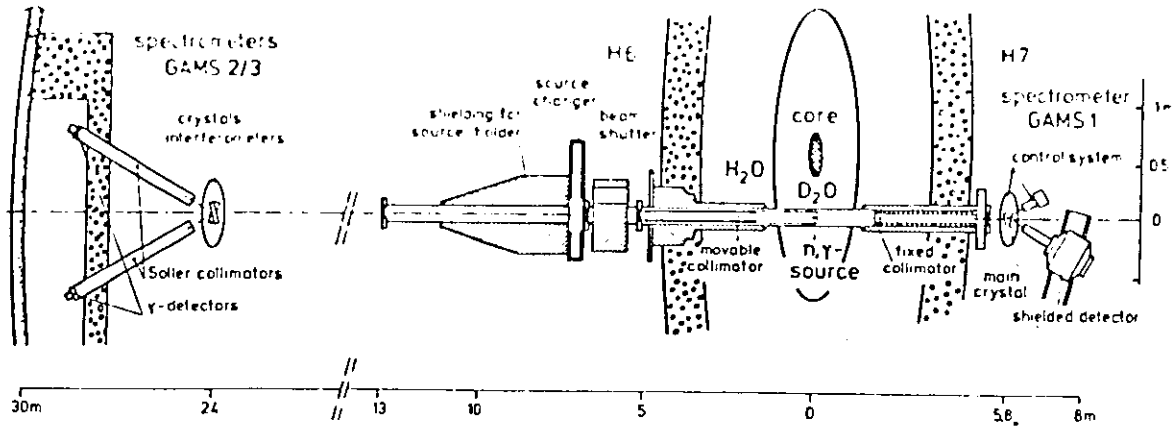

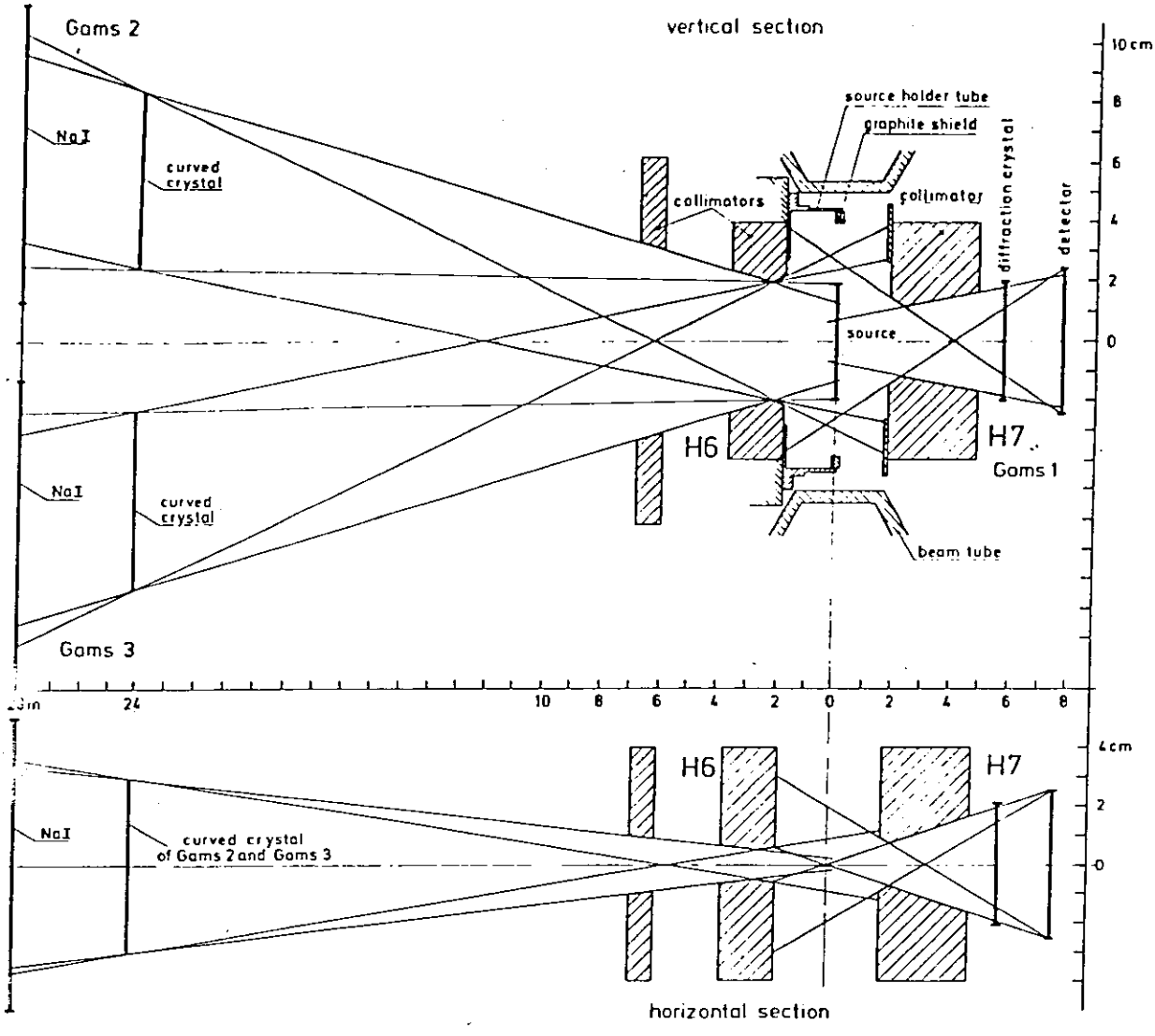

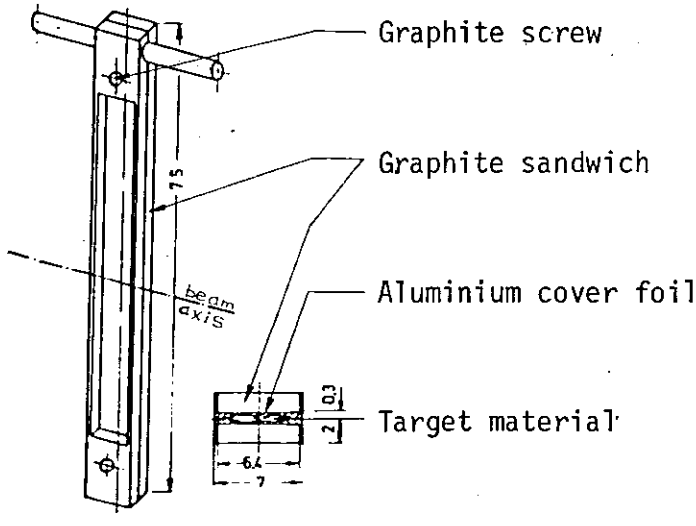

Fig. 4. Target Arrangement for GAMS Curved-Crystal Spectrometer (ref.31)

2.2.3. Adjustment

The target has to be arranged in the beam tube direction by rotating the source holder, which causes a local minimum of gamma-ray intensity profile due to the large self-absorption of gamma-rays in the target, but achieves the best resolution. Also the collimators have to be arranged in the beam direction. Further optimization of resolution can be done by tilting the crystal itself in the case that the source is not suspended perfectly vertically.

These adjustments have to be done after several hours of irradiation, since it takes 12 to 20 hours until the source reaches an equilibrium with its surroundings.

2.2.4. Control Crystal

An intense gamma-ray has to be selected to be observed by the control system of the GAMS 1. The control crystal is then set to follow the shift of the gamma-ray diffraction direction which is caused by the slight movement of the source with respect to the interferometer system. This angular shift of the control crystal is recorded so that the relevant correction of the reflection angle can be made after the data acquisition.

2.2.5. Data Acquisition

As in the case of the 'BILL' system, all the measurements are controlled by PDP-11 computers in both GAMS 1 and GAMS 2/3 systems. Main items controlled by the computers are

1) Fringe number measurement and crystal and NaI(Tl) detector position control.
2) Control crystal position measurement and calculation of a statistical factor which controls the crystal movement so that the Bragg condition can be sustained. (GAMS 1)

3) Gamma-ray counting and recording.

4) Automatic calibration including discriminator window control and amplifier gain control.

An integer number of interferometer fringes is chosen to be an increment of an angular step width. In the present experiment, two fringes were increased at each step from smaller reflection angle to larger i.e. from higher gamma-ray energy to lower. The counting time for each step was 70 sec and 80 sec, on GAMS 1 and GAMS 2/3, respectively.

Consequently, during the 12-day irradiation, the energy range of 34 ∿ 192keV (by the first order reflection) was scanned by the GAMS 1 and the range of 150 ∿ 795keV (also by the first order) by the GAMS 2/3.

2.2.6. Data Evaluation

Data evaluation has been done following the flow-chart shown in Fig. 5.

2.2.6.1. PLOT

The integral gamma-spectrum and the five orders of reflection are plotted on the same graph as function of interferometer fringe number. Fig. 6 shows a part of the spectrum. Simultaneously an automatic peak search is carried out based on the smoothed first derivative method[33]. Approximate peak positions found are then fed into the automatic peak fit routine.

2.2.6.2. FITSP, FITPIC

All the peaks are fitted by a simple Gaussian form with linear back ground. Even though the line shape is not a real Gaussian form, the deviation seems to be very small except in the case of intense peaks.

Since the transition density in the reaction $^{109}Ag(n,\gamma)^{110}Ag$ is

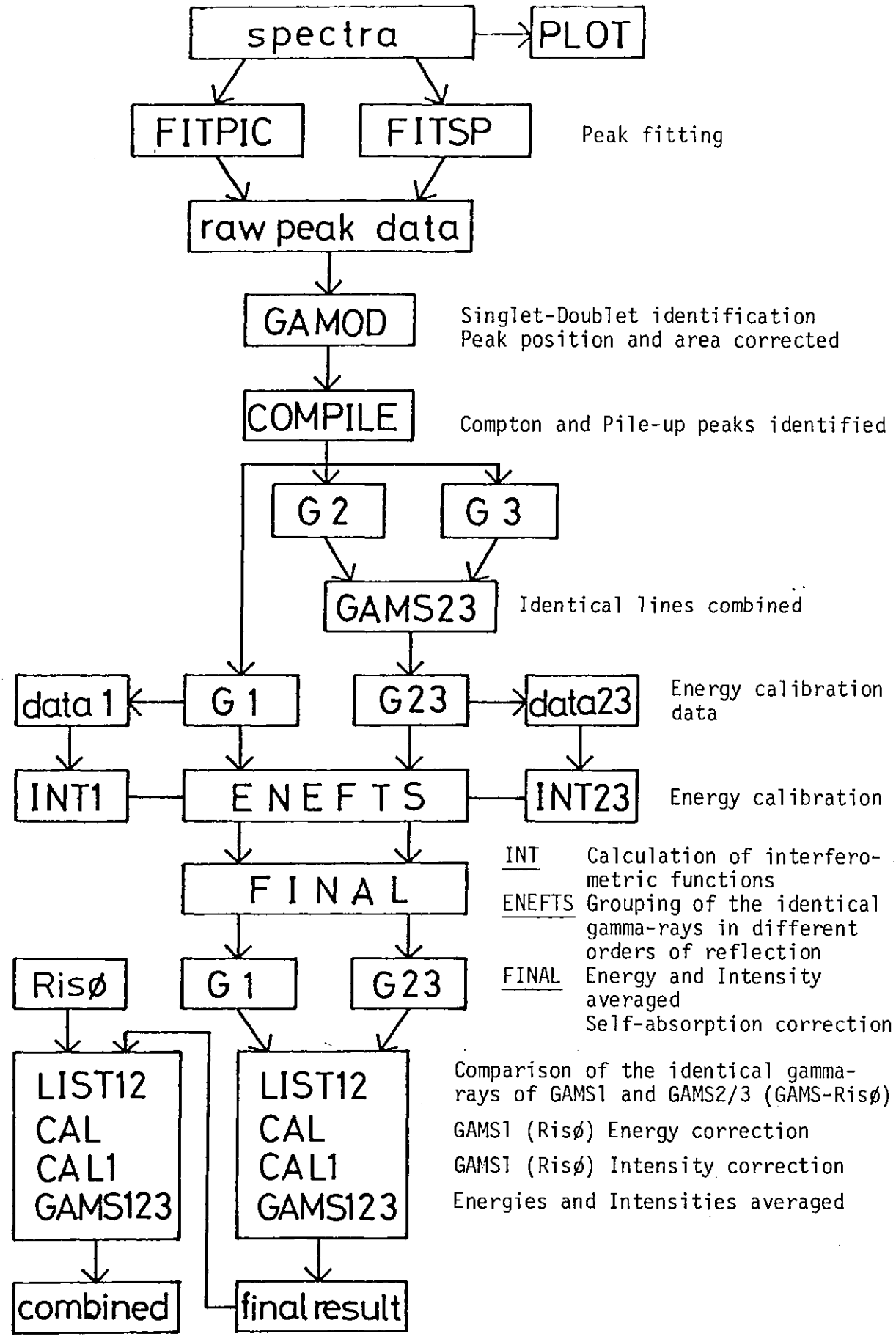

Fig. 5. Data Evaluation Flow for GAMS Spectrometer

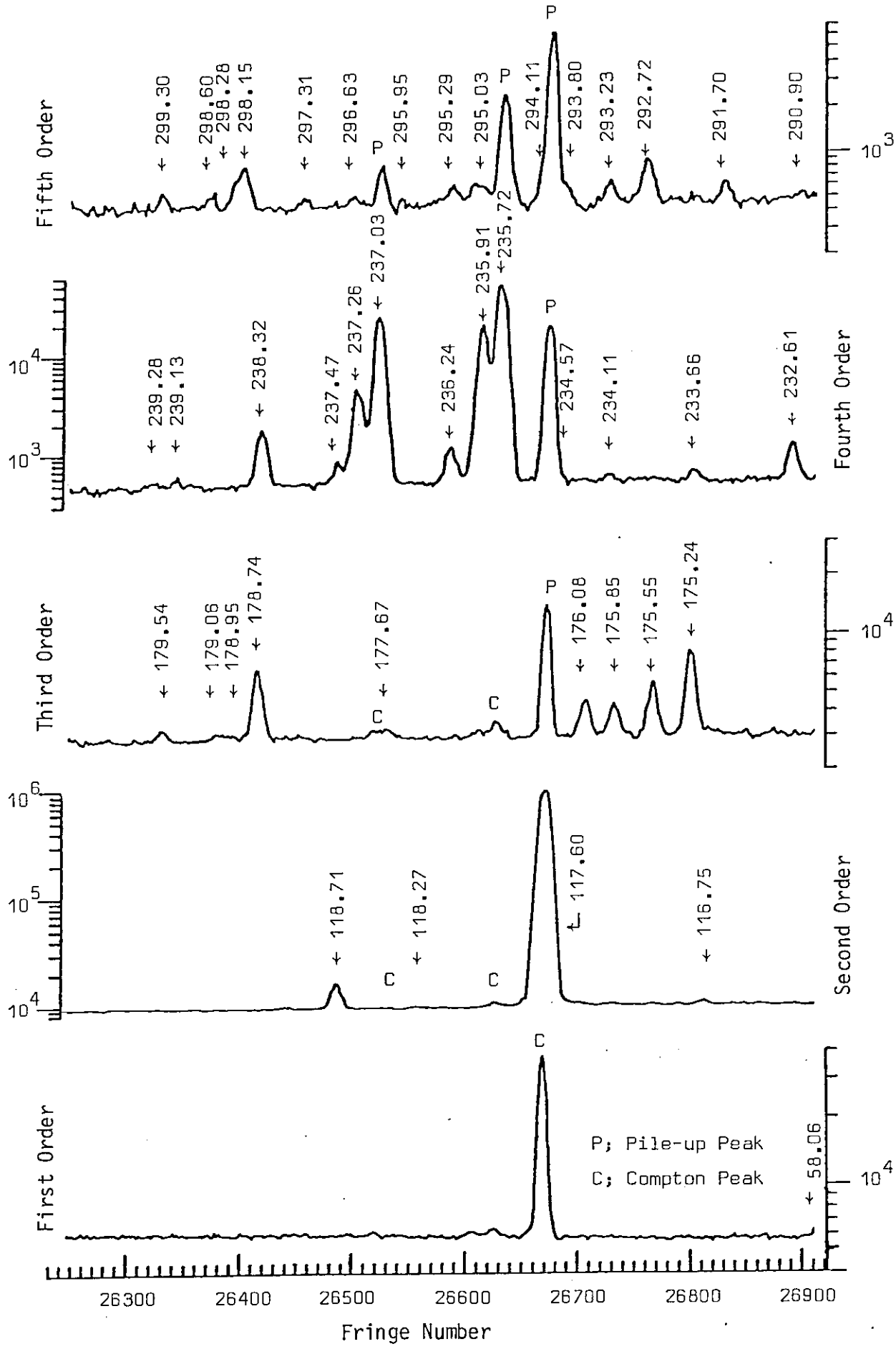

Fig. 6. Example of GAMS Spectrum (GAMS1)

very high (roughly two or three peaks per 1keV ~~at~~ in the 400keV region), the automatic routine FITSP was not very useful. Therefore, for most regions of the spectra, the manual routine FITPIC was used. This programme was originally designed for the initial fitting in order to determine the value of peak width in the spectrum. Many amendments were made to facilitate the fitting work as follows:

1) Graphic output shown in Fig. 7.
2) Automatic peak search routine (same as in PLOT).
3) Simultaneous two-width fitting for pile-up peaks (as will be explained ~~mentioned~~).
4) Peak addition and deletion.
5) Manual control of parameters.
6) 15-peak fitting (depending on dimension statements in the programme.

The fitted result contains peak position in fringe number and corrected fringe number (GAMS 1), error, peak intensity, its error and reflection order.

2.2.6.3. GAMOD

As can be seen in the spectrum, many peaks can be fitted in a certain region of spectrum. ~~And for~~ In the case of intense peaks or for slightly assymmetric peaks, small peaks can be fitted at their tails because of the non-realistic peak shape function. Therefore, it is necessary to introduce a criteria on which identifies a singlet, which has been fitted with two or more peaks.

In this programme, the criteria on was set by visual means as will be ~~mentioned~~ discussed in Appendix 2. Some weak lines which lie on the tails of intense peaks were rejected using this criteria on, and the peak position and intensity of the singlet were corrected.

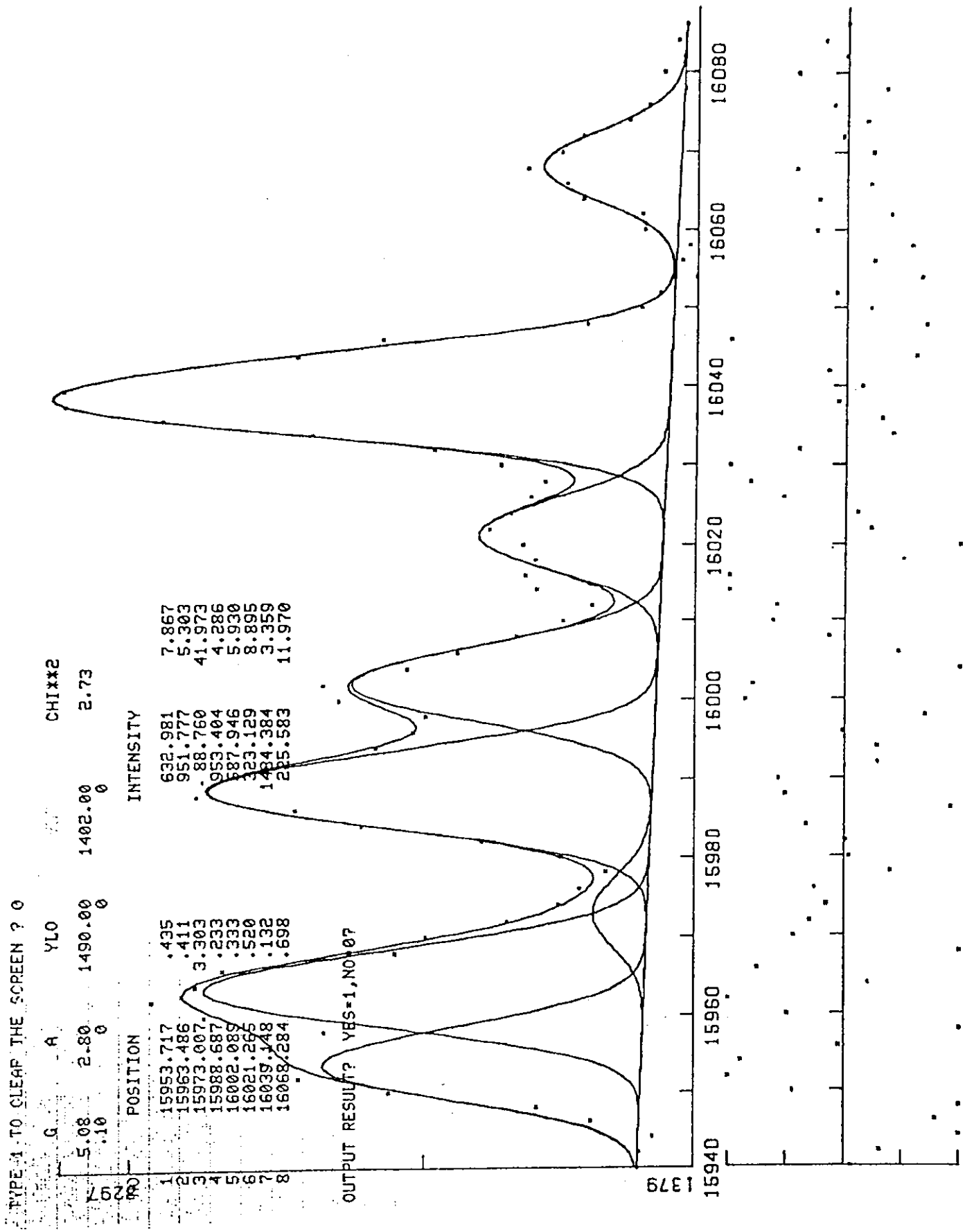

Fig. 7. Example of FITPIC Graphic Output

2.2.6.4. COMPILE

It is easily understood that an intense peak of an order of reflection can interfere with the countings of the other orders, with the current GAMS system, by creating additional spurious peaks.

If an intense peak is scanned in the second order of reflection, the Compton scattering of the gamma-ray in the NaI(Tl) detector will create lower energy back-ground, which falls in the first order discriminator window. This gives a rise in the first order count at the same fringe number where the true intense peak is observed in the second order, and makes a false peak with almost the same peak shape. This is known as 'Compton peak'.

In addition to this, there is a finite probability of detecting accidental coincidence counts of pair of the gamma-rays or the gamma-ray and a Compton back-ground pulse. They fall in the fourth order and the third order discriminator windows, respectively, making spurious peaks with slightly narrower peak width. This is known as 'Pile-up peak'.

These effects are caused when an intense gamma-ray is observed not only at the second order of reflection but also at any order. Therefore, if two or more peaks are found at the same fringe number within a reasonable width, their intensities must be compared each other and it has to be decided whether or not they are spurious.

2.2.6.5. GAMS23

The fitted data of GAMS 2 and GAMS 3 are combined to make $\theta_2 + \theta_3$, practically the corresponding sum of peak position fringe numbers, and peak intensities are summed. The peak to peak correspondence has to be found by comparing their intensities and peak positions.

10% systematic intensity error was added quadratically to each

intensity error before the summing.

2.2.6.6. INT1, INT23

In order to compare the exact values of the parameters of the interferometric functions which have been described above, a set of the strong gamma-lines which are found at several orders of reflection has to be chosen for each of INT1 and INT23.

For the GAMS 1, 22 transitions measured in a total of 76 reflections were used in the calculation INT1. The fringe number correction factor (of the control crystal position) was obtained so that the chi-squares can be minimized. For the GAMS 2/3, 14 transitions measured in 51 reflections were used in the calculation INT23.

In both of the calculation INT1 and INT23, a systematic fringe number error of 0.2 was quadratically added to each calibration line.

2.2.6.7. ENEFTS, FINAL

Finally, energies and intensities of all the peaks are calculated and averaged if a gamma-ray has been found in several orders of reflections. The most intense decay line of 657.7622keV was used as a reference energy[34]. Absolute energies can be calculated from the lattice constant of the crystal and the Miller indices. However, this may give some additional systematic errors due to the errors of the lattice constant, Plank's constant, speed of light etc., and absolute energies are not necessary to construct a level scheme according to the Ritz combination principle.

Using the interferometric functions obtained with the programmes INT1 and INT23, peak energies were calculated and they were sorted out by the two-way balanced merge and sort method in descending order of energy. Gamma-lines with approximately the same energies and intensities within a certain error are considered as an identical transition. This

grouping has to be examined very carefully line by line, and some peaks may be deleted if necessary. The final result is obtained by taking averages of energies and intensities after a systematic error addition and the self-absorption correction.

Since the errors of the interferometric function parameters were not included in the calculation input, the same systematic error of fringe number 0.2 as used in the INT calculation was again added quadratically to each peak position error.

The intensity efficiency curves for all orders of reflection have been well established semi-empirically using the energy dependence of the crystal reflectivity and the efficiency of the NaI(Tl) detector. However, the self-absorption correction gives a large uncertainty in gamma-ray intensities, because the average path length of gamma-rays in the target cannot be defined due to the imperfect flatness and the continuous movement of the target during the measurement. Therefore, a reduced target density of $9.0 g/cm^3$ was used instead of the correct density $10.5 g/cm^3$ to calculate attenuation coefficients with the narrow beam total photon cross sections given by Storm and Israel[35], since this value showed the best agreement above 200keV with the intensities which were calculated by alternative efficiency curves based on a Ge(Li) detector anti-Compton measurement carried out at the University of London Reactor Centre. Since a thin target was used in this measurement, the self-absorption correction is included in the efficiency curves. However, the detection efficiency of the anti-Compton system below 100keV was not well known, therefore, the self-absorption with the reduced target density was preferred.

Further, 15% systematic intensity error was quadratically added to GAMS 1 peaks and 10% to GAMS 2/3 peaks.

2.2.6.8. LIST12, CAL, CAL1, GAMS123

Two sets of independent peak data have been obtained by GAMS 1 and GAMS 2/3. Since there is certain deviation in their energy calibrations and efficiency data, identical gamma-rays in the overlapping energy range are listed by LIST12, and using these corresponding gamma-rays the energies and intensities of GAMS 1 are normalized to those of GAMS 2/3.

Finally, in GAMS123 these gamma-ray energies and intensities are averaged.

2.2.7. Absolute Intensity Calibration

In order to determine absolute gamma-ray intensities, the decay line 657.76keV was used as a reference. The number of the decay gamma-ray emitted per 100 neutron captures in ^{110}Ag was calculated to be 4.27 ± 0.26, assuming that the neutron cross section leading to the ground state σ_g is 89 barns, cross section leading to the isomeric state σ_m 4.5 barns[36], ground state half-life $\tau_{\frac{1}{2}g}$ 24.6 sec, isomeric state half-life $\tau_{\frac{1}{2}m}$ 249.9 days, emission probability of the decay line from the ground state b_g 4.49%, emission probability from the isomeric state b_m 94.74% [37] and the thermal neutron flux $5.5 \times 10^{14} ncm^{-2} sec^{-1}$.

In fact, the decay from the isomeric state does not contribute very much to the intensity as shown in Fig. 8. The contribution is approximately 3% of the ground state contribution after 10-day irradiation. Further, the increase of the isomeric state contribution with time compensates for the decrease of the ground state contribution after the saturation. Therefore, the total intensity of the decay gamma-ray can be considered as the saturation intensity of the ground state contribution and the decay from the isomeric state can be neglected.

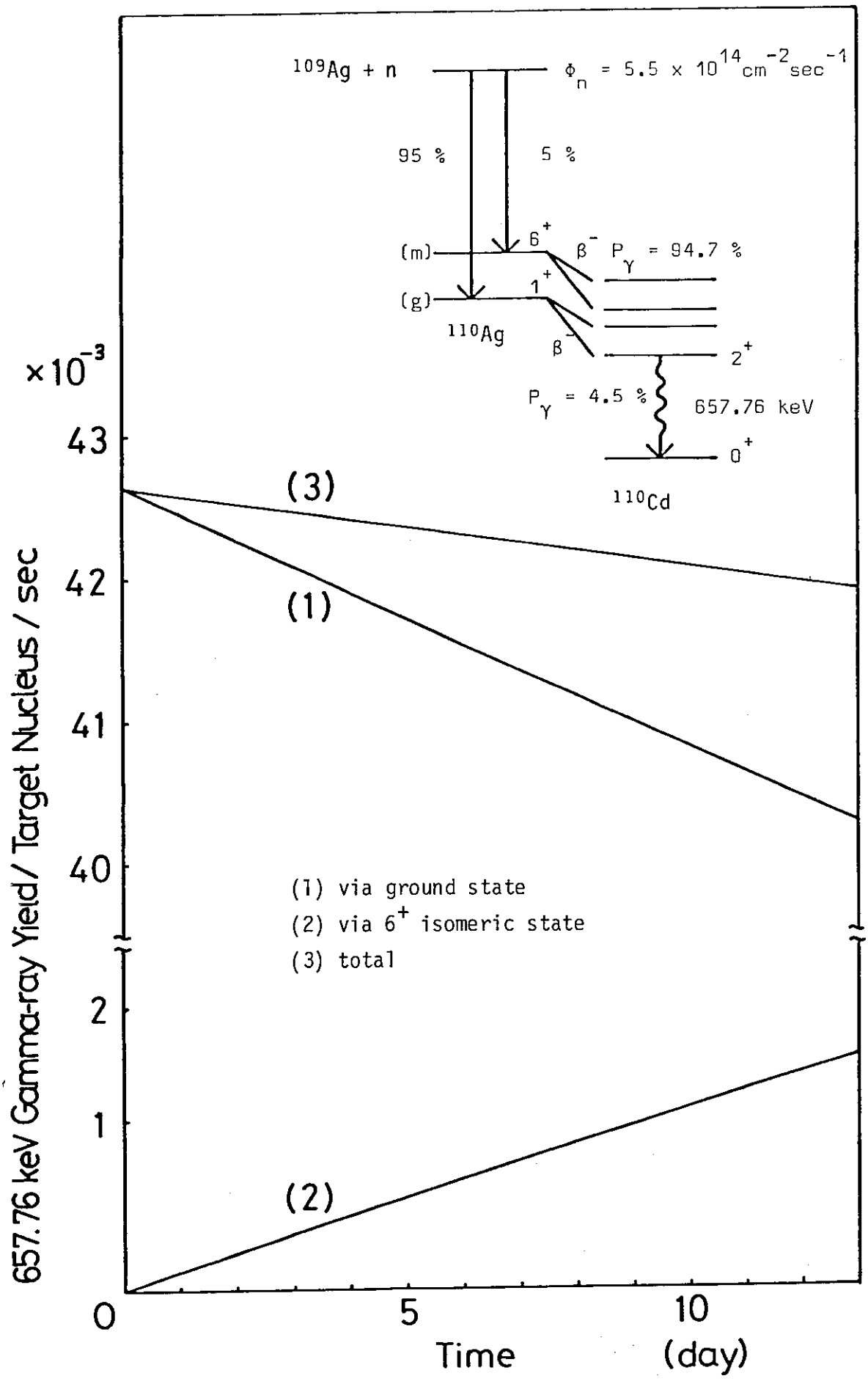

Fig. 8. Yield of 657.76 keV Decay Line in ^{110}Cd

2.2.8. Combination of Grenoble Data and Risø Data

Finally, the Risø data were normalized to the Grenoble data and both were combined ~~at~~ in the low energy region up to 467keV, above which energy the Risø data have been ignored. ~~as well as GAMS 1 result.~~ This averaging procedure was done using the same routines used in the averaging of GAMS 1 and GAMS 2/3 data. (LIST12, CAL, CAL1, GAMS123)

2.3. Measurement of High Energy Gamma-Transitions

High energy primary gamma-rays are of particular interest and importance in the neutron capture process. Level energies of low-lying excited states will be given by the differences between the primary gamma transition energies and the neutron binding energy plus neutron incident energy, which is negligible in the case of thermal neutron capture. This is the only direct information of level energies in neutron capture gamma-ray spectroscopy. In addition to this, the intensities of primary gamma-rays may identify the characteristics of low-lying states such as spins and parities, especially in the case of average resonance capture. Therefore, the earlier theoretical studies were devoted ~~in~~ to the primary gamma-ray emission process as mentioned before.

Since a common target is used in the pair spectrometer 'PN4' with the 'GAMS' system described before, at the High Flux Reactor in Grenoble, simultaneous measurement of the high energy gamma-rays in the reaction $^{109}Ag(n,\gamma)^{110}Ag$ has been carried out. An attempt was made to observe double neutron capture in ^{109}Ag via ^{110m}Ag leading to ^{111}Ag by examining the gamma-ray energy region between the neutron binding energies of ^{110}Ag and ^{111}Ag.

2.3.1. Instrument

The detector system is situated at the back of the GAMS1 spectrometer, and the gamma-rays penetrating the GAMS 1 crystals are observed. Therefore, the gamma-ray beam is not available while the GAMS 1 is scanning low Bragg angle reflections, in which the NaI(Tl) detector lead shielding prevents the beam from going further.

The instrument consists of a planar Ge(Li) detector with its active volume of $7cm^3$ placed between two 6"ϕ x 4" NaI(Tl) scintillation detectors. The associated electronics are made of some NIM units in order to obtain good fast coincidences between double escape peaks and two annihilation gamma-rays emitted in oposite directions. Complete suppression of photo and single escape events can be achieved and optimum energy resolution has been reported as 2.3keV at E_γ = 2.3MeV and 5.5keV at E_γ = 7.6MeV [38].

2.3.2. Data Acquisition

The amplifier gain was set to cover the energy range up to 9.5MeV gamma-ray energy with an 8K multi-channel analyser. The data were dumped on to a magnetic tape every three hours in case there is any ADC channel shifts.

In order to reduce too strong activity a lead attenuator of 2.45cm thick was placed at the back of the beam collimator behind the GAMS 1 spectrometer.

2.3.3. Data Evaluation

Data evaluation has been done following the flow-chart shown in Fig. 9.

2.3.3.1. FITPIC, LINTP

Since there was no significant channel shift, all the spectra measured for 130 hours at the end of a 12-day irradiation were summed.

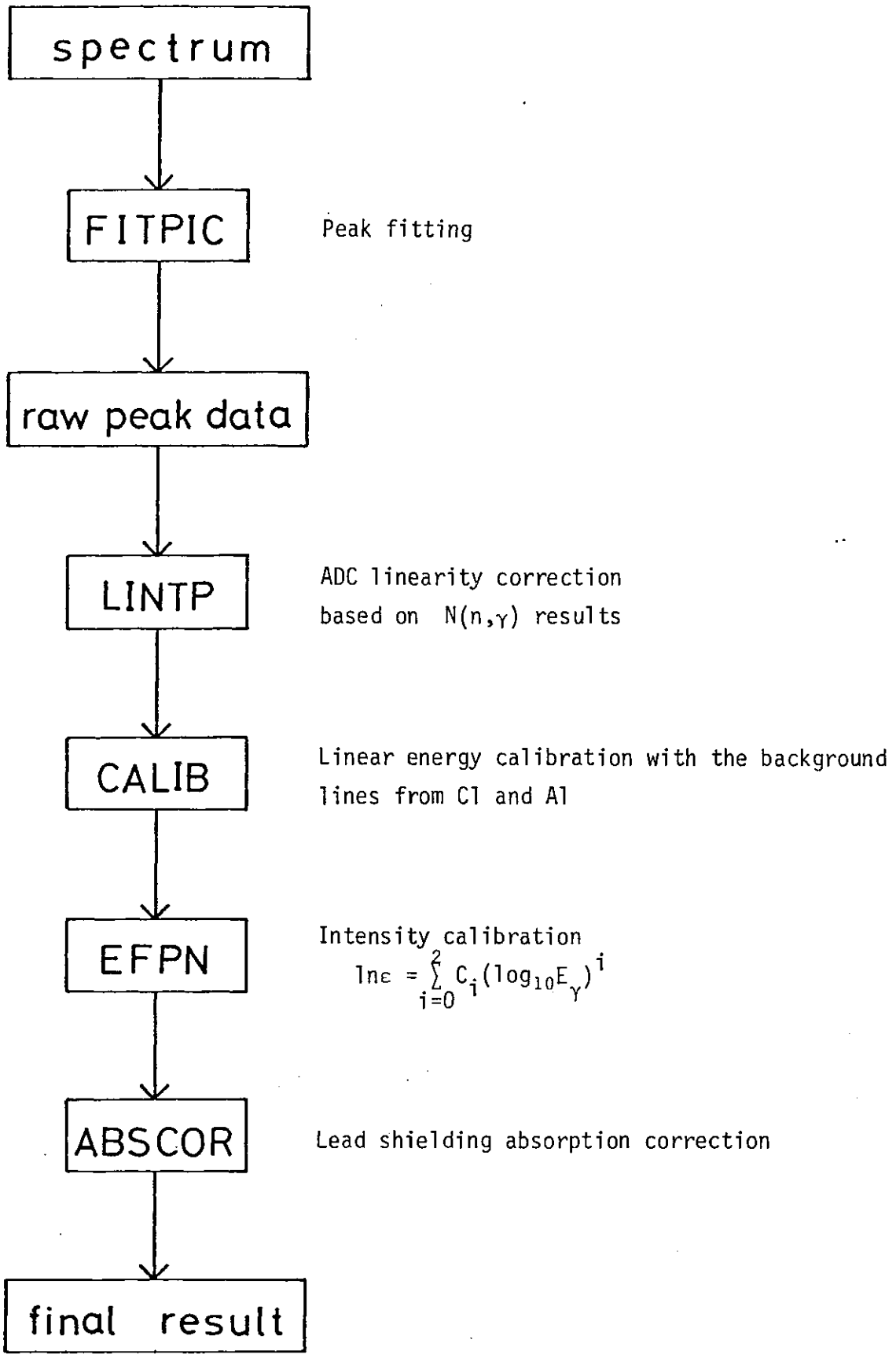

Fig. 9. Data Evaluation Flow for PN4 pair spectrometer

The peak shape was fitted by a Gaussian form with linear back-ground using the computer programme FITPIC described earlier.

It is known that there is a certain non-linearity in the ADC of the spectrometer. This has been investigated in routine measurements by Hofmyer and Tokunaga[39] as shown in Fig. 10. This correction was made after the peak fitting.

2.3.3.2. CALIB

Energy calibration was done using some back-ground peaks originating from neutron capture in aluminium and chlorine, whose energies were taken from the measurements by Stelts and Chrien[40]. These calibration data used are listed in Table 2. Some strong peaks have not been used, because contaminations from other isotopes or ^{110}Ag were suspected. e.g. 6111keV Cl peak, 4946keV C peak etc.

Further linearity correction was made by dividing the calibration data into several regions resulting in a zig-zag calibration line.

This programme CALIB is a simple linear fitting routine including errors of two dimensions equally. The minimization function S is expressed by

$$S = \sum_i \frac{\{y_i - (ax_i + b)\}^2}{(a\Delta x_i)^2 + (\Delta y_i)^2}$$

where $x_i \pm \Delta x_i$, $y_i \pm \Delta y_i$ are experimental data and calibration data, respectively, and a and b are parameters to be optimized.

2.3.3.3. EFPN

The intensity calibration has been done using the efficiency curve of the spectrometer which has been established as shown in Fig. 11 [39]. The efficiency fitting function has the form

$$\ln\varepsilon = \sum_{i=0}^{2} C_i (\log_{10} E_\gamma(\mathrm{keV}))^i$$

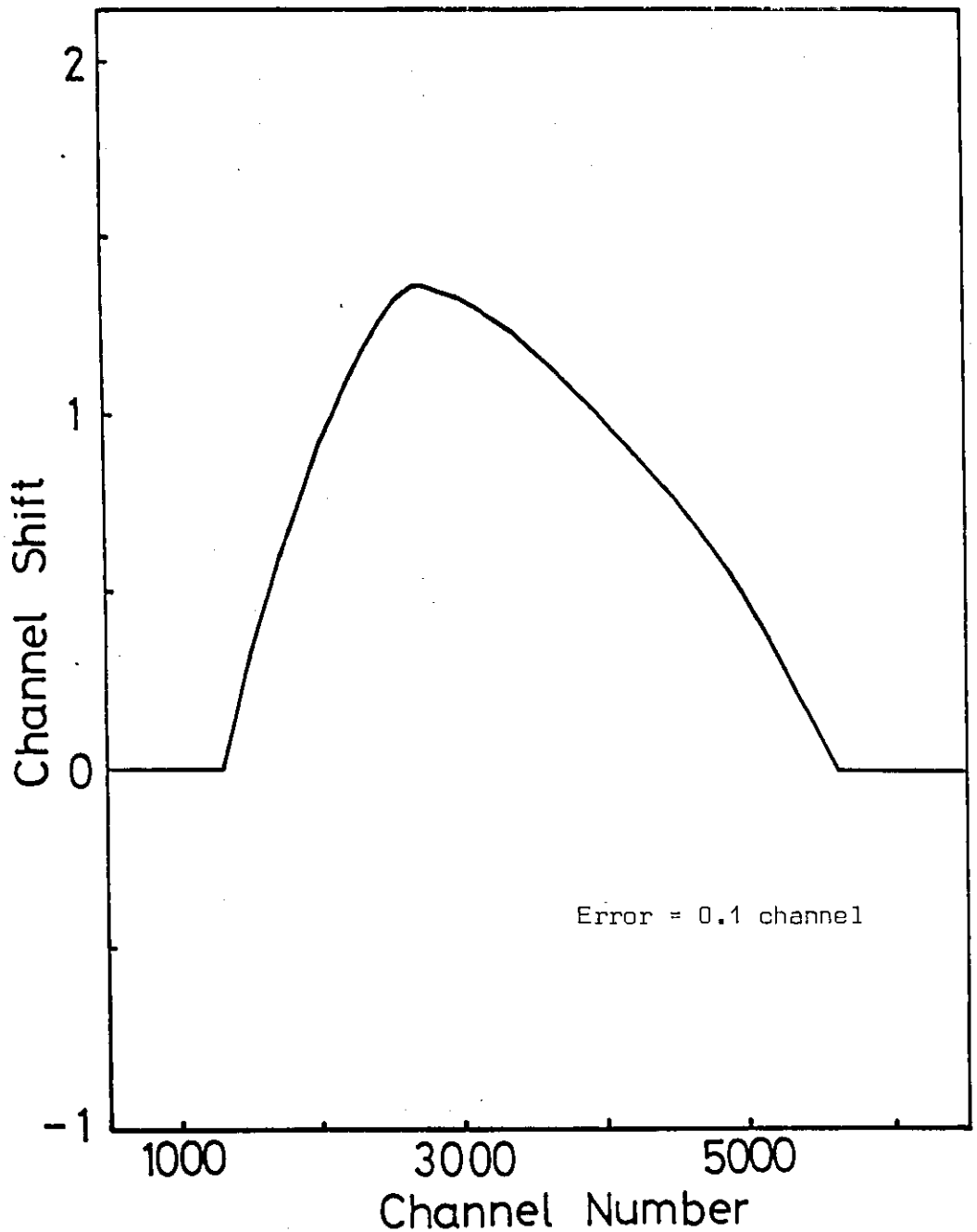

Fig. 10. ADC Non-linearity of PN4 spectrometer

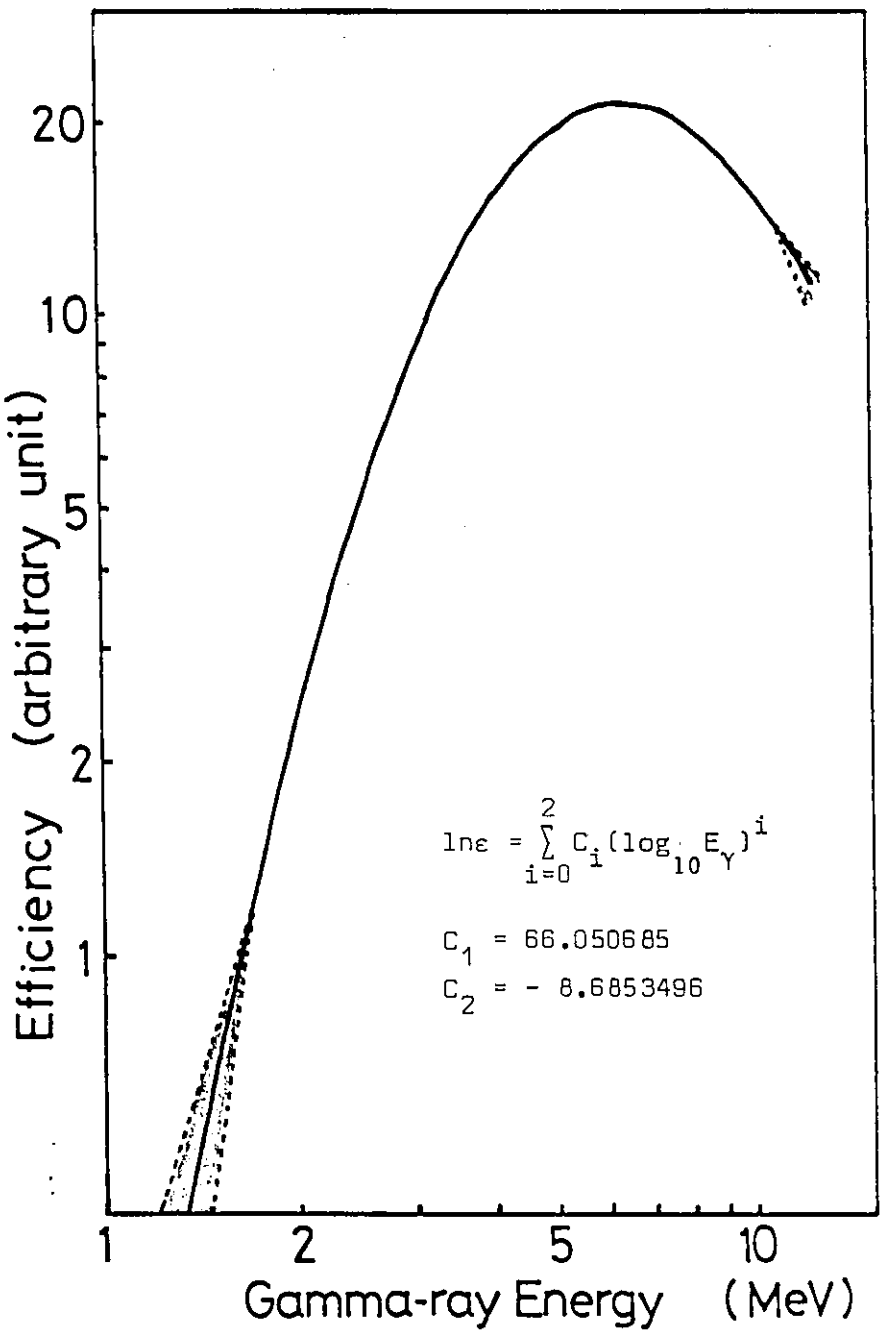

Fig. 11. Relative Efficiency of PN4 spectrometer

Table 2. Energy Calibration Lines for PN4 Pair Spectrometer

CHANNEL NO. (a)	ERROR	ENERGY(IN) (b)	ERROR		ENERGY(CAL) (c)	ERROR	DEV	D/E
514.4018	.0350	1778.7900	.0800	Al	1778.9236	.0834	-.1336	-1.16
1040.4893	.3400	2282.6800	.1000	Al	2282.1726	.3324	.5074	1.46
1361.7249	.2870	2590.1500	.1000	Al	2589.4627	.2819	.6873	2.30
1604.3660	.1920	2821.3900	.1000	Al	2821.5703	.1934	-.1803	-.83
1749.4700	.0680	2959.9300	.1000	Al	2960.3751	.0877	-.4451	-3.35
1826.3979	.1910	3033.8000	.1000	Al	3033.9634	.1917	-.1634	-.76
2276.9353	.4690	3465.0400	.1000	Al	3464.9421	.4517	.0979	.21
2408.6307	.1060	3591.1700	.1000	Al	3590.9204	.1136	.2496	1.65
2677.6696	.2170	3849.1200	.1000	Al	3848.2798	.2132	.8402	3.57
2975.1603	.1180	4133.4200	.1000	Al	4132.8558	.1220	.5642	3.58
3107.9120	.0920	4259.6100	.1000	Al	4259.8445	.0991	-.2345	-1.67
3603.4468	.1160	4734.0100	.1000	Al	4733.8672	.1191	.1428	.92
3779.8591	.1330	4903.0900	.1000	Al	4902.6211	.1343	.4689	2.80
5257.3384	.1170	6315.9700	.1000	Al	6315.9602	.1223	.0098	.06
5669.7943	.1310	6710.5600	.1000	Al	6710.5106	.1362	.0494	.29
6697.2223	.0850	7693.2000	.1000	Al	7693.3360	.1051	-.1360	-.94
6729.1531	.0480	7723.8800	.1000	Al	7723.8806	.0813	-.0006	-.00
5574.9526	.1570	6619.7600	.1000	Cl	6619.7862	.1591	-.0262	-.14
5583.4254	.2900	6627.9500	.1100	Cl	6627.8911	.2823	.0589	.19
5949.2019	.2480	6977.8500	.1000	Cl	6977.7886	.2439	.0614	.23
6405.3576	.0930	7414.0100	.1000	Cl	7414.1417	.1088	-.1317	-.89
6798.8676	.1010	7790.4000	.1000	Cl	7790.5687	.1182	-.1687	-1.09
7622.6536	.2070	8578.6500	.1000	Cl	8578.5926	.2137	.0574	.24

Comments (a) Peak positions (with ADC linearity correction)

(b) Energy calibration data (ref. 40)

(c) Linear energy calibration (CALIB)

where C_i are constants and E_γ is the full gamma-ray energy in keV. C_i have been obtained as C_o = arbitrary constant, C_1 = 66.050685 and C_2 = -8.6853496.

2.3.3.4. ABSCOR

Since a lead absorber was used in the measurement, the absorption in the lead must be taken into account. The attenuation coefficients have been taken from ref. 41, and values between the listed energies have been calculated by log-log interpolation.

The intensity conversion factor to calculate absolute intensities has been obtained using some strong lines at the overlapping region with the GAMS measurement. Since the detection efficiencies of the GAMS and PN4 spectrometers are very low at this gamma-ray energy region 1.3MeV ∿ 1.8MeV, this normalization may include a large systematic error.

CHAPTER 3.

LEVEL SCHEME CONSTRUCTION

In thermal neutron capture reactions, a considerable number of gamma-transitions and internal conversion electrons can be observed in the energy range up to the neutron binding energy. This shows that the capture state (if it exists) decays down to the ground state in several steps of electromagnetic transitions. This cascade of ~~the~~ electromagnetic transitions enables us to construct low-lying nuclear excited levels according to the Ritz combination principle and the Kirchhoff law within a reasonable uncertainty as described earlier. Additional experimental data are utilized in order to assign the spin and parity of each level.

Since many data are handled in the procedure, the analysis may be carried out with the aid of computers. A series of computer programmes ~~have~~ has been created in order to facilitate systematic compilation of the neutron capture data into a detailed level scheme[40]. The Ritz combination principle has been widely applied to the programmes for different purposes. The programmes and their I/O media are listed in Table 3. The actual analysis is carried out, following the flow chart shown in Fig. 12.

Some of the programmes will be discussed here, and the application of them will be shown in the next chapter.

3.1. Programme LEVELS

Each gamma-ray energy is compared with all the differences between two of the known level energies. Practically, the deviation $D = E_\gamma - (E_i - E_f)$ is compared with its quadratically summed error σ.

$$\sigma = \sqrt{(\Delta E_\gamma)^2 + (\Delta E_i)^2 + (\Delta E_f)^2}$$

PROGRAMME	INPUT	OUTPUT
LEVELS (LVLS)	Transition assignment Level energies	Gamma-ray energy fitting result printed
LEVELSØ	Gamma-ray data Preliminary level energies	Preliminary transition assignment file created
LEVELS1 LEVELS2 LEVELS3	Transition assignment	Level energy calculation
LEVELS4	Transition assignment Level energies	Gamma-ray energy fitting varying a new level energy
LEVELS5	Transition assignment Level energies Coincidence data Expected coinc. data	Comparison between level scheme and experiment, Possible new levels printed
LEVELS6 LEVELS7 LEVELS9	Transition assignment Level energies	Gamma-ray energy fitting with new levels based on the Ritz combination
LEVELS8	Transition assignment Level energies Primary assignment	Level scheme drawn on KINGMATIC/MICROFILM
TABLE HAGER	Electron data Gamma-ray data Hager-Seltzer data	Preliminary electron assignment file created
MPFILE	Electron assignment Transition assignment Hager-Seltzer data	Multipolarity assignment file created
PRIM	Primary gamma-ray data	Calculation of final level energies
BINDING	Primary gamma-ray data Level energies	Binding energy calculation Primary assignment file created
INFORM	All assignment files Level energies	Calculation of branching ratios and expected coincidence strengths

Table 3. I/O Media of Computer Programmes

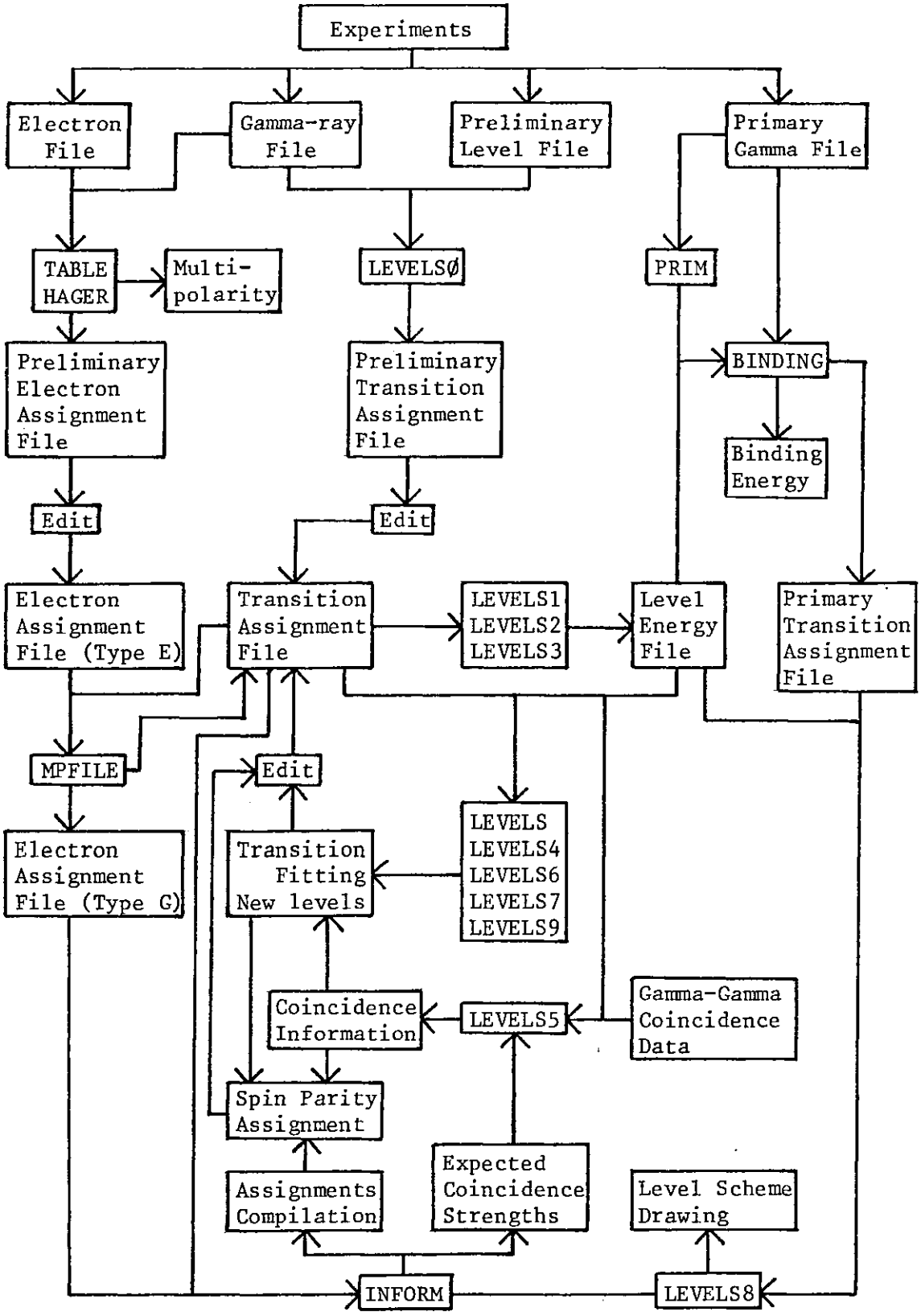

Fig. 12. Analysis Flow in Level Scheme Construction

where E_γ: gamma-ray energy

E_i: initial level energy

E_f: final level energy

ΔE: errors

Results will be listed if the fitting is accepted within a certain confidence limit, i.e. $|D| < \sigma \cdot S$, where the factor S is chosen appropriately.

All the possible fits are sorted out in different ways and the following lists are made with the result of fitting calculation.

1) for each gamma-ray
2) depopulating gamma-rays from each level
3) populating gamma-rays to each level

Since a particular gamma-ray energy can be fitted at more than one place occasionally, the output lists are designed so that this multiple assignment can be easily recognized. Obviously in most cases, the gamma-rays which have already been assigned are fitted at the corresponding positions. However, a few changes in a level scheme may cause some shifts of level energies, therefore, this programme is essential to be run whenever the level energies are modified or a new level is investigated.

Needless to say, the fitting result suggests only the possibility of gamma-ray assignment between the corresponding levels, but incorrect assignments may be excluded. A great care must be taken for a final decision, referring to other information such as gamma-ray intensities, gamma-gamma coincidence results, transition multipolarities, spins and parities of levels and so on.

This programme does not do any level energy corrections,which must be done by the programmes 'LEVELS 1', 'LEVELS2' or 'LEVELS3'. A shorter version of the programme 'LVLS', which has achieved shorter CPU time by the use of binary searching method, is available in a time-sharing mode.

3.2. Programme LEVELS3

The method adopted in this programme to calculate level energies with assigned transitions and their energies is a simple averaging technique by introducing the following likelihood function F.

$$F = \exp(-S)$$

$$S(E_1, E_2, \ldots, E_N) = \sum_{\gamma} \frac{(E_i - E_f - E_\gamma)^2}{2(\Delta E_\gamma)^2}$$

where E_1, E_2, ... , E_N are level energies to be calculated. (E_1 to be the ground state level)

E_γ: gamma-transition energy

E_i: initial level energy

E_f: final level energy

ΔE_γ: error of gamma-transition energy

N: number of levels

The summation is taken over all assigned transitions.

From the fact that the level energy of ground state E_1 can be chosen to have any value, usually zero, the function F must have (N - 1) independent variables to be optimized. Therefore, the problem can be considered as the maximization of the likelihood function F in (N - 1) degrees of freedom. Since an excitation energy of a particular level is the energy difference between the level and the ground state, a set of (N - 1) variables X_n can be introduced as

$$X_n = E_{n+1} - E_1 . \qquad (n = 1,2, \ldots , N-1)$$

Then, F may be written as follows :

$$F(E_1, E_2, \ldots , E_N) = F_1(X_1, \ldots, X_{N-1}) = \exp(-S_1)$$

$$S(E_1, E_2, \ldots , E_N) = S_1(X_1, X_2, \ldots , X_{N-1})$$

$$= \sum_{\gamma \text{ ground state transitions}} \frac{(X_{i-1} - E_\gamma)^2}{2(\Delta E_\gamma)^2} + \sum_{\gamma \text{ non-ground state transitions}} \frac{(X_{i-1} - X_{f-1} - E_\gamma)^2}{2(\Delta E_\gamma)^2}$$

$(i, f \neq 1)$

For simplicity, the function S may be written by replacing N - 1 by N, i - 1, by i, f - 1 by f, S_1 by S and F_1 by F without any confusions. Then,

$$S(X_1,X_2,\ldots,X_N) = \sum_{\gamma} \text{gst} \frac{(X_i - E_\gamma)^2}{2(\Delta E_\gamma)^2} + \sum_{\gamma} \text{ngst} \frac{(X_i - X_f - E_\gamma)^2}{2(\Delta E_\gamma)^2}$$

The expectation values $\bar{X}_n$ are given by

$$\bar{X}_n = \frac{\int_v X_n F(X_1,X_2,\ldots,X_N)\, dX_1 dX_2 \ldots dX_N}{\int_v F(X_1,X_2,\ldots,X_N)\, dX_1 dX_2 \ldots dX_N}$$

and also their standard deviations σ_n are given by

$$\sigma_n = \sqrt{\overline{X_n^2} - \bar{X}_n^2}$$

where

$$\overline{X_n^2} = \frac{\int_v X_n^2 F(X_1,X_2,\ldots,X_N)\, dX_1 dX_2 \ldots dX_N}{\int_v F(X_1,X_2,\ldots,X_N)\, dX_1 dX_2 \ldots dX_N}$$

The integrations span over all the space V of the N variables X_1 ..... X_N. The method to calculate these integrals will be ~~mentioned~~ described in Appendix 1.

Level energies have to be calculated by this programme if some corrections are made in a level scheme. Since this programme is an optimization of all the transition assignments, any alteration in a level scheme may lead to certain shifts of level energies.

3.3. Programme LEVELS4

When an unknown level is expected in a small range of excitation energy, this programme can be used. Having set up the range with lower and upper limits, a new level energy is varied step by step between the two limits. For each tentative level energy, gamma-ray energy fitting is made under the condition.

$$E_\gamma - |E_{TL} - E_n| \leq \sigma \cdot S$$

where S: confidence limit — E_γ: gamma-ray energy

E_{TL}: tentative level energy — E_n: known level energy

$\sigma = \sqrt{(\Delta E_\gamma)^2 + (\Delta E_n)^2}$ — ΔE: errors

In addition to the fitting procedure at each step, two values, which should indicate gradual maximum at the most probable tentative level energy, are calculated for populating and depopulating groups of the fitted transitions. These values I are calculated by the following equation;

$$I = \frac{N}{100 \sqrt{\dfrac{\sum_{\gamma} \dfrac{(E_\gamma - |E_{TL} - E_n|)^2}{(\Delta E_\gamma)^2 + (\Delta E_n)^2} + 10^{-4}}{(N-1) \sum_{\gamma} \dfrac{1}{(\Delta E_\gamma)^2 + (\Delta E_n)^2}}}}$$

where N is the number of transitions fitted. The factor (N - 1) is replaced by 1 if N = 1. An additional term 10^{-4} prevents accidental maxima. It is empirically known that the value I shows its maximum approximately 50 to 100 at actual levels.

Other indications can also be considered such as

1) $$I = \sum_{\gamma} \frac{1}{\sigma_\gamma} \exp\{ - \frac{(E_\gamma - |E_{TL} - E_n|)^2}{2 \sigma_\gamma^2} \}$$

2) $$I = 1 - \{ \prod_{\gamma} \{(2S\sigma_\gamma N_i)^{K_i} + W_n(1 - (2S\sigma_\gamma N_i)^{K_i})\}\}^{N/\mu} = 1 - W_{TL}$$

μ: total number of levels in the level scheme less 1,

N_i: transition density at the gamma-ray energy,

K_i: inverse of the number of places where the i-th gamma-ray has been assigned,

W_n: probability of the n-th level to be accidental. [43]

etc.

These alternatives have not been introduced to the programme yet.

3.4. Programme LEVELS5

This programme gives possible new level energies tentatively based on coincidence data using the Ritz combination principle. Sets of coincidence data are necessary to run the programme and their

strengths are compared with expected strengths which can be calculated by the programme INFORM as will be mentioned later.

The programme is made of the following procedures:

1) Find out possible gamma-rays in coincidence within the window widths given. Several gamma-ray combinations may be found in the same coincidence data.

2) Carry out the following examination for each combination.

1. If $E_{\gamma 1}$ and $E_{\gamma 2}$ are both assigned transitions,

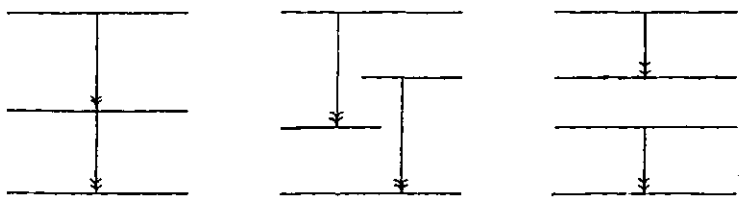

the indications 'COINCIDENT', 'OVERLAP' and 'INDIRECT' will be given in the cases (a), (b) and (c), respectively. In the case (c), the intermediate energy difference is given with its error. In the case (b), obviously no coincidence can be expected. Care must be taken, and the other gamma-ray combinations of the same coincidence data should be examined carefully.

2. If one of the two gamma-rays is assigned, two tentative levels can be considered as shown in the figure provided that the lower one E_{TL2} is not less than zero. If the tentative levels fit one of the known levels, 'GAMMA-FIT' will be indicated.

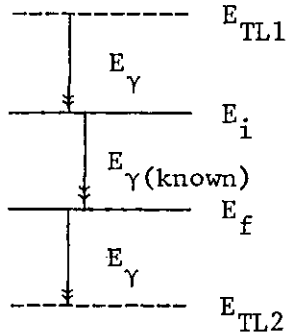

If not, 'TENTATIVE' and expected level energies and their errors will be given.

3. If $E_{\gamma 1}$ and $E_{\gamma 2}$ are both unassigned, the sum of $E_{\gamma 1}$ and $E_{\gamma 2}$ is compared with every level energy difference. If $E_{\gamma 1} + E_{\gamma 2} = E_i - E_f$

within a certain confidence limit, two tentative levels can be considered as shown in the figure. If the tentative level fits one of the known levels, 'SUCCESSIVE' will be indicated. If not, 'TENTATIVE' and the expected level energy and error will be given. The level energy is calculated by weighted average of $E_i - E_{\gamma 1}$ and $E_f + E_{\gamma 2}$ for E_{TL1}, or $E_i - E_{\gamma 2}$ and $E_f + E_{\gamma 1}$ for E_{TL2}.

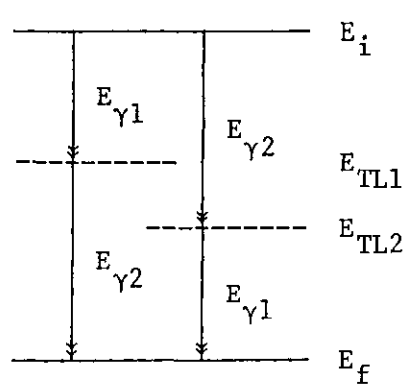

3) Gamma-ray energy fitting will be carried out for each tentative level obtained in the former part of the programme. The procedure is the same as in the programme LEVELS.

Since coincidence data are very important information for the construction of a level scheme, the output of this programme has more reliability than the others based purely on the Ritz combination principle. Therefore, this programme may not be used unless very precise γ-γ coincidence data are available with clearly stated coincidence windows i.e. channel widths or detector resolutions.

3.5. Programmes LEVELS7 and LEVELS9

The programme LEVELS7 searches possible successive transitions between two levels given and calculates tentative level energies. Any number of successive transitions can be chosen, but CPU time increases astronomically as the number increases. Two or three are reasonable to be used with 1000 transition data.

The programme LEVELS9 searches for pairs of gamma-rays such that the energy difference of them can be fitted to the difference of two given levels, and calculates tentative level energies.

These programmes are useful to search for a missing level in a

band structure of nuclear excited states. However, many possibilities can usually be found, so the programmes should not be used until some reliable levels are confirmed.

3.6. Programme LEVELS8

This programme draws a level scheme on 35mm microfilm or on the Kingmatic flat bed plotter at the Imperial College Computer Centre in London. A magnetic tape output is produced by the programme and then it will control the microfilm plotter or the Kingmatic drawing machine off-line. Since the subroutines included in the programme are CALCOMP compatible, it may not be difficult to make the programme available at any other computer centre.

Several remarks have to be mentioned.

1) Arrow widths

The maximum and minimum widths W_{max} and W_{min} are chosen appropriately for the strongest and weakest transitions in the data I_{max} and I_{min}, respectively. For a given intensity I, the arrow width W is calculated logarithmically by the following equation.

$$W = \frac{W_{max} - W_{min}}{\log \frac{I_{max}}{I_{min}}} \log \frac{I}{I_{min}} + W_{min}$$

2) Level heights

If the level scheme has multiplets of levels in a small range of excitation energy, it is impossible to draw them at the positions whose heights from the ground state level should be proportional to their level energies. And there must be enough space to draw level energies and spin and parity assignments between underlines, which are connected to the corresponding levels. Therefore, minimum limit distances must be chosen for minimum gaps between the level energy lines and the level energy underlines according to the size of drawing.

The values y_i to which the level heights are proportional are determined in a subroutine by minimizing $S = \sum_i (x_i - y_i)^2$ under the constraints $y_1 = 0$ and $y_{i+1} - y_i \geq a$, where x_i are level energies and a is one of the minimum lengths converted to energy scale.

Since level scheme diagrams give visual and direct compilation of the transition data, they can be very useful when interpreting characteristics of the nuclear structure, such as collective bands in heavier nuclei, I(I + 1) dependence etc.

3.7. Programmes TABLE and HAGER

In order to determine multipolarities of transitions, the programme TABLE has been made by T. von Egidy to search for electron lines corresponding to known gamma-transitions measured separately and to calculate experimental internal conversion coefficients as well as theoretical values of Hager and Seltzer[43]. Multipolarities can be determined by the comparison between the experimental and theoretical internal conversion coefficients or L-electron intensity ratios.

Since these results are listed in order of transition energy, it is difficult to estimate the intensity ratio if an electron line is doubly assigned. In order to overcome this difficulty, an alternative programme HAGER was made to list expected electron energies and intensities for some multipolarities calculated from experimental gamma-ray data in order of electron energy using the theoretical values of internal conversion coefficients, and experimental electron lines are placed beside corresponding energies.

Both programmes need some intensity calibration lines before their execution to combine electron and gamma-ray intensity data unless the data have been obtained absolutely. The multipolarity of at least one transition has to be assumed to do the calibration.

Details of the intensity calibration of the present work will be shown in the next chapter.

3.8. Programme INFORM

Since many data are involved in the process of level scheme construction, this kind of programme is necessary to compile all the data and to give detailed information of the level scheme and the transitions. The calculation in this programme INFORM includes energy deviations from the Ritz combination principle for each transition assignment, populating and depopulating intensities of each level, gamma-ray branching ratios, neutron binding energy and expected γ-γ coincidence strengths. These are examined very carefully to assign spins and parities of the levels, referring to the other experimental data, which are not included in the programme. Also, wrong transition assignments can be easily identified based on the transition selection rule.

One of the remarkable features of this programme is the calculation of the expected γ-γ coincidence strength S given by

$$S = I_{\gamma 1} B_{\gamma 2} \sum B_{t1} B_{t2} \cdots B_{tN}$$

where $I_{\gamma 1}$: intensity of the gate channel gamma-transition $\gamma 1$,

$B_{\gamma 2}$: depopulating or populating branching ratio of the spectrum channel gamma-transition $\gamma 2$, according to ~~that~~ whether the gate channel gamma-transition $\gamma 1$ is assigned upper or lower than $\gamma 2$, respectively,

B_{ti}: depopulating or populating branching ratios of transitions between $\gamma 1$ and $\gamma 2$.

The summation is taken over every possible combination of the transitions between the two gamma-transitions. If the gate channel gamma-ray is the upper transition, the summation is calculated as follows;

Put the final level of upper transition to be the i-th level and the initial level of lower transition the j-th level. If i = j, it is convenient to assume that the summation A = 1, and if i < j, this is not the case of coincidence, because the two gamma-rays are overlapping. Therefore, the case is limited to i > j. If the summation from the k-th level to the j-th level is expressed by A_{kj}, then $A_{k+1,j}$ will be given by the following equation;

$$A_{k+1,j} = B_{k+1,j} + \sum_{m=j+1}^{k} B_{k+1,m} A_{mj}$$

$$= \sum_{m=j}^{k} B_{k+1,m} A_{mj}$$

where B_{ij} is the depopulating branching ratio of the transition which depopulates the i-th level and populates the j-th level. According to the given equation, A_{ij} can be calculated step by step, using the fact that $A_{j+1,j} = B_{j+1,j}$. If the gate channel gamma-ray is the lower transition, the summation can be calculated in ~~the~~ a similar manner, but using populating branching ratios.

In the current version of the programme, gamma-ray branching ratios $B_{\gamma i}$ are used instead of transition branching ratios B_{ti} due to limited central memory space of computer. Therefore, in the case that an intense low energy transition is involved in the cascade between the two transitions of interest, the expected coincidence strength will be slightly underestimated because of the high internal conversion coefficient of the intense low energy transition.

A detailed discussion will be carried out in Appendix 3. including life-times of levels and angular correlations.

CHAPTER 4.

Application of the Methods and the Results

The computer programmes have been extensively used to process the many experimental data in the thermal neutron capture reactions in ^{107}Ag and ^{109}Ag. Actual procedures, following the flow chart shown in Fig. 12, will be presented in this chapter together with examples of computer output and the results obtained. The sequence of the programmes in the flow chart is a guideline to the level scheme construction and can be modified if necessary.

It has to be emphasized that the programmes are mostly based on the Ritz combination principle due to the good energy resolution of the crystal spectrometer, even though the probability of random fitting increases as energy increases. Therefore, other essential physical principles such as Kirchhoff's law and selection rules of transitions have to be taken into account, referring to the results of other nuclear reactions. Gamma-gamma coincidence data play an especially vital role in the level scheme construction.

4.1. ^{108}Ag

The level scheme construction starts with preliminary level energies suggested in earlier studies. The levels presented by Massoumi [17] were adopted in the current study. The Ritz combination principle can then assign gamma-transitions at one, or occasionally more, appropriate places within a reasonable uncertainty, e.g. twice the standard deviation. All the assignments have to be checked very carefully and some of them may be ignored if the other physical laws are not satisfied.

The primary gamma-rays are also assigned to corresponding low-lying levels. The neutron binding energy can be calculated based on the

assignments. A final calculation has to be done after the low-lying levels are well-established, since some of the primary gamma-ray peaks may be spurious peaks. In the present work, the neutron binding energy of ^{108}Ag has been determined to be 7269.59 ± .60 keV, the error arising mainly from the absolute energy calibration of the primary gamma-ray detector.

The internal conversion electron lines have been assigned to corresponding gamma-transitions and a relevant electron shell has been determined by Massoumi using the programme TABLE. Fig. 13 shows a part of its output. Special attention has to be paid to possible electron multiplets in order not to overestimate internal conversion coefficients. Absolute electron intensities were determined assuming pure E1 multipolarity for the strong 79.1 keV transition normalized to the theoretical internal conversion coefficients of Hager and Seltzer[44]. Multipolarities for other lines can be determined to some extent by comparing the experimental internal conversion coefficients with the theoretical values.

Based on the gamma-ray transition assignments, level energies are recalculated using LEVELS3. This process has to be repeated whenever some transition assignments are altered or a new level is established.

Outputs of INFORM and LEVELS5 give a useful compilation of all the experimental data and the assignments, and can be examined very easily. Parts of the outputs are shown in Figs. 14 and 15. Spins and parities can be determined according to the selection rule and the transition multipolarities obtained. Simultaneously, other experimental results are taken into account in order to establish a more reliable level scheme. The (d,p) reaction data [28] can confirm the existence of levels, and the information of angular momentum transfer is very useful to

N	E-GAMMA KEV	DEG KEV	IG /100N	DIG %	E-ELEC KEV	DEE KEV	IE /100N	DIE %	S	E-TRANS KEV	A-CAP	EA %	THEOR. CONV. COEFF. E1	E2	M1	COMMENTS	
17	113.799	.002	2.439	7	88.287	.002	6.1973	1	K	113.801	.254E+00	7	.964E-01	.717E+00	.255E+00		
					109.999	.006	.7584	6	L1	113.805	.311E-01	9	.953E-02	.663E-01	.293E-01		
18	113.931	.002	.348	7	88.419	.004	.3628	6	K	113.933	.104E+00	9	.960E-01	.715E+00	.254E+00		
19	117.886	.003	7.650	7	92.368	.00216	.8037	2	K	117.882	.220E+00	7	.871E-01	.636E+00	.231E+00		
					114.081	.002	1.8609	1	L1	117.887	.246E-01	7	.865E-02	.591E-01	.266E-01		
					114.348	.011	.1583	23	L2	117.872	.207E-02	24	.760E-03	.373E-01	.161E-02		
					114.548	.011	.1068	14	L3	117.899	.140E-02	15	.111E-02	.444E-01	.459E-03		
					117.173	.003	.3637	2	M1	117.891	.475E-02	7	.161E-02	.109E-01	.500E-02		
					117.312	.018	.0574	22	M2	117.915	.750E-03	23	.149E-03	.747E-02	.322E-03		
20	121.449	.004	.117	10	95.948	.005	.2414	15	K	121.462	.206E+00	18	.801E-01	.575E+00	.213E+00		
21	126.367	.005	.051	12	100.864	.016	.1214	26	K	126.378	.238E+00	28	.715E-01	.502E+00	.190E+00	+ 11(M2)	
					100.864	.016	.1214	26	K	126.378	.238E+00	28	.715E-01	.502E+00	.190E+00	+ 11(M2)	
23	129.232	.003	.198	7	103.718	.004	.3901	3	K	129.232	.197E+00	7	.671E-01	.465E+00	.179E+00		
25	134.473	.004	.123	8	108.953	.003	.2572	10	K	134.467	.209E+00	13	.599E-01	.406E+00	.160E+00		
26	136.243	.004	.195	7	110.710	.012	.0747	22	K	136.224	.383E-01	23	.577E-01	.384E+00	.155E+00		
28	140.895	.005	.048	12	115.383	.025	.0474	32	K	140.897	.987E-01	34	.524E-01	.345E+00	.141E+00		
30	147.349	.003	.822	7	121.834	.002	1.0088	3	K	147.349	.123E+00	7	.461E-01	.296E+00	.125E+00		
					133.555	.011	.1146	14	L1	147.360	.139E-01	15	.467E-02	.284E-01	.144E-01		
32	148.855	.003	.924	7	123.341	.002	1.3276	1	K	148.855	.144E+00	7	.448E-01	.286E+00	.121E+00		
					145.046	.005	.1804	15	L1	148.852	.195E-01	17	.454E-02	.274E-01	.140E-01		
					148.144	.016	.0426	17	M1	148.861	.461E-02	18	.844E-03	.507E-02	.262E-02	+ 46(K)	
					148.144	.016	.0426	17	M1	148.861	.461E-02	18	.844E-03	.507E-02	.262E-02	+ 46(K)	
34	155.450	.003	.672	7	129.933	.002	.7377	4	K	155.447	.110E+00	8	.396E-01	.246E+00	.108E+00		
					151.643	.017	.0876	8	L1	155.449	.130E-01	11	.403E-02	.238E-01	.124E-01		
41	170.058	.003	.402	7	144.543	.003	.3299	2	K	170.057	.821E-01	7	.307E-01	.181E+00	.847E-01		
					166.247	.015	.0578	27	L1	170.053	.144E-01	28	.314E-02	.176E-01	.971E-02		
42	170.615	.006	.021	15	166.808	.013	.1631	13	L1	170.613	.777E+00	20	.311E-02	.175E-01	.963E-02	+ 43(L1)	
43	170.615	.006	.021	15	166.808	.013	.1631	13	L1	170.613	.777E+00	20	.311E-02	.175E-01	.963E-02	+ 42(L1)	
46	173.648	.006	.021	15	148.144	.016	.0426	17	K	173.658	.203E+00	23	.289E-01	.168E+00	.800E-01	+ 32(M1)	
					148.144	.016	.0426	17	K	173.658	.203E+00	23	.289E-01	.168E+00	.800E-01	+ 32(M1)	
47	174.658	.003	.183	7	149.139	.005	.1254	8	K	174.653	.685E-01	11	.285E-01	.165E+00	.788E-01		
48	178.425	.003	1.545	7	152.910	.002	1.0486	0	K	178.424	.679E-01	7	.268E-01	.153E+00	.744E-01		
					174.620	.007	.1171	8	L1	178.426	.758E-02	11	.275E-02	.150E-01	.853E-02		
					174.881	.020	.0495	20	L2	178.404	.320E-02	21	.179E-03	.545E-02	.458E-03	+ 63(K)	
					174.881	.020	.0495	20	L2	178.404	.320E-02	21	.179E-03	.545E-02	.458E-03	+ 63(K)	
50	179.010	.009	.015	25	175.513	.005	.9487	1	L2	179.037	.632E+01	25	.177E-03	.536E-02	.453E-03	+ 64(K)	
52	180.582	.012	.018	25	177.251	.022	.0419	22	L3	180.602	.233E+00	33	.245E-03	.547E-02	.127E-03		
56	190.858	.008	.018	15	187.057	.016	.0750	15	L1	190.862	.417E+00	21	.228E-02	.120E-01	.711E-02	+ 75(K)	
57	192.003	.004	.099	7	166.502	.010	.1226	10	K	192.016	.124E+00	12	.218E-01	.119E+00	.612E-01		
58	192.356	.008	.015	18	166.808	.013	.1631	13	K	192.322	.109E+01	22	.217E-01	.118E+00	.609E-01	+ 42(L1) 43(L1)	
59	193.078	.004	14.970	5	167.559	.006	8.3496	0	K	193.073	.559E-01	5	.214E-01	.117E+00	.603E-01		
					189.274	.008	1.1560	5	L1	193.080	.772E-02	7	.221E-02	.116E-01	.689E-02		
63	200.358	.008	.021	15	172.361	.005	.2019	7	M1	193.078	.135E-02	9	.413E-03	.214E-02	.130E-02		
					174.881	.020	.0495	20	K	200.395	.236E+00	25	.193E-01	.103E+00	.546E-01	+ 48(L2)	
64	201.013	.004	1.752	7	174.881	.020	.0495	20	K	200.395	.236E+00	25	.193E-01	.103E+00	.546E-01	+ 48(L2)	
					175.513	.005	.9487	1	K	201.027	.541E-01	7	.191E-01	.102E+00	.542E-01	+ 50(L2)	
65	201.749	.004	1.839	7	197.228	.009	.1213	5	L1	201.034	.693E-02	8	.198E-02	.101E-01	.618E-02		
					176.243	.004	.9638	1	K	201.757	.524E-01	7	.189E-01	.101E+00	.536E-01		
					197.941	.006	.1160	5	L1	201.747	.631E-02	9	.196E-02	.100E-01	.612E-02		
67	202.507	.006	.036	9	201.785	.008	.0920	8	MT	202.503	.256E+00	12	.418E-03	.308E-02	.122E-02	+ 88(K)	
68	203.290	.004	.271	6	177.772	.006	.1553	5	K	203.286	.573E-01	8	.185E-01	.980E-01	.526E-01		
70	204.428	.004	.024	7	178.911	.006	.2981	16	K	204.425	.478E-01	17	.183E-01	.961E-01	.518E-01		
71	206.608	.003	22.350	7	181.096	.00611	.0311	0	K	206.610	.494E-01	7	.177E-01	.927E-01	.503E-01		
					202.806	.003	1.2871	0	L1	206.612	.576E-02	7	.184E-02	.925E-02	.575E-02		
					203.113	.012	.0765	11	L2	206.637	.342E-03	13	.108E-03	.280E-02	.294E-03		
					205.900	.003	.2820	2	MT	206.617	.126E-02	7	.395E-03	.285E-02	.116E-02		
72	207.310	.004	.336	7	181.826	.004	.1648	3	K	207.340	.491E-01	7	.176E-01	.915E-01	.499E-01		
74	212.310	.003	.618	7	186.802	.004	.2893	5	K	212.316	.468E-01	8	.164E-01	.844E-01	.468E-01		
					208.532	.011	.0533	20	L1	212.338	.863E-02	21	.171E-02	.845E-02	.534E-02		
75	212.553	.004	.101	6	187.057	.015	.0750	15	K	212.571	.739E-01	16	.164E-01	.841E-01	.467E-01	+ 56(L1)	
					211.353	.007	.1946	5	MT	212.570	.192E+00	8	.364E-03	.256E-02	.107E-02	+ 79(L2)	
76	213.049	.004	.420	7	187.541	.004	.1837	9	K	213.055	.437E-01	11	.163E-01	.834E-01	.464E-01		
77	213.410	.005	.078	8	187.927	.015	.0482	13	K	213.441	.618E-01	15	.162E-01	.829E-01	.462E-01		
79	215.383	.003	8.490	7	189.863	.003	6.6440	0	K	215.377	.783E-01	7	.158E-01	.804E-01	.451E-01		
					211.576	.003	.7065	1	L1	215.382	.832E-02	7	.164E-02	.806E-02	.514E-02		
					211.853	.007	.1946	5	L2	215.376	.229E-02	8	.935E-04	.232E-02	.259E-03	+ 75(MT)	
					212.934	.005	.2030	4	L3	215.346	.239E-02	8	.133E-03	.235E-02	.756E-04	+ 80(L2)	
					214.660	.012	.1378	5	MT	215.378	.162E-02	8	.351E-03	.243E-02	.104E-02		

Fig. 13. Example of TABLE Output for ^{108}Ag

NO PRIMARY TRANSITION TO THIS LEVEL

---

(8) 294.5608 (.0018) KEV LEVEL 2+

DEPOPULATING TRANSITIONS

EG	EF	SPIN	TYPE	ET	DET	I	DI	DEV	SIG	DBL	BR(ICC)	DBR(DICC)	MULT.
			G	87.9470	.0050	.120	18.0	-.0022	-.39	1	BR	.16	M1
87.9470	206.6	2+	K	87.9433	.0030	.058	3.8	-.0059	-1.50	1	.486E+00	18.4	M1
			AV	87.9443	.0026	.178	12.2	-.0049	-1.36				
			G	101.4820	.0020	2.202	7.0	-.0040	-1.26	1	16.07	1.42	M1
			K	101.4820	.0015	.725	1.3	-.0040	-1.38	1	.329E+00	7.1	M1
101.4820	193.1	1+	L1	101.4849	.0028	.084	6.2	-.0011	-.29	1	.380E-01	9.4	M1
			L3	101.7840	.1888	.014	62.7	.2980	1.58	1	.630E-02	63.1	M1+E2
			M1	101.4985	.0102	.022	12.1	.0125	1.19	1	.991E-02	14.0	M1+E2
			M2	101.4662	.0162	.012	26.0	-.0198	-1.21	2	.552E-02	26.9	M1+E2
			AV	101.4826	.0011	3.053	5.1	-.0034	-1.27				
			G	294.5670	.0040	10.230	7.0	.0062	1.41	1	74.64	6.58	M1
			K	294.5591	.0034	.214	3.0	-.0017	-.44	1	.209E-01	7.6	M1
294.5670	0	1+	L1	294.5713	.0100	.025	1.7	.0105	1.03	1	.242E-02	7.2	M1
			MT	294.5638	.0180	.005	11.2	.0030	.17	1	.491E-03	13.2	M1
			AV	294.5630	.0025	10.474	6.8	.0022	.71				

TOTAL DEPOPULATING INTENSITY 13.705 (5.3)

POPULATING TRANSITIONS

EG	EI	SPIN	TYPE	ET	DET	I	DI	DEV	SIG	DBL	ICC	DICC	MULT.
			G	113.7990	.0020	2.439	7.0	-.0027	-.81	1			M1
			K	113.8010	.0019	.620	1.1	-.0007	-.21	1	.254E+00	7.1	M1
113.7990	408.4	3+	L1	113.8052	.0062	.076	6.1	.0035	.52	1	.311E-01	9.3	M1
			AV	113.8003	.0013	3.135	5.4	-.0014	-.47				
			G	213.9110	.0050	.060	8.0	-.0056	-.97	1			
213.9110	508.5	2-	G	248.2880	.0050	.348	7.0	.0015	.25	2			M1+E2
248.2880	542.8	2-,3-	K	248.2916	.0072	.012	6.3	.0051	.65	1	.352E-01	9.4	M1+E2
			L2	248.2898	.0425	.002	17.3	.0033	.08	1	.479E-02	18.7	
			AV	248.2892	.0041	.181	55.9	.0027	.52				
			G	269.2530	.0040	.996	7.0	.0011	.22	1			M1
			K	269.2477	.0032	.026	1.2	-.0042	-.97	1	.259E-01	7.1	M1
269.2530	563.8	2+	L1	269.2434	.0193	.003	12.9	-.0085	-.44	1	.314E-02	14.7	M1
			L2	269.2210	.0158	.005	23.7	-.0309	-1.92	2	.483E-02	24.7	
			AV	269.2490	.0024	1.027	6.8	-.0029	-.77				
			G	311.9620	.0050	.231	7.0	-.0091	-1.57	1			E1
311.9620	606.5	1-	K	312.0126	.0529	.001	21.9	.0415	.78	1	.485E-02	23.0	E1
			AV	311.9624	.0050	.232	7.0	-.0087	-1.50				
			G	317.1060	.0050	.936	7.0	.0064	1.06	1			M1,E2
			K	317.0970	.0090	.016	2.1	-.0026	-.27	1	.171E-01	7.3	M1
317.1060	611.7	2+,3+	L1	317.0969	.0199	.002	8.2	-.0027	-.13	1	.249E-02	10.8	E2
			AV	317.1036	.0043	.954	6.9	.0040	.72				
322.3770	616.9	2-	G	322.3770	.0250	.021	18.0	-.0042	-.17	1			
350.9410	645.5	3+,(4+)	G	350.9410	.0060	.465	7.0	.0005	.06	1			
414.3070	708.8	2-	G	414.3070	.0200	.039	12.0	.0257	1.27	1			
485.1700	779.7	2-,3-	G	485.1700	.0400	.054	17.0	.0045	.11	1			
524.6000	819.1	2-	G	524.6000	.0800	.063	30.0	.0712	.89	1			
603.9100	898.4	1-	G	603.9100	.0300	.195	10.0	.0374	1.21	1			
708.1300	1002.6	1+,(2)	G	708.1300	.1800	.054	30.0	.0907	.50	1			
756.9800	1051.7	1+,2-,(3-)	G	756.9800	.2000	.126	40.0	-.1141	-.57	1			

TOTAL POPULATING INTENSITY BY SECONDARY AND PRIMARY TRANSITIONS 7.393 (3.1)

PRIMARY TRANSITION

ENERGY = 6974.74 6974.98 (.10) INTENSITY = .787 (1.7)

---

(9) 324.4964 (.0023) KEV LEVEL 3+

DEPOPULATING TRANSITIONS

EG	EF	SPIN	TYPE	ET	DET	I	DI	DEV	SIG	DBL	BR(ICC)	DBR(DICC)	MULT.
			G	117.8860	.0030	7.650	7.0	.0012	.29	1	78.87	7.04	M1
117.8860	206.6	2+	K	117.8823	.0021	1.680	2.2	-.0025	-.69	1	.220E+00	7.3	M1
			L1	117.8867	.0020	.188	1.8	-.0019	.54	1	.246E-01	7.2	
			L2	117.8715	.0105	.016	23.8	-.0133	-1.22	1	.207E-02	24.8	M1
			L3	117.8987	.0114	.011	14.2	.0139	1.18	1	.140E-02	15.8	M1+E2
			M1	117.8910	.0025	.036	2.5	.0062	1.61	1	.475E-02	7.4	M1
			M2	117.9147	.0176	.006	22.5	.0299	1.68	1	.750E-03	23.6	M1+E2
			AV	117.8863	.0011	9.587	5.6	.0015	.46				
			G	324.4930	.0070	.111	7.0	-.0034	-.46	1	1.14	.10	M1,E2
324.4930	0	1+	K	324.5028	.0395	.002	18.5	.0064	.16	1	.151E-01	19.8	M1
			AV	324.4933	.0069	.113	6.9	-.0031	-.43				

TOTAL DEPOPULATING INTENSITY 9.700 (5.5)

POPULATING TRANSITIONS

EG	EI	SPIN	TYPE	ET	DET	I	DI	DEV	SIG	DBL	ICC	DICC	MULT.
			G	192.3560	.0080	.015	18.0	.0090	1.03	1			M1
192.3560	516.8	3-	G	239.3160	.0040	1.974	7.0	-.0003	-.06	1			
239.3160	563.8	2+	K	239.3204	.0030	.065	2.6	.0041	.93	1	.330E-01	7.5	M1
			L1	239.3269	.0102	.006	4.1	-.0126	1.18	1	.327E-02	8.1	
			MT	239.3023	.0177	.003	24.1	-.0140	-.78	1	.173E-02	25.1	E2
			AV	239.3191	.0023	2.049	6.7	.0028	.69				
			G	274.1730	.0090	.024	12.0	.0017	.17	2			
274.1730	548.7	3-,4-	G	287.1650	.0050	.156	7.0	.0010	.16	1			M1,E2
287.1650	611.7	2+,3+	K	287.1303	.0514	.004	9.3	-.0337	-.65	1	.273E-01	11.6	M1+E2
			AV	287.1647	.0050	.160	6.8	.0007	.11				
			G	292.4310	.0080	.042	9.0	-.0146	-1.67	1			
292.4310	616.9	2-	G	320.9990	.0100	.036	9.0	-.0059	-.53	1			
320.9990	645.5	3+,(4+)	G	332.1580	.0060	.156	7.0	.0023	.30	1			M1,E2
332.1580	656.7	3+,4+	K	332.1427	.0248	.003	10.8	-.0130	-.51	1	.180E-01	12.9	E2
			AV	332.1572	.0058	.159	6.9	.0015	.19				
			G	384.3550	.0090	.159	7.0	.0093	.97	1			
384.3550	708.8	2-	G	533.0000	.0300	.150	9.0	-.0060	-.18	1			M1,E2
533.0000	857.5	2-	K	533.0734	.0852	.001	29.4	.0674	.78	1	.361E-02	30.8	M1,E2
			AV	533.0081	.0283	.151	9.0	.0021	.07				
876.2500	1200.4	<=3+	G	876.2500	.5500	.081	40.0	.3750	.68	1			

TOTAL POPULATING INTENSITY BY SECONDARY AND PRIMARY TRANSITIONS 2.864 (5.0)

NO PRIMARY TRANSITION TO THIS LEVEL

Fig. 14. Example of INFORM Output for ^{108}Ag

```
RESULT
======
                (*) INDICATES AN UNASSIGNED TRANSITION
                (!) INDICATES AN EXPECTED INTERMEDIATE TRANSITION
                (?) INDICATES A  TENTATIVE LEVEL

( 1) COINCIDENCE (   46.43  AND   102.31 )     STRENGTH      .3000E+00

      46.430       101.482      INDIRECT       155.899 ---(  46.430  1.200)---  109.469  (  .00)
                                                294.561 ---( 101.482  2.202)---  193.075  (-1.26)
                                 (STRENGTH)          0
                                 (INTRMDT)      37.1756        .0060                              (!)

      46.430       102.310      INDIRECT       155.899 ---(  46.430  1.200)---  109.469  (  .00)
                                                708.842 ---( 102.310   .882)---  606.532  ( -.05)
                                 (STRENGTH)      .1948
                                 (INTRMDT)     450.6327        .0062                              (!)

      46.430       102.310      INDIRECT       155.899 ---(  46.430  1.200)---  109.469  (  .00)
                                                587.385 ---( 102.310   .882)---  485.075  ( -.06)
                                 (STRENGTH)      .1948
                                 (INTRMDT)     329.1754        .0066                              (!)

      46.430       103.016 (*)  TENTATIVE       258.915 ---( 103.016   .171)---  155.899          (?)
                                                155.899 ---(  46.430  1.200)---  109.469  (  .00)
                                   (LEVEL)     258.9152        .0065                              (?)

                                 TENTATIVE      109.469 ---( 103.016   .171)---    6.453          (?)
                                                155.899 ---(  46.430  1.200)---  109.469  (  .00)
                                   (LEVEL)       6.4532        .0083                              (?)

        STRENGTH RATIO EXPERIMENT/EXPECTED      .7700E+00
=============================================================================================================

( 2) COINCIDENCE (   46.43  AND   113.70 )     STRENGTH      .1020E+01

      46.430       113.593      INDIRECT       155.899 ---(  46.430  1.200)---  109.469  (  .00)
                                                598.668 ---( 113.593  2.817)---  485.075  ( -.02)
                                 (STRENGTH)      .1948
                                 (INTRMDT)     329.1754        .0066                              (!)

      46.430       113.799      INDIRECT       155.899 ---(  46.430  1.200)---  109.469  (  .00)
                                                408.362 ---( 113.799  2.439)---  294.561  ( -.81)
                                 (STRENGTH)          0
                                 (INTRMDT)     138.6616        .0061                              (!)

      46.430       113.931      OVERLAP        155.899 ---(  46.430  1.200)---  109.469  (  .00)
                                                193.075 ---( 113.931   .348)---   79.140  (-1.19)

        STRENGTH RATIO EXPERIMENT/EXPECTED      .5236E+01
=============================================================================================================

( 3) COINCIDENCE (   46.43  AND   174.66 )     STRENGTH      .6600E-01

      46.430       172.625      INDIRECT       155.899 ---(  46.430  1.200)---  109.469  (  .00)
                                                379.242 ---( 172.625   .030)---  206.612  ( -.99)
                                 (STRENGTH)          0
                                 (INTRMDT)      50.7124        .0061                              (!)

      46.430       174.658      INDIRECT       155.899 ---(  46.430  1.200)---  109.469  (  .00)
                                                974.346 ---( 174.658   .183)---  799.689  (  .14)
                                 (STRENGTH)      .1306
                                 (INTRMDT)     643.7898        .0065                              (!)

      46.430       173.648 (*)  TENTATIVE       329.547 ---( 173.648   .021)---  155.899          (?)
                                                155.899 ---(  46.430  1.200)---  109.469  (  .00)
                                   (LEVEL)     329.5472        .0083                              (?)

        STRENGTH RATIO EXPERIMENT/EXPECTED      .5054E+00
=============================================================================================================

( 4) COINCIDENCE (   46.43  AND   201.01 )     STRENGTH      .6300E+00

      46.430       199.870      INDIRECT       155.899 ---(  46.430  1.200)---  109.469  (  .00)
                                                579.111 ---( 199.870   .045)---  379.242  (  .21)
                                 (STRENGTH)          0
                                 (INTRMDT)     223.3431        .0062                              (!)

      46.430       200.358      INDIRECT       155.899 ---(  46.430  1.200)---  109.469  (  .00)
                                                [illegible]
=============================================================================================================

( 8) COINCIDENCE (   46.43  AND   329.18 )     STRENGTH      .1160E+01

      46.430       327.457      INDIRECT       155.899 ---(  46.430  1.200)---  109.469  (  .00)
                                                542.847 ---( 327.457   .177)---  215.384  ( -.89)
                                 (STRENGTH)          0
                                 (INTRMDT)      59.4850        .0062                              (!)

      46.430       329.175      COINCIDENT     155.899 ---(  46.430  1.200)---  109.469  (  .00)
                                                465.075 ---( 329.175  3.450)---  155.899  ( -.05)
                                 (STRENGTH)      .1974

      46.430       326.950 (*)  TENTATIVE       462.849 ---( 326.950   .021)---  155.899          (?)
                                                155.899 ---(  46.430  1.200)---  109.469  (  .00)
                                   (LEVEL)     482.8492        .0189                              (?)

        STRENGTH RATIO EXPERIMENT/EXPECTED      .5876E+01
=============================================================================================================

( 9) COINCIDENCE (   74.60  AND    74.60 )     STRENGTH      .1800E+00

      74.521 (*)   74.521 (*)   ASSIGNMENT      IMPOSSIBLE

      74.521 (*)   74.831 (*)   TENTATIVE      1143.917 ---(  74.521  2.070)---  1069.421  (  .64)  (?)
                                                1069.421 ---(  74.831   .252)---   994.592  (  .13)  (?)
                                   (LEVEL)     1069.4209        .0098                              (?)

                                 TENTATIVE      1143.917 ---(  74.831   .252)---  1069.111  (  .65)  (?)
                                                1069.111 ---(  74.521  2.070)---   994.592  (  .12)  (?)
                                   (LEVEL)     1069.1112        .0090                              (?)
```

Fig. 15. Example of LEVELS5 Output for ^{108}Ag

determine definite parities as well as the range of possible spins. The angular distribution of gamma-rays in the (p,nγ) reaction [29] gives spin assignments of a few low-lying levels. Especially, the results of average resonance neutron capture [22] are very powerful to determine both spins and parities.

As spins and parities are determined level by level, some transitions may be found incorrectly assigned even though they satisfy energy combinations. These transitions have to be removed from the level scheme and new levels have to be searched for so that more transitions can be assigned in the level scheme.

The levels proposed in the present work are listed in Table 4 and the level scheme drawn by LEVELS8 is shown in Fig. 16. The details can be found elsewhere [45].

4.2. ^{110}Ag

Extensive studies of ^{110}Ag have been carried out during past years and have recently been summarized by Bertrand [37]. However, the spins and parities of only the lowest three states, including the ground state, have been determined unambiguously. A few more states have been established since the summary of Bertrand by Bogdanovic et al [25], which is based on the Risø curved-crystal spectrometer data and the time differential gamma-gamma coincidence measurement using Ge(Li) and NaI(Tl) detectors.

In the present work, the level scheme construction was carried out in the same manner as for ^{108}Ag, mainly based on the experimental results presented here. The neutron binding energy of ^{110}Ag has been determined to be 6806.62 ± .20 keV. Absolute electron intensities have been calculated assuming that the 117.6 keV and 118.7 keV transitions are pure

LIST OF LEVELS T4 -(1)

LEVEL (KEV)	ERROR (KEV)	SPIN & PARITY
	(a)	(b)
0	0	1+
79.1402	.0015	2-
109.4692	.0077	6+
155.8992	.0058	5+,6+
193.0748	.0017	1+
206.6116	.0018	2+
215.3842	.0021	3+
294.5608	.0018	2+
324.4964	.0023	3+
338.4188	.0021	3-
364.2389	.0036	4+,(3+)
379.2423	.0022	1-
408.3625	.0020	3+
460.0830	.0050	(2,3,4)-
465.6410	.0031	0-
485.0746	.0031	4-,5-
508.4774	.0022	2-
516.8434	.0026	3-
542.8473	.0026	2-,3-
563.8127	.0023	2+
579.1108	.0048	0-
587.3849	.0030	3-,4-
598.6677	.0029	3-,4-
606.5319	.0023	1-
611.6604	.0029	2+,3+
616.9420	.0026	2-
645.5013	.0045	3+,(4+)
656.3565	.0093	3-,(4-)
656.6521	.0043	3+,4+
679.0949	.0051	1-
700.8712	.0065	3-
703.5887	.0054	2-,3,4-
705.6954	.0053	2-
708.8421	.0023	2-
715.8151	.0042	2-,(1-)
718.7779	.0142	1-,2
765.4676	.0030	2-
779.7263	.0042	2-,3-
799.6890	.0030	2-,3-
803.7325	.0043	2-

LIST OF LEVELS T4 - (2)

LEVEL (KEV)	ERROR (KEV)	SPIN & PARITY
819.0896	.0036	2-
857.5024	.0136	2-
880.6979	.0085	2+
896.4334	.0075	1-
899.9434	.0036	1-
942.3389	.0071	2-,(2+,3-)
959.8503	.0167	2+,(2-,3-)
974.3462	.0036	1-,2-
994.5917	.0088	(1,2,3)-
1002.6001	.0158	1+,(2)
1012.7351	.0049	1-,2
1051.6549	.0146	1+,2-,(3-)
1079.8253	.0122	<=3-
1105.9241	.0191	<=3+
1112.1380	.0138	1+
1137.0763	.0087	
1143.9166	.0380	<=3+
1157.0781	.0069	<=3+
1200.3714	.0153	<=3+
1231.5541	.0185	
1355.4860	.1447	
1462.6400	.1500	

Comments (a) Level energies calculated by LEVELS3

(b) Spin-parity assignments based on several experiments (cf. text)

Table 4. Levels in ^{108}Ag

Fig. 16. ^{108}AG LEVEL SCHEME

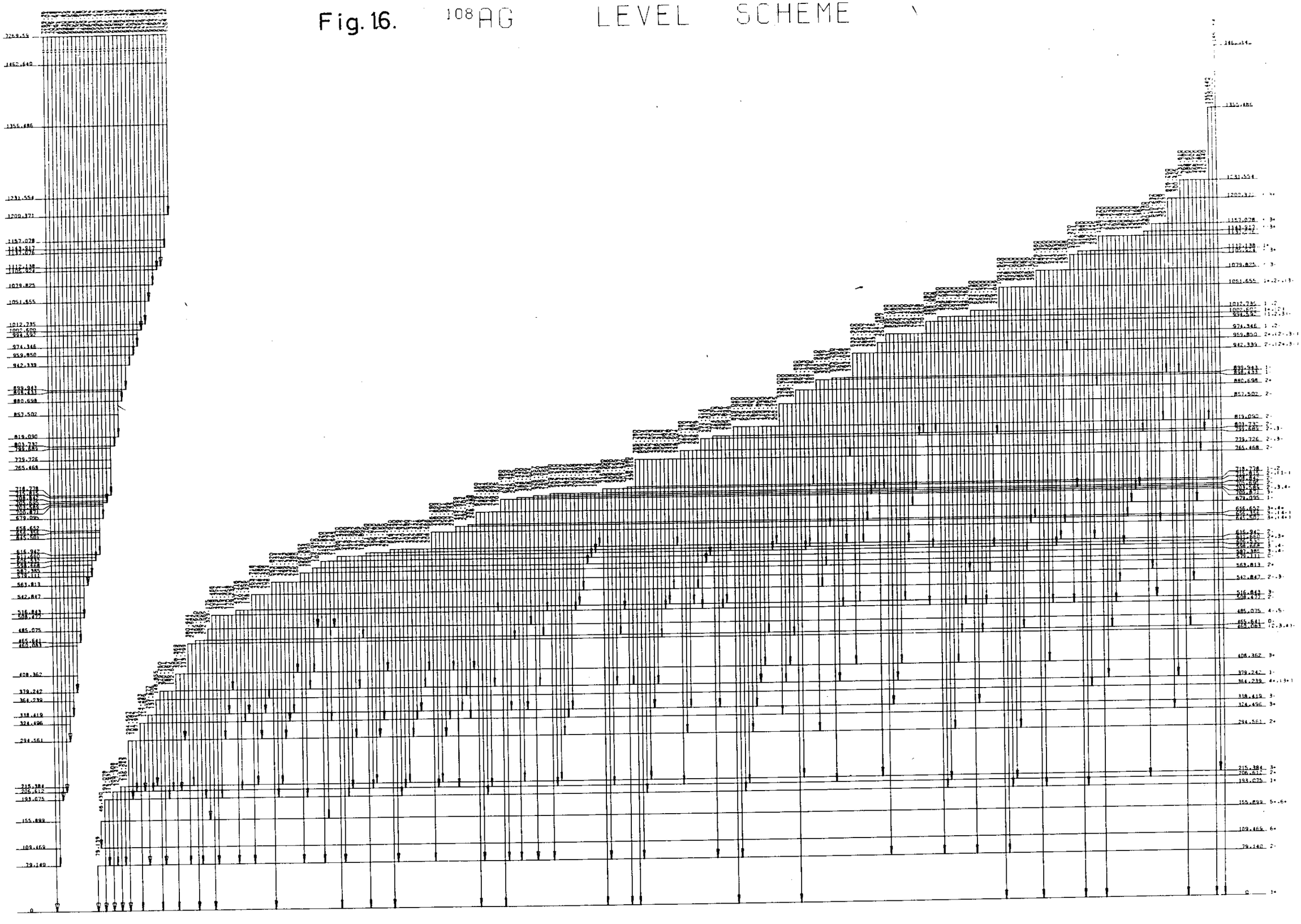

E1 and E2 transitions, respectively [26].

The final level scheme is shown in Fig. 17, which is placed in the back cover pocket, and the details are described in the next section.

4.3. Levels in ^{110}Ag

The details of the transitions in ^{110}Ag are listed in Tables 5, 6, 7 and 8 at the end of this chapter, including the assigned and unassigned gamma-transitions, the internal conversion electron assignments and the high energy gamma-transitions. Some assumptions have been put forward to assign spins and parities.

(1) Thermal neutron capture is restricted to s-wave neutrons and the capture state will be 0^- and/or 1^-.

(2) E1, M1, E2 and E0 transitions can be observed in the present experiment.

The Ground State 1^+

The spin and parity of the ground state has been determined in the earlier studies as 1^+ [37]. This assignment is based on an atomic beam experiment [46] and the allowed β-decay to the ^{110}Cd ground state 0^+ [47]. Other characteristics of the ground state have been investigated during past years, including the half-life 24.6 sec and magnetic moment 2.85 ± 0.05 [48].

1.1 keV Level 2^-

This state has been of interest to explain the M4 isomeric transition from the next 6^+ state. It is necessary to postulate a low-lying 2^- state, since a transition from the 6^+ state to the 1^+ ground state cannot have an M4 character. The earlier neutron capture investigations provided evidence of a low-lying state with 1.28 ± 0.10 keV excitation energy [49]. A hypothesis has been put forward that these two states

are identical and tested by Clark et al [50] using an inner-shell-vacancy detector, which can detect the time of decay although it cannot determine the transition energy. The half-life of the 2^- state was determined in the decay of ^{110m}Ag as 660 ± 40 ns, and the study of the $^{109}Ag(n,\gamma)$ ^{110}Ag reaction gives a consistent result for the low-lying state half-life.

In the present work, one 2^- level was assumed and its excitation energy was determined as 1.1143 ± 0.0011 keV from the gamma-transition energies in the current level scheme using the programme LEVELS3. The result shows that the excitation energy reported in the earlier study was an overestimation probably due to the doublet fitting procedure.

In the (d,p) reaction study [28], this state is populated by $\ell = 2$ angular momentum transfer, which is consistent with the 2^- assignment.

117.5 keV Level 6^+

The 6^+ assignment for this 249-day isomeric state has been determined in the earlier studies by an atomic beam experiment and the allowed β-decay character to an even-parity level in ^{110}Cd [51]. The excitation energy has been reported as 117.76 keV [37] as the combination of the 116.48 ± 0.05 keV M4 transition energy [37] and 1.28 ± 0.10 keV excitation energy of the 2^- level as previously determined [49]. This has now to be corrected to 117.59 ± 0.05 keV.

Although the 5% partial capture cross-section to this isomeric state relative to the total capture cross-section has been reported[36], evidence of the populating transitions to this level is not very strong. In the present work, a cascade of strong transitions which have not been placed in the level scheme was tentatively placed above this level as shown in Fig. 18. This implies the existence of other six tentative levels at 174.5 keV, 255.0 keV, 446.5 keV, 551.3 keV, 557.0 keV and

579.2 keV.

The excitation energy was determined by LEVELS3 calculation as 117.5359 ± 0.0046 keV, mainly based on the transition energies in this cascade. The result does not agree very well with the value 117.59 ± 0.05 keV mentioned above. The isomeric transition has to be studied with better accuracy.

The expected gamma-gamma coincidences are consistent with the experimental data of Winkler[27] except that the experiment was not able to find the coincidence between 57.0 keV and 80.4 keV, which are expected to be in strong coincidence.

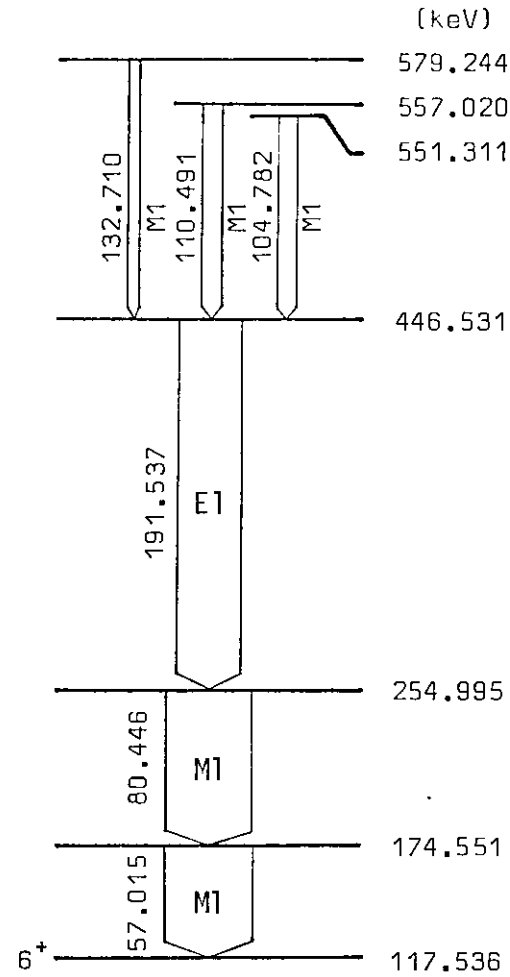

Fig. 18. Cascade Populating 6^+ Isomeric State

118.7 keV Level 3^+

The existence of this level is demonstrated by the existence of depopulating transitions 117.6 keV to the 1.1 keV 2^- state and 118.7 keV ground state transition, which are known to have E1 and E2 character, respectively. The character of these transitions require even parity and the spin has been assigned as 3 in the (p,nγ) experiment based on the 117.6 keV gamma-ray angular distribution [29]. Other experimental data are consistent with the 3^+ assignment.

The half-life has been measured as 36.7 ± 0.7 ns [29]. Since the depopulating 117.6 keV transition is very intense, the time differential gamma-gamma coincidence measurement with this transition[25]

has been used to confirm the existence of upper lying levels.

174.6 keV Level 5^+, 6^+

This level is a ~~totally~~ tentative level based on the assumption that the 57.0 keV transition populates the 6^+ isomeric state. If this state exists, the parity will be even because of the M1 character of the transition. The spin is restricted to 5, 6 or 7, but 7 can be excluded due to the rather strong population.

Apart from the 80.4 keV transition connecting this level with the next member of the cascade populating the 6^+ level, this level can be connected to the other existing levels at 471.2 keV and 613.0 keV by the 296.6 keV and 438.3 keV transitions, respectively. However, these transitions may both be assigned to other places in the level scheme, and there is no strong evidence for this level.

191.6 keV Level 2^+, 3^+, 4^+

The gamma-gamma coincidence between the transitions in the 120 keV and 74 keV regions suggests the existence of this level. However, the existence is rather doubtful since the time differential coincidence measurement has not confirmed the coincidence between the 117.6 keV and 72.9 keV transitions. This level may be suspect also from the fact that the populating intensity is very weak compared with the depopulating intensity although some strong transitions may be assigned to populate this level from levels which have not yet been established.

If this level exists, the M1 character of the 72.9 keV transition will indicate even parity and spin possibilities 2, 3 and 4. No primary transition was observed, but it could have been masked by the 6619 keV background line from chlorine.

The 191.5 keV E1 transition cannot be the ground state transition depopulating this level, because the energy combination and the selec-

tion rule are not satisfied. Therefore, the 191.5 keV gamma-ray angular distribution result in the (p,nγ) reaction cannot be used to assign the spin of this level.

198.7 keV Level 2^+

This level is well established by the two depopulating transitions 198.7 keV and 197.6 keV, which give the same energy difference as the 118.7 keV and 117.6 keV transitions. The M1 character of the 198.7 keV ground state transition determines even parity and spin 0, 1 or 2. Although the multipolarity of the 197.6 keV transition cannot be determined correctly due to the low energy tail of the 198.7 keV intense transition in the electron spectrum, the 0^+ assignment can be ruled out by the existence of the 197.6 keV transition to the 2^- state. .

The (p,nγ) work suggests spin 2 from the angular distribution of the 198.7 keV transition. It is consistent with the fact that a primary transition populates this level.

236.8 keV Level 1^-, 2^-, 3^- and 237.0 keV Level 1^-, 2^-

Population by a primary transition and in the (d,p) reaction with $\ell = 0$ indicates a level at approximately 237 keV. The 237.0 keV level has been established with three depopulating transitions and thirteen populating transitions apart from the primary transition. The 237.0 keV E1 transition to the ground state 1^+ and the 235.9 keV M1 transition to the 1.1 keV 2^- state assign the spin and parity to be 1^- or 2^- for this level.

The additional 236.8 keV level was first introduced by Bogdanovic et al [25] probably based on the coincidence between 236 keV and 195 keV transitions. It is based also on Breitig's precise energy measurement [18] in which the 235.8 keV gamma-ray was found to be a doublet. The Ritz combination principle has assigned twenty transitions populat-

ing this level. The M1 character of the 235.7 keV depopulating transition to the 1.1 keV 2^- state determines odd parity and spin possibilities 1, 2 and 3.

It is difficult to determine whether the primary transition and the (d,p) reaction populate the 236.8 keV level or the 237.0 keV level. Probably a large fraction of the primary transition populates the 237.0 keV level, since the transition energy is fitted to this level better than to the 236.8 keV level. However, both levels are equally possible to be populated in the (d,p) reaction. Spin and parity can be limited to 1^- for both levels if the population with $\ell = 0$ is confirmed.

(248 keV Level)

This level was introduced by the primary transition measurement of Bolotin and Namenson [24]. In the present work, however, this line was not observed.

255.0 keV Level 4^+, 5^+

This is one of the levels introduced as part of the cascade populating the 6^+ isomeric state. The M1 character of the 80.4 keV transition determines even parity but the spin can be 4, 5 or 6. The 6^+ assignment can be excluded by the E1 character of the 191.5 keV populating transition from the 446.5 keV 3^- or 4^- state as will be described when discussing that level.

267.2 keV Level 1^+, (2^+)

This level is well establised by three depopulating transitions 267.2 keV M1 + E2 to the ground state, 266.1 keV E1 to the 1.1 keV 2^- state and 68.5 keV M1 to the 198.7 keV 2^+ state. These define the spin and parity assignment 1^+ or 2^+. The strong primary transition prefers the 1^+ assignment.

271.4 keV Level 2^+, 3^+, (4^+)

The existence of this level is suggested by the time differential coincidence between 117.6 keV and 152.7 keV transitions. The M1 character of the 152.7 keV transition to the 118.7 keV 3^+ state assigns the spin and parity to be 2^+, 3^+ or 4^+. The 4^+ assignment is not ~~die~~favoured if the transitions 393.4 keV from the 664.9 keV 1^- or 2^- state and 454.3 keV from the 725.7 keV 0^-, 1^- or 2^- state exist.

304.5 keV Level 2^+, 3^+

The coincidence between the 105 keV and 199 keV transitions establishes this level. The M1 character of the 105.8 keV transition to the 198.7 keV 2^+ level suggests the spin and parity assignment 1^+, 2^+ or 3^+. If this level is 1^+, the levels at 380.1 keV, 468.8 keV, 471.2 keV, 536.1 keV, 663.4 keV and 683.1 keV will be assigned to be low spin even parity states without primary transition population, which is statistically very unlikely. Therefore, the 1^+ assignment can be excluded.

338.9 keV Level 0^-, (1^-)

The existence of this level is supported by the two depopulating transitions to the ground state and the 1.1 keV 2^- state and by the population in the (d,p) reaction with $\ell = 0$. The E1 character of the 338.9 keV ground state transition assigns the spin and parity 0^-, 1^- or 2^-. The zero angular momentum transfer excludes 2^-. Since no primary transition was observed, the 0^- assignment is preferred.

The 101.8 keV transition may depopulate this level to the 237.0 keV level. However, the energy combination is not satisfied, probably because the error of transition energy may have been underestimated. The coincidence data of Winkler cannot distinguish this coincidence from the indirect coincidence between the 237.2 keV and 105.8 keV

transitions.

360.6 keV Level 1^+, 2^+

This level is depopulated by eight transitions. The E2 character of the ground state transition determines the spin and parity to be 1^+, 2^+ or 3^+. The 123.6 keV and 123.8 keV transitions to the 237.0 keV and 236.8 keV levels, respectively, can exclude the 3^+ assignment, since at least one of these levels is a 1^- state. This is consistent with the existence of a primary transition.

380.1 keV Level 1^+, 2^+, 3^+, (4^+)

This level is based on the assumption that the 75.6 keV and 181.5 keV transitions depopulate this level and populate the 304.5 keV 2^+ or 3^+ state and the 198.7 keV 2^+ state, respectively. Transition assignments are totally based on the energy combination principle. Even parity is expected for this level from the M1 character of the 75.6 keV transition, but the spin cannot be determined uniquely and 1^+ to 4^+ assignments are possible. If the 143.1 keV transition to the 237.0 keV 1^- or 2^- state exists, the 4^+ assignment will be excluded. However, the existence is rather doubtful.

381.2 keV Level 1^-, 2^-

This level is populated by a primary transition and in the (d,p) reaction with $\ell = 2$, and is depopulated by five transitions including the transitions to the ground state and 1.1 keV 2^- state. These five transitions suggest the spin and parity 0^-, 1^- or 2^-. The angular momentum transfer $\ell = 2$ in the (d,p) reaction excludes the 0^- assignment.

424.7 keV Level 0^-, 1^-, (2^-) and 432.3 keV Level 2^-, (3^-)

The (d,p) reaction results suggest a possible doublet at excitation energy 433 keV with $\ell = 2$ and/or $\ell = 0$ angular momentum transfer.

Two corresponding primary transitions have been observed at 6381.8 keV and 6374.1 keV, which require low spin states at 424.6 keV and 432.3 keV. The energy combination principle can establish these levels at 424.7 keV and 432.3 keV each with four depopulating and seven populating transitions.

Although the 423.6 keV transition from the 424.7 keV level to the 1.1 keV 2^- state has been doubly assigned in the present level scheme, if this transition depopulates this level, its M1 or E2 character will determine odd parity and spin possibilities 0 to 4 for this 424.7 keV level. This is consistent with the E2 character of the 187.6 keV transition to the 237.0 keV 1^- or 2^- state. The 3^- and 4^- assignments can be excluded by the existence of a primary transition and ground state transition.

The M1 character of the 195.5 keV transition from the 432.3 keV level to the 236.8 keV requires odd parity and spin possibilities 0 to 4 for this 432.3 keV level. The 0^- and 1^- assignments can be excluded by the existence of the 313.6 keV transition to the 118.7 keV 3^+ state, and the 4^- assignment can be excluded by the primary transition population, ehich prefers the 2^- assignment.

Therefore, both levels are possibly populated in the (d,p) reaction. Probably the 424.7 keV level is populated with $\ell = 0$ and the 432.3 keV level with $\ell = 2$. The 0^- or 1^- assignment is favoured for the 424.7 keV level.

446.5 keV Level 3^-, 4^-

This is one of the levels in the cascade populating the 6^+ isomeric state. The E2 character of the 209.7 keV transition to the 236.8 keV 3^- state and E1 character of the 191.5 keV transition to the 255.0 keV state define the possible spin and parity assignments

3^-, 4^- and 5^-. By the 445.4 keV transition to the 1.1 keV 2^- state, the 5^- assignment can be excluded, and also the 6^+ assignment for the 255.0 keV level can be excluded as has been mentioned. This level may be populated by the (d,p) reaction.

468.8 keV Level 2^+, 3^+

The time differential coincidence between 117.6 keV and 350.1 keV transitions confirms the existence of this level although the energy combination is not satisfied very well. The M1 + E2 character of the 350.1 keV transition to the 118.7 keV 3^+ state and the M1 character of the 270.1 keV transition to the 198.7 keV 2^+ state require the spin and parity assignment 2^+ or 3^+.

It is interesting to note that the 350.1 keV transition can be placed to populate this level from the 818.9 keV level with good energy fitting. This transition may be a doublet, and a large fraction of intensity may belong to the upper transition from the 818.9 keV level.

471.2 keV Level 3^+, 4^+

The existence of this level is confirmed by the coincidence between the 105 keV and 166 keV transitions. Other transitions have been placed by the Ritz combination principle. The M1 character of the 166.7 keV transition to the 304.5 keV 2^+, 3^+ state allows spin and parity 1^+, 2^+, 3^+ or 4^+.

If the 296.6 keV transition, which has been placed twice in the level scheme, depopulates this level to the 174.6 keV 5^+ or 6^+ state, the 1^+ and 2^+ assignments can be excluded. This is consistent with the fact that no primary transition was observed.

485.7 keV Level 1^+, 2^+, 3^+

This level comes from the time differential coincidence between

the 117.6 keV and 367.0 keV transitions. The M1 character of the 125.1 keV transition to the 360.6 keV 1^+ or 2^+ state requires even parity and possible spins 0, 1, 2 and 3. The 0^+ assignment can be excluded by the 367.0 keV transition to the 118.7 keV 3^+ state.

496.8 keV Level 1^-, 2^-

This level is populated by a primary transition, and is depopulated by seven transitions including the transitions to the ground state and the 1.1 keV 2^- state. The M1 character of the 115.7 keV transition to the 381.2 keV 1^- or 2^- state requires spin 0 to 3 and odd parity. The 3^- assignment can be excluded by the 496.8 keV ground state transition. The population in the (d,p) reaction around this energy is not very clear, but the weak population is probably to this level because there ~~is~~ are no other odd parity states in the 484 ± 20 keV excitation energy region. The 0^- assignment can be excluded by the M1 character of the 82.4 keV transition from the 579.2 keV 2^- or 3^- state as will be mentioned when discussing that level.

525.6 keV Level 1^-, 2^-

This level is populated by a primary transition and in the (d,p) reaction of Lopez [52], and is depopulated by six transitions including the transitions to the ground state and the 1.1 keV 2^- state. The M1 or E2 character of the 524.5 keV transition to the 1.1 keV 2^- state requires odd parity and spin 0 to 4. The 3^- and 4^- assignments are excluded by the existence of the 525.6 keV ground state transition. The 0^- assignment is also excluded by the M1 + E2 character of the 101.0 keV and 186.7 keV transitions. The exsistence of the primary transition is consistent with this assignment.

527.5 keV Level 1^+, 2^+, 3^+

This level is suggested by the time differential coincidence

between the 117.6 keV and 408.8 keV transitions. The E1 character of the 526.3 keV transition to the 1.1 keV 2^- state requires the spin and parity assignment to be 1^+, 2^+ or 3^+.

536.1 keV Level 1^+, 2^+, 3^+

This level was originally thought to be present according to the population in the (d,p) reaction. However, the characters of the depopulating transitions, which have been assigned by the energy combination principle, suggest even parity for this level and possible spins 1, 2 and 3. There may be a small contribution of primary transition on the high energy tail of the primary transition to the next level.

539.5 keV Level 0^-, 1^-

This level is populated by a primary transition and in the (d,p) reaction with $\ell = 0$. The spin and parity can be assigned to be 0^-, 1^- or 2^- by the characters of depopulating transitions. The zero angular momentum transfer in the (d,p) reaction can exclude the 2^- assignment. If the 338.9 keV level is a 0^- state, then the 0^- assignment for this level can be excluded by the 200.6 keV transition to the 338.9 keV level.

549.3 keV Level 1^+, 2^+

A primary transition indicates the existence of a level at about 549.5 keV excitation energy. Sixteen populating and six depopulating transitions have been assigned by the energy combination principle. The characters of the depopulating transitions limit the spin and parity assignment to be 1^+, 2^+ or 3^+. The 3^+ assignment can be excluded by the existence of the primary transition.

551.3 keV Level 2^-, 3^-, 4^-

This is one of the levels related to the cascade feeding the 6^+

isomeric state. The M1 character of the 104.8 keV transition to the 446.5 keV 3^- or 4^- state requires odd parity, but the spin cannot be defined uniquely. The assignments 2^-, 3^- and 4^- are possible.

557.0 keV Level 2^-, (3^-)

This is another level which is related to the 6^+ isomeric level. The case is very similar to the 551.3 keV level, but eight depopulating transitions have been assigned by the energy combination principle. The M1 character of the 110.5 keV transition to the 446.5 keV 3^- or 4^- state and the M1 + E2 character of the 175.8 keV transition to the 381.2 keV 1^- or 2^- state limit the spin and parity assignment to 2^- or 3^-.

The existence of the ground state transition may exclude the 3^- assignment. However, this exclusion based on only one transition will result in definite spin assignments for all members of the cascade feeding the 6^+ isomeric level and can be dangerous. The 438.3 keV transition has been placed to populate the 118.7 keV 3^+ state, but no time differential coincidence was observed. This transition assignment is doubtful.

579.2 keV Level 2^-, 3^-

As well as the last two levels, this level is related to the 6^+ isomeric state. The M1 character of the 132.7 keV transition to the 446.5 keV 3^- or 4^- state determines odd parity and spin possibilities 2 to 5. This lower limit of spin 2 and the M1 character of the 82.4 keV transition to the 496.8 keV level can exclude the 0^- assignment for the 496.8 keV level as has been mentioned. This transition can also exclude the 4^- and 5^- assignments for this level.

589.7 keV Level $\leq 3^-$

The existence of this level is suggested by the presence of a

primary transition. The M1 or E2 character of the 588.6 keV transition to the 1.1 keV level requires odd parity and spin possibilities 0 to 4. The 4^- assignment can be excluded by the existence of the primary transition. The population in the (d,p) reaction has been observed at 594 keV with $\ell = 2$ angular momentum transfer. If this level is populated in the reaction, the 0^- assignment can be excluded.

595.0 keV Level 2^-, 3^-

The time differential coincidence between the 117.6 keV and 476.3 keV transitions confirms the existence of this level. The Ritz combination principle can assign only two depopulating transitions, and their M1 or E2 characters are contradictory in the parity assignment for this level. Since the K-elctron line of the 476.3 keV transition cannot be resolved from the 476.1 keV K-electron line, the multipolarity assignment of the 476.3 keV transition is doubtful.

The M1 or E2 character of the 358.1 keV transition to the 236.8 keV 1^-, 2^- or 3^- state requires odd parity and spin possibilities 0 to 5. The 0^-, 1^- and 5^- assignments can be excluded by the existence of the 476.3 keV transition to the 118.7 keV 3^+ state. The 4^- assignment can be excluded by the M1 character of the 38.4 keV transition from the 633.4 keV level, as will be explained. If this level is populated in the (d,p) reaction, this exclusion is consistent with the $\ell = 2$ angular momentum transfer.

613.0 keV Level 1, 2, 3, 4, 5^+

This level is also required by the time differential coincidence result between the 117.6 keV and 494.3 keV transitions. However, the existence of this level is very doubtful because of the very small depopulation. This level can be a high spin state. Possible spins 1 to 5 have been tentatively assigned because of the 494.3 keV transi-

tion to the 118.7 keV 3^+ state.

615.1 keV Level 1^-, 2^-, 3^-

This level is populated by a primary transition. The M1 character of the 182.7 keV transition to the 432.3 keV 2^- or 3^- state determines odd parity and possible spins 1 to 4. The 4^- assignment can be excluded by the existence of the primary transition.

633.4 keV Level 1^-, 2^-

The existence of this level is confirmed by the presence of a primary transition and eight depopulating transitions. The M1 character of the 93.9 keV transition to the 539.5 keV 0^- or 1^- state suggests odd parity and spin 0, 1 or 2. The 0^- assignment can be excluded by the M1 + E2 character of the 136.5 keV transition to the 496.8 keV 1^- or 2^- state and by the M1 character of the 38.4 keV transition to the 595.0 keV 2^- or 3^- state. The 38.4 keV M1 transition can also exclude the 4^- assignment for the 595.0 keV level.

653.9 keV Level 1^-, 2^-, 3^-

This level is populated by a primary transition. The M1 character of the 96.8 keV transition to the 557.0 keV 2^- or 3^- state requires odd parity and spin possibilities 1 to 4. The 4^- assignment can be excluded by the existence of the primary transition.

663.4 keV Level $\leq 3^+$

Evidence for the existence of this level is not very strong. However, the Ritz combination principle can assign nine depopulating transitions. The M1 character of the 114.1 keV transition to the 549.3 keV 1^+ or 2^+ state requires even parity and spins 0, 1, 2 or 3.

664.9 keV Level 1^-, 2^-

This level is populated by a weak primary transition and is depopulated by eleven transitions including the transitions to the

ground state and the 1.1 keV 2^- state. The M1 character of the 125.3 keV transition to the 539.5 keV 0^- or 1^- state determines odd parity and spin 0, 1 or 2. Since the 107.8 keV transition to the 557.0 keV 2^- or 3^- state has been doubly assigned in the level scheme, its M1 character cannot exclude the 0^- assignment completely. However, from the fact that this level is populated in the (d,p) reaction with $\ell = 2$, the 0^- assignment can be excluded.

If the 393.4 keV transition to the 271.4 keV level exists, the 4^+ assignment for the 271.4 keV level can be excluded. However, its existence cannot be confirmed.

683.1 keV Level $1^+, 2^+, 3^+, 4^+$

This level has been introduced by the energy combination principle with six depopulating and three populating transitions. However, five of them are also assigned at other places in the level scheme, and no primary transition was observed. The existence of this level is very doubtful. The character of the depopulating transitions would require even parity and spin possibilities 1 to 4.

698.5 keV Level $1^+, 2^+$

This level is populated by a primary transition. The M1 character of the 149.2 keV transition to the 549.3 keV 1^+ or 2^+ state and the E1 character of the 461.5 keV transition to 237.0 keV require even parity and spin possibilities 0 to 3. The 3^+ assignment can be excluded by the existence of the primary transition and the 0^+ assignment can also be excluded by the 697.3 keV transition to the 1.1 keV 2^- state.

706.1 keV Level $1^+, 2^+$

This level is populated by a primary transition. The M1 characters of the 345.5 keV transition to the 360.6 keV 1^+ or 2^+ state and the 237.3 keV transition to the 468.8 keV 2^+ or 3^+ state require even

parity and spin 1, 2 or 3. The existence of the primary transition excludes the 3^+ assignment.

725.7 keV Level 0^-, 1^-, 2^-

This level is also populated by a primary transition. The M1 character of the 186.2 keV transition to the 539.5 keV 0^- or 1^- state suggests 0^-, 1^- or 2^- assignment for this level. Population in the (d,p) reaction has been observed at 711 keV and 725 keV excitation energies. The angular momentum transfer has been obtained for the 711 keV to be $\ell = 0$, but no level has been established at this energy in the present work. The angular momentum transfer for the 725 keV has not been reported. The 454.3 keV transition to the 271.4 keV level may exclude the 4^+ assignment for the 271.4 keV level. This is the second transition excluding the 4^+ assignment for that level.

(746.8 keV Level), 748.5 keV Level 0^+, 1^+, 2^+ and 750.8 keV Level 0^+, 1^+, 2^+

These levels are populated by two or three unresolved strong primary transitions, but the primary transition energies cannot be fitted to the level energies 748.5 keV and 750.8 keV, which have been determined by the secondary transition energies. The peak fitting result with two peaks indicates that level may be found at 746.75 ± .24 keV and at 750.23 ± .21 keV.

The Ritz combination principle suggests a possible level at 746.807 ± .003 keV with the depopulating transitions 628.1 keV, 555.2 keV, 548.1 keV, 386.2 keV, 322.2 keV, 314.5 keV, 221.1 keV, 195.5 keV and 189.8 keV to the levels at 118.7 keV, 191.6 keV, 198.7 keV, 360.6 keV, 424.7 keV, 432.3 keV, 525.6 keV, 551.3 keV and 557.0 keV, respectively. However, the strong 195.5 keV transition has been placed at between the 432.3 keV and 236.8 keV levels in the

present level scheme to satisfy the coincidence result between the 236 keV and 195 keV transitions. The assignment of the 195.5 keV M1 transition from this tentative 746.8 keV level to the 551.3 keV 2^-, 3^- or 4^- state would require odd parity and possible spins 1 to 5 for this 746.8 keV level. The 1^-, 2^- and 3^- assignments are consistent with the population by the primary transition and in the (d,p) reaction with $\ell = 2$ at 751 keV. However, this assignment of the 195.5 keV transition cannot explain the coincidence with the 236 keV transition, unless the 195.5 keV transition is a doublet. Therefore, without the 195.5 keV transition assignment, this tentative level may exist, and the primary transition may be a triplet.

The 748.5 keV level is depopulated by seven transitions. The M1 or E2 character of the 549.8 keV transition to the 198.7 keV 2^+ state and the M1 character of the 212.4 keV transition to the 536.1 keV 1^+, 2^+ or 3^+ state require even parity and spin possibilities 0 to 4. The 3^+ and 4^+ assignments can be excluded by the exsistence of the primary transition.

The 750.8 keV level is depopulated by nine transitions. The M1 character of the 201.5 keV transition to the 549.3 keV 1^+ or 2^+ state determines the spin and parity assignment as 0^+, 1^+, 2^+ or 3^+. The 3^+ assignment can be excluded by the exsistence of the primary transition.

759.6 keV Level 3

This level is populated by a primary transition. However, the depopulating transitions cannot define the spin and parity very well. If the (d,p) reaction populates this level with $\ell = 2$, odd parity is expected for this level.

767.0 keV Level 0^+, 1, 2, 3^+

This level has been introduced by the energy combination principle with ten depopulating transitions and eight populating transitions. The spin and parity have tentatively been assigned based on the spin and parity assignments of levels fed by depopulating transitions.

773.6 keV Level and above

These levels are based on the primary transition data and the time differential coincidence results. Since multipolarities of transitions above 500 keV cannot be determined, because internal conversion electron data are not available, spins and parities are tentatively assigned ($\leq$ 3) for the levels populated by the primary transition and (1, 2, 3, 4) for those based on the time differential coincidence data.

Table 5.

SUMMARY OF THE AG-109(N,GAMMA)AG-110 REACTION

NUCLEAR STATES			DEEXCITATION GAMMA-TRANSITIONS						PRIMARY TRANSITIONS			
ENERGY (KEV)	ERROR (KEV)	SPIN & PARITY	ENERGY (KEV)	ERROR (KEV)	INTENSITY (I/100N,%)		MULTI-POLARITY	FINAL LEVEL	ENERGY (KEV)	ERROR (KEV)	INTENSITY (I/100N,%)	
0	0	1+										
1.1143	.0011	2-						(d)6805.45		.20	.0158	2
117.5359	.0046	6+										
118.7106	.0010	3+	118.7077	.0018	.0767	16	E2	0				
			117.5962	.0007	12.9432	11	E1	1.1				
174.5507	.0046	5+,6+	57.0149	.0013	2.1340	14	M1	117.5				
191.6086	.0016	2+,3+,4+	72.8987	.0029	2.0506	14	M1	118.7				
198.6774	.0010	2+	198.6756	.0029	16.1424	9	M1	0	6607.87	.20	.0338	2
			197.5641	.0025	.1819	8	E1	1.1				
236.8335	.0012	1-,2-,3-	235.7211	.0023	6.9096	9	M1	1.1				
237.0283	.0009	1-,2-	237.0309	.0015	3.2224	8	E1	0	6569.57	.20	.0473	2
			235.9129	.0023	2.4622	9	M1+E2	1.1				
			38.3519	.0009	.0980	26	E1	198.7				
254.9951	.0031	4+,5+	137.4578	.0050	.0039	31		117.5				
			80.4464	.0048	3.2821	14	M1	174.5				
267.1946	.0011	1+,(2+)	267.1973	.0039	4.8354	8	M1	0	6539.28	.20	.3259	1
			266.0805	.0045	.8413	8	E1	1.1				
			68.5195	.0021	1.1967	16	M1	198.7				
271.4492	.0013	2+,3+,4+	152.7406	.0013	.9753	10	M1	118.7				
			79.8403	.0014	.1351	15	M1+E2	191.6				
304.5041	.0012	2+,3+	304.5092	.0042	.1607	9	E2	0				
			105.8272	.0031	3.5091	15	M1	198.7				
338.8761	.0019	0-,(1-)	338.8753	.0067	.9782	8	E1	0				
			337.7665	.0098	.0175	10		1.1				
360.5869	.0010	1+,2+	360.5856	.0050	2.1495	8	E2	0	6445.88	.20	.0829	1
			359.4709	.0045	.2970	8	E1	1.1				

SUMMARY OF THE AG-109(N,GAMMA)AG-110 REACTION

NUCLEAR STATES			DEEXCITATION GAMMA-TRANSITIONS					PRIMARY TRANSITIONS			
ENERGY (KEV)	ERROR (KEV)	SPIN & PARITY	ENERGY (KEV)	ERROR (KEV)	INTENSITY (I/100N,%)	MULTI-POLARITY	FINAL LEVEL	ENERGY (KEV)	ERROR (KEV)	INTENSITY (I/100N,%)	
			241.8758	.0126	.0051 36		118.7				
			161.9051	.0023	.4952 8	M1	198.7				
			123.7538	.0025	.0188 22		236.8				
			123.5580	.0018	.0157 29	(E1)	237.0				
			93.3941	.0008	1.7419 15	M1	267.2				
			56.0823	.0013	.0808 22	M1+E2	304.5				
380.1406	.0023	1+2+3+(4+)	181.4554	.0084	.0039 27		198.7				
			143.1175	.0034	.0055 23		237.0				
			75.6329	.0030	.4862 12	M1	304.5				
381.1636	.0010	1-,2-	381.1659	.0055	1.8761 8	E1	0	6425.37	.20	.0604	1
			380.0533	.0063	.4836 8	E2	1.1				
			144.3314	.0017	.0095 14	M1,E2	236.8				
			144.1368	.0009	.3513 13	M1	237.0				
			113.9681	.0017	.0329 19		267.2				
424.6614	.0015	0-,1-,(2-)	424.6625	.0084	.0935 24		0	6382.00	.20	.0390	2
		*	423.5572	.0083	.6821 21	M1,E2	1.1				
			187.6350	.0019	.0287 9	(E2)	237.0				
		*	157.4688	.0050	.0179 10		267.2				
432.3303	.0017	2-,(3-)	313.6127	.0037	.0311 10		118.7	6374.32	.37	.0032	9
			240.7338	.0070	.0066 18		191.6				
			233.6572	.0083	.0198 9		198.7				
			195.4984	.0021	1.2260 8	M1	236.8				
446.5309	.0014	3-,4-	445.3980	.0134	.1366 10		1.1				
			209.6972	.0016	.0336 9	E2	236.8				
			191.5366	.0029	4.1278 8	E1	255.0				
468.8063	.0011	2+,3+	467.6936	.0053	.0200 25		1.1				
			350.0909	.0017	1.0988 8	M1+E2	118.7				
			270.1248	.0019	.9529 8	M1	198.7				
		*	197.3588	.0022	.0163 11		271.4				
			164.3008	.0024	.0730 9	M1	304.5				
			108.2220	.0010	.1999 22	M1	360.6				
471.1979	.0019	3+,4+	* 296.6387	.0208	.0053 31		174.5				
			272.5194	.0028	.0493 12		198.7				

SUMMARY OF THE AG-109(N,GAMMA)AG-110 REACTION

NUCLEAR STATES			DEEXCITATION GAMMA-TRANSITIONS					PRIMARY TRANSITIONS			
ENERGY (KEV)	ERROR (KEV)	SPIN & PARITY	ENERGY (KEV)	ERROR (KEV)	INTENSITY (I/100N,%)		MULTI-POLARITY	FINAL LEVEL	ENERGY (KEV)	ERROR (KEV)	INTENSITY (I/100N,%)	
			* 216.1850	.0169	.0023	43		255.0				
			166.6945	.0023	.5010	8	M1	304.5				
485.7266	.0013	1+,2+,3+	367.0147	.0043	.2102	8	M1,E2	118.7				
			294.1131	.0037	.0396	12		191.6				
			287.0459	.0045	.6289	11	M1+E2	198.7				
			248.8985	.0037	.0182	10		236.8				
			218.5328	.0081	.0077	24		267.2				
			* 214.2814	.0022	.0343	11	E2	271.4				
			125.1397	.0022	.5297	15	M1	360.6				
496.8359	.0011	1-,2-	496.8168	.0354	.1639	25		0	6309.68	.21	.0266	1
			495.6992	.0124	1.2454	43	M1,E2	1.1				
			* 298.1505	.0073	.0442	15		198.7				
			* 259.9926	.0238	.0051	34		236.8				
			229.6387	.0024	.0422	12		267.2				
			136.2473	.0028	.0077	36		360.6				
			115.6734	.0007	.0674	15	M1	381.2				
525.6147	.0015	1-,2-	525.6044	.0179	.0221	33		0	6280.91	.20	.0711	1
			524.4992	.0297	.9028	43	M1,E2	1.1				
			288.7900	.0235	.0071	34		236.8				
			288.5893	.0029	.0401	12		237.0				
			186.7409	.0031	.0270	9	M1+E2	338.9				
			100.9593	.0056	.0181	21	M1+E2	424.7				
527.4609	.0018	1+,2+,3+	526.3299	.0332	.4958	47	E1	1.1				
			408.7541	.0057	.6168	13	M1,E2	118.7				
			328.7731	.0066	.0469	12		198.7				
			290.6344	.0110	.0116	14		236.8				
			260.2541	.0110	.0037	64		267.2				
			256.0099	.0087	.0086	13		271.4				
			188.6029	.0101	.0067	17		338.9				
			166.8759	.0022	.1940	9	M1	360.6				
536.1334	.0012	1+,2+,3+	536.1266	.0224	1.2378	64	M1,E2	0				
			299.2996	.0089	.0099	27		236.8				
			268.9341	.0033	.1079	8	M1	267.2				
			231.6343	.0046	.3992	9	M1	304.5				
			175.5466	.0016	.0424	10	M1	360.6				

SUMMARY OF THE AG-109(N,GAMMA)AG-110 REACTION

NUCLEAR STATES			DEEXCITATION GAMMA-TRANSITIONS						PRIMARY TRANSITIONS			
ENERGY (KEV)	ERROR (KEV)	SPIN & PARITY		ENERGY (KEV)	ERROR (KEV)	INTENSITY (I/100N,%)		MULTI-POLARITY	FINAL LEVEL	ENERGY (KEV)	ERROR (KEV)	INTENSITY (I/100N,%)	
				154.9711	.0123	.0027	34		381.2				
539.5216	.0013	0-,1-		538.3937	.0168	1.0009	70	M1,E2	1.1	6267.05	.21	.0887	1
				302.5069	.0091	.0236	13		237.0				
				200.6433	.0021	.0797	8	M1	338.9				
				178.9517	.0091	.0028	39		360.6				
				158.3581	.0099	.0026	36		381.2				
				114.8634	.0020	.0135	22	M1	424.7				
549.3296	.0013	1+,2+		549.3251	.0166	.9542	73	M1,E2	0	6257.14	.21	.0270	1
				312.4929	.0041	.0130	12		236.8				
				282.1278	.0036	.0785	11	M1,E2	267.2				
				277.8491	.0176	.0060	29		271.4				
				244.8277	.0015	.3676	8	M1	304.5				
				188.7487	.0035	.0556	12	M1	360.6				
551.3111	.0013	2-,3-,4-	*	314.4755	.0023	.0206	11		236.8				
				171.1760	.0099	.0074	28		380.1				
				170.1479	.0012	.0253	9		381.2				
				104.7824	.0018	.9592	13	M1	446.5				
557.0198	.0014	2-,(3-)		557.0220	.0110	.0198	18		0				
				555.8830	.0181	.0303	24		1.1				
			*	438.3410	.1032	.0115	45		118.7				
				320.1805	.0039	.1171	9	M1	236.8				
				196.4268	.0074	.0131	18		360.6				
				175.8567	.0017	.0232	10	M1+E2	381.2				
				124.6883	.0054	.0143	30	E2	432.3				
				110.4909	.0021	.9842	18	M1	446.5				
579.2444	.0013	2-,3-		578.1355	.0090	.0308	17		1.1				
				387.6109	.0328	.0131	12		191.6				
				342.1584	.0296	.0187	16		237.0				
				307.8008	.0081	.0115	12		271.4				
				218.6681	.0150	.0040	33		360.6				
			*	198.0730	.0060	.0105	15		381.2				
				146.9190	.0060	.0573	12		432.3				
				132.7103	.0016	.5829	13	M1	446.5				
				82.4090	.0008	.0708	15	M1	496.8				

SUMMARY OF THE AG-109(N,GAMMA)AG-110 REACTION

NUCLEAR STATES			DEEXCITATION GAMMA-TRANSITIONS						PRIMARY TRANSITIONS			
ENERGY (KEV)	ERROR (KEV)	SPIN & PARITY	ENERGY (KEV)	ERROR (KEV)	INTENSITY (I/100N,%)		MULTI-POLARITY	FINAL LEVEL	ENERGY (KEV)	ERROR (KEV)	INTENSITY (I/100N,%)	
589.7432	.0022	(0,1,2,3)-	588.6239	.0062	1.1515	19	M1,E2	1.1	6216.83	.21	.0177	2
			250.8791	.0120	.0078	22		338.9				
			208.5868	.0049	.0045	26		381.2				
594.9688	.0022	2-,3-	476.2581	.0047	.0648	19	M1,E2	118.7				
			* 358.1371	.0048	.4357	8	M1,E2	236.8				
613.0284	.0029	(1 - 5)+	494.3120	.0075	.0209	31		118.7				
			* 438.3410	.1032	.0115	45		174.5				
			341.5772	.0070	.0114	14		271.4				
			232.9063	.0298	.0069	21		380.1				
615.0712	.0020	1-,2-,3-	613.9538	.0027	.3370	17	M1,E2	1.1	6191.56	.20	.0600	1
			378.2434	.0056	.5043	9	M1,E2	236.8				
			378.0486	.0056	.5126	10	M1,E2	237.0				
			254.4773	.0103	.0075	16		360.6				
			182.7415	.0029	.0638	9	M1	432.3				
633.3816	.0012	1-,2-	633.3887	.0061	.0786	16		0	6173.26	.21	.0232	2
			396.3529	.0024	.1143	14	M1,E2	237.0				
			366.1795	.0055	.2449	8	E1	267.2				
			272.7906	.0018	.0638	10		360.6				
			252.2176	.0017	.2377	9	M1	381.2				
			136.5468	.0063	.0508	17	M1+E2	496.8				
			93.8615	.0011	.0405	17	M1	539.5				
			38.4137	.0024	.0338	45	M1	595.0				
653.8573	.0016	1-,2-,3-	417.0230	.0065	.4054	20	M1,E2	236.8	6152.82	.21	.0176	2
			315.0523	.0385	.0092	52		338.9				
			185.0495	.0061	.0073	13		468.8				
			157.0252	.0058	.0095	23		496.8				
			96.8369	.0010	.0410	24	M1	557.0				
663.4029	.0014	<=3+	464.7332	.0081	.3935	16	M1,E2	198.7				
			426.6163	.0282	.0079	16		236.8				
			358.9012	.0095	.0611	13		304.5				
			302.8150	.0024	.1728	12	E2	360.6				
			194.5946	.0087	.0078	13		468.8				
			177.6724	.0039	.0060	18		485.7				
			135.9483	.0049	.0080	47	(M1)	527.5				

SUMMARY OF THE AG-109(N,GAMMA)AG-110 REACTION

NUCLEAR STATES			DEEXCITATION GAMMA-TRANSITIONS						PRIMARY TRANSITIONS			
ENERGY (KEV)	ERROR (KEV)	SPIN & PARITY		ENERGY (KEV)	ERROR (KEV)	INTENSITY (I/100N,%)		MULTI-POLARITY	FINAL LEVEL	ENERGY (KEV)	ERROR (KEV)	INTENSITY (I/100N,%)	
				127.2675	.0021	.0105	26		536.1				
				114.0744	.0018	.0704	14	M1	549.3				
664.8676	.0013	1-,2-		664.8534	.0131	.3989	16		0	6141.80	.26	.0061	6
				663.7335	.0145	.0940	21		1.1				
				428.0021	.0383	.2977	19	M1,E2	236.8				
			*	393.4496	.0459	.0083	32		271.4				
				325.9763	.0101	.0195	9		338.9				
				304.2755	.0128	.0143	17		360.6				
				283.7069	.0083	.0305	16	(E2)	381.2				
				139.2528	.0014	.0117	14		525.6				
				125.3423	.0023	.0206	17	M1	539.5				
				113.5575	.0014	.0291	21	M1,E2	551.3				
			*	107.8492	.0016	.0301	21	M1	557.0				
683.0860	.0018	(1,2,3,4)+		484.3874	.0148	.2427	44	M1,E2	198.7				
				378.5863	.0083	.0599	13		304.5				
			*	214.2814	.0022	.0343	11	E2	468.8				
				211.8962	.0235	.0024	40		471.2				
			*	197.3588	.0022	.0163	11		485.7				
			*	157.4688	.0050	.0179	10		525.6				
698.4895	.0012	1+,2+		698.4845	.0037	.3471	18		0	6107.98	.22	.0653	2
				697.3322	.0474	.0120	36		1.1				
				461.4594	.0020	.3224	12	E1	237.0				
			*	337.9233	.0790	.0087	58		360.6				
			*	317.3171	.0049	.0073	28		381.2				
			*	273.8306	.0059	.0086	18		424.7				
				201.6609	.0064	.0191	13		496.8				
				162.3559	.0010	.1339	8	M1	536.1				
				149.1623	.0061	.2609	10	M1	549.3				
706.0615	.0014	1+,2+	*	704.9641	.0116	.0353	21		1.1	6100.65	.20	.1081	1
				587.3586	.0104	.1459	27		118.7				
				514.4584	.0035	.0509	40		191.6				
				345.4739	.0018	.2753	8	M1	360.6				
				237.2567	.0032	.5622	9	M1	468.8				
				220.3361	.0028	.0827	8		485.7				
				169.9261	.0019	.0271	11	(M1)	536.1				
				156.7364	.0053	.0103	17	(E2)	549.3				

SUMMARY OF THE AG-109(N,GAMMA)AG-110 REACTION

NUCLEAR STATES			DEEXCITATION GAMMA-TRANSITIONS					PRIMARY TRANSITIONS			
ENERGY (KEV)	ERROR (KEV)	SPIN & PARITY	ENERGY (KEV)	ERROR (KEV)	INTENSITY (I/100N,%)	MULTI-POLARITY	FINAL LEVEL	ENERGY (KEV)	ERROR (KEV)	INTENSITY (I/100N,%)	
725.7324	.0017	0-,1-,2-	725.7392	.0067	.1735 20		0	6080.91	.20	.0648	1
			488.7010	.0025	.2795 26	M1,E2	237.0				
			458.5560	.0167	.0676 11		267.2				
			454.2743	.0155	.0115 63		271.4				
			386.8627	.0089	.0671 9		338.9				
			344.5685	.0039	.0366 9		381.2				
			301.0287	.0375	.0058 35		424.7				
			* 279.2190	.0150	.0106 24		446.5				
			228.8974	.0057	.0101 14		496.8				
			186.2114	.0028	.1203 8	M1	539.5				
			110.6595	.0243	.0115 63		615.1				
748.5022	.0017	0+,1+,2+	748.4957	.0078	.5295 18		0				
			549.8369	.0059	.5095 30	M1,E2	198.7				
			409.6444	.0240	.0270 18		338.9				
			367.3416	.0043	.0282 12		381.2				
			* 323.8332	.0045	.0426 8		424.7				
			212.3697	.0018	.1569 8	M1	536.1				
			199.1687	.0081	.0147 10		549.3				
750.8275	.0019	0+,1+,2+	749.7278	.0179	.0856 18		1.1	(d)6056.22	.20	.6946	10
			632.1096	.0085	.1826 17		118.7				
			483.6352	.0140	.1225 38		267.2				
			446.3270	.0068	.1393 15	M1,E2	304.5				
			390.2204	.0123	.0114 21		360.6				
			223.3613	.0047	.1114 10	(M1)	527.5				
			214.6938	.0023	.0631 10	E2	536.1				
			201.5013	.0035	.1553 9	M1	549.3				
			193.8011	.0118	.0044 20		557.0				
759.5604	.0018	<=3	759.6043	.0293	.0343 21		0	6047.23	.24	.0219	6
			758.4512	.0077	.3747 21		1.1				
			522.7246	.0521	.1686 58	M2,E3	236.8				
			522.5249	.0056	.0788 19		237.0				
			288.3611	.0056	.0164 14		471.2				
			* 273.8306	.0059	.0086 18		485.7				
			262.7220	.0063	.0094 23		496.8				
			220.0368	.0042	.0113 13		539.5				
			169.8192	.0029	.0309 10	(M1)	589.7				

NUCLEAR STATES			DEEXCITATION GAMMA-TRANSITIONS						PRIMARY TRANSITIONS			
ENERGY (KEV)	ERROR (KEV)	SPIN & PARITY		ENERGY (KEV)	ERROR (KEV)	INTENSITY (I/100N,%)		MULTI-POLARITY	FINAL LEVEL	ENERGY (KEV)	ERROR (KEV)	INTENSITY (I/100N,%)	
766.9640	.0018	0+,1,2,3+	*	766.9618	.0036	.3822	21		0				
				499.7869	.0179	.1330	66		267.2				
				462.4469	.0129	.1566	13		304.5				
				406.3843	.0149	.0201	21		360.6				
			*	298.1505	.0073	.0442	15		468.8				
				281.2476	.0051	.0218	12		485.7				
				239.5198	.0117	.0081	15		527.5				
				227.4484	.0099	.0103	14		539.5				
				217.6390	.0080	.0051	22		549.3				
				153.9352	.0029	.0220	10	M1	613.0				
773.5937	.0016	<=3(+)		773.5832	.0063	.3360	15		0	6033.02	.21	.0966	2
				772.4877	.0103	.1287	18		1.1				
				574.9165	.0032	.4455	21	M1,E2	198.7				
				506.3907	.0080	.0286	29		267.2				
				469.0692	.0287	.0664	29	M1,E2	304.5				
				413.0412	.0373	.0197	21		360.6				
			*	393.4496	.0459	.0083	32		380.1				
			*	348.9503	.0127	.0187	11		424.7				
				276.7656	.0077	.0152	16		496.8				
				237.4664	.0043	.0462	12		536.1				
				234.1061	.0312	.0041	45		539.5				
				224.2607	.0035	.0617	9	M1	549.3				
785.5723	.0018	<=3		784.4520	.0241	.0955	21		1.1	6021.50	.20	.3069	1
				666.8502	.0091	.0521	19		118.7				
				586.8945	.0035	.7730	26	M1,E2	198.7				
				514.1236	.0134	.0411	36		271.4				
				249.4432	.0035	.1460	9	M1	536.1				
				236.2452	.0036	.0941	9	E2	549.3				
811.3347	.0028	<=3(+)		812.6703	.0057	.1183	20		198.7	5995.24	.20	.1625	1
			*	544.1371	.0508	.4092	45	M1,E2	267.2				
				506.8238	.0070	.0524	29		304.5				
				450.7389	.0110	.1749	20	M1,E2	360.6				
				342.5874	.0331	.0110	36		468.8				
				325.6152	.0065	.0233	9		485.7				
				275.2008	.0141	.0089	12		536.1				
				261.9750	.0163	.0124	14		549.3				

NUCLEAR STATES			DEEXCITATION GAMMA-TRANSITIONS					PRIMARY TRANSITIONS			
ENERGY (KEV)	ERROR (KEV)	SPIN & PARITY	ENERGY (KEV)	ERROR (KEV)	INTENSITY (I/100N,%)		MULTI-POLARITY	FINAL LEVEL	ENERGY (KEV)	ERROR (KEV)	INTENSITY (I/100N,%)	
			* 259.9926	.0238	.0051	34		551.3				
			* 157.4688	.0050	.0179	10		653.9				
818.8976	.0024	(1,2,3,4)	* 700.1490	.0269	.0379	20		118.7				
			627.2645	.0325	.0145	29		191.6				
			551.7082	.0125	.0869	16		267.2				
			* 458.2818	.0613	.0352	17		360.6				
			* 333.1265	.1099	.0061	17		485.7				
			282.7662	.0037	.0535	11		536.1				
			269.5646	.0055	.0212	12		549.3				
			185.4943	.0167	.0039	24		633.4				
820.6035	.0033	<=3	820.6201	.0199	.0471	18		0	5986.54	.20	.0983	1
			819.4732	.0160	.1781	23		1.1				
			553.4035	.0245	.0193	25		267.2				
			439.4352	.0172	.0300	21		381.2				
			284.4710	.0034	.0927	10	(E2)	536.1				
854.0261	.0042	(1,2,3,4)	735.2906	.0235	.0290	19		118.7	5952.39	.21	.0390	1
			* 421.6896	.0213	.0216	23		432.3				
			304.6982	.0059	.0498	12	(E2)	549.3				
			259.0174	.0241	.0032	37		595.0				
880.4397	.0030	(1,2,3,4)	761.7231	.0342	.0276	39		118.7				
			681.7501	.0280	.0098	47		198.7				
			643.6032	.0050	.1884	15		236.8				
			354.8332	.0043	.0107	16		525.6				
881.4431	.0018	<=3	880.3290	.0090	.1172	21		1.1	5925.10	.39	.0080	15
			501.2943	.0085	.0152	30		380.1				
			449.1455	.0790	.0191	21		432.3				
			355.8360	.0045	.0227	12		525.6				
			341.9134	.0269	.0157	18		539.5				
			330.1327	.0069	.0308	9		551.3				
			302.1967	.0039	.1823	11	M1,E2	579.2				
			291.7042	.0051	.0156	18		589.7				
			182.9480	.0050	.0108	15		698.5				
			* 107.8492	.0016	.0301	21	M1	773.6				
896.5671	.0028	<=3	895.4620	.0056	.4744	18		1.1	5910.05	.21	.0545	1

SUMMARY OF THE AG-109(N,GAMMA)AG-110 REACTION

NUCLEAR STATES			DEEXCITATION GAMMA-TRANSITIONS					PRIMARY TRANSITIONS			
ENERGY (KEV)	ERROR (KEV)	SPIN & PARITY	ENERGY (KEV)	ERROR (KEV)	INTENSITY (I/100N,%)	MULTI-POLARITY	FINAL LEVEL	ENERGY (KEV)	ERROR (KEV)	INTENSITY (I/100N,%)	
			* 704.9641	.0116	.0353 21		191.6				
			516.3147	.0609	.0115 27		380.1				
			515.4003	.0064	.0126 44		381.2				
			* 317.3171	.0049	.0073 28		579.2				
			301.6067	.0165	.0110 20		595.0				
			* 198.0730	.0060	.0105 15		698.5				
910.8141	.0018	<=3	910.7989	.0268	.0808 20		0	5895.85	.20	.1072	1
			792.1030	.0036	.5377 17		118.7				
			478.4824	.0127	.0486 45		432.3				
			441.9973	.0098	.1839 22	M1,E2	468.8				
			425.0885	.0028	.0575 19		485.7				
			361.4601	.0161	.0232 14		549.3				
			* 331.5687	.0050	.0321 9		579.2				
			* 321.0706	.0045	.0248 10		589.7				
			315.8387	.0364	.0056 27		595.0				
			247.4130	.0118	.0056 28		663.4				
			204.7548	.0036	.0099 11		706.1				
			143.8452	.0085	.0056 29		767.0				
913.3548	.0037	(1,2,3,4)	794.6427	.0063	.2176 14		118.7				
			532.1729	.0104	.0185 37		381.2				
			364.0411	.0127	.0265 18		549.3				
			298.2768	.0127	.0155 24		615.1				
925.0445	.0029	(1,2,3,4)	806.3344	.0074	.0718 16		118.7				
			733.4219	.0112	.0369 30		191.6				
			564.4521	.0138	.0228 23		360.6				
			310.0044	.0174	.0056 29		615.1				
			158.0822	.0044	.0175 15	M1+E2	767.0				
954.3219	.0021	<=3	954.3121	.0176	.1002 24		0	5852.56	.23	.0228	3
			687.0727	.0346	.1323 18		267.2				
			521.9918	.0065	.0261 43		432.3				
			* 485.5202	.0111	.0612 42		468.8				
			428.7747	.1098	.0062 153		525.6				
			404.9836	.0384	.0190 21		549.3				
			290.8970	.0205	.0033 35		663.4				
			248.2647	.0070	.0132 11		706.1				
			205.8411	.0132	.0061 15		748.5				

NUCLEAR STATES			DEEXCITATION GAMMA-TRANSITIONS					PRIMARY TRANSITIONS			
ENERGY (KEV)	ERROR (KEV)	SPIN & PARITY	ENERGY (KEV)	ERROR (KEV)	INTENSITY (I/100N,%)		MULTI-POLARITY	FINAL LEVEL	ENERGY (KEV)	ERROR (KEV)	INTENSITY (I/100N,%)	
			187.3519	.0049	.0079	21		767.0				
			180.7251	.0093	.0048	20		773.6				
			168.7486	.0042	.0095	13		785.6				
979.7109	.0029	(1,2,3,4)	860.9774	.0150	.1458	21		118.7				
			781.0471	.0107	.0778	22		198.7				
			708.2675	.0270	.0217	33		271.4				
			* 443.5453	.0192	.0107	22		536.1				
			314.7801	.0402	.0048	38		664.9				
			* 296.6387	.0208	.0053	31		683.1				
			212.7509	.0038	.0106	15		767.0				
994.9763	.0024	<=3	796.2833	.0112	.0956	17		198.7	5811.75	.20	.3276	1
			739.9730	.0335	.0188	20		255.0				
			727.7810	.0055	.3188	19		267.2				
			509.2575	.0058	.0773	36		485.7				
			458.8450	.0151	.0816	16		536.1				
			437.9426	.0416	.0211	21		557.0				
			* 331.5687	.0050	.0321	9		663.4				
			288.9508	.0253	.0065	35		706.1				
			244.1307	.0095	.0061	23		750.8				
			221.3921	.0059	.0032	37		773.6				
			176.0784	.0032	.0244	11	M1	818.9				
1012.9672	.0019	<=3	1012.9526	.0163	1.0709	23		0	5793.56	.20	.6194	1
			814.2963	.0050	.3466	18		198.7				
			* 544.1371	.0508	.4092	45	M1,E2	468.8				
			516.1291	.0107	.0145	33		496.8				
			* 485.5202	.0111	.0612	42		527.5				
			463.6212	.0283	.0238	17		549.3				
			* 314.4755	.0023	.0206	11		698.5				
			253.4073	.0019	.0343	10	(E2)	759.6				
1034.8108	.0025	<=3	1034.8382	.0199	.0824	16		0	5771.93	.20	.2358	1
			767.6017	.0096	.1410	15		267.2				
			653.6636	.0093	.0634	18		381.2				
			563.6037	.0116	.0108	34		471.2				
			498.6698	.0107	.0409	43		536.1				
			371.4271	.0124	.0304	11		663.4				
			309.0783	.0070	.0057	19		725.7				

SUMMARY OF THE AG-109(N,GAMMA)AG-110 REACTION

NUCLEAR STATES			DEEXCITATION GAMMA-TRANSITIONS					PRIMARY TRANSITIONS			
ENERGY (KEV)	ERROR (KEV)	SPIN & PARITY	ENERGY (KEV)	ERROR (KEV)	INTENSITY (I/100N,%)		MULTI-POLARITY	FINAL LEVEL	ENERGY (KEV)	ERROR (KEV)	INTENSITY (I/100N,%)	
			267.8466	.0141	.0191	16		767.0				
			215.9088	.0073	.0056	27		818.9				
1036.7803	.0039	(1,2,3,4)	918.1347	.0263	.0507	18		118.7				
			656.6502	.0353	.0173	28		380.1				
			655.6249	.0119	.0887	27		381.2				
			551.0582	.0085	.0222	46		485.7				
			* 421.6896	.0213	.0216	23		615.1				
			277.2140	.0049	.0157	14		759.6				
			* 216.1850	.0169	.0023	43		820.6				
1066.5093	.0076	<=3	*1066.5272	.0114	.1514	19		0	5740.16	.21	.1265	1
			476.7462	.0162	.0745	61		589.7				
			* 453.4649	.0135	.0098	26		613.0				
			* 383.4595	.0376	.0161	59		683.1				
1097.4306	.0022	<=3	1097.4214	.0193	.1977	21		0	5709.09	.21	.2849	1
			898.7481	.0056	.3753	14		198.7				
			502.4561	.0643	.0699	34		595.0				
			* 443.5453	.0192	.0107	22		653.9				
			432.5694	.0130	.0079	25		664.9				
			* 348.9503	.0127	.0187	11		748.5				
			* 346.6230	.0254	.0069	17		750.8				
			* 337.9233	.0790	.0087	58		759.6				
			* 330.4776	.0115	.0102	20		767.0				
			* 323.8332	.0045	.0426	8		773.6				
			311.8589	.0021	.0354	9		785.6				
			278.5336	.0105	.0095	20		818.9				
1106.6389	.0021	<=3	1106.6445	.0111	.5111	20		0	5700.24	.20	.8328	1
			907.9644	.0076	.5447	18		198.7				
			869.6677	.0335	.0291	20		237.0				
			835.1133	.0389	.0538	27		271.4				
			746.0504	.0073	.1692	17		360.6				
			* 423.5572	.0083	.6821	21	M1,E2	683.1				
			* 358.1371	.0048	.4357	8	M1,E2	748.5				
			* 333.1265	.1099	.0061	17		773.6				
			* 321.0706	.0045	.0248	10		785.6				
			* 295.2963	.0086	.0171	14		811.3				
			181.5950	.0066	.0048	20		925.0				

NUCLEAR STATES			DEEXCITATION GAMMA-TRANSITIONS					PRIMARY TRANSITIONS			
ENERGY (KEV)	ERROR (KEV)	SPIN & PARITY	ENERGY (KEV)	ERROR (KEV)	INTENSITY (I/100N,%)	MULTI-POLARITY	FINAL LEVEL	ENERGY (KEV)	ERROR (KEV)	INTENSITY (I/100N,%)	
			152.3142	.0026	.0072 21		954.3				
			126.9334	.0053	.0063 28	E2	979.7				
			69.8440	.0203	.0049 124		1036.8				
1164.3234	.0037	<=3	1164.3159	.0356	.1287 17		0	5641.82	.21	.1493	2
			897.2051	.0692	.0433 34		267.2				
			* 458.2818	.0613	.0352 17		706.1				
			239.2784	.0040	.0146 13		925.0				
			184.6128	.0040	.0103 10		979.7				
1168.9967	.0026	<=3	1167.8685	.0231	.2291 29		1.1	5637.69	.28	.0443	/
			* 700.1490	.0269	.0379 20		468.8				
			504.1336	.0092	.0095 52		664.9				
			402.0356	.0040	.1241 19	E2	767.0				
			* 383.4595	.0376	.0161 59		785.6				
			314.9685	.0086	.0058 24		854.0				
			134.1856	.0014	.0207 16	M1	1034.8				
1175.7303	.0036	<=3	690.0070	.0268	.0335 30		485.7	5630.81	.21	.1035	1
			650.1409	.0203	.0185 21		525.6				
			648.2789	.0071	.1008 21		527.5				
			477.2353	.0067	.0207 31		698.5				
			* 295.2963	.0086	.0171 14		880.4				
			* 264.9047	.0132	.0152 18		910.8				
			262.3711	.0055	.2993 13	M1	913.4				
1178.2515	.0053	(1,2,3,4)	1059.4948	.0678	.0390 29		118.7				
			817.6614	.0440	.0649 23		360.6				
			707.0547	.0068	.0713 23		471.2				
			583.2749	.0152	.0150 28		595.0				
			563.1592	.0196	.0206 22		615.1				
			404.6667	.0167	.0235 25		773.6				
			* 264.9047	.0132	.0152 18		913.4				
1185.2142	.0034	<=3	* 1066.5272	.0114	.1514 19		118.7	5621.37	.21	.0567	2
			824.6252	.0118	.0831 19		360.6				
			804.0070	.0276	.0193 18		381.2				
			716.3714	.0378	.0221 23		468.8				
			595.4602	.0126	.0273 29		589.7				
			486.7168	.0088	.0272 25		698.5				

SUMMARY OF THE AG-109(N,GAMMA)AG-110 REACTION

NUCLEAR STATES			DEEXCITATION GAMMA-TRANSITIONS					PRIMARY TRANSITIONS			
ENERGY (KEV)	ERROR (KEV)	SPIN & PARITY	ENERGY (KEV)	ERROR (KEV)	INTENSITY (I/100N,%)		MULTI-POLARITY	FINAL LEVEL	ENERGY (KEV)	ERROR (KEV)	INTENSITY (I/100N,%)	
			459.4785	.0053	.0448	12		725.7				
			230.8998	.0060	.0777	10	M1	954.3				
1192.5850	.0050	<=3	1192.6573	.0393	.0805	18		0	5613.96	.20	.2245	1
			925.3963	.0233	.0567	38		267.2				
			433.0063	.0168	.0322	16		759.6				
			425.6119	.0177	.0199	32		767.0				
			* 279.2190	.0150	.0106	24		913.4				
			267.5429	.0052	.0217	18		925.0				
1227.0581	.0037	<=3	1227.0254	.0226	.2627	28		0	5579.53	.20	.3501	1
			990.2084	.0292	.0657	25		236.8				
			888.2127	.0301	.0506	32		338.9				
			* 755.8432	.0329	.0372	34		471.2				
			699.5694	.0167	.0359	18		527.5				
			677.7820	.0269	.0403	17		549.3				
			675.8362	.0502	.0284	24		551.3				
			* 453.4649	.0135	.0098	26		773.6				
			441.5070	.0245	.0302	18		785.6				
			373.0288	.0076	.0065	20		854.0				
			* 346.6230	.0254	.0069	17		880.4				
			* 330.4776	.0115	.0102	20		896.6				
			192.2506	.0045	.0211	10	(E1)	1034.8				
1252.6889	.0027	<=3	1251.6433	.0946	.1362	27		1.1	5554.14	.26	.1026	12
			827.9110	.0685	.0216	20		424.7				
			783.8801	.0041	.4822	17		468.8				
			* 766.9618	.0036	.3822	21		485.7				
			* 755.8432	.0329	.0372	34		496.8				
			372.2603	.0071	.1328	8	M1,E2	880.4				
			356.1077	.0640	.0068	16		896.6				

Comments * Gamma-transition placed at two or more positions in the level scheme.

(d) Unresolved doublet of primary transitions

Table 6.

LIST OF INTERNAL CONVERSION ELECTRONS

E-GAMMA (KEV)	SHELL		E-ELECTRON (KEV)	ERROR (KEV)	INTENSITY (I/100N)	ERROR (%)	I.C.C. (m)	MULTI-POLARITY (f)	FINAL ASSIGNMENT
38.3519	L1		34.5375	.0051	.0140	10.7	.411E+00	E1	E1
	M1	*	37.6425	.0057	.0091	9.8	.267E+00		
38.4137	L1		34.6083	.0042	.0163	6.9	.139E+01	M1	M1
	M1	*	37.6425	.0057	.0091	9.8	.774E+00	E2	
56.0823	K		30.5692	.0036	.2469	3.3	.879E+01	M1+E2	M1+E2
	L1		52.2828	.0122	.0391	51.0	.139E+01	M1,E2	
	M1		55.3752	.0160	.0135	29.9	.482E+00	E2	
57.0149	K		31.5003	.0033	3.1272	1.1	.422E+01		M1
	L1		53.2093	.0047	.4095	2.4	.552E+00	M1	
	L2		53.4882	.0053	.0538	5.4	.725E-01	M1+E2	
	M1		56.2976	.0049	.0630	7.8	.850E-01		
58.0571	K		32.5429	.0034	.0609	3.1	.191E+01	E1	E1
	L1		54.2422	.0107	.0841	11.4	.264E+01		
63.5551	K		38.0197	.0088	.0053	20.3	.107E+01	E1	E1
63.7629	K		38.2510	.0038	.0837	1.4	.200E+01		E1
	L1		59.9581	.0074	.0149	8.1	.355E+00		
	L2		60.2244	.0184	.0051	45.6	.121E+00	M1+E2	
	L3		60.4284	.0123	.0062	22.0	.149E+00	M1+E2	
	M1		63.0548	.0176	.0048	19.3	.113E+00	M1	
68.5195	K		43.0075	.0040	1.3075	1.5	.315E+01	M1	M1
	L1		64.7131	.0061	.1229	5.2	.296E+00		
	L2		65.0050	.0082	.0117	7.3	.281E-01	M1	
	L3		65.1510	.0135	.0056	22.8	.135E-01	M1+E2	
72.8987	K		47.3861	.0043	1.8707	.9	.263E+01	M1	M1
	L1		69.0956	.0064	.1789	5.3	.251E+00		
	L2		69.3762	.0074	.0128	10.9	.180E-01	M1	
	L3		69.5447	.0119	.0058	17.3	.815E-02	M1+E2	
	M1		72.1844	.0067	.0349	3.7	.490E-01		
	M2	*	72.2792	.0106	.0063	15.8	.886E-02	M1+E2	
75.6329	K		50.1184	.0045	.3171	1.4	.188E+01		M1
	L1		71.8295	.0066	.0352	2.2	.209E+00		
	L3	*	72.2792	.0106	.0063	15.8	.374E-01	M1+E2	
	M1		74.9269	.0176	.0073	12.7	.433E-01	M1	
79.8403	K		54.3339	.0058	.1614	3.2	.344E+01	M1+E2	M1+E2
	L1		76.0341	.0085	.0141	8.3	.301E+00	M1+E2	
80.4464	K		54.9285	.0048	1.9824	.9	.174E+01	M1	M1
	L1		76.6408	.0069	.2097	1.8	.184E+00		
	L2		76.9182	.0074	.0127	4.8	.111E-01		
	L3		77.0842	.0105	.0049	26.6	.431E-02	M1	
	M1		79.7237	.0076	.0699	9.6	.613E-01	M1+E2	
	M2		79.7832	.0104	.0254	16.1	.223E-01	M1+E2	
	M3		79.8759	.0094	.0217	10.3	.190E-01	M1+E2	
82.4090	K		56.9037	.0050	.0528	2.6	.215E+01	M1	M1

E-GAMMA (KEV)	SHELL	E-ELECTRON (KEV)	ERROR (KEV)	INTENSITY (I/100N)	ERROR (%)	I.C.C.	MULTI-POLARITY	FINAL ASSIGNMENT
	L1	78.6082	.0134	.0095	13.8	.384E+00	M1+E2	
93.3941	K	67.8968	.0082	.7411	3.0	.123E+01	M1	M1
	L1 *	89.5917	.0078	.0820	1.1	.136E+00	M1	
	L2	89.8604	.0097	.0087	14.4	.144E-01	M1+E2	
	L3	90.0597	.0113	.0066	10.2	.110E-01	M1+E2	
	M1	92.6773	.0072	.0150	13.8	.247E-01	M1	
93.8615	K	68.3428	.0068	.0256	52.2	.182E+01	M1	M1
	L1 *	90.0597	.0113	.0066	10.2	.473E+00		
96.8369	K	71.3192	.0075	.0136	32.8	.952E+00	M1	M1
100.9593	K	75.4506	.0186	.0096	15.9	.153E+01	M1+E2	M1+E2
101.8546	K	76.3391	.0069	.0424	1.8	.879E+00	M1	M1
	L1 *	98.0377	.0147	.0061	15.4	.126E+00	M1	
102.5408	K	77.0021	.0150	.0034	29.6	.482E+00	E1	E1
	L1	98.7244	.0255	.0023	27.4	.324E+00	E2	
103.9407	K	78.4413	.0123	.0143	7.9	.132E+01	M1+E2	M1+E2
	L3	*100.3866	.0201	.0033	21.3	.306E+00	E2	
	L2	*100.3866	.0201	.0033	21.3	.306E+00		
104.2191	K	78.7217	.0136	.0088	11.7	.404E+01		
	L1	*100.3866	.0201	.0033	21.3	.152E+01	M2,E3	
104.7824	K	79.2699	.0071	.3202	2.0	.961E+00	M1	M1
	L1	100.9748	.0119	.0319	2.3	.956E-01	M1	
	* L2	101.2173	.0345	.0038	28.1	.113E-01	M1+E2	
	* L2	101.2611	.0242	.0039	21.4	.117E-01	M1+E2	
	L3	*101.4061	.0150	.0039	17.3	.116E-01	M1+E2	
	M1	*104.0658	.0141	.0075	10.1	.226E-01	M1	
105.8272	K	80.3153	.0075	1.0793	.5	.886E+00	M1	M1
	L1	102.0178	.0119	.1163	3.6	.954E-01	M1	
	L2	102.3049	.0125	.0085	4.7	.694E-02	M1	
	M1	105.1116	.0123	.0234	3.2	.192E-01	M1	
	M2	*105.2606	.0267	.0049	20.9	.406E-02	M1+E2	
	M3	*105.2606	.0267	.0049	20.9	.406E-02	M1+E2	
107.1307	K	81.6267	.0162	.0050	18.6	.862E+00	M1	M1
107.7742	K	82.2489	.0103	.0066	30.1	.114E+01	M1	M1
107.8492	K	82.3415	.0081	.0093	6.9	.886E+00	M1	M1
	L1	*104.0658	.0141	.0075	10.1	.720E+00		
108.2220	K	82.7114	.0073	.0571	1.8	.822E+00	M1	M1
	L1	104.4227	.0132	.0071	11.4	.103E+00	M1	
	L2	104.6762	.0190	.0030	17.8	.432E-01	M1+E2	
	M1	107.5178	.0281	.0032	22.1	.459E-01	E2	
108.8643	K	83.3917	.0230	.0040	24.7	.879E+00	M1	M1
	L3	105.5721	.0397	.0018	42.3	.400E+00		
109.6954	K	84.1774	.0076	.0244	3.7	.897E+00	M1	M1
	L1	105.8949	.0160	.0042	20.2	.153E+00	M1+E2	

E-GAMMA (KEV)	SHELL	E-ELECTRON (KEV)	ERROR (KEV)	INTENSITY (I/100N)	ERROR (%)	I.C.C.	MULTI-POLARITY	FINAL ASSIGNMENT
	L2	106.1574	.0405	.0031	51.3	.115E+00		
	L3	*106.3304	.0277	.0042	12.9	.154E+00		
	M1	*108.9804	.0153	.0052	8.5	.193E+00	M2,E3	
109.9225	K	* 84.4481	.0106	.0088	13.6	.222E+01	E2	M1
	L1	106.1107	.0242	.0045	27.7	.113E+01	M2,E3	
110.1529	K	* 84.4481	.0106	.0088	13.6	.166E+01	M1+E2	M1
	L1	*106.3304	.0277	.0042	12.9	.786E+00		
110.4909	K	84.9769	.0076	.2920	1.5	.854E+00	M1	M1
	L1	106.6741	.0124	.0347	1.4	.101E+00	M1	
	M1	*109.7701	.0164	.0077	19.1	.226E-01	M1	
112.1323	K	86.6233	.0077	.0411	1.9	.791E+00	M1	M1
	L1	108.3237	.0135	.0051	12.5	.985E-01	M1	
	L2	*108.6619	.0211	.0032	23.4	.626E-01	M1+E2	
	M1	111.3989	.0267	.0031	20.0	.605E-01		
112.7852	K	87.2752	.0077	.0306	2.0	.900E+00	M1	M1
	L1	*108.9804	.0153	.0052	8.5	.154E+00	M1+E2	
113.5575	K	88.0406	.0092	.0108	17.0	.107E+01	M1+E2	M1,E2
	L1	*109.7701	.0164	.0077	19.1	.765E+00	M2	
114.0744	K	88.5631	.0084	.0178	6.3	.728E+00	M1	M1
	L1	110.2662	.0307	.0025	27.2	.100E+00	M1	
	M1	113.3345	.0223	.0047	19.4	.191E+00	M2,E3	
114.8634	K	89.3644	.0131	.0040	19.1	.856E+00	M1	M1
115.6734	K	90.1649	.0085	.0163	6.1	.695E+00	M1	M1
	L1	111.7656	.0186	.0027	23.0	.117E+00	M1+E2	
117.5962	K	92.0855	.0086	1.0838	.8	.241E+00	E1	E1
	L1	113.7923	.0128	.1058	.7	.235E-01	E1	
	L2	114.0741	.0138	.0096	6.1	.214E-02	E1	
	L3	114.2505	.0133	.0142	7.4	.316E-02	E1	
	M1	116.8841	.0131	.0203	7.0	.452E-02	E1	
	M2	*117.0207	.0142	.0056	25.6	.126E-02	M1	
	M3	*117.0207	.0142	.0056	25.6	.126E-02	M1+E2	
118.7077	K	93.2002	.0070	.0421	6.8	.158E+01	E2	E2
	L1	114.9143	.0139	.0051	16.6	.193E+00	E2	
	L2	115.1972	.0256	.0034	28.0	.129E+00	E2	
	L3	115.3652	.0144	.0045	8.5	.169E+00		
	M1	*118.0391	.0251	.0030	27.3	.111E+00		
123.5580	K	* 98.0377	.0147	.0061	15.4	.111E+01	M1+E2	(E1)
124.6883	K	99.1753	.0136	.0064	8.5	.128E+01	E2	E2
	L3	*121.3618	.0138	.0163	4.2	.328E+01		
125.1397	K	99.6250	.0118	.0993	3.2	.540E+00	M1	M1
	L1	*121.3618	.0138	.0163	4.2	.886E-01	M1+E2	
	M1	124.3997	.0288	.0028	32.6	.151E-01	M1	
125.3423	K	99.8314	.0159	.0049	16.6	.689E+00	M1	M1

LIST OF INTERNAL CONVERSION ELECTRONS

E-GAMMA (KEV)	SHELL	E-ELECTRON (KEV)	ERROR (KEV)	INTENSITY (I/100N)	ERROR (%)	I.C.C.	MULTI-POLARITY	FINAL ASSIGNMENT
126.9334	K	*101.4061	.0150	.0039	17.3	.177E+01	E2	E2
129.0332	K	103.5644	.0261	.0048	19.0	.104E+01	M1+E2	M1+E2
132.7103	K	107.1971	.0123	.0967	1.2	.478E+00	M1	M1
	L1	128.9089	.0142	.0110	6.5	.542E-01	M1	
	M1	*131.9922	.0165	.0053	17.1	.264E-01	E2	
134.1856	K	*108.6619	.0211	.0032	23.4	.452E+00	M1	M1
135.9048	K	*110.4191	.0290	.0032	23.9	.935E+00	E2	(M1)
135.9483	K	*110.4191	.0290	.0032	23.9	.115E+01	E2	(M1)
136.5468	K	111.0439	.0130	.0104	11.8	.588E+00	M1+E2	M1+E2
	L1	132.7766	.0284	.0028	15.8	.160E+00		
137.0285	K	111.5127	.0150	.0047	16.2	.824E+00	M1+E2	M1+E2
137.4578	K	111.9320	.0220	.0051	11.8	.373E+01	M2	
137.9512	K	112.4334	.0142	.0056	17.1	.443E+00	M1	M1
	L1	134.1422	.0275	.0029	28.2	.235E+00		
142.6905	K	117.1781	.0189	.0042	15.3	.633E+00	M1+E2	M1+E2
143.5209	K	*118.0391	.0251	.0030	27.3	.189E+01		
144.1368	K	118.6236	.0131	.0538	1.1	.441E+00	M1+E2	M1
	L1	140.3114	.0165	.0063	10.9	.520E-01	M1	
	L3	140.7825	.0178	.0043	12.4	.356E-01	M2	
144.3314	K	118.8108	.0190	.0040	14.7	.123E+01		M1,E2
148.5258	K	122.9931	.0314	.0028	24.7	.118E+01	E2	
149.1623	K	123.6505	.0135	.0306	1.4	.338E+00	M1	M1
	L1	145.3651	.0214	.0048	14.4	.533E-01	M1+E2	
	M1	148.4055	.0329	.0036	23.2	.395E-01		
152.7406	K	127.2265	.0137	.1066	1.0	.315E+00	M1	M1
	L1	148.9224	.0128	.0124	5.4	.366E-01	M1	
	L2	149.2154	.0331	.0029	23.6	.867E-02	M1+E2	
	L3	149.3956	.0317	.0030	19.6	.879E-02	M1+E2	
	M1	152.0182	.0217	.0025	27.1	.732E-02	M1	
153.9352	K	128.4053	.0295	.0031	19.8	.408E+00	M1	M1
156.2459	K	130.7271	.0142	.0122	3.7	.282E+00	M1	M1
	L1	152.4523	.0360	.0034	12.6	.775E-01	E2	
156.7364	K	131.1790	.0208	.0029	15.5	.806E+00	E2	(E2)
157.4688	K	*131.9922	.0165	.0053	17.1	.860E+00		
157.5424	K	*131.9922	.0165	.0053	17.1	.113E+01		
158.0822	K	132.5576	.0174	.0030	11.7	.502E+00	M1+E2	M1+E2
159.2676	K	133.9087	.0314	.0027	33.4	.928E+00	E2	(E2)
161.9051	K	136.3884	.0144	.0419	1.4	.243E+00		M1
	L1	158.1062	.0139	.0055	5.9	.318E-01	M1	
	M1	*161.2120	.0149	.0036	6.7	.207E-01		
162.3559	K	136.8416	.0146	.0122	8.2	.262E+00	M1	M1
164.3008	K	138.7803	.0160	.0067	7.5	.262E+00	M1	M1
	L1	160.5430	.0318	.0026	16.2	.101E+00		

LIST OF INTERNAL CONVERSION ELECTRONS

E-GAMMA (KEV)	SHELL	E-ELECTRON (KEV)	ERROR (KEV)	INTENSITY (I/100N)	ERROR (%)	I.C.C.	MULTI-POLARITY	FINAL ASSIGNMENT
164.6804	K	139.1685	.0286	.0029	14.8	.681E+00	E2	(E2)
164.9471	K	139.3731	.0274	.0030	26.2	.882E+00		
165.1215	K	139.6252	.0287	.0047	15.8	.284E+00	M1	M1
166.6945	K	141.1757	.0147	.0391	2.0	.225E+00		M1
	L1	162.8782	.0210	.0055	6.9	.317E-01	M1	
166.8759	K	141.3595	.0151	.0156	3.0	.231E+00		M1
	L1 *	163.0780	.0228	.0039	30.1	.579E-01	E2	
167.0515	K	141.5370	.0152	.0132	6.5	.236E+00	M1	M1
	L1 *	163.2459	.0148	.0058	6.3	.104E+00		
169.9261	K	144.3873	.0226	.0072	14.5	.765E+00		(M1)
172.8197	K	147.2971	.0163	.0061	7.0	.194E+00		M1
	L1 *	169.0789	.0384	.0040	12.8	.128E+00		
175.2403	K	149.7190	.0134	.0070	7.9	.230E+00	M1	M1
	L1	171.4403	.0291	.0041	13.8	.133E+00		
175.5466	K	150.0225	.0155	.0038	8.0	.259E+00	M1+E2	M1
175.8567	K	150.3417	.0301	.0026	19.0	.327E+00	M1+E2	M1+E2
176.0784	K	150.5688	.0436	.0017	32.4	.196E+00	M1	M1
178.7429	K	153.2274	.0169	.0036	9.6	.151E+00		M1
	L1	174.8503	.0360	.0025	33.2	.105E+00		
	L3 *	175.3752	.0386	.0020	37.2	.833E-01		
179.0562	L2	175.5842	.0281	.0033	21.8	.162E+01		
180.9651	K	155.4767	.0254	.0027	16.3	.368E+00	E2	M1+E2
	L1	177.1138	.0441	.0029	28.2	.392E+00		
181.2506	K	155.7411	.0232	.0034	12.9	.354E+00	M1+E2	M1+E2
182.7415	K	157.2097	.0149	.0046	10.5	.210E+00	M1	M1
186.2114	K	160.6919	.0138	.0074	3.8	.176E+00	M1	M1
186.7409	K *	161.2120	.0149	.0036	6.7	.380E+00	E2	M1+E2
187.6350	K	162.1600	.0396	.0032	14.9	.326E+00	E2	(E2)
187.7665	K	162.2687	.0407	.0033	22.0	.486E+00	E2	(E2)
188.6029	K *	163.0780	.0228	.0039	30.1	.168E+01	E3	
188.7487	K *	163.2459	.0148	.0058	6.3	.299E+00	M1+E2	M1
190.3362	K	164.8975	.0280	.0033	22.1	.594E+00		(E2)
191.5366	K	166.0188	.0154	.0910	1.5	.635E-01	E1	E1
	L1	187.7267	.0266	.0100	3.1	.696E-02	E1	
	L2 *	188.0158	.0390	.0032	14.7	.226E-02	M1+E2	
	L3	188.2285	.0452	.0026	26.9	.185E-02	M1+E2	
	M1	190.8156	.0416	.0046	14.2	.318E-02		
194.1778	K	168.6090	.0371	.0035	10.4	.590E+00		(E2)
194.5946	K *	169.0789	.0384	.0040	12.8	.147E+01	E3	
194.7044	K	169.2902	.0387	.0035	13.5	.802E+00		
195.4984	K	169.9835	.0157	.0721	1.5	.169E+00	M1	M1
	L1	191.6834	.0270	.0095	7.7	.223E-01	M1+E2	
196.3368	K *	170.8821	.0207	.0029	13.0	.127E+01	M2,E3	

E-GAMMA (KEV)	SHELL	E-ELECTRON (KEV)	ERROR (KEV)	INTENSITY (I/100N)	ERROR (%)	I.C.C.	MULTI-POLARITY	FINAL ASSIGNMENT
196.4268	K	*170.8821	.0207	.0029	13.0	.641E+00		
197.3588	K	171.8445	.0182	.0066	20.0	.117E+01	M2,E3	
197.5641	K	172.0550	.0168	.0114	9.2	.181E+00	M1	E1
	L1	193.7041	.0442	.0028	23.7	.438E-01		
198.6756	K	173.1662	.0160	.9292	1.4	.166E+00	M1	M1
	L1	194.8659	.0271	.1184	1.3	.211E-01	M1+E2	
	L2	195.1660	.0292	.0066	19.3	.118E-02	M1	
	L3	195.3757	.0364	.0029	28.4	.516E-03	E1	
	M1	197.9563	.0274	.0235	7.3	.418E-02	M1+E2	
199.1687	K	173.6769	.0407	.0034	23.9	.673E+00		
200.6433	K	175.1364	.0175	.0058	7.6	.209E+00	M1+E2	M1
201.0169	K	*175.5842	.0281	.0033	21.8	.116E+01	M2,E3	
201.5013	K	176.0009	.0166	.0093	7.9	.173E+00	M1	M1
	L1	*197.7937	.0473	.0032	25.4	.587E-01		
203.7252	K	178.2120	.0172	.0079	5.7	.187E+00	M1+E2	M1+E2
204.5825	K	179.0996	.0486	.0022	35.0	.640E+00	M2	(M2)
206.7599	K	181.2261	.0520	.0019	40.1	.252E+00	E2	E2
209.0564	K	183.5820	.0545	.0015	42.3	.974E+00	M2,E3	
209.6972	K	184.1799	.0319	.0033	15.4	.285E+00	E2	E2
211.3350	K	185.8305	.0413	.0026	15.5	.216E+00	E2	E2
212.3697	K	186.8535	.0269	.0079	6.7	.144E+00	M1	M1
	L1	*208.5746	.0372	.0026	23.6	.473E-01		
213.5330	K	*188.0158	.0390	.0032	14.7	.383E+00		M1+E2
214.2814	K	188.7552	.0300	.0028	12.3	.236E+00	E2	E2
214.6938	K	189.2342	.0304	.0057	15.4	.261E+00	E2	E2
	L1	*210.9593	.0467	.0028	24.9	.130E+00	E3	
214.8453	K	189.3475	.0403	.0045	18.4	.169E+00	M1+E2	M1+E2
	L1	*210.9593	.0467	.0028	24.9	.108E+00	M2,E3	
215.6353	K	190.1043	.0400	.0036	17.2	.420E+00		(E2)
219.1163	K	193.5218	.0436	.0026	22.9	.309E+00		M1,E2
223.3613	K	*197.7937	.0473	.0032	25.4	.819E-01		(M1)
224.2607	K	198.7377	.0339	.0028	18.7	.131E+00	M1	M1
230.8998	K	205.3844	.0315	.0023	14.0	.867E-01		M1
231.6343	K	206.1153	.0282	.0158	8.5	.114E+00	M1	M1
	L1	*227.8521	.0318	.0032	9.7	.234E-01		
232.6074	K	207.0883	.0294	.0048	8.4	.135E+00	M1+E2	M1+E2
233.6572	K	208.2370	.0527	.0022	32.0	.318E+00		
234.1061	K	*208.5746	.0372	.0026	23.6	.182E+01		
235.2444	K	209.7330	.0452	.0065	17.3	.118E+01		
235.7211	K	210.1982	.0284	.2660	1.6	.111E+00	M1	M1
	L1	231.9200	.0302	.0306	2.1	.127E-01	M1	
	L2	*232.1280	.0308	.0125	5.6	.519E-02	M2	
	L3	*232.3897	.0338	.0026	17.3	.107E-02	M1+E2	

E-GAMMA (KEV)	SHELL		E-ELECTRON (KEV)	ERROR (KEV)	INTENSITY (I/100N)	ERROR (%)	I.C.C.	MULTI-POLARITY	FINAL ASSIGNMENT
	MT		235.0266	.0312	.0067	8.0	.278E-02	M1+E2	
235.9129	K		210.3941	.0285	.1075	2.7	.126E+00	M1+E2	M1+E2
	L1	*	232.1280	.0308	.0125	5.6	.146E-01	M1+E2	
	L2	*	232.3897	.0338	.0026	17.3	.300E-02	M1+E2	
	L3		232.5692	.0518	.0022	23.6	.256E-02	M1+E2	
	MT		235.2441	.0446	.0028	14.4	.326E-02	M1+E2	
236.2452	K		210.7143	.0293	.0045	20.6	.138E+00	E2	E2
237.0309	K		211.5113	.0285	.0399	1.5	.356E-01	E1	E1
	L1		233.2466	.0326	.0042	9.8	.378E-02	E1	
	MT		236.3941	.0616	.0025	39.0	.219E-02	M1	
237.2567	K		211.7402	.0286	.0209	2.3	.107E+00	M1	M1
	L1		233.4860	.0362	.0026	13.7	.135E-01	M1	
238.3200	K		212.8066	.0291	.0066	9.1	.986E-01	M1	M1
	L1	*	234.4905	.0656	.0019	42.6	.286E-01	E2	
244.8277	K		219.3127	.0292	.0125	2.5	.981E-01	M1	M1
	L1		241.0725	.0367	.0041	12.5	.325E-01		
249.4432	K		223.9268	.0317	.0040	11.6	.795E-01	M1	M1
252.2176	K		226.7016	.0302	.0068	6.7	.826E-01	M1	M1
253.4073	K	*	227.8521	.0318	.0032	9.7	.273E+00		(E2)
259.7975	K		234.2328	.0612	.0021	39.1	.135E+00	E2	E2
259.9926	K	*	234.4905	.0656	.0019	42.6	.108E+01		
262.3711	K		236.8772	.0307	.0086	12.2	.824E-01	M1	M1
265.0598	K		239.5573	.0451	.0034	14.0	.183E+00		(E2)
266.0805	K		240.5900	.0314	.0089	5.2	.305E-01		E1
	L1		262.2972	.0568	.0030	26.2	.103E-01	M1,E2	
267.1973	K		241.7018	.0309	.1356	1.9	.808E-01	M1+E2	M1
	L1		263.4357	.0329	.0168	3.0	.998E-02	M1+E2	
	L2	*	263.7464	.0617	.0020	34.4	.121E-02	M1+E2	
	L3	*	263.7464	.0617	.0020	34.4	.121E-02	M1+E2	
	MT		266.5627	.0469	.0039	10.7	.230E-02	M1+E2	
268.2947	K		242.8042	.0332	.0046	35.3	.860E-01	M1,E2	M1,E2
268.9341	K		243.4387	.0346	.0032	20.1	.858E-01	M1	M1
269.3320	K		243.8828	.0523	.0023	22.7	.131E+00	E2	E2
270.1248	K		244.6360	.0312	.0261	1.8	.787E-01	M1+E2	M1
	L1		266.4114	.0678	.0035	35.0	.105E-01	M1,E2	
282.1278	K		256.6307	.0386	.0022	28.2	.807E-01	M1,E2	M1,E2
283.7069	K	*	258.1935	.0679	.0016	42.3	.150E+00	E2	(E2)
283.8242	K	*	258.1935	.0679	.0016	42.3	.226E+00	M2	(E2)
284.4710	K		258.9876	.0532	.0036	20.9	.112E+00	E2	(E2)
287.0459	K		261.5811	.0326	.0163	2.9	.746E-01	M1+E2	M1+E2
	L1		283.3207	.0534	.0023	14.8	.106E-01	E2	
292.7221	K		267.2373	.0550	.0029	21.2	.197E+00		(M2)
294.1131	K		268.6258	.0534	.0026	22.9	.189E+00		

LIST OF INTERNAL CONVERSION ELECTRONS

E-GAMMA (KEV)	SHELL		E-ELECTRON (KEV)	ERROR (KEV)	INTENSITY (I/100N)	ERROR (%)	I.C.C.	MULTI-POLARITY	FINAL ASSIGNMENT
301.3819	K		275.9304	.0537	.0020	17.6	.722E-01	E2	E2
302.1967	K		276.7410	.0361	.0041	17.7	.653E-01	M1,E2	M1,E2
302.8150	K		277.3677	.0350	.0044	6.9	.731E-01	E2	E2
304.5092	K		279.0639	.0354	.0050	7.0	.903E-01		E2
304.6982	K		279.2779	.0638	.0027	31.5	.154E+00		(E2)
307.0053	K		281.6013	.0626	.0013	29.9	.173E+00	M2	(M2)
308.0027	L1		304.1618	.0427	.0015	18.9	.536E-01		
318.6650	K		293.2357	.0686	.0011	44.1	.280E+00	M2,E3	
320.1805	K		294.6805	.0380	.0019	14.1	.461E-01	M1	M1
321.3978	K		295.8742	.0561	.0016	32.3	.736E-01	E2	E2
326.9336	K		301.4643	.0403	.0015	17.0	.693E-01	E2	E2
328.1987	K		302.6831	.0363	.0022	11.3	.621E-01	E2	E2
333.7300	K		308.2553	.0644	.0012	38.0	.357E+00		
338.8753	K		313.3643	.0270	.0046	7.0	.134E-01	E1	E1
	L1	*	335.0773	.0252	.0293	2.3	.863E-01		
342.4226	K		316.8790	.0429	.0020	19.1	.100E+00		
345.4739	K		319.9664	.0274	.0039	10.6	.410E-01	M1	M1
350.0909	K		324.5870	.0248	.0161	2.5	.423E-01	M1+E2	M1+E2
	L1		346.2986	.0378	.0025	9.3	.643E-02		
357.5090	K		331.9886	.0258	.0061	8.8	.420E-01	E2	M1,E2
	L1		353.6614	.0464	.0014	18.8	.926E-02		
358.1371	K		332.6265	.0254	.0061	3.8	.403E-01	E2	M1,E2
359.4709	K		333.9823	.0422	.0014	16.1	.139E-01	E1	E1
360.5856	K	*	335.0773	.0252	.0293	2.3	.393E-01	E2	E2
	L1		356.7967	.0292	.0029	9.0	.384E-02	M1	
	MT		359.8900	.0496	.0018	21.6	.239E-02		
366.1795	K		340.6739	.0701	.0011	40.6	.132E-01	E1	E1
	L1	*	362.4459	.0416	.0018	12.8	.217E-01		
367.0147	K		341.5342	.0295	.0026	10.1	.354E-01	M1,E2	M1,E2
372.2603	K		346.7263	.0410	.0023	14.3	.498E-01		M1,E2
375.7853	K		350.3746	.0477	.0018	22.2	.101E+00	M2,E3	(M2)
376.7593	K		351.2320	.0272	.0058	6.5	.356E-01	E2	M1,E2
377.3430	K		351.8452	.0361	.0019	17.2	.563E-01		
378.0486	K		352.5448	.0294	.0064	9.0	.357E-01	E2	M1,E2
378.2434	K		352.7277	.0284	.0052	8.3	.296E-01	M1	M1,E2
380.0533	K		354.5291	.0262	.0066	6.2	.390E-01	E2	E2
381.1659	K		355.6298	.0261	.0070	3.0	.107E-01	E1	E1
	L1		377.3736	.0538	.0015	24.6	.231E-02		
384.6277	K		359.1287	.0474	.0023	19.3	.649E-01		
387.9327	K	*	362.4459	.0416	.0018	12.8	.671E-01		
391.7204	K		366.2976	.0467	.0016	18.6	.172E+00		
392.5965	K		367.0552	.0554	.0016	26.7	.669E-01		
396.3529	K		370.8534	.0376	.0014	32.6	.342E-01	M1,E2	M1,E2

E-GAMMA (KEV)	SHELL	E-ELECTRON (KEV)	ERROR (KEV)	INTENSITY (I/100N)	ERROR (%)	I.C.C.	MULTI-POLARITY	FINAL ASSIGNMENT
402.0356	K	376.4776	.0337	.0018	23.7	.415E-01	E2	E2
407.9761	K	382.4613	.0534	.0013	22.6	.973E-01	M2,E3	M2,E3
408.4629	K	382.8923	.0390	.0015	22.8	.324E-01	M1,E2	M1,E2
408.7541	K	383.2419	.0277	.0058	4.7	.273E-01	M1,E2	M1,E2
	L1	404.9924	.0387	.0016	17.0	.753E-02		
410.3291	K	384.8792	.0479	.0021	18.7	.352E-01	E2	E2
417.0230	K	391.5073	.0289	.0033	6.7	.234E-01	M1,E2	M1,E2
419.7801	K	394.2298	.0501	.0010	20.6	.230E-01	M1,E2	M1,E2
423.5572	K	398.0191	.0280	.0061	4.1	.258E-01	M1,E2	M1,E2
	L1	*419.8467	.0488	.0026	17.2	.109E-01	M2,E3	
	MT	422.8188	.0387	.0018	14.7	.762E-02		
428.0021	K	402.4480	.0402	.0022	14.3	.217E-01	M1,E2	M1,E2
431.2406	K	405.7368	.0288	.0042	9.5	.277E-01	E2	M1,E2
441.9973	K	416.4003	.0492	.0023	18.4	.365E-01		M1,E2
443.1247	K	417.5894	.0525	.0012	21.3	.137E+00		
445.3980	K	*419.8467	.0488	.0026	17.2	.544E-01	E3	
445.7124	K	420.2122	.0592	.0015	24.4	.805E-01	M2,E3	M2,E3
446.3270	K	420.8046	.0418	.0016	18.1	.339E-01		M1,E2
450.7389	K	425.1962	.0363	.0018	13.4	.293E-01		M1,E2
452.1509	K	426.6456	.0337	.0022	11.7	.234E-01	M1,E2	M1,E2
461.4594	K	435.9488	.0860	.0012	45.9	.106E-01	E1	E1
464.7332	K	439.1983	.0351	.0027	19.5	.197E-01	M1,E2	M1,E2
468.5735	K	443.0838	.0395	.0014	15.4	.366E-01		M1,E2
476.0894	K	*450.7394	.0840	.0009	40.1	.591E-01	M2,E3	M1,E2
476.2581	K	*450.7394	.0840	.0009	40.1	.406E-01	M2,E3	M1,E2
484.3874	K	458.8412	.0467	.0016	13.1	.184E-01	M1,E2	M1,E2
488.7010	K	463.2193	.0486	.0022	14.2	.227E-01	M1,E2	M1,E2
495.6992	K	470.1941	.0303	.0095	3.1	.220E-01	M1,E2	M1,E2
	L1	491.9197	.0526	.0019	10.9	.435E-02	M2,E3	
502.9754	K	477.4735	.0587	.0021	23.6	.434E-01	M2,E3	M2,E3
507.3653	K	481.8717	.0569	.0010	20.8	.270E-01		
522.7246	K	497.1809	.0571	.0021	20.0	.351E-01		M2,E3
524.4992	K	498.9787	.0316	.0060	12.0	.192E-01	M1,E2	M1,E2
526.3299	K	500.7908	.0589	.0011	21.2	.626E-02	E1	E1
536.1266	K	510.6083	.0320	.0072	3.6	.168E-01	M1,E2	M1,E2
	L1	532.2498	.0524	.0014	14.9	.328E-02		
538.3937	K	512.8973	.0320	.0069	9.6	.200E-01		M1,E2
	L1	534.5771	.0507	.0015	12.6	.437E-02		
544.1371	K	518.6211	.0361	.0018	9.2	.124E-01	M1,E2	M1,E2
549.3251	K	523.8133	.0324	.0065	3.5	.197E-01		M1,E2
549.8369	K	524.3475	.0365	.0022	8.6	.123E-01	M1,E2	M1,E2
550.1861	K	524.6688	.0375	.0020	12.1	.125E-01	M1,E2	M1,E2
552.5916	K	527.1110	.0652	.0012	24.0	.142E-01	M1,E2	M1,E2

E-GAMMA (KEV)	SHELL	E-ELECTRON (KEV)	ERROR (KEV)	INTENSITY (I/100N)	ERROR (%)	I.C.C.	MULTI-POLARITY	FINAL ASSIGNMENT
574.1173	K	548.5716	.0663	.0012	25.2	.766E-01		
574.9165	K	549.4140	.0373	.0020	9.6	.126E-01	M1,E2	M1,E2
583.8035	K	558.1911	.0627	.0008	22.4	.130E-01	M1,E2	M1,E2
586.8945	K	561.4021	.0390	.0023	9.4	.853E-02	M1,E2	M1,E2
588.6239	K	563.1110	.0344	.0037	9.9	.922E-02	M1,E2	M1,E2
	L1	*584.7819	.0588	.0017	17.2	.429E-02	M2	
593.8377	K	568.3393	.0366	.0030	7.9	.106E-01	M1,E2	M1,E2
610.3374	K	*584.7819	.0588	.0017	17.2	.326E-01	M2,E3	
610.9268	K	585.3437	.0606	.0014	18.5	.678E-01		
613.9538	K	588.3229	.0642	.0014	22.0	.119E-01	M1,E2	M1,E2
620.2095	K	594.6888	.0375	.0028	7.9	.110E-01	M1	M1,E2
628.5062	K	602.9163	.1173	.0008	50.3	.177E-01		
632.1096	K	606.5275	.0658	.0012	21.5	.194E-01	E3	
648.2789	K	622.8678	.0740	.0008	27.6	.235E-01	M2,E3	
652.7190	K	627.2192	.0599	.0013	16.2	.821E-02	M1,E2	M1,E2

Comments * Electron line assigned to two or more corresponding gamma-transitions

(m) Multipolarities assigned by MPFILE within intensity errors

(f) Final assignment of multipolarities taking doublet assignments, L1:L2:L3 ratios and experimental conditions into account

Table 7.

LIST OF UNASSIGNED GAMMA-TRANSITIONS (1)

E-GAMMA (KEV)	ERROR (KEV)	INTENSITY (I/100N)	ERROR (%)	MULTI-POLARITY
35.2281	.0016	.0424	38.2	
50.7983	.0019	.0405	28.6	
50.8321	.0045	.0167	47.5	
58.0571	.0012	.0917	21.1	E1
63.5551	.0086	.0141	52.4	E1
63.7629	.0013	.1207	19.7	E1
65.7813	.0052	.0163	35.8	
66.0019	.0060	.0138	39.3	
66.0613	.0097	.0084	54.9	
101.8546	.0019	.1389	16.1	M1
102.5408	.0017	.0201	26.8	E1
103.9407	.0014	.0313	18.8	M1+E2
104.2191	.0023	.0063	25.8	
107.1307	.0022	.0167	20.4	M1
107.7742	.0013	.0165	31.2	M1
108.8643	.0015	.0131	19.9	M1
109.6954	.0020	.0783	24.0	M1
109.9225	.0033	.0115	31.6	M1
110.1529	.0032	.0153	22.6	M1
111.5740	.0039	.0052	30.2	
112.1323	.0033	.1493	18.4	M1
112.7852	.0026	.0981	21.5	M1
116.7533	.0045	.0150	30.0	
118.2789	.0085	.0052	31.9	
118.9903	.0024	.0074	22.7	
126.5428	.0033	.0063	23.6	
129.0332	.0024	.0133	16.1	M1+E2
131.4934	.0062	.0057	26.3	
132.1484	.0012	.0197	13.4	
135.9048	.0091	.0097	45.8	(M1)
137.0285	.0041	.0163	12.7	M1+E2
137.9512	.0019	.0362	12.8	M1
141.1598	.0052	.0048	29.4	
142.0353	.0025	.0078	16.1	
142.6905	.0011	.0193	12.0	M1+E2
143.5209	.0053	.0045	32.7	
145.0306	.0096	.0033	29.4	
145.4511	.0044	.0048	31.0	
146.0166	.0141	.0023	37.8	
148.5258	.0034	.0069	21.8	
154.1448	.0021	.0106	12.9	
154.5307	.0049	.0107	14.9	
156.2459	.0030	.1247	9.6	M1

LIST OF UNASSIGNED GAMMA-TRANSITIONS (2)

E-GAMMA (KEV)	ERROR (KEV)	INTENSITY (I/100N)	ERROR (%)	MULTI-POLARITY
157.5424	.0024	.0136	16.7	
158.6088	.0048	.0054	20.5	
159.2676	.0097	.0084	25.8	(E2)
160.1954	.0042	.0076	29.4	
160.3777	.0028	.0227	11.8	
163.3497	.0114	.0031	26.6	
164.6804	.0031	.0121	12.7	(E2)
164.7764	.0050	.0057	20.8	
164.9471	.0071	.0098	13.9	
165.1215	.0027	.0479	15.4	M1
165.4410	.0028	.0120	14.2	
167.0515	.0021	.1605	8.4	M1
167.5079	.0037	.0104	11.6	
171.4419	.0034	.0182	11.6	
172.8197	.0022	.0898	8.6	M1
173.2091	.0034	.0108	12.0	
175.0495	.0072	.0064	51.4	
175.2403	.0025	.0881	9.7	M1
178.7429	.0032	.0690	11.0	M1
179.0562	.0064	.0060	21.9	
179.5380	.0035	.0073	16.5	
180.9651	.0025	.0213	9.3	M1+E2
181.2506	.0031	.0276	9.2	M1+E2
182.3379	.0060	.0073	15.4	
183.0736	.0054	.0044	23.0	
187.2625	.0034	.0086	14.0	
187.7665	.0031	.0196	9.7	(E2)
188.2347	.0079	.0055	15.8	
188.8343	.0059	.0113	17.4	
189.3794	.0044	.0038	22.4	
189.7968	.0165	.0020	37.1	
190.3362	.0016	.0162	13.3	(E2)
190.9150	.0034	.0059	65.6	
191.9022	.0036	.0081	17.4	
194.1778	.0016	.0170	9.5	(E2)
194.7044	.0058	.0126	11.2	
196.3368	.0095	.0066	22.6	
199.7848	.0176	.0064	17.0	
199.8771	.0058	.0071	15.4	
200.5031	.0079	.0092	15.0	
201.0169	.0093	.0083	18.2	
201.5799	.0064	.0205	18.0	
203.7252	.0029	.1218	8.3	M1+E2

LIST OF UNASSIGNED GAMMA-TRANSITIONS T7(3)

E-GAMMA (KEV)	ERROR (KEV)	INTENSITY (I/100N)	ERROR (%)	MULTI-POLARITY
203.9458	.0041	.0101	13.3	
204.5825	.0054	.0099	10.9	(M2)
204.8829	.0035	.0176	10.1	
205.4451	.0026	.0175	11.4	
206.7599	.0021	.0219	9.5	E2
207.4422	.0062	.0048	24.9	
208.3683	.0081	.0022	80.8	
208.7643	.0092	.0031	39.2	
209.0564	.0084	.0046	18.8	
210.3419	.0136	.0041	26.4	
211.3350	.0037	.0348	11.2	E2
213.0389	.0242	.0041	45.8	
213.5330	.0021	.0243	10.2	M1+E2
214.1275	.0029	.0120	11.1	
214.8453	.0014	.0759	9.6	M1+E2
215.6353	.0018	.0249	10.6	(E2)
216.8438	.0141	.0032	44.6	
217.1465	.0039	.0224	11.4	
217.3176	.0245	.0053	33.4	
217.9687	.0059	.0051	22.8	
218.8711	.0051	.0057	22.6	
219.1163	.0014	.0241	11.2	M1,E2
221.1001	.0858	.0024	33.0	
221.9997	.0049	.0207	11.4	
225.6726	.0021	.0248	12.3	
226.0145	.0131	.0130	14.4	
226.2918	.0067	.0054	24.5	
226.8929	.0204	.0051	24.1	
228.2586	.0017	.0263	9.9	
229.5481	.0026	.0303	11.9	
230.4123	.0099	.0077	17.1	
231.3200	.0098	.0059	32.1	
231.8175	.0069	.0137	23.3	
232.2855	.0035	.0132	12.7	
232.6074	.0069	.1030	9.9	M1+E2
234.5661	.0060	.0080	12.1	
235.2444	.0034	.0159	13.2	
238.3200	.0015	.1922	8.3	M1
239.1296	.0112	.0069	19.2	
240.2569	.0108	.0041	44.8	
241.3982	.0057	.0345	12.8	
241.5112	.0092	.0135	19.3	
241.6976	.0059	.0252	10.6	

LIST OF UNASSIGNED GAMMA-TRANSITIONS T7(4)

E-GAMMA (KEV)	ERROR (KEV)	INTENSITY (I/100N)	ERROR (%)	MULTI-POLARITY
242.3865	.0200	.0031	47.5	
242.7597	.0020	.0207	8.9	
243.1718	.0152	.0043	36.0	
244.6457	.0187	.0088	35.4	
245.2356	.0038	.0159	13.0	
246.6076	.0081	.0056	24.9	
247.0261	.0047	.0348	9.0	
247.7706	.0108	.0204	12.3	
249.2863	.0059	.0155	14.5	
250.6107	.0111	.0073	25.1	
251.3729	.0257	.0056	25.1	
253.8253	.0142	.0058	15.8	
255.4649	.0210	.0062	14.1	
256.4417	.0113	.0054	24.2	
256.8290	.0042	.0161	12.4	
257.2301	.0061	.0064	17.4	
257.7718	.0151	.0063	15.5	
258.2905	.0099	.0053	19.1	
258.7336	.0134	.0054	28.3	
259.7975	.0024	.0443	8.7	E2
261.7069	.0171	.0064	52.9	
263.3551	.0199	.0110	22.1	
263.6204	.0035	.0206	10.4	
263.9358	.0029	.0467	8.6	
265.0598	.0062	.0537	10.5	(E2)
266.7654	.0051	.0158	16.8	
268.2947	.0033	.1555	10.9	M1,E2
269.3320	.0030	.0514	11.1	E2
270.3817	.0063	.0215	16.7	
270.6843	.0043	.0371	10.3	
274.1116	.0237	.0085	17.9	
274.6715	.0179	.0039	28.2	
275.8314	.0054	.0181	13.2	
277.0454	.0051	.0143	13.6	
279.5123	.0025	.0248	14.0	
283.8242	.0095	.0202	19.8	(E2)
286.2145	.0184	.0071	27.4	
286.4211	.0106	.0116	20.0	
289.1806	.0053	.0109	17.2	
292.7221	.0036	.0422	11.0	(M2)
293.2306	.0042	.0249	14.6	
293.8021	.0062	.0329	12.1	
295.0265	.0060	.0142	13.5	

LIST OF UNASSIGNED GAMMA-TRANSITIONS T7(5)

E-GAMMA (KEV)	ERROR (KEV)	INTENSITY (I/100N)	ERROR (%)	MULTI-POLARITY
295.5274	.0132	.0066	23.5	
295.9533	.0168	.0039	27.0	
297.3144	.0271	.0085	23.6	
298.6042	.0134	.0112	16.9	
300.5807	.0123	.0078	26.3	
301.3819	.0060	.0782	12.7	E2
306.3719	.0109	.0112	14.6	
306.7371	.0108	.0090	18.0	
307.0053	.0079	.0222	11.9	(M2)
307.3593	.0039	.0156	14.0	
308.0027	.0034	.0790	10.8	
309.5357	.0225	.0044	27.4	
310.1445	.0712	.0057	66.4	
310.8489	.0295	.0048	13.8	
313.2611	.0119	.0050	14.9	
316.2686	.0057	.0058	20.8	
316.4487	.0060	.0055	21.1	
316.8096	.0043	.0276	23.1	
318.6650	.0082	.0114	18.6	
319.5789	.0107	.0105	16.0	
320.8762	.0241	.0090	24.3	
321.3978	.0061	.0626	9.0	E2
321.9741	.0141	.0061	18.7	
322.1770	.0292	.0091	15.7	
322.4894	.0024	.0752	8.5	
322.6914	.0051	.0116	16.1	
324.3431	.0069	.0243	9.5	
324.7991	.0080	.0389	10.4	
324.9470	.0093	.0198	11.9	
326.4043	.0191	.0030	27.9	
326.9336	.0046	.0604	8.5	E2
327.2098	.0083	.0058	33.1	
328.1987	.0023	.1021	9.3	E2
329.5853	.0339	.0043	342.3	
330.8715	.0311	.0053	54.7	
332.4966	.0135	.0080	15.6	
333.7300	.0082	.0097	11.0	
334.7582	.0049	.0283	9.1	
335.4711	.0120	.0190	10.0	
335.8208	.0029	.0633	15.7	
336.4366	.0167	.0094	15.0	
337.3692	.0230	.0090	12.5	
339.4669	.0063	.0068	19.7	

LIST OF UNASSIGNED GAMMA-TRANSITIONS T7(6)

E-GAMMA (KEV)	ERROR (KEV)	INTENSITY (I/100N)	ERROR (%)	MULTI-POLARITY
341.2049	.0190	.0103	20.3	
342.4226	.0051	.0576	8.6	
342.9168	.0108	.0093	15.3	
346.2890	.0031	.0201	9.7	
347.4187	.0600	.0061	21.9	
347.9655	.0028	.0468	10.0	
350.7634	.0357	.0118	21.7	
351.1284	.0047	.0266	13.7	
351.7399	.0052	.0248	12.0	
352.2341	.0139	.0067	21.8	
352.6171	.0060	.0107	17.7	
353.8594	.0160	.0059	28.6	
354.3142	.0414	.0043	24.4	
355.1816	.0272	.0074	18.5	
356.5717	.0181	.0080	19.4	
357.5090	.0043	.4215	9.0	M1,E2
360.0752	.0134	.0277	14.6	
361.7416	.0209	.0078	15.7	
362.7892	.0102	.0106	26.9	
364.2357	.0273	.0153	24.8	
364.7779	.0137	.0056	33.6	
365.1058	.0070	.0747	9.2	
365.5033	.0182	.0088	13.1	
366.4553	.0114	.0404	11.6	
366.7948	.0129	.0106	24.2	
368.3206	.0072	.0672	8.4	
368.7592	.0994	.0052	62.4	
369.4900	.0181	.0073	16.5	
374.9415	.0121	.0229	10.9	
375.7853	.0060	.0513	10.0	(M2)
376.7593	.0052	.4657	8.1	M1,E2
377.3430	.0034	.0974	8.6	
379.0599	.0058	.0416	12.1	
382.2368	.0420	.0046	37.4	
384.6277	.0065	.1002	8.9	
384.8660	.0125	.0198	19.1	
385.2921	.0226	.0137	12.8	
385.5949	.0079	.0131	12.1	
386.2255	.0109	.0407	8.9	
386.6123	.0208	.0211	12.4	
387.9327	.0083	.0791	10.4	
388.3275	.0088	.0484	15.7	
389.2977	.0102	.0053	19.4	

LIST OF UNASSIGNED GAMMA-TRANSITIONS T7(7)

E-GAMMA (KEV)	ERROR (KEV)	INTENSITY (I/100N)	ERROR (%)	MULTI-POLARITY
389.5766	.0098	.0050	18.4	
391.4313	.0307	.0233	26.3	
391.7204	.0155	.0275	13.5	
392.5965	.0253	.0668	13.0	
393.1006	.0195	.0303	10.3	
394.0763	.0125	.0038	34.1	
395.0706	.0264	.0136	18.7	
396.9744	.0132	.0185	22.2	
397.9927	.0084	.0225	16.0	
399.2642	.0235	.0040	23.6	
399.7837	.0092	.0446	21.4	
400.6679	.0269	.0201	13.8	
401.2475	.0070	.0724	22.1	
403.2500	.0320	.0128	35.6	
407.1745	.0079	.0402	19.4	
407.9761	.0169	.0395	24.3	M2,E3
408.4629	.0078	.1299	9.9	M1,E2
409.9276	.0111	.0200	30.9	
410.3291	.0074	.1678	19.7	E2
411.0944	.0094	.0333	16.9	
411.9128	.0124	.0168	33.9	
413.8201	.0244	.0149	15.5	
415.7726	.0081	.0110	30.4	
419.2017	.0070	.0204	27.0	
419.7801	.0066	.1285	15.2	M1,E2
421.1511	.0292	.0165	24.5	
423.3343	.0251	.0484	34.7	
424.2266	.0157	.0309	20.0	
425.9499	.0492	.0112	28.9	
429.8656	.0360	.0316	28.1	
431.2406	.0072	.4322	16.4	M1,E2
433.8142	.0069	.0395	16.0	
434.5974	.0069	.0499	18.0	
435.9356	.0428	.0178	13.6	
439.8000	.0172	.0235	22.4	
440.0394	.0267	.0172	54.5	
440.6600	.0165	.0095	20.2	
442.8533	.0140	.0099	21.5	
443.1247	.0370	.0250	22.7	
445.7124	.0230	.0534	11.4	M2,E3
447.6216	.0232	.0085	27.7	
448.1474	.0091	.0083	36.8	
449.4242	.1297	.0176	38.2	

LIST OF UNASSIGNED GAMMA-TRANSITIONS T7(8)

E-GAMMA (KEV)	ERROR (KEV)	INTENSITY (I/100N)	ERROR (%)	MULTI-POLARITY
452.1509	.0067	.2743	13.6	M1,E2
455.2220	.0125	.0654	11.6	
456.1824	.0193	.0646	12.2	
457.5859	.0204	.0236	13.6	
460.4844	.0072	.0144	27.1	
464.3174	.0119	.1179	12.9	
465.7733	.0132	.0186	29.2	
466.1614	.0105	.0700	12.1	
467.0330	.0053	.0251	32.5	
467.2882	.0114	.0186	33.2	
468.2370	.0069	.0410	21.6	
468.5735	.0048	.1099	26.8	M1,E2
469.4058	.0080	.0181	34.4	
470.9186	.0149	.0079	27.9	
472.4302	.0091	.0082	21.3	
473.1816	.0035	.0386	27.1	
473.5419	.0051	.0141	32.4	
474.3723	.0057	.0187	31.0	
474.6021	.0140	.0109	23.6	
476.0894	.0061	.0445	19.8	M1,E2
479.0367	.0075	.0157	26.4	
479.3960	.0043	.0556	35.8	
479.7150	.0081	.0544	33.4	
480.0714	.0058	.0376	32.2	
480.4792	.0100	.0219	26.5	
481.1407	.0142	.0275	24.2	
482.2763	.0109	.0171	19.1	
483.0490	.0249	.0140	32.2	
484.7254	.0302	.0157	20.2	
485.1260	.0163	.0239	17.3	
486.4357	.0124	.0303	36.0	
489.3240	.0308	.0068	68.9	
490.0266	.0097	.0392	34.5	
490.8190	.0077	.0149	37.0	
491.4529	.0029	.0478	57.7	
492.1791	.0102	.0759	48.8	
493.3359	.0235	.0121	35.7	
494.9075	.0138	.0058	46.8	
497.5657	.0241	.0218	29.6	
498.0782	.0196	.1486	32.1	
500.6018	.0172	.0680	54.9	
502.1931	.0071	.0405	33.9	
502.9754	.0058	.1382	55.4	M2,E3

LIST OF UNASSIGNED GAMMA-TRANSITIONS T7(9)

E-GAMMA (KEV)	ERROR (KEV)	INTENSITY (I/100N)	ERROR (%)	MULTI-POLARITY
503.2058	.0086	.0372	20.4	
503.5988	.0119	.0118	50.3	
504.8418	.0078	.0198	30.6	
505.4970	.0098	.0187	38.3	
507.3653	.0027	.1105	28.5	
508.6207	.0054	.0401	23.8	
509.6632	.0047	.0438	32.4	
513.0145	.0118	.0134	45.8	
516.9505	.0118	.0351	22.9	
518.7836	.0038	.0646	19.4	
521.0391	.0033	.0876	22.3	
521.5213	.0132	.0114	51.3	
523.1506	.0126	.0196	24.0	
524.9590	.0113	.1144	19.7	
525.2503	.0170	.0270	28.8	
527.0977	.0124	.0593	20.2	
528.4697	.0097	.0183	21.3	
530.4803	.0059	.0442	18.9	
531.0336	.0121	.0235	26.7	
531.7638	.0091	.0208	42.2	
537.7539	.0213	.0233	22.6	
539.5102	.0037	.0724	27.8	
540.1093	.0071	.0275	21.5	
541.6307	.0199	.0106	34.7	
542.2426	.0073	.0260	23.9	
542.8932	.0389	.1229	55.7	
544.7360	.0114	.0240	41.8	
545.1314	.0139	.0254	27.8	
547.6181	.0043	.0797	22.2	
548.1226	.0088	.0294	18.3	
550.1861	.0039	.4707	30.4	M1,E2
552.5916	.0048	.2414	24.4	M1,E2
554.6054	.0081	.1240	16.0	
555.1910	.0103	.0285	19.5	
557.6435	.0086	.0310	16.6	
558.5805	.0081	.0179	33.7	
559.5066	.0288	.0275	20.5	
560.4381	.0064	.0503	21.1	
560.8245	.0079	.0727	23.8	
561.3579	.0134	.0289	22.1	
561.6555	.0080	.0875	17.1	
564.8285	.0053	.0788	17.9	
565.4715	.0455	.0247	24.1	

LIST OF UNASSIGNED GAMMA-TRANSITIONS T7(10)

E-GAMMA (KEV)	ERROR (KEV)	INTENSITY (I/100N)	ERROR (%)	MULTI-POLARITY
566.0231	.0035	.0940	25.0	
567.7362	.0100	.0103	42.6	
568.7054	.0294	.0130	55.3	
569.4387	.0052	.0295	32.1	
570.4614	.0058	.0254	40.8	
571.1414	.0179	.0103	49.3	
574.1173	.0065	.0452	20.5	
576.2010	.0276	.0057	30.7	
578.6335	.0100	.0207	17.1	
579.6647	.0069	.0365	16.5	
580.2173	.0143	.0155	31.0	
580.9290	.0065	.0452	19.5	
581.8844	.0059	.0374	24.5	
583.0400	.0436	.0108	32.9	
583.8035	.0051	.1872	18.0	M1,E2
584.3341	.0072	.0278	24.4	
585.2001	.0095	.0687	17.5	
586.4065	.0170	.0523	22.9	
590.0607	.0122	.0210	19.3	
591.0191	.0080	.0379	18.3	
591.4931	.0074	.0399	21.2	
592.1890	.0161	.0296	17.6	
593.8377	.0050	.8259	20.6	M1,E2
594.9614	.0108	.0323	17.3	
596.6165	.0536	.0138	29.4	
597.1472	.0119	.0200	20.8	
597.8844	.0121	.0562	20.4	
598.9707	.0102	.0275	26.4	
599.9002	.0200	.0126	21.0	
600.3615	.0263	.0291	23.6	
601.0252	.0100	.0328	30.2	
601.2388	.0215	.0546	17.1	
602.5350	.0237	.0129	26.7	
604.3618	.0078	.0223	18.4	
607.7183	.0413	.0321	39.2	
608.8132	.0069	.0505	22.2	
610.3374	.0041	.1514	27.0	
610.9268	.0096	.0607	32.8	
611.7540	.0222	.0235	22.3	
615.2871	.0069	.0582	15.6	
616.8509	.0206	.0205	25.5	
617.7619	.0103	.0690	31.0	
619.0641	.0116	.0280	19.2	

LIST OF UNASSIGNED GAMMA-TRANSITIONS T7(11)

E-GAMMA (KEV)	ERROR (KEV)	INTENSITY (I/100N)	ERROR (%)	MULTI-POLARITY
620.2095	.0042	.7383	16.5	M1,E2
621.3198	.0176	.0305	21.3	
622.8781	.0114	.0479	24.4	
624.0280	.0429	.0093	25.5	
624.9873	.0038	.1008	17.8	
627.6053	.0268	.0184	26.2	
628.1120	.0251	.0576	17.4	
628.5062	.0050	.1331	15.8	
628.8216	.0047	.1496	21.7	
629.8265	.0089	.1120	23.0	
630.1525	.0078	.0902	18.3	
631.1475	.0132	.0242	25.2	
634.4669	.0065	.0668	22.7	
635.0554	.0102	.0538	26.4	
635.9755	.0163	.0246	23.9	
637.6669	.0091	.0455	16.4	
639.2922	.0056	.0640	18.4	
639.8821	.0333	.0377	16.7	
640.7784	.0069	.0592	24.8	
644.5917	.0062	.0748	22.3	
645.0572	.0192	.0404	30.8	
646.0411	.0073	.0828	18.5	
646.6596	.0303	.0238	31.9	
647.4221	.0162	.0814	19.8	
649.7054	.0304	.0274	18.0	
651.7898	.0104	.0614	17.0	
652.7190	.0037	.4577	21.4	M1,E2
654.7215	.0212	.0305	22.3	
655.2635	.0115	.0599	59.0	
659.3976	.0250	.0297	23.1	
662.1709	.0165	.0592	23.8	
663.1753	.0193	.0286	19.8	
665.2014	.0115	.1793	16.5	
667.3535	.0396	.0220	23.5	
668.0105	.0094	.0505	24.3	
668.6125	.0176	.0280	27.9	
669.5486	.0074	.0513	22.2	
670.6365	.0061	.1486	16.6	
673.3184	.0147	.0262	20.5	
674.1889	.0103	.0934	18.8	
677.1262	.0141	.0366	17.6	
678.9846	.0223	.0175	22.8	
679.6731	.0372	.0095	24.3	

LIST OF UNASSIGNED GAMMA-TRANSITIONS T7(12)

E-GAMMA (KEV)	ERROR (KEV)	INTENSITY (I/100N)	ERROR (%)	MULTI-POLARITY
680.4829	.0262	.0351	24.9	
681.0445	.0086	.0531	25.3	
684.2153	.0080	.0534	21.6	
685.8761	.0048	.1717	20.0	
687.5637	.0101	.1019	16.6	
688.0364	.0070	.1132	17.0	
689.0937	.0166	.0272	29.4	
690.9764	.0101	.0463	16.2	
691.9486	.0100	.0488	23.0	
692.5891	.0145	.0325	19.1	
693.3640	.0234	.0186	26.6	
694.0111	.0079	.0702	14.9	
694.6963	.0349	.0174	27.1	
695.3699	.0165	.0427	16.8	
702.5056	.0200	.0359	26.9	
705.5504	.0213	.0188	27.9	
706.1522	.0149	.0468	21.1	
708.8608	.0236	.0259	18.5	
710.6491	.0208	.0293	20.0	
711.8117	.0453	.0326	22.5	
712.7955	.0079	.1120	17.4	
714.1141	.0063	.3105	16.0	
717.4295	.0140	.0868	32.0	
718.3969	.0062	.2177	25.9	
720.9029	.0515	.0681	24.6	
723.2317	.0130	.0530	25.2	
724.0499	.0128	.0816	17.9	
724.5557	.0062	.1753	15.2	
726.2154	.0099	.1456	18.4	
729.7088	.0216	.0255	19.6	
730.3629	.0118	.0802	23.6	
732.5504	.0100	.0463	18.6	
735.7849	.0615	.0274	19.2	
736.8733	.0078	.1350	17.9	
738.0064	.0360	.0265	27.4	
739.2090	.0334	.0221	21.2	
742.5031	.0202	.0218	33.8	
744.8775	.0297	.0437	20.9	
747.3662	.0078	.1394	25.0	
750.8038	.0073	.9200	14.3	
754.4019	.0053	.2094	14.4	
757.1356	.0108	.0707	15.8	
760.4661	.0136	.1247	15.9	

LIST OF UNASSIGNED GAMMA-TRANSITIONS T7(13)

E-GAMMA (KEV)	ERROR (KEV)	INTENSITY (I/100N)	ERROR (%)	MULTI-POLARITY
765.4932	.0362	.0539	17.7	
766.0530	.0546	.0868	16.3	
775.7024	.0150	.0878	14.6	
777.3825	.0422	.0419	19.8	
777.7568	.0139	.0498	18.8	
784.8875	.0399	.0705	18.9	
785.5592	.0040	.4117	14.6	
788.0143	.0094	.0845	15.7	
789.6064	.0100	.0894	21.4	
790.4902	.0412	.0330	21.7	
795.4186	.0275	.1690	16.3	
795.8493	.0117	.1313	17.5	
798.2168	.0116	.0749	14.9	
799.2399	.0166	.0476	19.2	
802.2883	.0159	.0471	15.8	
808.1075	.0335	.0123	37.8	
808.9093	.0218	.0236	21.3	
811.1830	.0481	.0261	21.9	
812.1641	.0080	.1057	14.4	
813.6420	.0185	.0644	26.6	
815.3551	.0113	.0838	15.1	
816.4416	.0170	.0642	15.7	
819.1317	.0316	.2459	25.0	
825.7314	.0232	.0268	25.3	
831.0088	.0237	.0874	15.6	
832.1399	.0278	.0366	17.5	
833.0466	.0493	.0385	22.3	
836.9575	.0219	.1093	15.9	
839.2237	.0094	.1007	15.2	
847.2985	.0200	.0499	16.7	
847.9785	.0336	.0257	19.9	
849.2523	.0239	.0527	16.5	
850.0160	.0740	.0275	19.2	
850.8818	.0239	.0570	16.5	
851.9310	.0732	.0304	17.9	
853.2701	.0223	.1928	14.5	
854.3150	.0099	.1380	15.4	
856.9674	.0170	.0554	21.3	
860.3220	.0125	.0910	16.1	
862.8651	.0164	.0623	21.4	
864.1202	.0325	.0347	23.4	
866.5761	.0326	.0840	30.8	
867.0958	.0738	.1532	30.5	

LIST OF UNASSIGNED GAMMA-TRANSITIONS T7(14)

E-GAMMA (KEV)	ERROR (KEV)	INTENSITY (I/100N)	ERROR (%)	MULTI-POLARITY
867.7751	.0114	.3428	16.9	
871.0597	.0659	.0820	25.1	
873.9443	.0512	.0217	22.6	
875.8303	.0390	.0360	20.0	
877.6965	.0859	.0430	25.8	
881.1573	.0183	.1383	16.6	
882.1871	.0211	.0811	16.0	
883.2690	.0192	.0717	16.5	
884.0223	.0374	.0522	21.8	
884.6960	.0339	.0527	21.7	
890.7929	.0213	.0484	28.8	
893.6378	.0181	.0610	26.8	
902.0757	.0609	.0379	23.0	
904.6141	.0464	.0295	21.4	
905.7751	.0199	.0827	16.0	
912.8356	.0203	.0704	16.6	
916.0655	.0078	.1982	14.6	
923.3810	.0272	.0500	26.5	
930.7946	.0431	.1004	18.5	
932.3482	.0065	.3482	20.4	
934.9658	.0205	.0736	17.0	
937.8332	.0222	.1013	16.0	
938.8262	.0123	.1304	15.5	
942.0571	.0205	.0639	17.0	
948.6767	.0142	.0883	18.9	
953.0637	.0213	.2491	20.4	
959.4028	.0159	.1050	17.4	
960.0684	.0095	.2183	30.9	
963.1247	.0385	.0609	16.3	
964.8122	.0325	.0426	18.0	
969.2856	.0468	.0854	19.3	
984.7230	.0273	.0976	35.2	
987.9928	.0270	.0937	25.5	
993.3543	.0339	.1043	19.7	
994.1302	.0178	.1511	23.6	
995.1415	.0448	.0779	20.9	
995.8936	.0426	.0741	21.3	
997.8630	.0415	.0330	19.5	
999.9673	.0379	.0406	18.5	
1003.1024	.0918	.0823	21.3	
1009.9414	.0724	.0665	28.6	
1023.2734	.0274	.0690	21.5	
1025.0996	.0396	.0331	18.4	

LIST OF UNASSIGNED GAMMA-TRANSITIONS T7(15)

E-GAMMA (KEV)	ERROR (KEV)	INTENSITY (I/100N)	ERROR (%)	MULTI-POLARITY
1028.4537	.0194	.0707	15.3	
1031.8809	.0209	.1257	15.1	
1039.0510	.0296	.0593	16.0	
1040.6002	.0183	.0511	16.4	
1042.8679	.0394	.0364	18.5	
1048.0327	.0192	.0845	15.6	
1050.6434	.0120	.1925	15.0	
1052.1065	.0317	.0614	20.6	
1055.0048	.1111	.0468	24.0	
1072.3644	.0286	.0759	33.0	
1080.1408	.0257	.1541	21.3	
1104.2308	.0528	.1466	25.4	
1110.1223	.0565	.0665	25.1	
1113.6633	.0554	.0951	26.8	
1117.5320	.0728	.0549	22.3	
1136.4970	.0135	.1948	18.1	
1149.8529	.0146	.2634	22.8	
1158.0073	.0269	.0936	18.6	
1175.1115	.0133	.3451	22.0	
1182.5957	.0371	.0819	18.0	
1185.4767	.0447	.0700	41.0	
1200.6807	.0251	.1215	16.8	
1205.6314	.0758	.0866	17.4	
1208.0213	.0548	.0825	31.3	
1213.2155	.0838	.0758	18.2	
1219.9276	.0273	.1924	17.7	
1229.2077	.0479	.0936	17.5	
1233.7228	.0650	.0630	21.5	
1257.2916	.0636	.0759	41.8	
1268.4780	.0399	.1337	21.2	
1282.5198	.0779	.0509	19.9	
1288.6885	.0566	.0933	20.5	
1290.6517	.0568	.1328	22.1	
1294.1169	.0651	.1112	39.1	
1302.8089	.0438	.1241	42.5	
1319.1578	.0602	.1553	23.6	
1325.2239	.1004	.1063	17.9	
1327.9070	.0724	.0931	31.7	
1339.9649	.0662	.1395	39.6	
1358.2076	.0854	.0603	19.5	
1383.3922	.0694	.1267	31.5	
1392.8673	.0976	.1019	17.4	
1397.1104	.0573	.0998	17.5	

LIST OF UNASSIGNED GAMMA-TRANSITIONS T7(16)

E-GAMMA (KEV)	ERROR (KEV)	INTENSITY (I/100N)	ERROR (%)	MULTI-POLARITY
1414.6975	.0920	.0614	20.0	
1495.7185	.0652	.0732	29.9	
1526.1431	.0841	.0876	18.9	
1566.0316	.0644	.1447	17.7	
1611.7239	.1161	.1574	23.0	
1752.2221	.0615	.2123	18.5	

Table 8.

LIST OF GAMMA-RAYS (PN4) T8 -(1)

E-GAMMA (KEV)	ERROR (KEV)	INTENSITY (I/100N)	ERROR (%)
1383.3984	.3162	.0731	14.2
1387.8204	.6311	.0349	28.4
1437.7730	.9258	.0371	38.9
1442.0951	.6850	.0734	24.1
1445.7973	.4966	.1244	15.1
1449.3509	.5362	.0824	23.0
1455.6106	.6603	.0489	28.3
1460.0593	.3307	.1015	13.9
1479.8419	.2123	.1588	9.4
1489.4243	.5550	.0556	25.3
1495.0393	.3668	.0851	16.8
1526.6229	.2705	.0808	12.3
1537.3634	.5445	.0411	23.8
1542.0813	.4774	.0469	20.8
1550.2495	.6487	.0309	29.9
1565.5391	.1941	.1214	8.1
1570.7028	.5047	.0439	21.3
1575.7567	.2813	.0773	12.2
1588.2910	.7009	.0265	32.6
1600.6022	.1715	.1277	7.3
1607.7220	.3208	.0754	13.4
1611.6241	.1714	.1587	6.6
1627.6518	.4536	.0404	21.1
1634.8295	.3766	.0493	17.3
1645.6295	1.2938	.0122	67.4
1652.0849	.5594	.0460	24.6
1655.3897	.5679	.0448	25.1
1666.3104	.3122	.0544	13.9
1671.9104	.4281	.0388	19.2
1678.4559	.6067	.0265	27.6
1684.1615	.3103	.0535	13.9
1690.8719	.5290	.0608	30.2
1693.8552	.8282	.0988	38.9
1695.9955	.9569	.0734	66.1
1706.8825	.4996	.0350	23.1
1713.9777	.1597	.1290	6.7
1720.9461	.3213	.0558	14.6
1730.2750	.3772	.0465	17.3
1738.0808	.4675	.0369	21.6
1747.2831	.5052	.0373	22.0
1752.0747	.1118	.2449	3.8
1759.6558	.3081	.0568	14.0
1789.5933	.5999	.0340	27.8

LIST OF GAMMA-RAYS (PN4) T8 -(2)

E-GAMMA (KEV)	ERROR (KEV)	INTENSITY (I/100N)	ERROR (%)
1797.0296	.4777	.0425	22.3
1808.7362	.2858	.0740	13.0
1824.0953	.3135	.0537	14.4
1830.4557	.5941	.0273	27.7
1840.8798	.5941	.0353	25.1
1844.7016	.3348	.0640	14.0
1861.0146	.5059	.0323	24.4
1866.3576	.8089	.0199	39.7
1876.7110	.2929	.0552	14.9
1886.8071	.3767	.0418	20.1
1897.2332	.3271	.0495	14.2
1901.9709	.5357	.0298	23.2
1907.9360	.3644	.0407	16.8
1913.6675	.5137	.0281	24.2
1920.9147	.3730	.0380	18.2
1929.3701	.2880	.0491	14.4
1939.6436	.3147	.0444	16.4
1948.6718	.5740	.0288	27.1
1952.8237	.4228	.0396	19.9
1959.0937	.4314	.0318	24.1
1970.3452	.1803	.0736	8.4
1977.1519	.5520	.0233	25.7
1983.8273	.3339	.0389	15.5
1993.2565	.2919	.0441	13.7
2006.3046	.3684	.0250	17.3
2015.9661	.3092	.0315	13.9
2021.0844	.3417	.0322	14.1
2025.5967	.5262	.0207	21.6
2031.0286	.7176	.0235	33.1
2033.9831	.5320	.0308	25.7
2048.4748	.1118	.1265	5.3
2051.4972	.2664	.0513	12.7
2058.8120	.4374	.0171	21.2
2065.9231	.5015	.0149	24.8
2074.4043	.8211	.0126	37.0
2077.9726	.1876	.0570	8.4
2085.5236	.6842	.0132	32.2
2089.5182	.4977	.0185	23.3
2095.4818	.2476	.0300	14.1
2107.8326	.2991	.0308	13.8
2113.6330	.3697	.0246	17.1
2127.9924	.3583	.0366	15.4
2131.4984	.6566	.0224	24.0

LIST OF GAMMA-RAYS (PN4) T8 -(3)

E-GAMMA (KEV)	ERROR (KEV)	INTENSITY (I/100N)	ERROR (%)
2136.2649	.6356	.0267	24.9
2139.3944	.4338	.0347	20.1
2146.3674	.6729	.0159	28.4
2150.4256	.3899	.0280	16.2
2156.3113	.3451	.0257	15.9
2163.2994	.2966	.0304	13.5
2168.8645	.2804	.0453	11.5
2172.4494	.2187	.0579	9.0
2178.2091	.2653	.0337	12.0
2184.4055	.0752	.1400	3.2
2189.6346	.2482	.0364	11.1
2203.7619	.4179	.0169	19.5
2215.6425	.3169	.0286	13.3
2219.6502	.4438	.0254	15.2
2223.8501	.5794	.0226	19.3
2227.3646	.2004	.0568	8.1
2232.7296	.2562	.0355	10.1
2237.2470	.3876	.0435	16.1
2240.5429	.6799	.0530	25.0
2242.8617	.8148	.0271	63.5
2252.4054	.2574	.0354	10.8
2256.1613	.1782	.0539	7.1
2261.6799	.2745	.0315	11.0
2265.8181	.2235	.0424	8.3
2270.3804	.2037	.0404	8.2
2275.7631	.4632	.0279	20.7
2278.9070	.3974	.0434	11.7
2287.1949	.3336	.0417	12.8
2290.2692	.3375	.0376	14.8
2295.5181	.2768	.0359	10.6
2299.1432	.3699	.0259	14.7
2304.3327	.3167	.0215	14.1
2312.8899	.2505	.0328	11.4
2318.8010	.3064	.0309	12.8
2323.1055	.5140	.0179	21.9
2334.8227	.2658	.0307	12.1
2340.4211	.3417	.0236	15.5
2347.1706	.1455	.0591	6.4
2352.6530	.3760	.0222	16.5
2358.0961	.3182	.0340	12.8
2361.8330	.3666	.0283	15.4
2372.4478	.7340	.0103	34.2
2388.2760	.4411	.0240	19.4

LIST OF GAMMA-RAYS (PN4) T8 -(4)

E-GAMMA (KEV)	ERROR (KEV)	INTENSITY (I/100N)	ERROR (%)
2391.5750	.2252	.0508	9.1
2396.6953	.1991	.0381	8.5
2402.4934	.2695	.0257	12.1
2408.5164	.3614	.0186	16.5
2414.8393	.1390	.0608	5.6
2419.3604	.4118	.0278	15.0
2422.8213	.4080	.0268	15.7
2427.6613	.4766	.0161	19.4
2432.6390	.1602	.0462	6.8
2439.2939	.2157	.0436	8.9
2442.9276	.2083	.0508	7.5
2447.5255	.3107	.0249	12.6
2452.7623	.9016	.0074	39.5
2458.2864	.7707	.0082	35.1
2470.6404	.3279	.0175	14.6
2475.8505	.2303	.0267	9.8
2481.4522	.6286	.0231	36.0
2484.1504	.7489	.0289	21.7
2487.3778	.5790	.0205	25.0
2492.5164	.4562	.0374	23.8
2495.8289	2.2051	.0152	48.7
2497.8905	.6573	.0200	54.5
2505.5110	.2757	.0212	12.0
2510.5778	.9984	.0076	38.9
2514.5082	.5992	.0174	19.3
2517.9561	.2376	.0355	10.1
2525.2185	.1652	.0553	6.6
2529.1700	.2882	.0323	11.0
2534.3553	.3297	.0423	15.2
2537.1658	.5213	.0247	26.6
2546.4530	.4786	.0295	26.8
2549.0340	.5461	.0259	30.3
2555.3346	.2503	.0266	11.4
2563.5396	.4626	.0190	18.9
2567.2271	.4239	.0208	17.3
2579.3500	.1944	.0482	7.1
2585.7346	.2020	.0532	6.9
2594.2429	.4450	.0249	15.3
2598.3511	.2956	.0329	11.2
2604.1578	.4111	.0263	16.5
2607.8498	.3165	.0521	9.1
2611.2851	.3484	.0379	12.8
2616.2747	.4867	.0286	19.8

LIST OF GAMMA-RAYS (PN4) T8 -(5)

E-GAMMA (KEV)	ERROR (KEV)	INTENSITY (I/100N)	ERROR (%)
2619.3446	.4586	.0303	18.8
2624.3541	.3155	.0390	11.4
2627.8712	.4774	.0271	15.8
2632.2105	.4215	.0297	14.0
2635.7753	.1836	.0668	6.6
2644.2486	.1546	.0467	5.6
2652.4246	.2773	.0227	11.5
2657.0640	.1710	.0422	6.3
2665.2911	.2117	.0588	10.2
2668.1048	.3218	.0453	11.7
2672.0690	.3674	.0204	15.0
2679.5623	.2924	.0261	11.9
2683.1626	.2214	.0358	8.7
2691.2007	.2029	.0380	7.8
2694.9270	.2297	.0324	9.1
2702.7669	.1582	.0425	6.0
2707.7711	.3740	.0270	15.5
2711.0726	.5910	.0253	15.7
2714.4057	.3913	.0323	12.4
2718.3330	.3566	.0247	12.1
2722.5875	.2276	.0290	9.1
2730.7906	.4035	.0222	16.5
2734.8585	.5834	.0232	19.5
2738.3471	.3423	.0440	10.3
2742.2321	.3020	.0426	9.5
2746.3505	.3521	.0377	11.2
2749.8616	.2324	.0480	9.3
2755.3615	.2900	.0326	11.4
2759.2737	.1409	.0850	4.6
2763.5297	.5787	.0139	24.2
2770.5198	.2409	.0443	10.3
2774.0477	.2490	.0646	7.2
2777.4716	.3496	.0351	13.4
2782.1204	.2801	.0279	11.6
2787.9461	.1334	.0685	5.1
2792.0683	.1954	.0424	8.0
2805.5288	.1121	.0601	4.3
2809.2378	.1500	.0665	4.4
2812.4413	.2684	.0258	12.4
2827.9899	.7295	.0139	37.3
2830.9660	.7789	.0190	22.6
2834.4000	.3884	.0227	16.9
2840.1555	.2526	.0211	11.4

LIST OF GAMMA-RAYS (PN4) T8 -(6)

E-GAMMA (KEV)	ERROR (KEV)	INTENSITY (I/100N)	ERROR (%)
2846.9622	.1615	.0370	6.8
2851.5687	.2908	.0196	12.6
2861.9565	.2026	.0569	11.4
2864.5166	.1988	.0584	11.1
2870.8365	.2295	.0254	9.6
2875.2561	.2080	.0277	8.8
2883.6600	.1912	.0479	9.3
2886.7218	.4192	.0309	12.0
2890.2168	.2905	.0266	12.3
2896.2212	.2773	.0264	11.5
2899.6511	.2529	.0344	8.4
2904.0839	.1618	.0554	5.2
2907.5834	.6463	.0117	24.7
2912.6235	.3086	.0222	11.4
2916.3137	.1083	.0637	4.2
2925.6023	.1087	.0408	4.1
2929.2766	.1246	.0380	4.3
2934.4323	.3155	.0171	12.8
2937.5380	.4822	.0103	21.8
2943.7453	.2090	.0261	9.5
2946.8674	.2407	.0295	7.4
2950.6918	.1081	.0451	3.8
2965.5007	.2986	.0197	11.5
2970.1586	.2025	.0336	7.1
2974.6275	.2367	.0260	8.9
2980.3733	.3181	.0289	13.9
2983.6731	.2898	.0455	7.7
2987.5211	.2355	.0498	6.3
2991.1666	.2048	.0384	8.3
2998.1323	.2279	.0456	11.3
3001.1941	.3718	.0349	9.5
3004.7463	.2092	.0459	6.4
3009.2262	.4353	.0247	16.0
3012.1591	.2885	.0336	12.6
3017.0695	.5056	.0119	16.9
3020.9413	.2790	.0185	11.2
3030.7488	.2779	.0275	15.3
3037.1548	.1572	.0392	6.7
3044.5278	.4150	.0305	34.9
3046.5935	.5893	.0265	37.2
3051.1182	.2251	.0321	6.2
3054.7828	.4244	.0144	13.8
3059.4715	.2493	.0222	7.8

LIST OF GAMMA-RAYS (PN4) T8 -(7)

E-GAMMA (KEV)	ERROR (KEV)	INTENSITY (I/100N)	ERROR (%)
3063.6365	.1951	.0454	6.3
3066.6418	.1859	.0362	9.1
3076.6530	.1572	.0657	10.8
3078.9358	.3236	.0350	19.1
3083.7318	.4166	.0097	15.7
3089.2068	.1470	.0347	5.6
3093.2247	.4203	.0204	13.9
3096.6124	.2828	.0392	7.2
3099.9644	.5022	.0151	19.1
3104.6234	.0806	.0649	3.4
3112.8043	.1815	.0200	6.9
3117.6984	.5403	.0112	19.5
3121.3565	.2693	.0358	6.7
3124.7396	.2101	.0378	6.9
3129.4625	.8087	.0094	26.6
3132.9590	.2138	.0523	4.9
3136.2736	.4744	.0168	17.1
3141.0951	.4734	.0161	16.8
3144.2309	.8689	.0084	32.5
3149.0331	.5631	.0102	17.5
3152.5907	.2202	.0216	9.0
3162.0142	.2154	.0259	8.1
3166.2443	.4180	.0167	12.5
3171.0971	.4771	.0322	25.7
3173.5501	.3229	.0433	20.0
3179.4451	.2022	.0395	7.4
3183.1356	.3618	.0318	8.9
3186.7420	.1919	.0461	6.6
3191.8386	.3942	.0185	12.8
3195.5100	.2708	.0231	10.8
3203.7059	.0991	.0540	3.5
3208.4773	.1908	.0295	6.4
3213.2262	.0847	.0665	2.9
3223.6678	.2376	.0242	9.3
3227.7600	.4474	.0289	16.1
3230.6052	1.0314	.0095	56.1
3236.2831	.0861	.0545	3.0
3244.7083	.2744	.0193	10.4
3249.0676	.1972	.0658	7.9
3251.9127	.1748	.0676	8.2
3257.3127	.3855	.0216	13.8
3260.7018	.4007	.0234	11.9
3264.9191	.1508	.0362	5.6

LIST OF GAMMA-RAYS (PN4) T8 -(8)

E-GAMMA (KEV)	ERROR (KEV)	INTENSITY (I/100N)	ERROR (%)
3275.2853	.0996	.0921	4.1
3278.5602	.2272	.0385	9.2
3284.5223	1.2860	.0053	45.8
3288.4315	.5590	.0154	15.3
3292.6435	.1804	.0341	6.6
3299.7684	.4484	.0134	16.8
3303.9457	.3931	.0248	10.7
3307.7134	.1398	.0701	4.0
3312.1352	.2527	.0221	9.4
3322.3223	.1573	.0316	5.9
3326.4194	.2113	.0398	5.7
3329.9350	.5066	.0132	18.4
3335.5533	.1889	.0432	8.2
3338.4669	.3580	.0200	18.4
3345.5625	.2736	.0194	10.8
3349.4317	.3323	.0313	9.4
3352.4754	.5028	.0140	26.2
3360.0083	.1150	.0421	4.2
3364.0769	.3182	.0247	8.4
3367.5317	.1752	.0343	7.1
3373.6624	.1340	.0235	5.0
3384.3558	.2757	.0179	10.1
3388.7319	.2757	.0322	7.8
3392.4105	.1754	.0547	4.6
3397.0147	.2380	.0388	6.2
3400.7419	.2862	.0310	7.8
3405.4108	.1802	.0469	4.7
3409.3582	.2400	.0365	5.9
3413.4193	.1509	.0374	5.6
3428.2043	.6147	.0196	35.9
3431.2102	.4269	.0556	8.8
3434.3005	.4145	.0284	23.1
3441.6959	.0885	.0582	3.1
3449.1170	.1192	.0762	4.7
3452.6396	.2951	.0380	8.0
3456.9890	.3320	.0217	10.2
3462.8412	.4290	.0377	27.5
3472.0999	.2313	.0212	12.4
3476.2605	.2652	.0221	11.5
3480.6341	.2035	.0218	10.3
3487.2592	.0861	.0424	5.0
3495.5704	.5893	.0070	23.9
3500.2587	.4483	.0174	14.2

LIST OF GAMMA-RAYS (PN4) T8 -(9)

E-GAMMA (KEV)	ERROR (KEV)	INTENSITY (I/100N)	ERROR (%)
3504.1467	.3562	.0465	11.9
3506.8857	.3212	.0385	17.5
3512.1810	.2235	.0245	6.1
3516.2659	.3251	.0128	12.0
3524.2290	.1932	.0309	8.6
3527.7006	.2847	.0343	6.2
3531.3949	.1443	.0426	5.4
3537.8450	.5076	.0090	17.5
3542.0233	.1482	.0545	3.4
3546.0138	.2493	.0352	5.3
3549.8237	1.0090	.0059	33.6
3555.4716	.0883	.0960	2.5
3559.4737	.1912	.0791	5.5
3562.6613	.4033	.0413	9.1
3565.9873	.3786	.0183	20.0
3575.9857	.3930	.0124	14.1
3581.9978	.1880	.0559	7.2
3585.4561	.2240	.0501	7.7
3594.8833	.1569	.0747	5.1
3600.3292	.2345	.0295	6.8
3605.6493	.2328	.0401	6.9
3609.6176	.7953	.0123	21.1
3614.4624	.1478	.0563	3.9
3619.9566	.3812	.0335	15.1
3623.1516	.2703	.0487	10.3
3628.6172	.6942	.0132	20.2
3632.3909	.2817	.0271	10.9
3641.9762	.2327	.0584	18.0
3644.0985	.2941	.0465	22.5
3651.5075	.2155	.0186	7.0
3656.7282	.2506	.0286	8.0
3660.3645	.2331	.0309	7.4
3665.6304	.0891	.0634	2.2
3679.4550	.5442	.0067	18.5
3684.7354	.1135	.1057	3.8
3688.1413	.4873	.0312	9.4
3691.9500	.2886	.0409	6.5
3696.6552	.1870	.0863	6.0
3699.6289	.3439	.0381	14.9
3704.4161	.3534	.0131	11.1
3710.9305	.5113	.0127	21.7
3714.1897	.2173	.0331	8.2
3720.2502	.1790	.0335	5.4

LIST OF GAMMA-RAYS (PN4) T8 -(10)

E-GAMMA (KEV)	ERROR (KEV)	INTENSITY (I/100N)	ERROR (%)
3724.0369	.3961	.0134	13.5
3729.9835	.1199	.0312	3.6
3738.2232	.1121	.0380	3.4
3746.9086	.0956	.0561	2.4
3753.9472	.3459	.0181	13.1
3757.7461	.4429	.0190	10.8
3762.1705	.1433	.0408	4.4
3770.6942	.1536	.0265	4.8
3775.0021	.1146	.0445	2.9
3781.6970	.1231	.0577	4.3
3785.0245	.3841	.0183	12.1
3789.9599	.2424	.0355	9.8
3792.7487	.1759	.0501	6.9
3797.6060	.1436	.0575	3.5
3801.0973	.1619	.0391	5.6
3807.0256	.2357	.0169	6.6
3811.5050	.4863	.0068	16.6
3820.5802	.2653	.0365	14.8
3823.3134	.1499	.0756	7.1
3830.7800	.2711	.0187	8.5
3835.6577	.3740	.0356	14.3
3838.9990	.1953	.1073	3.6
3842.6576	.1558	.0724	5.5
3848.9403	.2239	.0354	7.5
3852.3523	.2401	.0283	10.0
3861.2315	.1249	.0386	3.2
3866.3708	.1231	.0493	2.6
3871.7804	.1136	.0574	2.2
3877.2885	.1267	.0432	2.8
3882.9395	.1343	.0390	3.1
3888.7523	.5519	.0140	21.8
3891.9900	.1134	.0967	3.4
3901.0437	.1521	.0597	6.4
3903.9760	.2261	.0349	11.0
3913.0749	.1468	.0406	3.9
3918.4446	.2068	.0671	7.3
3921.9523	.3742	.0540	6.8
3925.6423	.1671	.0798	5.4
3931.4589	.4108	.0161	10.3
3935.9804	.1116	.0936	2.0
3943.2095	.2722	.0497	14.7
3946.3263	.3315	.0753	6.2
3950.4523	.5954	.0472	10.0

LIST OF GAMMA-RAYS (PN4) T8 -(11)

E-GAMMA (KEV)	ERROR (KEV)	INTENSITY (I/100N)	ERROR (%)
3954.2537	.7670	.0540	17.8
3957.1173	.7447	.0407	31.8
3961.2657	.4226	.0217	14.5
3971.1544	.5004	.0075	14.8
3977.0388	.2890	.0232	5.0
3984.7943	.2551	.0441	2.8
3991.1073	.3255	.0279	7.7
3995.0945	.2452	.0955	2.3
4000.7062	.2346	.0818	1.8
4009.9739	.2769	.0291	5.8
4014.8641	.4670	.0364	17.5
4018.1673	.9055	.0306	15.5
4021.0809	.6010	.0217	37.9
4032.3043	.2473	.0569	5.7
4036.2425	.2320	.1124	2.5
4040.8617	.2269	.0937	2.6
4046.3484	.2367	.1179	4.6
4050.0601	.3143	.0899	4.9
4053.7229	.2055	.1470	3.4
4062.1018	.3176	.0545	16.3
4064.6660	.3014	.0589	14.6
4071.6930	.2217	.0323	8.5
4078.9867	.1825	.1238	2.7
4083.9179	.3699	.0169	19.1
4091.5105	.2548	.0181	6.5
4097.9362	.1823	.0522	2.5
4106.1424	.1738	.0664	2.0
4117.0362	.2211	.0327	4.9
4122.5862	.2364	.0672	6.4
4125.8988	.4772	.0219	20.6
4138.7094	.2030	.0910	4.3
4142.2520	.1884	.1016	4.2
4148.9133	.2051	.0367	3.9
4155.2206	.1835	.0861	3.0
4159.5117	.3078	.0395	5.6
4164.4264	.7723	.0156	16.7
4168.5191	.3791	.0373	6.9
4173.0925	.2579	.0497	4.4
4178.3240	.5721	.0197	10.1
4180.1674	.2567	.0266	5.5
4186.1624	.1813	.0759	2.2
4191.8453	.1788	.0852	2.0
4198.1392	.2392	.0274	5.2

LIST OF GAMMA-RAYS (PN4) T8 -(12)

E-GAMMA (KEV)	ERROR (KEV)	INTENSITY (I/100N)	ERROR (%)
4204.5008	.1846	.0665	2.3
4212.0256	.7003	.0247	44.2
4214.9124	1.4256	.0225	30.2
4218.2861	.3472	.0410	17.0
4228.2375	.1862	.1105	1.4
4239.3977	.2733	.0148	7.0
4249.3285	.2409	.0467	5.6
4253.1953	.2285	.0652	3.9
4265.6561	.3459	.0137	8.8
4273.2508	.2794	.0206	5.8
4279.3216	.2268	.0600	2.2
4287.2166	.2490	.0839	5.2
4290.6609	.5095	.0265	13.7
4296.4164	.6097	.0315	27.5
4299.0021	.4004	.0351	27.0
4309.0923	.1107	.1448	5.7
4311.9158	.4931	.0328	22.8
4317.4807	.3680	.0175	8.4
4322.6299	.2163	.0212	6.6
4331.7048	.3271	.0305	16.3
4334.8809	.2745	.0414	11.4
4342.2090	.3166	.0618	19.4
4345.0285	.7959	.0356	27.1
4349.2695	.1432	.0731	5.3
4356.5536	.1625	.0258	4.8
4364.6776	.4678	.0336	29.7
4367.4672	.1234	.1871	4.9
4372.8515	.1189	.0640	3.1
4379.7336	.0894	.0767	2.1
4385.2140	.3281	.0162	8.5
4391.5353	.0723	.1189	1.4
4397.7578	.3895	.0313	16.0
4400.8920	.1765	.0609	8.9
4409.8962	.2188	.0191	7.2
4417.4536	.1102	.0442	3.4
4426.1986	.3768	.0289	17.6
4429.6586	.2296	.0639	7.0
4434.9367	.1932	.0328	6.0
4444.1475	.0800	.0971	2.1
4449.2104	.1135	.0569	3.4
4459.4495	.0658	.0996	1.6
4470.9938	.4011	.0112	12.4
4476.5577	.1639	.0292	5.0

LIST OF GAMMA-RAYS (PN4) T8 -(13)

E-GAMMA (KEV)	ERROR (KEV)	INTENSITY (I/100N)	ERROR (%)
4489.4823	.1239	.0403	3.7
4494.3924	.2711	.0185	7.5
4501.7779	.2691	.0373	12.4
4504.9735	.1792	.0566	8.3
4512.8504	.1689	.0390	5.3
4517.3176	.0671	.1533	1.5
4524.5000	.1957	.0710	9.1
4527.8473	.1504	.1275	4.3
4532.9734	.1430	.0730	2.8
4537.8844	.4208	.0143	11.5
4542.2405	.1549	.0177	14.1
4549.4797	.0515	.1487	1.6
4555.3256	.2396	.0173	11.1
4560.9944	.1974	.0298	6.9
4565.3305	.0714	.0895	2.4
4573.0875	.1149	.0495	4.1
4577.1335	.0824	.0752	2.8
4584.3700	.0574	.0860	1.5
4590.8739	.1547	.0266	4.3
4595.6908	.1648	.0231	4.8
4602.3734	.0865	.0320	2.5
4613.8266	.1438	.0296	4.5
4622.2053	.0491	.2731	.8
4632.3147	.1539	.0324	4.6
4638.2409	.1178	.0447	3.5
4649.3845	.6288	.0163	37.7
4652.4759	.2398	.0685	7.2
4657.6751	.4780	.0226	8.2
4667.8374	.4399	.0182	10.3
4672.3781	.1589	.0669	2.8
4677.9258	.3762	.0572	15.9
4680.9243	.3070	.0682	13.6
4686.3793	.1364	.0555	2.9
4692.3420	.0641	.1282	1.1
4698.2460	.0691	.0762	1.6
4710.2322	.0951	.0439	2.5
4716.0009	.1037	.0699	2.2
4720.8069	.0834	.0928	1.8
4727.0256	.0669	.0883	1.3
4741.3508	.2109	.0464	10.7
4744.2123	.8346	.0103	49.2
4758.1917	.0572	.1848	.9
4763.8935	.2458	.0160	6.9

LIST OF GAMMA-RAYS (PN4) T8 -(14)

E-GAMMA (KEV)	ERROR (KEV)	INTENSITY (I/100N)	ERROR (%)
4772.1566	.0626	.0958	1.2
4782.1923	.2275	.0130	6.7
4789.5941	.1057	.0622	2.9
4794.1477	.2009	.0321	5.1
4800.5165	.1045	.0486	2.3
4807.5093	.1250	.0768	4.1
4811.4273	.0872	.1353	2.3
4818.3136	.0662	.1193	1.1
4827.2707	.2091	.0192	5.8
4832.9502	.1236	.0674	2.8
4837.2594	.1595	.0367	5.5
4848.7766	.3659	.0677	34.3
4850.7150	.3782	.0662	35.0
4861.0783	.0687	.2126	1.1
4867.0267	.7657	.0312	37.9
4869.7755	.9462	.0218	56.3
4876.6464	.4051	.0285	12.8
4880.4852	.2792	.0449	7.8
4886.0760	.1009	.0657	2.5
4893.9342	.0992	.0419	2.6
4907.3474	.3771	.0149	12.2
4912.7729	.3392	.0114	8.4
4919.6701	.0722	.0934	1.4
4927.3444	.0814	.1009	1.7
4932.6048	.0713	.1336	1.4
4940.9362	.1184	.0609	3.3
4953.1537	.1295	.0293	3.5
4962.4433	.0875	.0741	2.2
4967.4621	.1586	.0353	4.1
4974.9731	.0843	.0708	1.8
4980.7534	.3428	.0107	9.6
4990.6968	.1179	.0386	3.2
4996.5194	.1136	.0616	2.3
5002.1530	.0660	.1445	1.2
5009.7300	.2758	.0110	8.1
5027.5285	.1809	.0211	5.2
5034.4810	.1049	.0476	2.7
5041.8834	.1974	.0235	5.0
5048.3842	.6210	.0101	14.5
5054.2945	.0706	.2593	1.2
5058.7745	.2335	.0352	8.6
5067.5801	.4287	.0077	12.5
5076.4523	.0653	.1625	1.3

LIST OF GAMMA-RAYS (PN4) T8 - (15)

E-GAMMA (KEV)	ERROR (KEV)	INTENSITY (I/100N)	ERROR (%)
5082.0945	.0735	.1253	1.6
5091.0048	.0591	.2734	1.0
5096.1986	.1009	.0784	2.7
5104.5928	.1255	.0360	3.3
5112.3544	.0538	.3592	.6
5120.5755	.1721	.0214	4.9
5127.7583	.2397	.0129	6.3
5135.0907	.0799	.0585	1.8
5142.1379	.1122	.0337	2.8
5149.6707	.0962	.0427	2.3
5156.9368	.0556	.1596	.9
5168.6849	.4095	.0057	12.7
5180.8222	.6837	.0034	20.8
5188.9682	.2310	.0112	6.9
5197.9016	.0798	.0532	2.0
5205.8946	.0507	.3701	.7
5214.4005	.2010	.0258	5.3
5219.6933	.2318	.0350	4.7
5224.8883	.0604	.1909	1.1
5232.4302	.2326	.0146	6.0
5240.5962	.0500	.3511	.7
5249.4374	.0675	.0650	1.6
5270.3525	.1620	.0444	8.9
5273.5785	.7036	.0154	22.5
5279.0356	.0780	.0930	2.1
5284.8780	.1464	.0270	4.2
5290.7933	.0971	.0366	2.8
5297.4379	.2090	.0216	5.0
5301.7153	1.1104	.0029	43.0
5316.8196	.2164	.0342	18.5
5318.9741	.7207	.0113	54.4
5326.0151	.0630	.0729	1.2
5330.8645	.2538	.0194	5.0
5334.6114	.4918	.0057	22.6
5346.6642	.0974	.0207	2.9
5357.9598	.0537	.1975	1.1
5362.4577	.4099	.0266	7.2
5366.6252	.4746	.0208	9.3
5370.9733	.1947	.0222	7.6
5379.2501	1.1190	.0016	29.9
5386.5234	.0517	.2086	1.0
5390.8505	.3776	.0228	6.1
5395.2282	.3671	.0171	7.9

LIST OF GAMMA-RAYS (PN4) T8 -(16)

E-GAMMA (KEV)	ERROR (KEV)	INTENSITY (I/100N)	ERROR (%)
5399.9462	.4061	.0066	14.3
5413.4371	.0644	.0344	1.6
5422.2846	.0476	.1254	.8
5429.8925	.0509	.0798	1.0
5439.1464	.0815	.0287	2.0
5444.8818	.7874	.0022	22.2
5455.6518	.0711	.0311	2.0
5466.9521	.0507	.1030	.9
5472.9794	.1207	.0238	3.4
5479.8879	.0927	.0284	3.1
5486.7774	.0770	.0347	2.9
5497.7445	.1179	.0214	3.2
5503.9276	.0728	.0455	1.7
5513.0200	.0515	.2162	1.1
5518.1103	.0975	.2245	2.9
5521.1187	.1772	.0677	11.7
5537.9949	.0511	.1341	.9
5544.6413	.0787	.0755	1.5
5551.5198	.4714	.0414	29.2
5553.9849	.1640	.1026	12.3
5572.8176	.1309	.0164	4.1
5579.3789	.0429	.3501	.7
5584.5380	.2152	.0149	9.3
5599.9973	.2623	.0143	8.7
5604.5146	.2803	.0145	8.3
5613.8037	.0435	.2245	.9
5621.2198	.0668	.0567	1.8
5630.6566	.0531	.1035	1.2
5637.5393	.1953	.0443	6.5
5641.6653	.0785	.1493	2.0
5647.2399	.2887	.0128	9.3
5661.1624	.3636	.0032	11.3
5691.6694	.3227	.0117	9.8
5700.0828	.0397	.8328	.6
5708.9282	.0501	.2849	.9
5714.6466	.3759	.0174	9.8
5721.7168	.4540	.0078	11.8
5729.6776	.3977	.0072	11.5
5739.9963	.0490	.1265	1.2
5756.0977	.2732	.0077	11.5
5771.7698	.0406	.2358	.6
5788.4792	.7039	.0066	29.4
5793.3961	.0441	.6194	.6

LIST OF GAMMA-RAYS (PN4) T8 -(17)

E-GAMMA (KEV)	ERROR (KEV)	INTENSITY (I/100N)	ERROR (%)
5797.1563	.2978	.0265	16.2
5811.5843	.0395	.3276	.6
5820.4355	.1157	.0266	3.3
5845.8023	.6848	.0017	19.4
5852.3903	.1228	.0228	3.4
5856.4344	.5253	.0040	21.2
5874.0647	.1273	.0096	3.8
5895.6767	.0389	.1072	.6
5901.6645	.4489	.0035	10.9
5909.8787	.0542	.0545	1.3
5914.6069	.9771	.0019	32.7
5924.9266	.3384	.0080	15.4
5928.3455	.8213	.0031	40.0
5952.2214	.0500	.0390	1.3
5986.3689	.0435	.0983	1.2
5995.0630	.0382	.1625	1.0
6014.3769	.8088	.0062	23.3
6021.3264	.0417	.3069	1.2
6032.8453	.0582	.0966	1.9
6047.0555	.1366	.0219	5.7
6056.2164	.0383	.6946	9.5
6059.6875	.1236	.0960	6.8
6080.7319	.0442	.0648	1.4
6100.4672	.0413	.1081	1.2
6107.7944	.0986	.0653	2.4
6141.6163	.1672	.0061	6.1
6152.6361	.0724	.0176	2.5
6173.0771	.0561	.0232	1.6
6191.3722	.0422	.0600	1.1
6197.3421	.3150	.0044	9.5
6216.6400	.0624	.0177	2.0
6256.9446	.0521	.0270	1.4
6266.8626	.0480	.0887	1.4
6271.1620	.2844	.0105	10.7
6280.7188	.0404	.0711	.9
6286.7978	.4981	.0027	14.1
6309.4866	.0525	.0266	1.4
6374.1168	.3053	.0032	8.6
6381.8019	.0431	.0390	1.8
6425.1665	.0375	.0604	.9
6431.2329	.6260	.0021	15.2
6439.4462	.5668	.0025	14.4
6445.6742	.0403	.0829	.8

LIST OF GAMMA-RAYS (PN4) T8 -(18)

E-GAMMA (KEV)	ERROR (KEV)	INTENSITY (I/100N)	ERROR (%)
6451.5301	.3710	.0037	11.1
6539.0685	.0344	.3259	.9
6543.4645	.3995	.0137	18.0
6569.3579	.0440	.0473	2.0
6607.6530	.0422	.0338	2.0
6724.9407	1.2751	.0003	38.2
6805.4477	.0576	.0158	1.7

CHAPTER 5.

THEORY OF ODD-ODD NUCELI

It has been known that an odd number of protons or neutrons has great importance at low excitation energy of nuclei due to the pairing interaction of nucleons. The pairing interaction between fermions by a short range force was understood in atomic physics many years ago, and the seniority coupling scheme was set up [53]. In nuclear physics, this effect was seen as a correction term in the semi-empirical mass formula of Weizsäcker and Bethe. Since the great success of the shell structure of nuclei, the concept of a pairing interaction has also been exploited to explain many schematic features of nuclei. These include ground state spins of even-even or odd-mass nuclei, and lead to the seniority coupling scheme [54], the BCS theory [55] and the interacting boson model [56] into nuclear physics.

However, the interpretation of odd-odd nuclei is somewhat more complicated at low excitation energy than even-even or odd-mass nuclei, probably because its larger seniority extends the shell model configuration space. The characteristics of the ground state of odd-odd nuclei were investigated by Nordheim [57] using spherical potential as in the usual j-j coupling model and by Gallagher and Moszkowsky [58] using the spheroidal Nilsson potential [59], in which j of each nucleon is no longer a good quantum number.

The isospin formalism has been considered to explain the characteristics of light nuclei including odd-odd nuclei. However, the symmetry between protons and neutrons is gradually destroyed as nuclei become heavier, and therefore an even-even nucleus core may be considered as an inert core and odd numbers of quasi-protons and quasi-neutrons

have to be coupled with each other to form an odd-odd nucleus. A typical example is the $(d_{3/2}, f_{7/2})$ multiplet in ^{38}Cl [60].

In addition to the shell model configuration, the coupling between the core and proton-neutron multiplet becomes considerable in much heavier nuclei. In order to explain this, a neighbouring even-even nucleus is chosen as the core and its collective motion is coupled to the proton-neutron multiplet. The standard example of the collective states in an odd-odd nucleus is the rotational levels in ^{166}Ho [61].

Recently, as an analogy to the Alaga model [62], the particle-quadrupole vibration interaction has been introduced into an odd-odd nucleus system by Paar [63] with the result that the energy splitting of a proton-neutron multiplet can be expressed by a quadratic polynomial with respect to the square of angular momentum magnitude $I(I + 1)$.

For the odd-odd nuclei around Z = 50 region, theoretical studies have not been carried out very extensively compared with those of even-even and odd-mass nuclei, simply because experimental results have not been available. However, calculations have been reported for Sb and In odd-odd nuclei by Gunsteren et al [64] using a particle (hole)- quasi-particle coupling model. Almost all states at low energy have been reproduced by the model. However, the deviations of the level energies are still large as can be seen in most of the theoretical calculations.

On the other hand, Paar's description and result are in very simple form in order to evaluate the splitting of a proton-neutron multiplet. This theory will be examined with the results obtained in the present work.

5.1. Residual Interaction

In the shell model approach to odd-odd nuclei, the most important assumption is a residual interaction between the unpaired proton and

neutron. This interaction possesses similar characteristics to the short range pairing interaction, but normally the unpaired proton and neutron occupy differnt major shells in heavier nuclei, and do not occupy time-reversal states with respect to each other, which is the case for the pairing interaction. Therefore, the residual interaction is expected to be weaker than the pairing interaction. In other words, the splitting of the proton-neutron multiplet may be smaller than the pairing interaction, i.e. the BCS energy gap.

In actual shell model calculations of the splitting of the level energies, a variety of functions is used to express the residual interaction, such as δ-potential [60], Gaussian force [64] and Schiffer interaction[64]. The shell model space is chosen appropriately assuming an inert core, e.g. doubly magic core.

5.2. j-j Coupling

In the many particle shell model scheme, j-j coupling is essential rather than LS-coupling to calculate the total spin of a nucleus by adding individual angular momenta of the nucleons, which occupy different single particle orbitals according to the Pauli principle. Generally, j-j coupling is applied to n equivalent particles, which occupy the same shell. This is known as $(j)^n$-coupling. Possible total angular momenta in the configuration $(j)^n$ have been obtained for equivalent identical particles. This knowledge is necessary in order to interpret experimental results.

The angular momentum coupling scheme has its mathematical complication due to the quantum mechanics involved, but is able to reveal the symmetry of nuclear structure under various types of two-body interaction by means of the group theory. The level degeneracies and their splitting must be made clear in terms of energy matrix in the coupling

scheme.

5.3. Parabolic Energy Dependence of Proton-Neutron Multiplets

As an analogy to the Alaga model and the geometric model of Bohr and Mottelson [65], the interaction between the odd number proton cluster and the odd number neutron cluster outside a closed shell (or hole states inside a closed shell) is treated as the exchange of quadrupole 2^+ phonon and spin-vibrational 1^+ phonon between the clusters. Its concept is quite similar to that of the interacting boson model except for the additional spin-vibrational phonon and the mathematical description of the system Hamiltonian.

The perturbation terms in the Hamiltonian are expressed by $H_2 + H_1$, where

$$H_2 = a_2 \{ Y_2(b_2^\dagger + b_2) \}_o$$

$$H_1 = a_1 \{ \sigma \times (b_1^\dagger + b_1) \}_o$$

a_i are the strength factors, Y_2 a spherical harmonic, σ spin operator and $b_i^\dagger$ and b_i phonon creation and annihilation operators, respectively. According to Paar's calculation, the contribution to the energy splitting $\delta E(I)$ of the multiplet $|j_p, j_n; I>$ is described by a quadratic polynomial of $I(I+1)$.

$$\delta E(I) = A \cdot \{I(I+1)\}^2 + B \cdot I(I+1) + C$$

The second order term is due to the contribution from the quadrupole phonon exchange H_2 and the first order is the spin-vibrational phonon exchange H_1 and a part of H_2. The zeroth order constant term does not give any spin dependence of the enegy splitting, but overall shift of the multiplet.

These coefficients are configuration dependent, and the result shows that the parabola is concave down ($A < 0$) for particle-particle and hole-hole states and concave up ($A > 0$) for particle-hole states. The position of the vertex $I_v(I_v + 1)$ is given by

$$I_v(I_v+1) = j_p(j_p+1) + j_n(j_n+1) - \frac{1}{2}$$

without the 1^+ phonon contribution. I_v is shifted with the 1^+ phonon exchange.

If j_p or j_n is equal to $\frac{1}{2}$, the energy splitting is due to the 1^+ phonon exchange only (i.e. A = 0). In this case, the sign of coefficient B depends on $N = j_p - \ell_p + j_n - \ell_n$, where ℓ_p and ℓ_n are corresponding orbital angular momenta. For N = 0, the higher spin state has higher excitation energy (B > 0) and for N = ±1, the lower spin state has higher excitation energy (B < 0).

CHAPTER 6.

DISCUSSION

Having constructed the level schemes of ^{108}Ag and ^{110}Ag, based on the recent experiments, several remarks have to be mentioned on the experiments, data analyses, the characteristics of the nuclear structure of these odd-odd silver isotopes and the neutron capture process.

6.1. Experiments and data analyses

During past years experimental methods have been improved considerably. Automated experimental procedures and data analyses with the aid of electronic computers have achieved quick data processing and precise calculations. However, there are still some important decisions to be made empirically, such as the choice of peak shape and peak identification in a spectrum. Also several energy and intensity calibration lines have to be very carefully selected. Especially in the absolute intensity calculation, usually only a few calibration data are available, which may include a large systematic error.

In the present work, two decay lines were used to determine the absolute intensities of gamma-transitions in ^{108}Ag and only one decay line for ^{110}Ag. Also, multipolarities had to be assumed to obtain absolute internal conversion electron intensities. As mentioned in Chapter 2, the intensity data ~~by~~ from the pair spectrometer were calibrated absolutely using several gamma-transition intensities at the overlapping enegy region with the GAMS measurement, where very low detection efficiencies can be achieved by both spectrometers.

Alternatively, absolute intensities can be calibrated based on the Kirchhoff's law and the Ritz combination principle. If all the transi-

tions have been detected, the sum of energy weighted transition intensities per one neutron capture must be equal to the neutron binding energy.

$$\alpha \sum_i E_i \cdot I_i = E_b$$

where α; normalization constant to be obtained

E_i; transition energies

I_i; relative transition intensities

E_b; neutron binding energy

Therefore, the present calibration can be tested by this method. The normalization constant α must be determined as 1, or slightly less than 1, due to unobserved transitions and the existence of long lived isomeric state. However, the calculation shows that

$$\sum_i E_i \cdot I_i = (\text{BILL}) + (\text{GAMS}) + (\text{PN4})$$

$$= (19.8 \pm 0.1) + (596.4 \pm 10.6) + (1554.3 \pm 6.0)$$

$$= 2170.5 \pm 12.2 \text{ (keV/n.c.)}$$

and $\alpha = 3.14 \pm 0.02$

This large discrepancy can be explained by the following reasons.

(1) There are many unobserved transitions forming flat background in the spectrum around 1 MeV to 5 MeV, resulting in a 69% missing energy-intensity product.

(2) The self-absorption correction for GAMS measurement may have been overestimated, resulting in a relatively overestimated efficiency at the 1 MeV region and underestimated efficiency at low energies.

(3) GAMS efficiency may be overestimated at 1 MeV to 2 MeV region.

The unobserved transitions must not be very strong. Thus, the contribution to the energy-intensity product may be very small, but cannot be estimated correctly. No improvement can be made with respect to (1). While, (2) and (3) can be improved by another careful measurement

of gamma-ray intensities using a Ge(Li) detector. By comparison of these intensities with GAMS peak areas, new efficiency curves can be obtained including the self-absorption correction automatically. This correction has been attempted by the author at the University of London Reactor Centre, as described in Chapter 2. However, the large uncertainty in the detector efficiency around 100 keV and above 1.4 MeV made this method very difficult, because the 100 keV region is important for calibrating absolute electron intensities (117.6 keV transition is known to be an E1) and the 1.3 MeV to 1.8 MeV region is also important for calibrating the pair spectrometer data. Very good statistics are necessary to establish the GAMS efficiency curves by this method.

If this procedure is carried out with good accuracy, then it will be possible to compare the energy-intensity products with the neutron binding energy and to deduce the missing transition intensities.

If a precise energy measurement is required, which is the case in neutron capture gamma-ray spectroscopy, the detection efficiency decreases inevitably. There seems to be a kind of uncertainty principle in energy and intensity measurements.

6.2. Comparison with Neighbouring Nuclei and Preliminary Interpretation

Characteristics of two proton-neutron multiplets in silver odd-odd nuclei have been compared as functions of neutron number by Massoumi [17]. However, the systematics cannot be generalized with these limited interpretations. In order to interpret more levels in ^{108}Ag and in ^{110}Ag, an attempt was made to compare them with the neighbouring even-even and odd mass nuclei, which are relatively well-known compared to odd-odd nuclei. The comparison was made as shown in Fig. 19, and excitation energies for various proton-neutron multiplets were roughly estimated

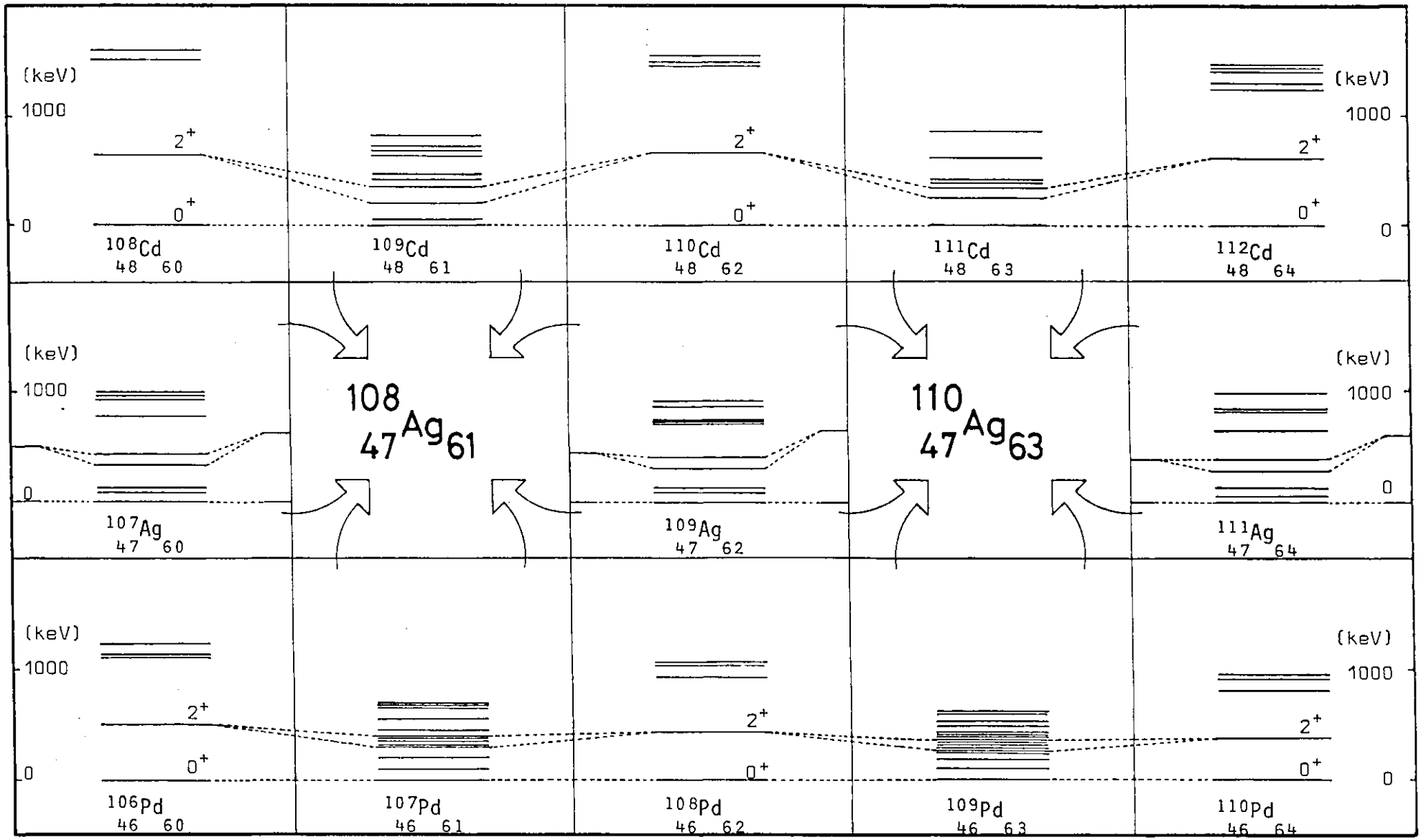

Fig. 19. Neighbouring Nuclei and Quasi-particle-Vibration Coupling

by coupling proton states in a neighbouring odd-even nucleus and neutron states in a neighbouring even-odd nucleus without the residual interaction which gives the multiplet splitting.

The sequence of the lowest five levels in odd silver isotopes ^{107}Ag, ^{109}Ag and ^{111}Ag is $(1/2)^-$, $(7/2)^+$, $(9/2)^+$, $(3/2)^-$ and $(5/2)^-$ at more or less the same excitation energies. They have been interpreted as $p_{1/2}$, $(g_{9/2})^{-3}_{7/2}$, $(g_{9/2})^{-3}_{9/2}$, $(p_{1/2} + 2^+\text{-phonon})_{3/2}$ and $(p_{1/2} + 2^+\text{-phonon})_{5/2}$, respectively, in terms of particle-vibration coupling [4]. The one phonon energy is expected to be about 500 keV compared with the neighbouring even-even nuclei. Two-phonon states can also be found around 800 keV to 1 MeV excitation energy region.

On the other hand, odd neutron nuclei ^{107}Pd, ^{109}Pd, ^{109}Cd and ^{111}Cd show more complicated structure at low excitation, as can be expected from the shell model configurations. The lowest $(5/2)^+$, $(1/2)^+$ and $(11/2)^-$ states can be interpreted as $d_{5/2}$, $s_{1/2}$ and $h_{11/2}$ neutron single-particle orbitals, respectively. However, one-phonon states coupled to the $d_{5/2}$ and $s_{1/2}$ exhibit very complicated structure. In particular, the $(3/2)^+$ and $(7/2)^+$ levels are difficult to interpret as they can be members of the one-phonon states or the single-particle neutron configurations $d_{3/2}$ and $g_{7/2}$.

If the configurations $p_{1/2}$, $(g_{9/2})^{-3}_{7/2}$ and $(g_{9/2})^{-3}_{9/2}$ for the unpaired proton, $g_{7/2}$, $d_{5/2}$, $d_{3/2}$, $s_{1/2}$ and $h_{11/2}$ for the unpaired neutron and one vibrational phonon are considered when interpreting the odd-odd nuclei ^{108}Ag and ^{110}Ag, possible combinations can be obtained by a simple coupling scheme. These combinations are shown in Table 9.

An attempt can be made to interpret the constructed level schemes in terms of proton-neutron multiplet coupled to core vibration. It is worthwhile to note that similar characteristics can be found in the present

proton / neutron	$p_{1/2}$ 0 keV	$(g_{9/2})^{-3}_{7/2}$ 80 keV	$(g_{9/2})^{-3}_{9/2}$ 130 keV
$d^{-1,3}_{5/2}$ 0 keV	− 2 0,1,2,3,4 3 1,2,3,4,5 1-phonon	+ 1 1,2,3 2 0,1,2,3,4 3 1,2,3,4,5 4 2,3,4,5,6 5 3,4,5,6,7 6 4,5,6,7,8 1-phonon	+ 2 0,1,2,3,4 3 1,2,3,4,5 4 2,3,4,5,6 5 3,4,5,6,7 6 4,5,6,7,8 7 5,6,7,8,9 1-phonon
$s_{1/2}$ 100 keV	− 0 2 1 1,2,3 1-phonon	+ 3 1,2,3,4,5 4 2,3,4,5,6 1-phonon	+ 4 2,3,4,5,6 5 3,4,5,6,7 1-phonon
$d_{3/2}$ 500 keV	− 1 1,2,3 2 0,1,2,3,4 1-phonon	+ 2 0,1,2,3,4 3 1,2,3,4,5 4 2,3,4,5,6 5 3,4,5,6,7 1-phonon	+ 3 1,2,3,4,5 4 2,3,4,5,6 5 3,4,5,6,7 6 4,5,6,7,8 1-phonon
$g^{-1}_{7/2}$ 300 keV	− 3 1,2,3,4,5 4 2,3,4,5,6 1-phonon	+ 0 2 1 1,2,3 2 0,1,2,3,4 3 1,2,3,4,5 4 2,3,4,5,6 5 3,4,5,6,7 6 4,5,6,7,8 7 5,6,7,8,9 1-phonon	+ 1 1,2,3 2 0,1,2,3,4 3 1,2,3,4,5 4 2,3,4,5,6 5 3,4,5,6,7 6 4,5,6,7,8 7 5,6,7,8,9 8 6,7,8,9,10 1-phonon
$h_{11/2}$ 300 keV	+ 5 3,4,5,6,7 6 4,5,6,7,8 1-phonon	− 2 0,1,2,3,4 3 1,2,3,4,5 4 2,3,4,5,6 5 3,4,5,6,7 6 4,5,6,7,8 7 5,6,7,8,9 8 6,7,8,9,10 9 7,8,9,10,11 1-phonon	− 1 1,2,3 2 0,1,2,3,4 3 1,2,3,4,5 4 2,3,4,5,6 5 3,4,5,6,7 6 4,5,6,7,8 7 5,6,7,8,9 8 6,7,8,9,10 9 7,8,9,10,11 10 8,9,10,11,12 1-phonon

Table 9. Possible Combinations of Proton-Neutron Configurations with One Phonon Coupling

level schemes of ^{108}Ag and ^{110}Ag. Although the spins and parities of low-lying levels in ^{110}Ag have not been determined uniquely, tentative assignments can be made by comparison with the spin and parity assignments in ^{108}Ag.

The ground states 1^+

Since a phonon state cannot be a ground state, the candidates for the ground state are limited to the configurations $((g_{9/2})^{-3}_{7/2},d_{5/2})$, $((g_{9/2})^{-3}_{7/2},g_{7/2})$ and $((g_{9/2})^{-3}_{9/2},g_{7/2})$. Considering the excitation energy combination and the parabola-like multiplet structure, the 1^+ of the $((g_{9/2})^{-3}_{7/2},d_{5/2})$ may be the ground state.

The 2^- states 79.1 keV (^{108}Ag) 1.1 keV (^{110}Ag)

The first 2^- state may be a member of the $(p_{1/2},d_{5/2})$ configuration, because the (d,p) reaction populates this level with $\ell = 2$. The intense 79.1 keV E1 transition in ^{108}Ag can be explained by the proton single particle transition, while the corresponding 1.1 keV transition in ^{110}Ag cannot be observed with the current experimental apparatus.

The isomeric 6^+ states 109.5 keV (^{108}Ag) 117.5 keV (^{110}Ag)

The possible candidates are members of the $((g_{9/2})^{-3}_{7/2},d_{5/2})$ and the $(p_{1/2},h_{11/2})$, or possibly of the $((g_{9/2})^{-3}_{9/2},d_{5/2})$. It is difficult to interpret these isomeric states, since the population to these levels is still ambiguous. The $(p_{1/2},h_{11/2})$ configuration may be excluded by the fact that these states are not populated in the (d,p) reactions. Also, the $((g_{9/2})^{-3}_{9/2},d_{5/2})$ can be excluded by the parabolic structure. The $((g_{9/2})^{-3}_{7/2},d_{5/2})$ is preferred.

The 1^+ states 193.1 keV (^{108}Ag) 267.2 keV (^{110}Ag)

These are the second 1^+ states. The strong transition to the ground state and the transition to the 2^- state in each nucleus imply that the neutron configuration is $d_{5/2}$. Since the $(g_{9/2})^{-3}_{9/2}$ proton configuration

cannot form a 1^+ state with the $d_{5/2}$ neutron, the configuration of these 1^+ levels must be the same as the ground state, but probably with one phonon $(((g_{9/2})^{-3}_{7/2},d_{5/2})_1,2^+)_1$.

The 2^+ states 206.6 keV (^{108}Ag) 198.7 keV (^{110}Ag)

Three configurations $((g_{9/2})^{-3}_{7/2},d_{5/2})_2$, $(((g_{9/2})^{-3}_{7/2},d_{5/2})_1,2^+)_2$ and $((g_{9/2})^{-3}_{9/2},d_{5/2})_2$ can be the candidates for these 2^+ states. If the splitting of the $((g_{9/2})^{-3}_{7/2},d_{5/2})$ multiplet is assumed to be around 500 keV analogous to the same multiplet in ^{106}Ag [67], these 2^+ states must be members of the $((g_{9/2})^{-3}_{7/2},d_{5/2})$ multiplet.

The 3^+ states 215.4 keV (^{108}Ag) 118.7 keV (^{110}Ag)

This level correspondence has been deduced from the fact that their half-lives have been measured as 46ns and 37ns, and the g-factors as 1.301 ± 0.011 and 1.242 ± 0.012 for the 215.4 keV state of ^{108}Ag and the 118.7 keV state of ^{110}Ag, respectively [29]. The values of g-factors suggest the configuration $((g_{9/2})^{-3}_{7/2},s_{1/2})$ by comparison with empirical calculations [68]. However, the strong E1 transition in ^{110}Ag cannot be explained by a single-particle transition. The different behaviour of the depopulating transitions (i.e. strong E2 to the ground state in ^{108}Ag and strong E1 to the 2^- state in ^{110}Ag) can partly be explained by the energy dependence of transition probabilities.

The 2^+ states 294.6 keV (^{108}Ag) 360.6 keV (^{110}Ag)

The candidates for these states are $(((g_{9/2})^{-3}_{7/2},d_{5/2})_1,2^+)_2$ and $((g_{9/2})^{-3}_{9/2},d_{5/2})_2$. Since the energy difference of the second 1^+ states (193.1 keV in ^{108}Ag and 267.2 keV in ^{110}Ag) is roughly the same as the difference of these 2^+ states, it is reasonable to suggest that these states are the members of the one-phonon states coupled to the ground state. However, the configuration $((g_{9/2})^{-3}_{9/2},d_{5/2})$ cannot be excluded completely.

The 3^+ states 324.5 keV (^{108}Ag) 304.5 keV (^{110}Ag)

The depopulating transitions feed only the 1^+ and 2^+ states of the $((g_{9/2})^{-3}_{7/2},d_{5/2})$ multiplet. These 3^+ states are probably members of the same multiplet.

The 3^- states 338.4 keV (^{108}Ag) 236.8 keV (^{110}Ag)

The strong depopulation to the 2^- state suggests the possibility of the $(p_{1/2},d_{5/2})$ configuration. Since the population in the (d,p) reaction has been observed with $\ell = 2$ in ^{108}Ag, the $(p_{1/2},g_{7/2})$ configuration can be excluded.

The 4^+, (3^+) states 364.2 keV (^{108}Ag) 191.6 keV (^{110}Ag)

The intense transition to the 3^+ short-lived isomeric state and no transition to the ground state nor to the first 2^- state, suggest that the possible candidate for these states is the $((g_{9/2})^{-3}_{9/2},s_{1/2})$ configuration, forming 4^+ states. It seems inconsistent that no state of the $((g_{9/2})^{-3}_{9/2},d_{5/2})$ multiplet has not appered at lower excitation energy. This is probably due to the effect of a complicated proton-neutron residual interaction, or the second 2^+ states may be members of the $((g_{9/2})^{-3}_{9/2}, d_{5/2})$ multiplet.

The 1^- states 379.2 keV (^{108}Ag) 237.0 keV (^{110}Ag)

The population in the (d,p) reaction with $\ell = 0$ suggests the $(p_{1/2}, s_{1/2})$ configuration. The depopulating transitions are consistent with this assignment except for the enhanced E1 transition to the ground state in ^{110}Ag.

The 3^+ states 408.4 keV (^{108}Ag) 468.8 keV or 485.7 keV (^{110}Ag)

These states may be members of the one-phonon states coupled to the ground state, according to the similar energy difference.

The 0^- states 465.6 keV (^{108}Ag) 338.9 keV (^{110}Ag)

The population in the (d,p) reaction with $\ell = 0$ suggests another

member of the $(p_{1/2},s_{1/2})$ doublet.

Odd parity states around 500 keV to 900 keV

Many low spin odd parity states can be found at this energy region, which is impossible to interpret in terms of proton-neutron multiplets with the present experimental data. These levels are probably the one-phonon or two-phonon states coupled to the odd parity proton-neutron multiplets.

Based on the above configurations, the low-lying levels can be decomposed into the proton neutron multiplet groups as shown in Fig. 20.

4^+ and 5^+ states are missing or ambiguous in the $((g_{9/2})^{-3}_{7/2},d_{5/2})$ multiplet. Compared with the members of the same multiplet in ^{106}Ag, the newly constructed levels, 155.9 keV in ^{108}Ag and 174.6 keV and 255.0 keV in ^{110}Ag are unlikely to be members of the multiplet. The two levels in ^{110}Ag may be interpreted as the members of $(p_{1/2},h_{11/2})$ doublet, 6^+ and 5^+ states. If this is correct, the 57.0 keV transition will be a two-particle transition. A coincidence measurement has to be carried out very carefully between the 57.0 keV and 80.4 keV transitions.

The 1^+, 2^+ and 3^+ states interpreted as the one-phonon states coupled to the ground state have some inconsistencies. The phonon energy seems to be much less than the 500 keV expected from the neighbouring even-even nuclei. And the splitting of the levels shows rather strong spin dependence of the quasi-particle-core coupling.

Since high spin states are not populated very strongly in the neutron capture reactions in ^{107}Ag and ^{109}Ag, it is difficult to obtain all the members of multiplets. In particular, the $((g_{9/2})^{-3}_{9/2},d_{5/2})$ multiplet shows no indication of its existence at low excitation energy in ^{108}Ag and ^{110}Ag except the second 2^+ states, although all members can be found in ^{106}Ag, i.e., 234.7 keV, 389.2 keV, 503.0 keV 556.8 keV, 542.4 keV and

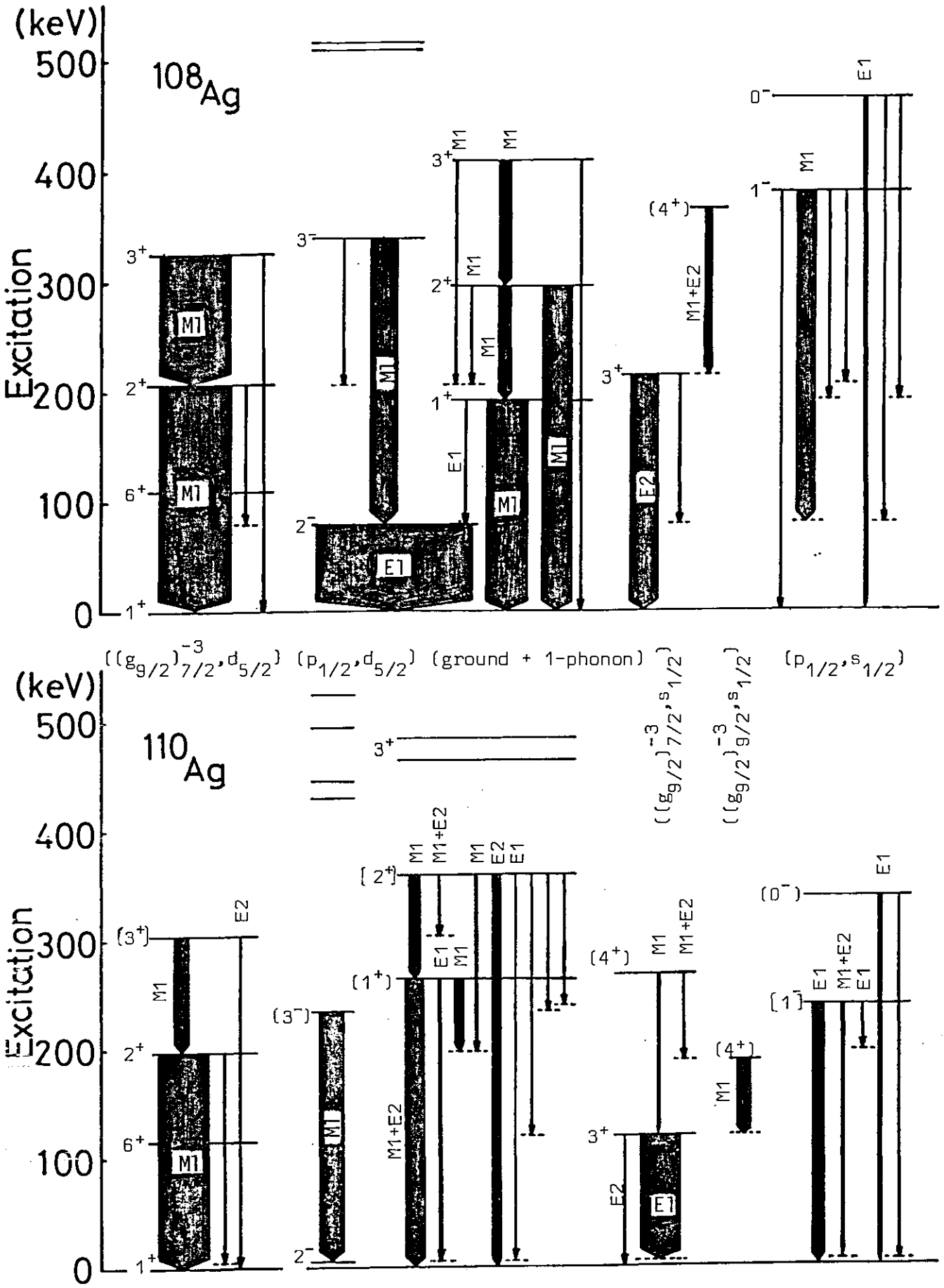

Fig. 20. Proton-Neutron Multiplets and Intra- and Inter-band Transitions

332.6 keV to be 2^+ to 7^+ states, respectively.

Some discrepancies can also be pointed out between the present level schemes and the (d,p) reaction results, which presumably include most of the odd parity states at low excitation energies. In particular, the 269 keV level in ^{110}Ag observed in the (d,p) reaction with $\ell = 2$ cannot correspond to any levels in the present level scheme.

6.3. Comparison with Parabolic Rule

As mentioned in the previous chapter, the parabolic energy dependence proposed by Paar is one of a few theories of odd-odd nuclei. Although it cannot predict correct energies, the systematics of proton-neutron multiplets can be explained. And experimental results are easily compared with the parabola of I(I + 1).

In the present work, however, few states have been interpreted in terms of proton-neutron configurations. And no multiplet has been found with all its members identified except for two doublet configurations. Since the four states 1^+, 2^+, 3^+ and 6^+ have been tentatively interpreted as members of the $((g_{9/2})^{-3}_{7/2}, d_{5/2})$ multiplet, the parabolic rule can be used to estimate the excitation energies of the missing 4^+ and 5^+ states. Although the parabolic rule does not include a particle configuration such as $(g_{9/2})^{-3}_{7/2}$, the general trend of the multiplet must follow the rule. Therefore, a simple quadratic polynomial has been fitted to the available four points for ^{108}Ag and ^{110}Ag as shown in Fig. 21.

According to this fit, the 4^+ and 5^+ states have to be found at 340 keV to 540 keV region. Candidates among the present levels are the 364.2 keV level for ^{108}Ag and the 380.1 keV and 471.2 keV levels for ^{110}Ag, but all are unlikely. For ^{110}Ag, an additional parabola was fitted assuming that the levels at 255.0 keV and 174.6 keV are the 4^+ and 5^+ states of

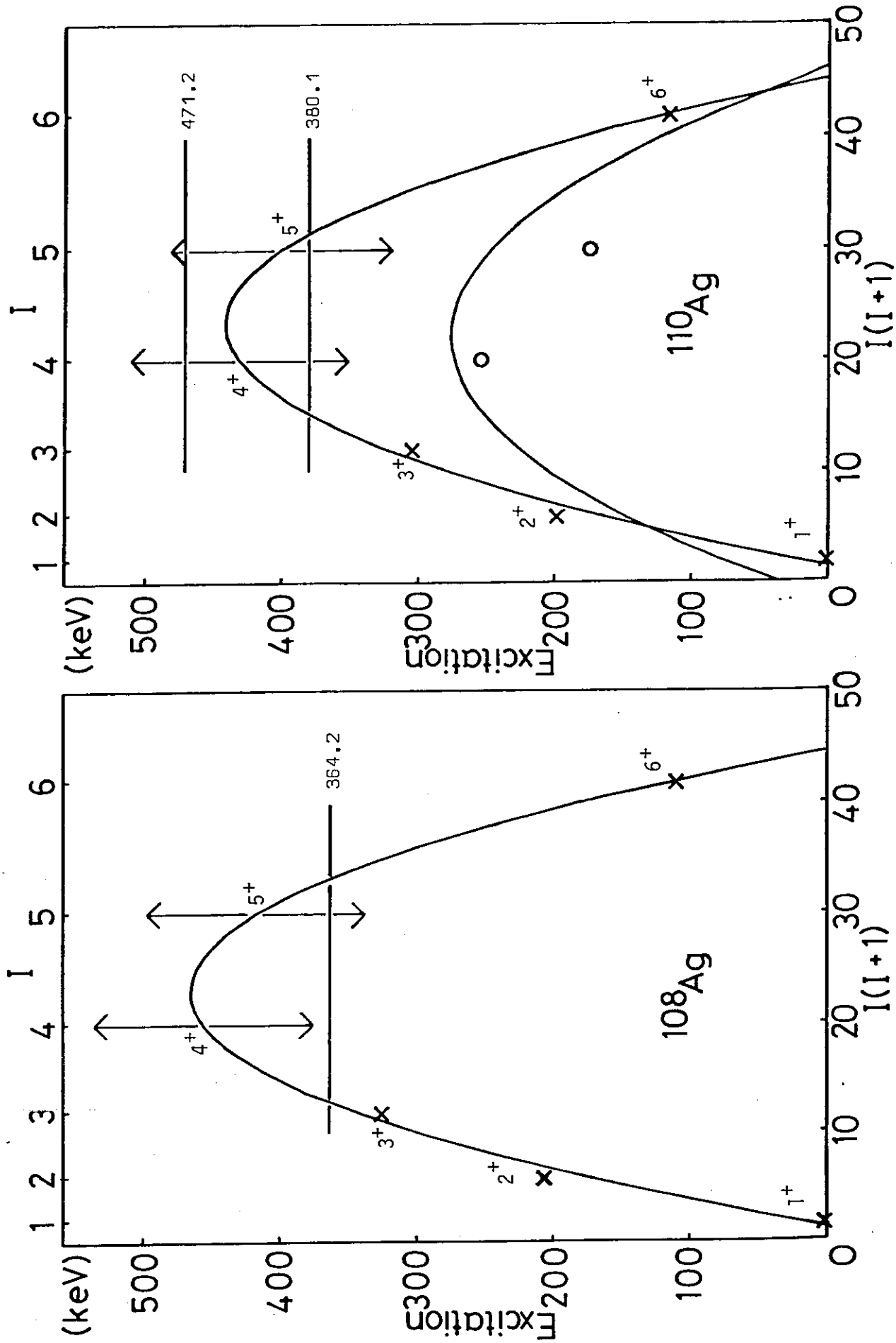

Fig. 21. Comparison with the Parabolic Energy Dependence of $((g_{9/2})^{-3}_{7/2}, d_{5/2})_{1^+ - 6^+}$ Multiplets in ^{108}Ag and ^{110}Ag

the multiplet, respectively. But the fitting looks awkward. The positions of the vertex have been obtained at reasonable places assuming that $j_p = 7/2$.

For ^{110}Ag, efforts have been made to search for the missing 4^+ and 5^+ states of this configuration. A very preliminary result has been obtained as shown in Fig. 22. The result shows that the 4^+ and 5^+ states lie at 612.507 ± 0.004 keV and 386.469 ± 0.006 keV, respectively. A parabola was fitted to the result as in Fig. 23. The 612.5 keV 4^+ state lies at slightly higher excitation energy than expected. But this feature is very similar to that of the same multiplet in ^{106}Ag.

The configurations $(p_{1/2},d_{5/2})$ and $(p_{1/2},s_{1/2})$ have been assigned to four levels each in ^{108}Ag and ^{110}Ag. The sequence of levels ~~have~~ has been compared with the special case of the parabolic rule (i.e., A = 0). The configuration $(p_{1/2},d_{5/2})$ with $N = j_p - \ell_p + j_n - \ell_n = 0$ must have the sequence $(2^-, 3^-)$, which agrees with the present interpretation. However, the configuration $(p_{1/2},s_{1/2})$ with N = 0 does not follow this rule.

The parabolic rule is in progress in the cases $|(j_p,\text{phonon})_J,j_n>$ or $|j_p,(j_n,\text{phonon})_J>$ [69]. However, the second $(1^+, 2^+, 3^+)$ sequence has been interpreted in the present work as one phonon coupling with the ground state, i.e., $|(j_p,j_n)_J,\text{phonon}>$ type. It seems that the coupling with one-phonon follows a somewhat linear energy energy dependence on spin I. The differences between these configurations have to be made clear.

6.4. Gamma-ray Yield

It may be interesting to treat the experimental data statistically. The primary transitions can be compared with the Porter-Thomas distribution and the spectrum can be compared with the theoretical calculation

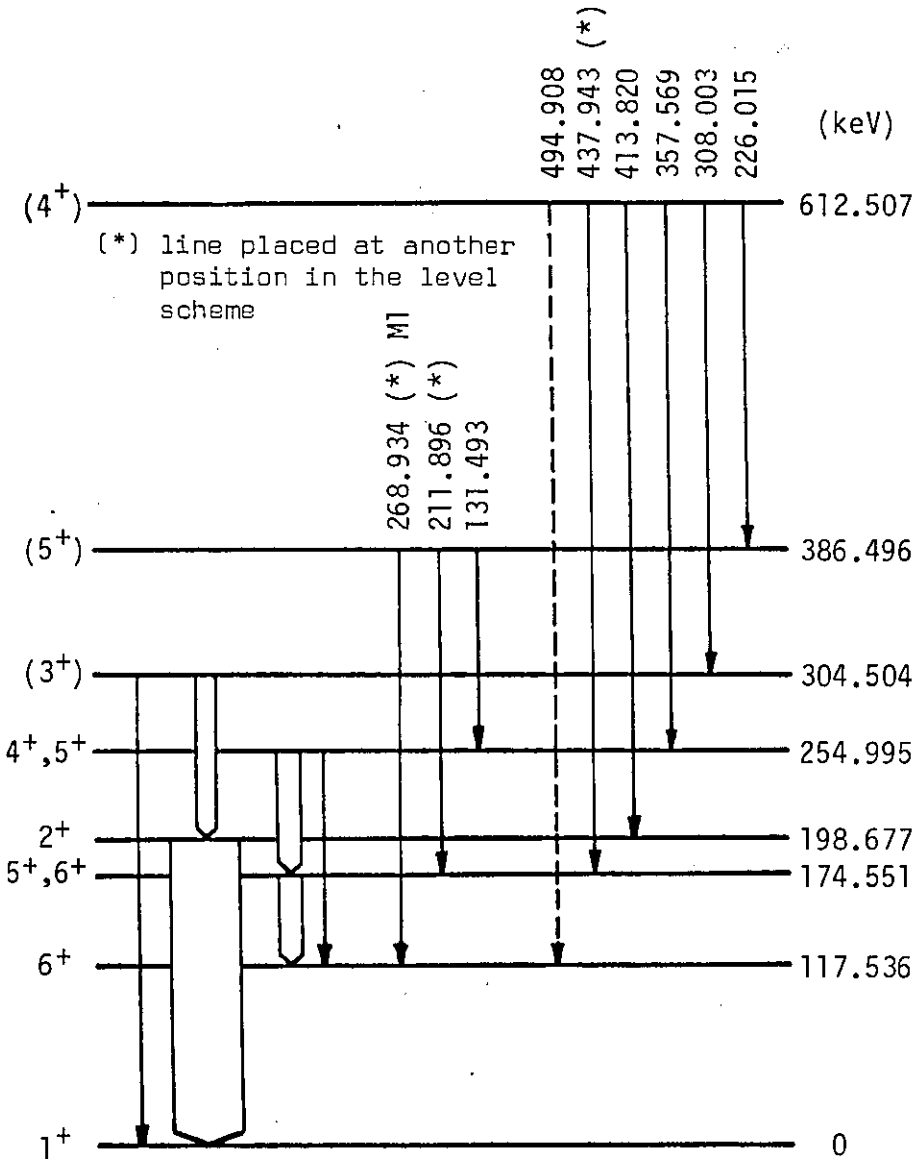

Fig. 22. Proposed 4^+ and 5^+ states of the multiplet $((g_{9/2})^{-3}_{7/2}, d_{5/2})$ in ^{110}Ag

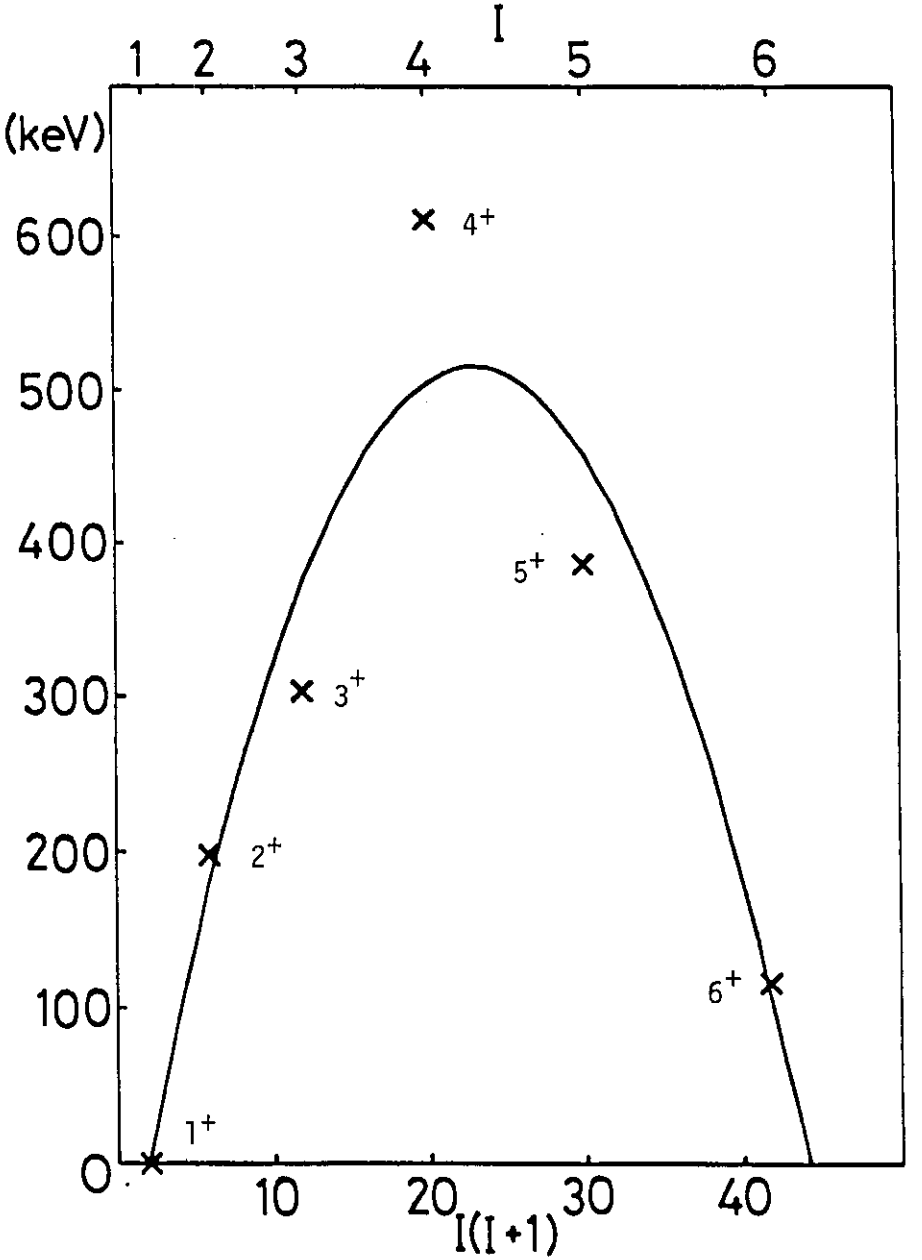

Fig. 23. Comparison with the Parabolic Energy Dependence

described in Chapter 1.

6.4.1. Primary Gamma-rays

The Porter-Thomas distribution can be applied to the fluctuation of primary gamma-transition partial widths of the thermal neutron capture compound state. Since the spin and parity of the compound state are not unique, all the primary transitions may be used for the statistics. The effectiveness of the Porter-Thomas distribution can then be examined in the case of thermal neutron capture. Assuming that the partial widths are proportional to the reduced intensities divided by the corresponding transition energies powered by a certain reduction factor n. For example, n = 3 can be used, because the transition probability is proportional to E_γ^3 in the case of E1 or M1 single particle transition.

In the present work, the reduced intensities of assigned transitions have been examined with the χ^2-distributions with one and two degrees of freedom as shown in Fig. 24. The fitting method is described in Appendix 4. The characteristics of the distributions for ^{108}Ag and ^{110}Ag differ from each other for each value of reductionfactor n = 1, 3 or 5. This is probably because all the spins and parities of final states have been ignored,and of course, not many data are available, especially two unresolved doublets (i.e. transitions to the ground state - 1.1 keV and 748.5 keV - 750.8 keV) have not been taken into account in ^{110}Ag.

The differences between ^{108}Ag and ^{110}Ag may suggest that the thermal neutron capture compound states of ^{108}Ag and ^{110}Ag can be very different, which is also indicated from the fact that the intensities of the ground state primary transitions per neutron capture are very different in ^{108}Ag and ^{110}Ag. These may be related to the difference of the neutron binding energies.

Since the gamma-ray measurement by PN4 includes the energy range

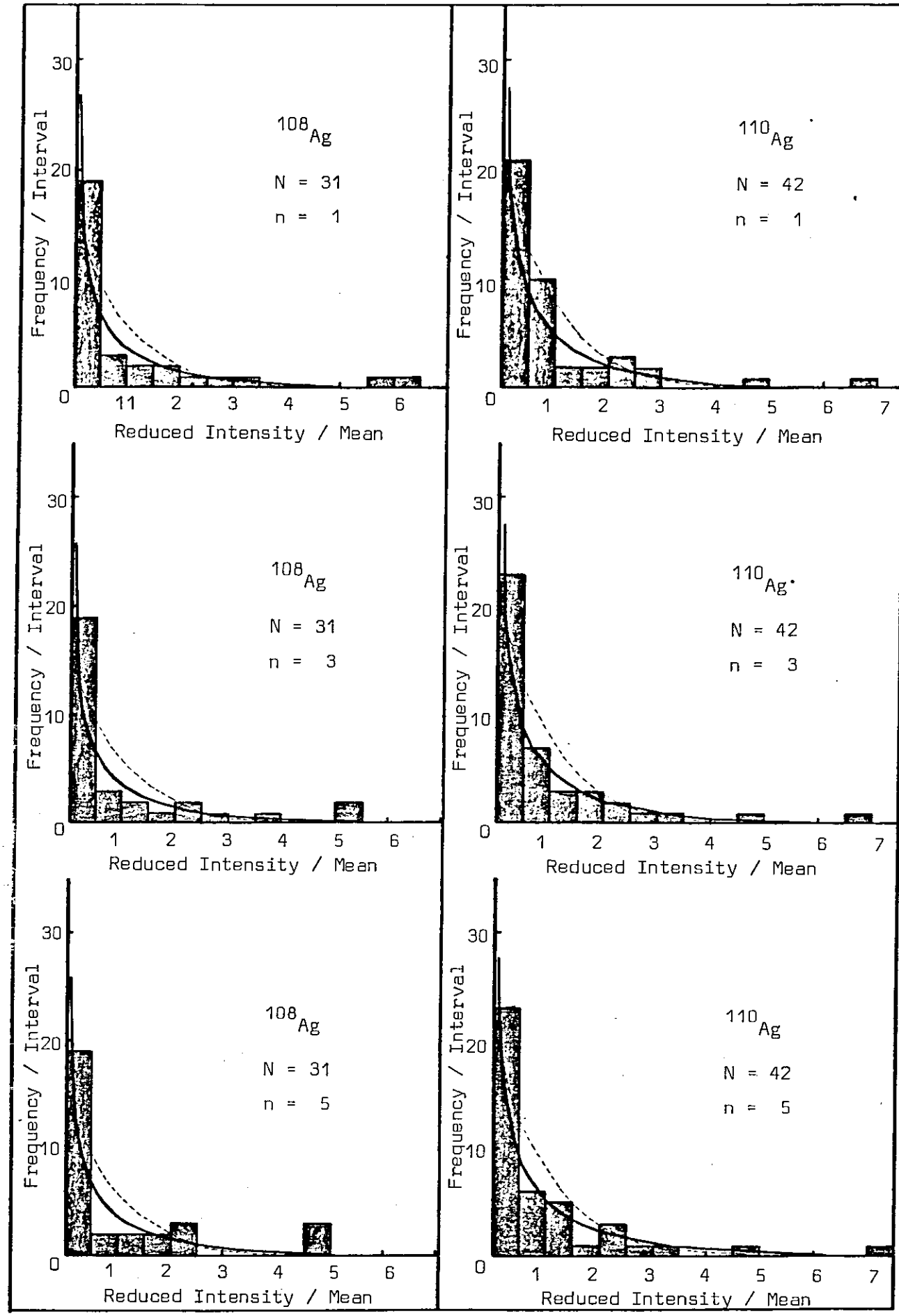

Fig. 24. Reduced Intensity Distribution of Primary Gamma-Transitions

—— χ^2-distribution with one degree of freedom

---- χ^2-distribution with two degrees of freedom

from 1.4 MeV up to the neutron binding energy in ^{110}Ag and very little is known about the level scheme, the Porter-Thomas distribution can be examined using these data including unassigned transitions as shown in Fig. 25. All the 395 transitions above 3.5 MeV were assumed as primary transitions, where 3.5 MeV was chosen arbitrarily around the half of neutron binding energy.

The result shows that the χ^2-distribution with two degrees of freedom can fit the data better than that with one degree. However, it must not be forgotten that some very weak intensity transitions have not been detected and some multiplets have not been resolved due to the limited detection efficiency and energy resolution. As can be seen in Fig. 25, an attempt was made to correct the frequency of the lowest intensity class-interval, assuming that the data follow the χ^2-distribution with one degree of freedom. This procedure is described also in Appendix 4. The correction estimates that approximately 170 transitions have not been detected with the total of 2.6% observed reduced intensities above 3.5 MeV in the present PN4 experiment.

This value disagrees with the 69% missing energy-intensity product. To explain this large discrepancy, it has to be assumed that many gamma-transitions with medium reduced intensities have not been observed at the medium energy 2 MeV to 6 MeV region in the present experiment; or the absolute intensity calibration for high energy gamma-rays has been underestimated as mentioned earlier.

6.4.2. Gamma-ray spectrum

The complete gamma-ray spectrum in the reaction ^{109}Ag(n,γ)^{110}Ag has been produced with the experimental data in the present work. In order to make a smooth spectrum the following equation has been used to calculate the intensity $f(E_\gamma)$ in the energy interval between E_γ and $E_\gamma + dE_\gamma$.

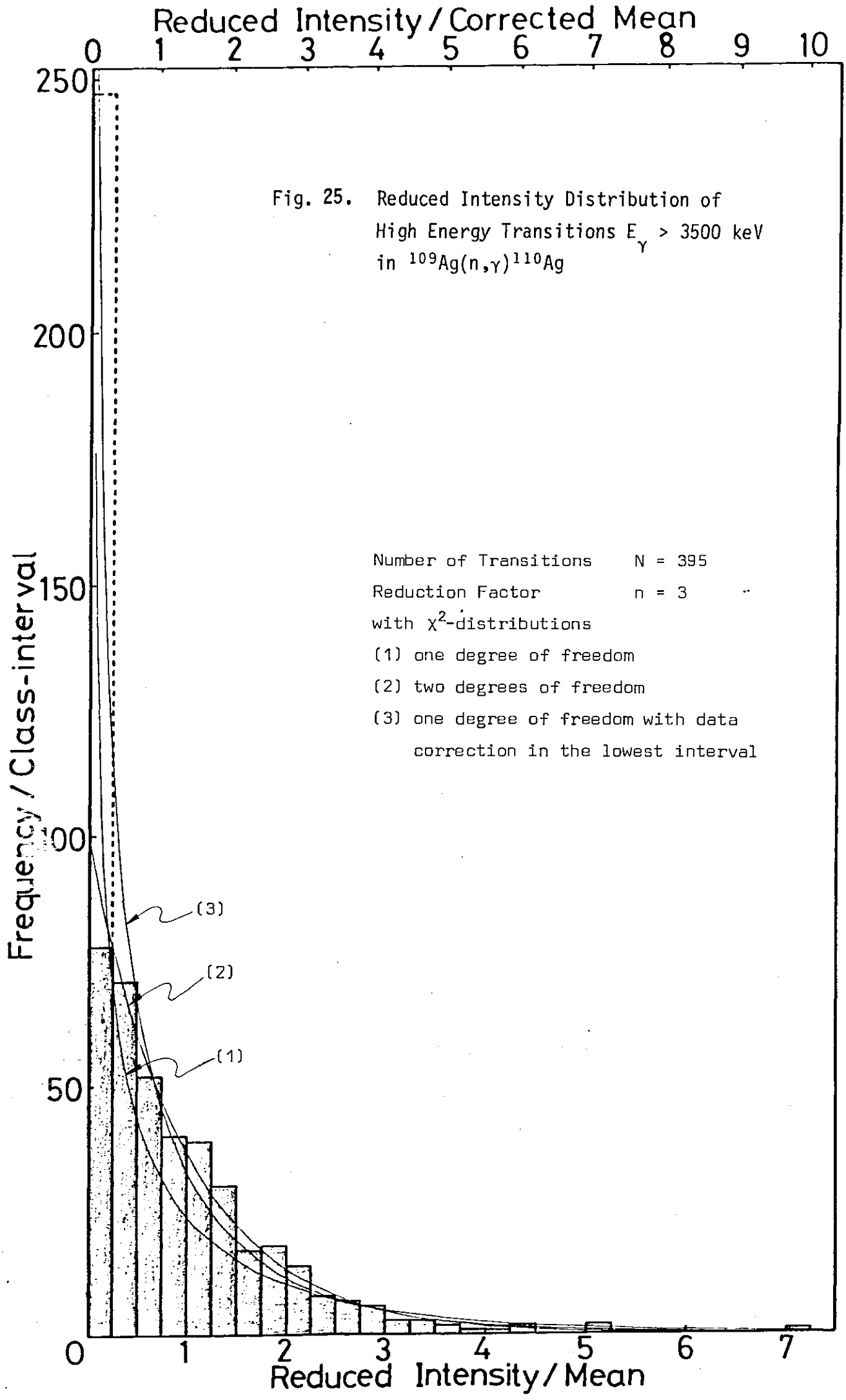

Fig. 25. Reduced Intensity Distribution of High Energy Transitions E_γ > 3500 keV in $^{109}Ag(n,\gamma)^{110}Ag$

Number of Transitions N = 395

Reduction Factor n = 3

with χ^2-distributions

(1) one degree of freedom

(2) two degrees of freedom

(3) one degree of freedom with data correction in the lowest interval

$$f(E_\gamma) = \sum_i \frac{I_i}{\sqrt{(2\pi)}\cdot\sigma} \exp\{ - \frac{(E_\gamma - E_i)^2}{2\sigma^2} \}$$

where, E_i and I_i are experimental data and σ is a smoothing factor. The result is shown in Fig. 26 with different smoothing factors.

This result with a very significant second peak at 5 MeV to 6 MeV region is different from the spectrum obtained by Starfelt [15], and shows similar character to the Au or Cs spectrum, which can be explained by the M1 giant resonance. It has been confirmed in the present work that M1 transitions are enhanced in ^{110}Ag for low transition energies. the enhanced M1 transitions may be present also at higher energies not due to the number of neutrons but to the characteristics of odd-odd nuclei.

6.5. Double Neutron Capture

An attempt has been made to observe double neutron capture via ^{110m}Ag in the high energy spectrum, since the neutron capture cross-section of ^{110m}Ag has been reported to be about 80 barns [36] and the neutron binding energy of ^{111}Ag has been estimated to be higher than the ^{110}Ag binding energy. However, no significant peak has been found in the spectrum, from which one may deduce that the capture cross-section of 80 barns may be an overestimation.

On the other hand, in the low energy experiment with GAMS 1, the 70.5 keV transition from the $(9/2)^+$ state to the $(7/2)^+$ state in ^{111}Ag can be seen at the first and second orders of reflection with increasing intensity with time, but the 59.9 keV transition from the $(7/2)^+$ state to the $(1/2)^-$ ground state has not been observed. This may be due to the 65sec half-life of the $(7/2)^+$ state and the high internal conversion coefficient of E3 multipolarity. The 34.4 keV electron line observed by BILL spectrometer may correspond to this 59.9 keV transition.

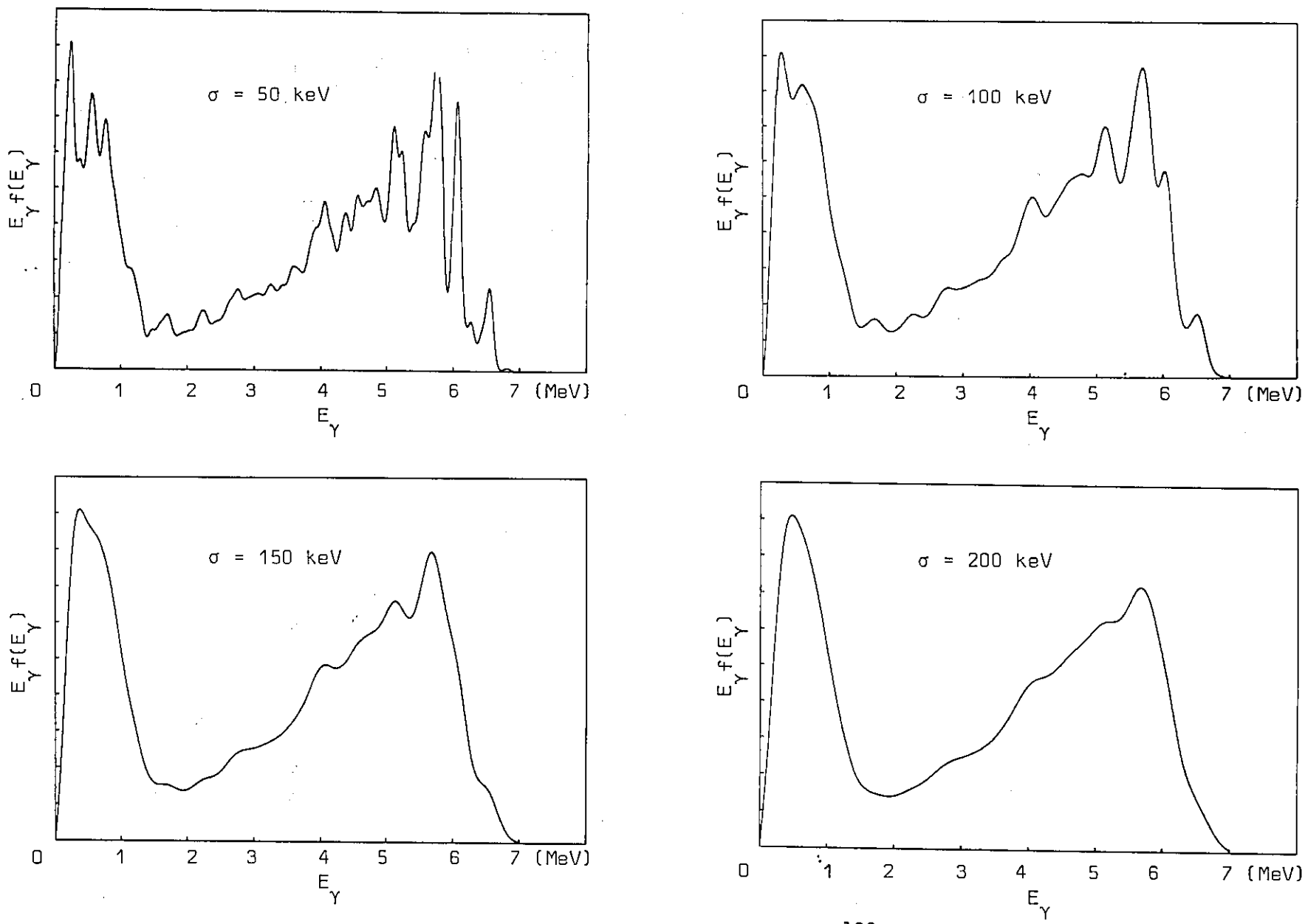

Fig. 26. Gamma-ray Spectrum in Thermal Neutron Capture Reaction in ^{109}Ag

Since double neutron capture probability is very sensitive to the neutron flux and the details of transitions in ^{111}Ag are not available, any quantitative argument cannot be discussed with these low energy transition data. However, it is still suspected that the capture cross-section of 80 barns may be overestimated and the isomeric transition ratio of 99.7% [70] from the $(7/2)^+$ state to the ground state in ^{111}Ag may also be overestimated.

CHAPTER 7.

CONCLUSION

With the present level schemes of ^{108}Ag and ^{110}Ag, it can be pointed out that there are some interesting features of proton-neutron multiplet coupled with a vibrational phonon as discussed in the previous chapter. But it is also pointed out that the complete multiplet of $((g_{9/2})^{-3}_{9/2}, d_{5/2})$ configuration is missing. As mentioned before, thermal neutron capture is not a very good method to observe high spin states, therefore it is difficult to interpret each level as a member of certain nuclear configurations. It is definitely necessary to perform some heavy ion reactions or high energy reactions to obtain high spin states in odd-odd silver isotopes. And much more precise (d,p) reactions have to be carried out to investigate the systematics of odd parity states. Currently, the (p,d) reaction is in progress to investigate ^{108}Ag. With these reactions, the existence of excited states must be confirmed, then the Ritz combination principle can be applied to the region of excitation energy with the precise gamma-ray energy data obtained in the present work to deduce very precise level energies. Those reactions and average resonance capture reactions are very useful to assign spins and parities.

Theoretical improvement will be expected in parallel with the progress of experiments, and the mechanism of odd-odd nuclei and the residual interaction between unpaired proton and neutron will be discussed much in detail. However, as long as the nuclear physics is based on quantum mechanics, some approximations are necessary because of the mathematical limitation in solving the Schrödinger's equation of many body system.

It is also expected that particle-hole states will be investigated in neighbouring even-even nuclei, which must show similar characteristics

to odd-odd nuclei. Then, the charge dependence of unpaired nucleon interaction can be justified.

REFERENCES

1) E. Amaldi et al; Proc. R. Soc. A149, 522 (1935)
Proc. R. Soc. A146, 483 (1934)

2) C.E. Porter and R.G. Thomas; Phys. Rev. 104, 483 (1956)

3) A.M. Lane and J.E. Lynn; Nucl. Phys. 17, 586 (1960)
J.E. Lynn; "The theory of neutron resonance reactions", Clarendon Press, (1968)

4) K. Hyde et al; Phys. Rev. C17, 1219 (1978)
R.E. Anderson et al; Phys. Rev. C15, 123 (1977)
R.M. Del Vecchio et al; Phys. Rev. C12, 845 (1975)
V. Paar; Nucl. Phys. A211, 29 (1973)

5) F.S. Levin and H. Feshbach; "Reaction dynamics", Gordon and Breach Science Publishers (1973)

6) H. Feshbach, C.E. Porter and V.F. Weisskopf; Phys. Rev. 96, 448 (1954)

7) D.F. Jackson; "Nuclear reactions", Methuen and Co. Ltd. (1970)

8) D.M. Brink and G.R. Satchler; "Angular momentum", Oxford Univ. Press, 2nd ed. (1968)

9) B.B. Kinsey and G.A. Bartholomew; Phys. Rev. 93,1260 (1954)

10) A.M. Lane; in "Neutron capture gamma-ray spectroscopy", 31 (1975) Proceeding of the second international symposium on neutron capture gamma-ray spectroscopy and related topics, Petten, 1974

11) S.F. Mughabghab; in "Nuclear structure study with neutrons", 167, ed. J. Erö and J. Szücs, Plenum Press (1974)

12) S.F. Mughabghab; in the proceeding ref.9, 53

13) J.M. Blatt and V.F. Weisskopf; "Theoretical nuclear physics", John Wiley and Sons. NY, (1952)

14) L.M. Bollinger and G.E. Thomas; Phys.Rev. C2, 1951 (1970)

15) N. Starfelt; Nucl. Phys. 53, 397 (1964)

16) D. Rabenstein and D. Harrach; Nucl. Phys. A242, 189 (1975)
V.L. Alexeev et al; Nucl. Phys. A297, 373 (1978)

17) M. Thein; Ph.D. Thesis, Univ. of London (1977)
G.R. Massoumi; Ph.D. Thesis, Univ. of London (1979)

18) D. Breitig and H.R. Koch; Unpublished data, private communication

19) M. Bogdanovic; Unpublised data, private communication

20) P. Sushkov; Unpublished data, private communication

21) G.B. Orr, W.R. Kane and G.J. Smith; in "Neutron capture gamma-ray spectroscopy", 707, Plenum Press, NY (1979)
Proceeding of the third international symposium on neutron capture gamma-ray spectroscopy and related topics, BNL, 1978

22) W.R. Kane; Unpublished data, private communication

23) M. Bogdanovic et al; Fizika 10, 133 (1978)

24) H.H. Bolotin and A.I. Namenson; Phys. Rev. 157, 1131 (1967)

25) M. Bogdanovic et al; Fizika 11, 157 (1979) and ref.21, 567

26) Th.W. Elze et al; Zeit. Phys. 209, 497 (1968)

27) P. Winkler; Forschungsbericht, ZfK Rossendorf bei Dresden 126 (1967)

28) C.E. Brient et al; Phys. Rev. C6, 1837 (1972)

29) H. Hattori, M. Adachi and T. Taketani; J. Phys. Soc. Japan 41, 1830 (1976)

30) W. Mampe et al; Nucl. Instr. Meth. 154, 127 (1978)

31) H.R. Koch et al; Nucl. Instr. Meth. 175, 401 (1980)

32) J.J. Reidy; in "The electromagnetic interaction in nuclear spectroscopy", 839, ed. W.D. Hamilton, North. Holl. Pub. Co. (1975)
J.W. Knowles; in "α,β and γ-spectroscopy", 203, ed. K. Siegbahn, North Holl. Pub. Co. (1966)

33) J.T. Routti and S.G. Prussin; Nucl. Instr. Meth. 72, 125 (1969)

34) R.G. Helmer et al; Atom. Data and Nucl. Data Tables 24, 39 (1979)

35) E. Storm and H.I. Israel; Nucl. Data Tables A7, 565 (1970)

36) S.F. Mughabghab and D.I. Garber; "Neutron cross sections", BNL 325, vol. 1 (1973)

37) F.E. Bertrand; Nucl. Data Sheets 22, 135 (1977)

38) B. Maier; "Neutron beam facilities at the HFR available for users", I.L.L. (1977)

39) C. Hofmyer, Y. Tokunaga and S. Kerr; Private communication

40) M.L. Stelts and R.E. Chrien; Nucl. Instr. Meth. 155, 253 (1978)

41) K. Siegbahn; "α,β and γ-spectroscopy"

42) T. Mitsunari; Internal Report, ULRC/RES/29 (1980)

43) T.A.A. Tielen; Private communication

44) R.S. Hager and E.C. Seltzer; Nucl. Data A4, 1 (1968)

45) G.R. Massoumi et al; to be published

46) G.H. Fuller and V.W. Cohen; Nucl. Data Tables A5, 433 (1969)

47) Y. Kawase et al; Nucl. Phys. A193, 204 (1972)

48) S. Malmskog and J. Konijn; Nucl. Phys. 38, 196 (1962)
C.J. Cussens, G.K. Rochester and K.F. Smith; J. Phys. A2, 658 (1969)

49) W.R. Kane and G. Scharff-Goldhaber; Phys. Rev. C2, 314 (1970)

50) D.D. Clark, V.O. Kostroun and N.E. Siems; Phys. Rev. C12, 595 (1975)

51) T. Katoh and Y. Yoshizawa; Nucl. Phys. 32, 5 (1962)

52) M.E. de Lopez; ref. 6 in ref. 28

53) G. Racah; Phys. Rev. 62, 438 (1942)

54) B.H. Flowers; Proc. R. Soc. A212, 248 (1952)

55) J. Bardeen, L.N. Cooper and J.R. Schrieffer; Phys. Rev. 108, 1175 (1957)
A. Bohr, B.R. Mottelson and D. Pines; Phys. Rev. 110, 936 (1958)

56) F. Iachello; "Interacting bosons in nuclear physics", Plenum Press, NY (1979)
A. Arima and F. Iachello; Phys. Rev. Lett. 35, 1069 (1975)

57) L.W. Nordheim; Phys. Rev. 78, 294 (1950)

58) C.J. Gallagher Jr. and S.A. Moszkowski; Phys. Rev. 111, 282 (1958)

59) S.G. Nilsson; Kgl. Danske Vid. Sel., Mat. Fys. Medd. 29, No.16 (1955)

60) P.J. Brussaard and P.W.M. Glaudemans; "Shell-model applications in nuclear spectroscopy", North Holl. Pub. Co. (1977)
A. de Shalit and H. Feshbach; "Theoretical nuclear physics", Vol. 1 Nuclear structure, John Wiley and sons Inc. (1974)

61) D.J. Rowe; "Nuclear collective motion, Models and theory", Methuen and Co. Ltd. (1970)

62) G. Alaga; Bull. Am. Phys. Soc. 4, 359 (1959)
V. Paar; Nucl. Phys. A211, 29 (1973)

63) V. Paar; Nucl. Phys. A331, 16 (1979)

64) W.F. van Gunsteren; Nucl. Phys. A265, 263 (1976)
W.F. van Gunsteren, K. Allaart and E. Boeker; Nucl. Phys. A266, 365 (1976)
W.F. van Gunsteren; Zeit. Phys. 282, 55 (1977)

65) A. Bohr and B.R. Mottelson; Kgl. Danske Vid. Sel., Mat. Fys. Medd. 27, No.16 (1953)

66) A. Bohr and B.R. Mottelson; "Nuclear structure", Vol. 2, Benjamin (1975)

67) B. Harmatz; Nucl. Data Sheets 30, 305 (1980)

68) H. Bertschat et al; Nucl. Phys. A229, 72 (1974)

69) V. Paar et al; in the prceeding of the fourth international symposium on neutron capture gamma-ray spectroscopy and related topics, Grenoble, 1981

70) C.M. Lederer and V.S. Shirley; "Table of isotopes", 7th ed. (1978)

APPENDIX 1.

A.1. Integrals in Level Energy Calculation

In order to calculate level energies, a method has been introduced to maximize the likelihood as described in Section 3.2. LEVELS3. However, the expression of the results is rather implicit including some integral forms. To calculate these integrals, a linear transformation of the variables X_n is introduced. Since the function S can be expressed as

$$S = \sum_{ij} A_{ij} X_i X_j + \sum B_k X_k + C$$

$$= \langle X|A|X\rangle + \langle B|X\rangle + C ,$$

the linear transformation T from $|X\rangle$ to $|Y\rangle$

$$|Y\rangle = T|X\rangle$$

may be chosen so that S can be written in the following form.

$$S = \sum_{k} (Y_k - D_k)^2 + E$$

$$= \langle X|T^{tr}T|X\rangle - 2\langle D|T|X\rangle + \langle D|D\rangle + E$$

where A and T are matrices and $|X\rangle$, $|Y\rangle$, $|B\rangle$ and $|D\rangle$ are vectors of dimension N. Hence, the following constraints are obtained to equate the above two expressions.

$$A = T^{tr}T$$

$$|B\rangle = -2T^{tr}|D\rangle$$

$$C = \langle D|D\rangle + E$$

In order to satisfy these constraints, A has to be a symmetric matrix. This implies, on the other hand, the number of the independent elements of T is N(N + 1)/2, and therefore all the off-diagonal elements of one side of T can be equated to zero.

$$T_{ij} = 0 \qquad (i < j)$$

Since all the diagonal elements of A are not zero, the determinant of T has a finite non-zero value. So,

$$\text{Rank}(T) = N$$

There is an inverse matrix of T, which is a necessary condition for the calculation to be feasible. Therefore,

$$|D\rangle = -\frac{1}{2} T^{tr\ -1}|B\rangle = -\frac{1}{2} T^{-1\ tr}|B\rangle$$

$$|X\rangle = T^{-1}|Y\rangle$$

Now, a complete preparation for the integral calculation has been obtained.

$$\int F(X_1, \ \ldots\ , X_N) dX_1 dX_2 \ \ldots\ dX_N$$

$$= \int \exp\{ -(\sum_k (Y_k - D_k)^2 + E)\} \det|T^{-1}| dY_1 dY_2 \ \ldots\ dY_N$$

$$= \det|T^{-1}| \prod_k \int_{-\infty}^{+\infty} \exp\{ -(Y_k - D_k)^2\} dY_k \cdot \exp(-E)$$

$$= \det|T^{-1}| \ \exp(-E)\ \pi^{N/2}$$

$$\int X_n\ F(X_1, \ \ldots\ , X_N) dX_1 dX_2 \ \ldots\ dX_N$$

$$= \int (\sum_i T^{-1}_{ni}\ Y_i)\ \exp\{ -(\sum_k (Y_k - D_k)^2 + E)\}\ \det|T^{-1}|\ dY_1 dY_2 \ \ldots\ dY_N$$

$$= \det|T^{-1}|\ \exp(-E)\ \{ \sum_i T^{-1}_{ni} \int Y_i\ \exp\{ -\sum_k (Y_k - D_k)^2\} dY_1 dY_2 \ \ldots\ dY_N\}$$

$$= \det|T^{-1}|\ \exp(-E)\ \{ \sum_i T^{-1}_{ni} \prod_{k\neq i} \int_{-\infty}^{+\infty} \exp\{ -(Y_k - D_k)^2\} dY_k \cdot \int_{-\infty}^{+\infty} Y_i\ \exp\{ -(Y_i - D_i)^2\} dY_i\ \}$$

$$= \det|T^{-1}|\ \exp(-E)\ \pi^{N/2} \sum_i T^{-1}_{ni}\ D_i$$

$$\int X_n^2\ F(X_1, \ \ldots\ , X_N) dX_1 dX_2 \ \ldots\ dX_N$$

$$= \int (\sum_i T^{-1}_{ni}\ Y_i)^2 \exp\{ -(\sum_k (Y_k - D_k)^2 + E)\}\ \det|T^{-1}|\ dY_1 dY_2 \ \ldots\ dY_N$$

$$= \det|T^{-1}|\ \exp(-E) \int \sum_{ij} T^{-1}_{ni}\ T^{-1}_{nj}\ Y_i\ Y_j\ \exp\{ -\sum_k (Y_k - D_k)^2\}\ dY_1 \ \ldots\ dY_N$$

$$= \det|T^{-1}|\ \exp(-E)\ \{ \sum_{i\neq j} T^{-1}_{ni}\ T^{-1}_{nj} \int Y_i Y_j \exp\{ -\sum_k (Y_k - D_k)^2\}\ dY1 \ \ldots\ dY_N$$

$$+ \sum_i (T^{-1}_{ni})^2 \int Y_i^2\ \exp\{ -\sum_k (Y_k - D_k)^2\}\ dY_1 dY_2 \ \ldots\ dY_N\ \}$$

$$= \det|T^{-1}|\ \exp(-E)\ \{\ \sum_{\substack{i,j \\ i\neq j}} \{T^{-1}_{ni}\ T^{-1}_{nj} \prod_{\substack{k\neq i \\ \neq j}} \int_{-\infty}^{+\infty} \exp\{-(Y_k - D_k)^2\}\ dY_k \cdot$$

$$\int_{-\infty}^{+\infty} Y_i\ \exp\{-(Y_i - D_i)^2\}\ dY_i \cdot \int_{-\infty}^{+\infty} Y_j\ \exp\{-(Y_j - D_j)^2\}\ dY_j\ \}$$

$$+ \sum_i (T^{-1}_{ni})^2 \prod_{k\neq i} \int_{-\infty}^{+\infty} \exp\{-(Y_k - D_k)^2\}\ dY_k \cdot \int_{-\infty}^{+\infty} Y_i^2\ \exp\{-(Y_i - D_i)^2\}\ dY_i\ \}$$

$$= \det|T^{-1}|\ \exp(-E)\ \pi^{N/2}\ \{\ 2 \sum_{i>j} T^{-1}_{ni}\ T^{-1}_{nj}\ D_i\ D_j + \sum_i (T^{-1}_{ni})^2 (D_i^2 + \frac{1}{2})\ \}$$

$$= \det|T^{-1}|\ \exp(-E)\ \pi^{N/2} \sum_{i,j} T^{-1}_{ni}\ T^{-1}_{nj}\ (D_i D_j + \delta_{ij}/2)$$

Therefore, the expectation values of level energies $\overline{X}_n$ are given by

$$\overline{X}_n = \sum_i T^{-1}_{ni}\ D_i$$

and the square of standard deviations σ_n^2 are given by

$$\sigma_n^2 = \overline{X_n^2} - \overline{X}_n^{\,2}$$

$$= \sum_i (T^{-1}_{ni})^2/2$$

APPENDIX 2.

A.2. Two-Gaussian Fit

If a peak cannot be fitted by a single Gaussian function in the cases where there is a significant high or low energy tail, or peak asymmetry, two Gaussians may be used to fit the peak. The peak shape is given by

$$f(x) = \frac{P}{\sqrt{(2\pi)}\sigma} \{ \exp(- \frac{x^2}{2\sigma^2}) + A \cdot \exp(- \frac{(x - x_o)^2}{2\sigma^2}) \}$$

Since the Gaussian fitting computer programmes are widely available, this two-Gaussian fit method can be used without changing the fitting function.

Obviously, there is a finite probability to observe a true doublet, which may be fitted also by two Gaussians. Therefore, it is necessary to set up a criterion which distinguishes a singlet from a doublet, using fitted results, the intensity ratio A, the peak separation x_o, their errors and the standard deviation σ = FWHM / $2\sqrt{(2\ln 2)}$.

In order to confirm a doublet visually, the following criterion can be considered.

(1) If there are four zero points in the second derivative f"(x), f(x) is regarded as a doublet.

The number of zero points in f"(x) can be expressed schematically as in Fig. A1.

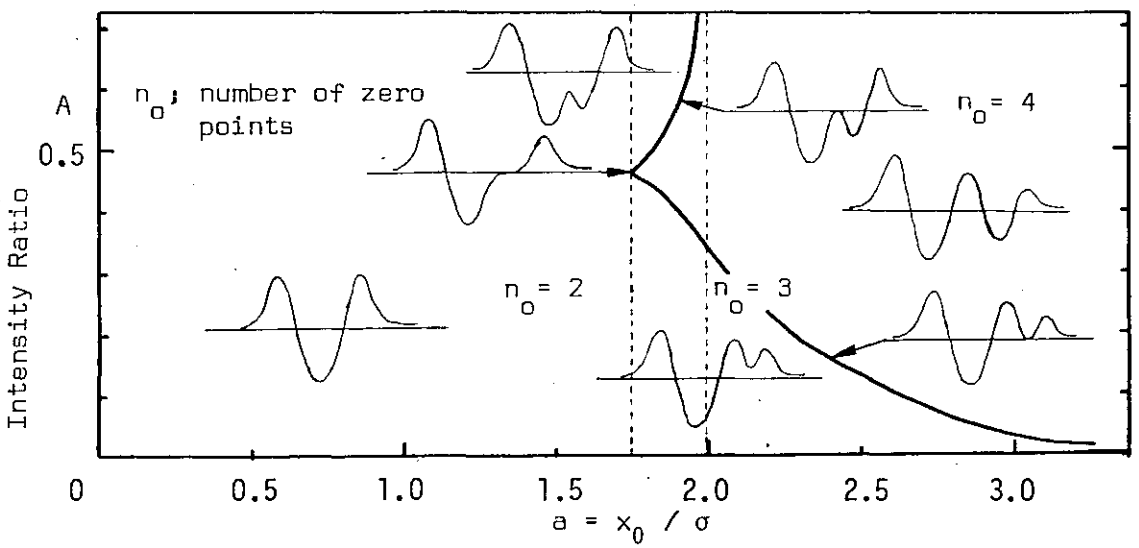

Fig. A1. Number of Zero Points in the Second Derivative

This criterion implies that the peak is a doublet if its curvature changes its sign four times. This criterion can be used if the intensity ratio is rather small (e.g. A < 0.3). However, if the intensity ratio is rather large, this is no more powerful, since the full width shows its increase very clearly.

Another criterion may be considered for higher intensity ratios.

(2) If there are five zero points in the third derivative f'''(x), f(x) can be regarded as a doublet.

This implies a smooth change of the curvature.

However, when considering higher derivatives, the criteria become meaningless, because they simply show how close the function is to a Gaussian function. Therefore, expected FWHM has to be calculated as a function of A and $a = x_o/\sigma$. The result is shown in Fig. A2. with the criteria (1) and (2) on the same a-A plane.

Consequently, it may be concluded that the peak shape is important for a > 2.0 and FWHM for a < 2.0. However, no additional criteria have been considered to connect the two criteria by a visual method. This kind of correction may have to be made during the peak fitting procedure, where the original spectrum is available.

Despite this fact, some efforts have been made to identify singlets for a > 1.6 using the mixed criteria of (1) and (2). Those for a < 1.6 are regarded as a singlet, which is not really correct, but the case occurs very rarely.

Practically, the peak identification is carried out with a set of fitted peak data ($x_i \pm \Delta x_i$, $I_i \pm \Delta I_i$) and neighbouring two peaks are tested under the condition, which requires a certain confidence limit to identify a doublet. Peak positions and peak areas are corrected appropriately for singlets.

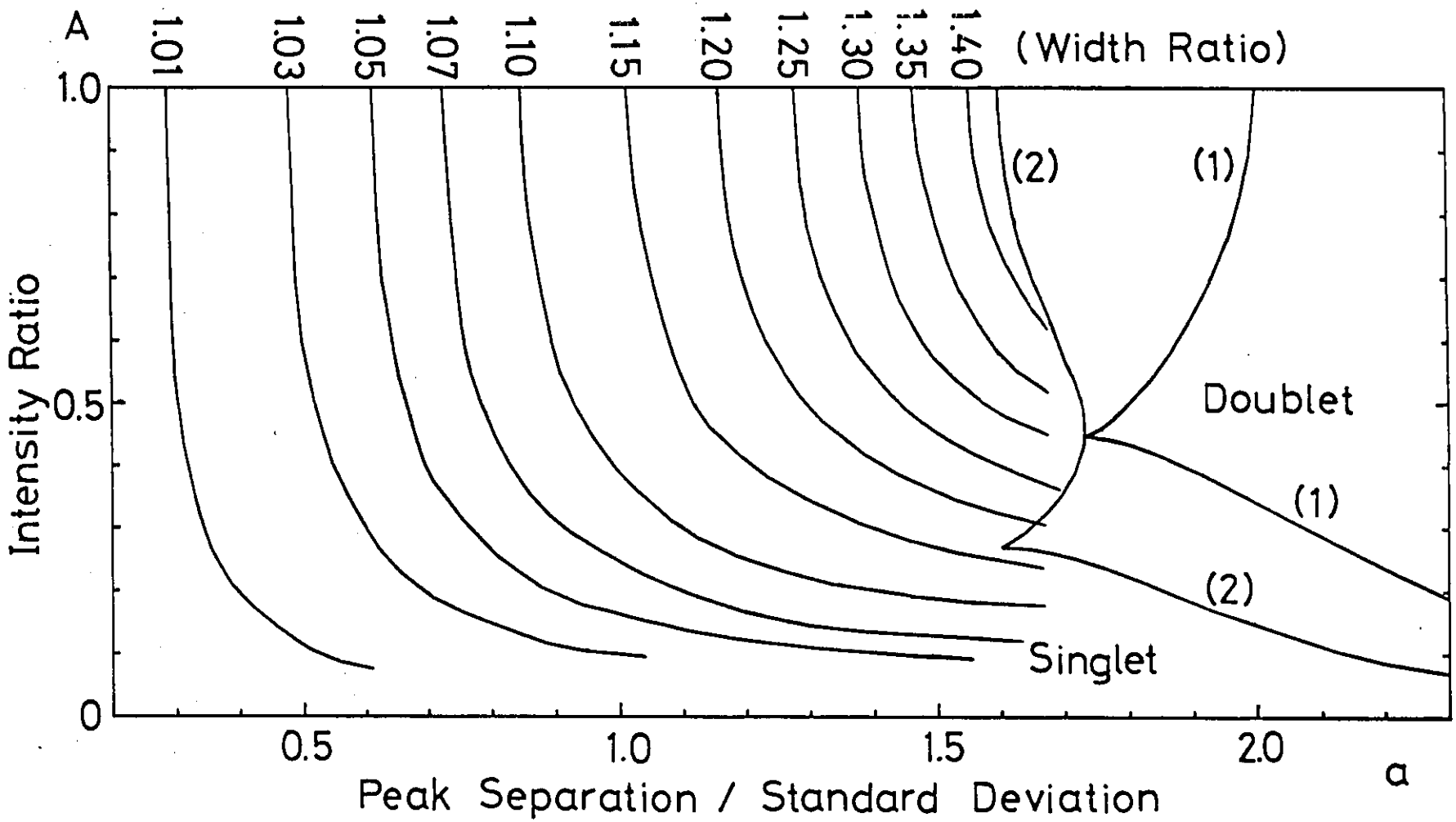

Fig. A2. Characteristics of Two-Gaussian Function

APPENDIX 3.

A.3. Coincidence Strength Calculation

A method has been presented in Section 3.8. INFORM to calculate coincidence strengths which can be expected from the level scheme and the experimental data of transitions. For simplicity, however, the method neglects two important factors. One is the life-time contributions of levels and the other is the angular correlation of coincident transitions.

A.3.1. Life-Time Contribution

Prior to the argument of the life-time contribution, the timing adjustment of coincidence system has to be considered. Assuming that the transmission time of gamma-ray pulsese (from the moment when the gamma-ray is emitted to the moment when the pulse enters the coincidence unit) follows a Gaussian-like distribution for both coincidence channels,

$$F_g(t_g) \approx \exp\left(- \frac{(t_g - \bar{t}_g)^2}{2\Delta t_g^2} \right) \qquad \text{for gate channel,}$$

$$F_s(t_s) \approx \exp\left(- \frac{(t_s - \bar{t}_s)^2}{2\Delta t_s^2} \right) \qquad \text{for spectrum channel,}$$

where, $\bar{t}_g$ and $\bar{t}_s$ are average delays, then overall system delay $t_o = t_s - t_g$ follows the distribution $D_o(t_o)$ given by

$$D_o(t_o) = \int_{-\infty}^{+\infty} F_g(t_s - t_o)\, F(t_s)\, dt_s$$

Obviously, $\bar{t}_o = \bar{t}_s - \bar{t}_g$, which is normally chosen to be zero for prompt gamma-gamma coincidence measurements.

In the case of direct coincidence via the i-th level, the delay t_i due to the (mean) life-time τ_i of the level will be expressed by

$$D_i(t_i) = \begin{cases} \exp(- t_i/\tau_i) & \text{for } t_i > 0 \\ 0 & \text{for } t_i < 0 \end{cases}$$

Therefore, the total delay time $t = t_i + t_o$ follows the distribution F(t).

$$F(t) = \int_{-\infty}^{+\infty} D_i(t - t_o)\, D_o(t_o)\, dt_o$$

and the probability P to detect the corresponding two gamma-ray pulses within the coincidence resolving time Δt can be given by

$$P = \int_o^{\Delta t} F(t)\, dt \Big/ \int_{-\infty}^{+\infty} F(t)\, dt$$

This argument is easily extended to the indirect coincidence between the i-th and j-th levels, considering every level concerning the coincidence. An implicit form of the delay time distribution for a particular cascade is given by

$$F_\nu(t) = \int_{-\infty}^{+\infty} \cdots \int_{-\infty}^{+\infty} D_i(t - t_{k_1})\, D_{k_1}(t_{k_1} - t_{k_2}) \cdots$$

$$\cdot\cdot\, D_{k_n}(t_{k_n} - t_j)\, D_j(t_j - t_o)\, D_o(t_o)\, dt_o dt_j dt_{k_n} \cdots dt_{k_1}$$

where, k_ℓ are the intermediate levels which the cascade transitions pass by and ν is the combination of these levels $(i,k_1,k_2, \cdots ,k_n,j)$. The probability P_ν can be given in the same form as

$$P_\nu = \int_o^{\Delta t} F_\nu(t)\, dt \Big/ \int_{-\infty}^{+\infty} F_\nu(t)\, dt$$

A.3.2. Angular Correlation

It is a well-known fact that successive transitions show angular correlation depending on the spins of the three levels. Since the detector sizes are limited, it is impossible to set up 4π-geometry. Therefore, for a fixed detector geometry, the contribution of angular correlations to the coincidence strength has to be taken into account.

For the gamma-ray cascade $(\gamma_g,\gamma_1,\gamma_2, \cdots ,\gamma_n,\gamma_{n+1},\gamma_s)$, which corresponds to the level combination $\nu = (i,k_1,k_2, \cdots ,k_n,j)$ between the two gamma-rays γ_g and γ_s of interest, assuming that the angular

correlation between γ_k and γ_{k+1} is given by $W_{k,k+1}(\theta_{k,k+1})$, the angular correlation $W(\theta)$ between γ_g and γ_s will be expressed as

$$W(\theta) = \int_{4\pi} \cdots \int_{4\pi} W_{g1}(\theta_1)\, W_{12}(\theta_1\phi_1 \vee \theta_2\phi_2) \cdots \cdots W_{n+1,s}(\theta_{n+1}\phi_{n+1} \vee \theta\phi)\, d\Omega_{n+1} d\Omega_n \cdots d\Omega_1$$

where, $\theta_1\phi_1 \vee \theta_2\phi_2$ denotes the angle between $\theta_1\phi_1$ and $\theta_2\phi_2$ directions. Neglecting the detector size effect and assuming an ideal detector efficiency, the probability such that the γ_s is detected in the spectrum channel when the γ_g is detected in the gate channel can be expressed by

$$C_\nu = \int_{\Delta\Omega \text{ at } \theta} W(\theta)\, d\Omega \Big/ \int_{4\pi} W(\theta)\, d\Omega$$

The actual calculation may be carried out using an expansion in terms of Legendre polynomials and spherical harmonics.

A.3.3. Corrections

Taking the above contributions into account, corrections can be made by multiplying the probabilities P_ν and C_ν. Then, the coincidence strength S can be given by

$$S = I_{\gamma_s} B_{\gamma_g} \sum_\nu B_{t_1} B_{t_2} \cdots B_{t_N} \cdot P_\nu \cdot C_\nu$$

However, since the programme INFORM is utilized to construct a level scheme, the necessary physical quantities (half-lives of levels and angular correlations) to make the corrections are hardly obtainable at this stage. Therefore, constant values for P_ν and C_ν (e.g. $P_\nu = C_\nu = 1$) have been exploited.

Special attention has to be paid to some isomeric states, the life-time of which is much longer than the coincidence resolving time.

APPENDIX 4.

A.4. χ^2-distribution Fit

A.4.1. Normalization

The frequency distribution of reduced intensities divided by their mean value $x_\gamma = I_\gamma / \overline{I}_\gamma$ can be fitted by χ^2-distributions by normalizing the total integral to be equal to the number of gamma-transitions N. The normalized χ^2-distribution functions $F_1(x)$ with one degree of freedom and $F_2(x)$ with two degrees of freedom can be given by

$$F_1(x) = N \cdot f_1(x) \qquad \text{and} \qquad F_2(x) = N \cdot f_2(x)$$

where

$$f_1(x) = (2\pi x)^{-\frac{1}{2}} \exp(-\frac{x}{2}) \qquad (x > 0)$$

$$f_2(x) = \exp(-x) \qquad (x > 0)$$

Therefore, if each class-interval for the variates x_γ is chosen as Δx, the expected frequency G_{ki} in the i-th interval will be given by

$$G_{ki}(\Delta x, N) = N \cdot \int_{x_i - \Delta x/2}^{x_i + \Delta x/2} f_k(x)\, dx \qquad k = 1, 2$$

where, x_i is the midpoint of the i-th interval and given by

$$x_i = i \cdot \Delta x - \Delta x/2$$

Or explicitly,

$$G_{1i}(\Delta x, N) = 2N \{ \Phi(\sqrt{(x_i + \Delta x/2)}) - \Phi(\sqrt{(x_i - \Delta x/2)}) \}$$

$$G_{2i}(\Delta x, N) = 2N \cdot \exp(-x_i) \cdot \sinh(\Delta x/2)$$

where, $\Phi(x)$ is the cumulative normal distribution function defined as

$$\Phi(x) = (2\pi)^{-\frac{1}{2}} \int_0^x \exp(-t^2/2)\, dt$$

In order to indicate the goodness of the fit, the sum of squared deviations can be used as

$$S = \sum_i (y_i - G_i)^2 / N^2$$

where, y_i are frequencies per class-interval. Of course, the lower S

is, the better is the fit.

A.4.2. Low Intensity Correction

Since very low intensity gamma-transitions cannot be detected, it is necessary to correct the frequency in the lowest intensity interval, assuming that reduced intensities follow the χ^2-distribution with one degree of freedom. This correction can be done by adding ΔN extra low intensity transitions with their total reduced intensity ΔI in the lowest class-interval to minimize the goodness of the fit S. These changes of total reduced intensity and the number of transitions alter the mean value of the reduced intensity as $\bar{I}_\gamma \cdot N + \Delta I = (N + \Delta N) \cdot I_o$

where, $\bar{I}_\gamma$ is the old mean and I_o the new mean. These changes also cause alteration of the normalization as well as that of the variate scaling. To be explicit, the new distribution F(x) will be

$$F(x) = (N + \Delta N) \cdot f_1(x)$$

and the width of class-interval will be converted to $\Delta x_o = \Delta x \, \bar{I}_\gamma / I_o$ without changing the original frequency distribution y_i, except that y_1 is replaced by $y_1 + \Delta N$.

Then, ΔI can be expressed by

$$\Delta I = (N + \Delta N) \cdot I_o \cdot \int_o^{\Delta x_o} x \cdot f_1(x) \, dx - \sum_{y_1} I_\gamma$$

where, the second term of the right hand side is the sum of reduced intensities in the lowest class interval. And the first term can be approximated as follows;

$$\text{(first term)} = 2(N + \Delta N) \cdot I_o \cdot \{ \Phi(\Delta x_o^{\frac{1}{2}}) - (\Delta x_o / 2\pi)^{\frac{1}{2}} \exp(-\Delta x_o / 2) \}$$

$$\simeq 2(N + \Delta N) \cdot (\Delta x_o / 2\pi)^{\frac{1}{2}} \{ \Delta x_o / 3 - (\Delta x_o)^2 / 10 + (\Delta x_o)^3 / 56 \}$$

ΔN and Δx_o can be obtained to minimize S

$$S = \frac{1}{(N+\Delta N)^2} \{ \{ G_{11}(\Delta x_o, N+\Delta N) - y_1 - N \}^2 + \sum_{i \neq 1} \{ G_{1i}(\Delta x_o, N+\Delta N) - y_i \}^2 \}$$

under the constraint

$$\bar{I}_\gamma \cdot N + \Delta I = (N + \Delta N) \cdot I_o$$

which can be written explicitly using the above approximation

$$N + 2(N+\Delta N) \cdot \Delta x \cdot (\Delta x_o/2\pi)^{\frac{1}{2}} \{\frac{1}{3} - \frac{x_o}{10} + \frac{(\Delta x_o)^2}{56}\} - \sum_{y_1} I_\gamma/\bar{I}_\gamma - (N+\Delta N)\frac{\Delta x}{\Delta x_o} = 0$$

The missing intensity ΔI can then be expressed using the optimized ΔN and Δx_o

$$\Delta I/\ \bar{I}_\gamma = (N + \Delta N)\ \frac{\Delta x}{\Delta x_o}\ - N$$

Error estimations have not been done as yet because of the very complicated structure of function S.

Fig. 17a ^{110}AG LEVEL SCHEME

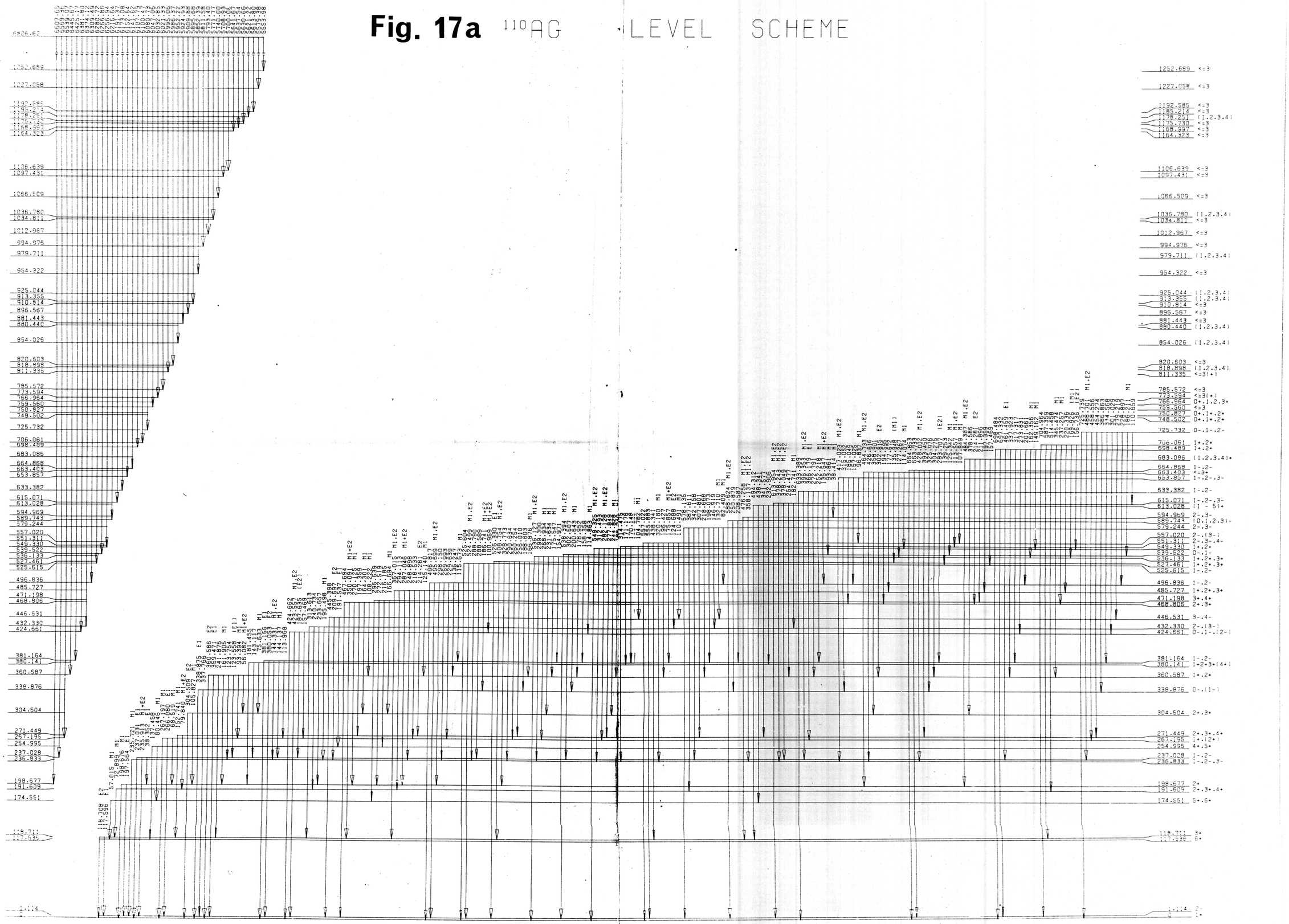

Fig. 17b ^{110}Ag LEVEL SCHEME